

University of Rajshahi

Rajshahi-6205

Bangladesh.

RUCL Institutional Repository

<http://rulrepository.ru.ac.bd>

Institute of Environmental Science (IES)

PhD Thesis

2020

Photocatalytic Decomposition of Selected Textile Industrial Effluent on Fe-Ti-Zn Oxide Catalysts

Tareque, Mahmud Hasan

University of Rajshahi

<http://rulrepository.ru.ac.bd/handle/123456789/1062>

Copyright to the University of Rajshahi. All rights reserved. Downloaded from RUCL Institutional Repository.

**PHOTOCATALYTIC DECOMPOSITION OF
SELECTED TEXTILE INDUSTRIAL EFFLUENT
ON Fe-Ti-Zn OXIDE CATALYSTS**



A Thesis

**Submitted to the Institute of Environmental science at the University of
Rajshahi in Partial Fulfilment of the Requirements for the Degree of**

DOCTOR OF PHILOSOPHY

IN

ENVIRONMENTAL SCIENCE

BY

MAHMUD HASAN TAREQUE

Principal Supervisor

Dr. Md. Golam Mostafa
Professor
Institute of Environmental Science
University of Rajshahi
Rajshahi-6205, Bangladesh

Co-Supervisor

Dr. Md. Azizul Islam
Professor (Retired)
Department of Chemistry
University of Rajshahi,
Rajshahi-6205, Bangladesh

**INSTITUTE OF ENVIRONMENTAL SCIENCE
UNIVERSITY OF RAJSHAH
RAJSHAH, BANGLADESH
JUNE, 2020**



DEDICATED

TO

MY BELOVED PARENTS

AND FAMILY MEMBERS

DECLARATION

It is hereby declared that the thesis entitled “**PHOTOCATALYTIC DECOMPOSITION OF SELECTED TEXTILE INDUSTRIAL EFFLUENT ON Fe-Ti-Zn OXIDE CATALYSTS**” is written based on my research work except where due acknowledgement has been stated. It has been carried out under the supervision and guidance of Professor Dr. Md. Golam Mostafa, Institute of Environmental Science and Dr. Md. Azizul Islam, former Professor and Director, Institute of Environmental Science, University of Rajshahi. This thesis is being humbly submitted to the Institute of Environmental Science at University of Rajshahi, Bangladesh for the fulfillment of Ph.D. degree in Environmental Science.

I further declare that any form of this thesis has not been submitted to any other University or Institution for any other degree or diploma.

Mahmud Hasan Tareque
Researcher
Institute of Environmental Science (IES)
University of Rajshahi
Rajshahi, Bangladesh

Certificate



This is to certify that the thesis entitled “**PHOTOCATALYTIC DECOMPOSITION OF SELECTED TEXTILE INDUSTRIAL EFFLUENT ON Fe-Ti-Zn OXIDE CATALYSTS**” submitted by Mahmud Hasan Tareque is the outcome of his research work carried out at the Institute of Environmental Science, University of Rajshahi, Bangladesh under our supervision. Any part or whole of the dissertation has not been submitted elsewhere for any degree.

We are forwarding this dissertation to be examined for the degree of Doctor of Philosophy in the Institute of Environmental Science at the University of Rajshahi, Bangladesh. The data presented in this thesis are genuine and original. The candidate, Mahmud Hasan Tareque has fulfilled all the requirements according to the rules of the University for the submission of a dissertation for the Ph.D. degree and made a distinct contribution to environmental science.

Principal Supervisor

Dr. Md. Golam Mostafa
Professor
Institute of Environmental Science
University of Rajshahi
Rajshahi-6205, Bangladesh

Co-Supervisor

Dr. Md. Azizul Islam
Professor (Retired)
Department of Chemistry
University of Rajshahi,
Rajshahi-6205, Bangladesh

ACKNOWLEDGEMENT

All praise and thanks to the supreme ruler of the universe Almighty Allah, who has given me the immeasurable opportunity, inspiration, encouragement, and patience to complete my research work. It is indeed a great pleasure to express my deepest sense of gratitude to my Principal Supervisor, Professor Dr. Md. Golam Mostafa, Institute of Environmental Science (IES), University of Rajshahi for his immense support, proper guidance, necessary suggestions, and continuous encouragement, without which this research would not have been successful. I am also grateful to my Co-supervisor Professor Dr. Md. Azizul Islam for his encouragement and suggestions.

I express my heartfelt gratitude to Professor Dr. Golam Sabbir Sattar, Director, IES, University of Rajshahi for providing administrative facilities and necessary support for my research work and continuous inspiration and suggestion during the research period. I am grateful to the former Director of IES, Professor Dr. Md. Sultan-Ul-Islam for his valuable suggestion and continuous inspiration.

I express my heartfelt gratitude to the honorable teachers of the Institute of Environmental Science, University of Rajshahi, for their continuous inspiration and suggestion during the research period. I greatly acknowledge all the officers and staff of this institute for their active cooperation.

I greatly acknowledge the Ministry of Science and Technology for granting me the NST (National Science and Technology) scholarship for this research work. I am also thankful to the Ministry of Education for sanctioning the deputation to complete this study. I also acknowledge the authority of BSCIC for their co-operation to collect effluents and necessary information related to the research.

I convey my sincere thanks to all the officers and staff of Central Science Laboratory, University of Rajshahi, and BCSIR Lab of Rajshahi and Dhaka for their co-operation in effluents analysis. I wish to express thanks to all my research colleagues for their friendly co-operation in the laboratory, information, and suggestion when needed.

I am deeply indebted to my parents, especially to my father, who was the continuous source of inspiration during my research work.

Finally, I wish to express my grateful acknowledgment to my wife, other family members and relatives, and friends for their encouragement and kind cooperation during this research period.

(Mahmud Hasan Tareque)

ABSTRACT

Textile dyeing industries produce a large volume of wastewater containing printing and dyeing residues of reactive dyes and chemicals. The release of colored organic compounds in the effluents contaminates the surface and ground water and is considered to be the source of nonaesthetic pollution and eutrophication. So, it is imperative to treat the discharge effluents before releasing them to the environment. The present study focused on the characterization of the untreated effluents to understand the pollution status as well as optimize the process parameters for their degradation and mineralization by heterogeneous photocatalysis. The dyeing effluents were collected from three (3) textile dyeing industries of Rajshahi and Sirajganj districts. The analyzed physicochemical parameters for these effluent samples included pH, EC, DO, TDS, TSS, COD, BOD, TOC, heavy metals, and anions. The analyses were done using several methods such as gravimetric, electrochemical, colorimetric, and optical. The effluents were subjected to photocatalytic degradation using three different photocatalysts as TiO_2 , ZnO , and Fe_2O_3 . The study optimized various operational parameters, including initial effluent concentration, catalyst concentration, catalyst type, pH, reaction time, and oxidizing agent dose to get the maximum degradation efficiency of an individual and mixed catalyst for a particular textile dyeing effluents.

The analysis results showed that the values of EC, TSS, TDS, BOD, and COD of the effluents exceeded the DoE, BD (Department Environment, Bangladesh) standard limits indicating that these effluents were highly polluted. The DO values of the effluents indicated that there was a depletion of necessary oxygen in the water. Among the effluents, SIER-1 (Silk Industry Effluent, Rajshahi-1) showed higher chloride and sulfate pollution than others, whereas SIER-2 (Silk Industry Effluent, Rajshahi-2) showed comparatively higher nitrate and bicarbonate pollution. All the effluents were almost free from phosphate pollution. The results of trace elements indicated that all the effluents had concentrations within the permissible limits of the DoE, BD standard with few exceptions. Only Cr in one effluent (SIER-1) and Pb in two effluents (SIER-1 and SIER-2) exceeded the limits of DoE, BD standard.

The photocatalytic degradation results showed that the percentage of decomposition decreased with increasing concentrations for all the effluents. All the three catalysts and their mixtures showed similar behavior. Among the photocatalysts, ZnO showed the best degradation capacity for the MB and SIER-1, whereas Fe₂O₃ and TiO₂ were most suitable for SIER-2 and YDIES (Yarn Dyeing Industry Effluent, Sirajganj), respectively. In most cases, the degradation efficiency of a single catalyst for the effluents, MB, SIER-1, and YDIES was higher than that of mixed catalysts. The decomposition percentage was sharply increased with the increase in irradiation time in the first few hrs and then increased slowly until reaching the equilibrium. The Kinetic study results showed that the photocatalytic degradation reactions followed approximately the pseudo-first-order reactions for all the effluents using TiO₂, ZnO, and Fe₂O₃ catalysts. The acidic pH level was favorable for the degradation of MB and YDIES, whereas SIER-1 and SIER-2 were better degraded in alkaline and neutral pH levels, respectively. The effect of catalyst concentration on the degradation of the effluents was not so significant. However, a higher catalyst dose increased turbidity and inhibited light penetration through the effluent solution, and reduced the degradation. Besides, an oxidizing agent, H₂O₂ concentration up to a certain limit to the photocatalytic treatment process was found to be enhanced the degradation to a large extent. The maximum decomposition of about 82.8, 81.6, 97.0, and 95.8% were achieved for MB, SIER-1, SIER-2, and YDIES, respectively at the optimized conditions. The photocatalytic degradation analyses using the TOC values showed that about 44.7, 97.9, 62.4, and 74.1%, of reductions, were achieved for the MB, SIER-1, SIER-2, and YDIES, respectively, indicated that a good efficiency with moderate to excellent levels of mineralization. Concerning COD value removal of the effluents, the results showed about 43.5, 40.8, and 57% of reduction were achieved for the SIER-1, SIER-2, and YDIES, respectively, that showed moderate mineralization of the effluents that occurred by the photocatalytic treatment. The study results indicated that ZnO and Fe₂O₃ could be an effective and suitable alternative to TiO₂ for the degradation of textile dyeing effluents. Photocatalytic degradation is not a self-sufficient treatment process for textile effluents on an industrial scale but, it can be an auxiliary process with the conventional treatment techniques because it is a unique destructive technology for non-biodegradable

organic components of the effluent. The results obtained in the present study show the efficiency of AOP's in removing dyes contained in textile effluents, which resists other conventional treatment processes. Photo oxidative degradation appears to be a promising technology that has many applications in environmental cleanup systems.

The result obtained from the UV/TiO₂/H₂O₂ treatment process made it the most appealing choice for complete degradation and substantial mineralization of textile effluents at a laboratory scale, which can be successfully extended to an industrial scale. The study observed that the optimum parameters for the photocatalytic degradation varied from one effluent to another. The selection of optimum degradation parameters such as catalyst, catalyst concentration, effluent concentration, pH, irradiation time, oxidizing agent dose, etc. is very important for photocatalytic treatment. Each of these parameters has to be optimized before the photocatalytic treatment of a particular effluent. Further study has to be required for the improvement of efficiency of these catalysts for harnessing solar light, which is an endless source of renewable energy. Efforts should be made to install the photocatalytic degradation unit in all textile dyeing as well as other industrial effluents treatment plants (ETP) before discharging them into surface water bodies.

CONTENTS

ACKNOWLEDGEMENT	i
ABSTRACT	ii-iv
CONTENTS	v-ix
LIST OF FIGURES	x-xii
LIST OF TABLES	xiii-xiv
LIST OF ABBREVIATIONS.....	xv
CHAPTER 1 INTRODUCTION.....	1-5
1.1 Significance of work	1
1.2 Statement of problems	3
1.3 Research gaps.....	4
1.4 Objectives of this research	4
CHAPTER 2 LITERATURE REVIEW.....	6-19
2.1 Textile effluents	7
2.2 Textile Industrial Effluent in Bangladesh	8
2.3 Characteristics of textile effluents	9
2.4 Adverse effects of textile effluents on environment	10
2.5 Treatment Processes for Textile Effluents	12
2.5.1 Traditional Treatment Processes and their drawbacks.....	12
2.5.2 Advanced Oxidation Processes (AOPs).....	14
2.5.2.1 Non-photochemical AOPs	14
2.5.2.2 Photochemical AOPs	14
2.6 Catalyst and Photocatalyst	17
2.7 Factors affecting photodegradation efficiency	18
2.8 Degradation of Textile Effluent by Photocatalysts	19
CHAPTER 3 MATERIALS AND METHODS	20-45
3.1 Study Area	20
3.2 Sample types	21

3.3 Sample collection	22
3.4 Sample analysis.....	23
3.4.1 pH, EC and DO	23
3.4.2 Total Suspended Solids (TSS)	23
3.4.3 Total Dissolved Solids (TDS).....	24
3.4.4 Determination of Biochemical Oxygen Demand (BOD ₅)	24
3.4.5 Determination of Chemical Oxygen Demand (COD)	25
3.4.6 Estimation of heavy metals.....	27
3.4.6.1 Iron (Fe)	27
3.4.6.2 Chromium (Cr)	28
3.4.6.3 Manganese (Mn)	28
3.4.6.4 Cadmium (Cd)	29
3.4.6.5 Zinc (Zn)	30
3.4.6.6 Lead (Pb)	31
3.4.6.7 Copper (Cu)	31
3.4.7 Estimation of major anions	32
3.4.7.1 Chloride ion (Cl ⁻)	32
3.4.7.2 Nitrate ion (NO ₃ ⁻).....	33
3.4.7.3 Bicarbonate ion (HCO ₃ ⁻)	34
3.4.7.4 Sulfate ion (SO ₄ ²⁻)	35
3.4.7.5 Phosphate ion (PO ₄ ³⁻).....	36
3.4.8 Determination of Total Organic Carbon (TOC)	37
3.5 Photocatalytic Treatment of Effluent Samples	38
3.5.1 Variable Parameters	38
3.5.2 Photocatalytic Reactor	38
3.5.3 Photocatalytic Decomposition Process	39
3.5.4 Assessment of Decomposed Effluents.....	40
3.6 Photocatalytic Reaction Mechanisms	41
3.6.1 Photocatalysts	41
3.6.2 Band Gap (E _{bg}).....	42
3.6.3 Photocatalytic Reactions	43
3.7 Equipment and Instruments	44

3.7.1 Centrifuge machine.....	44
3.7.2 Electric oven	44
3.7.3 UV-Vis spectrophotometer for colour measurement.....	45
3.7.4 Atomic absorption spectrophotometer (AAS)	45
3.7.5 TOC Analyzer.....	45
CHAPTER 4 RESULTS AND DISCUSSION.....	46-120
4.1 Introduction.....	46
4.2 Characterization of the Effluents	46
4.2.1 pH.....	47
4.2.2 Dissolved Oxygen (DO)	47
4.2.3 Total Suspended Solids (TSS)	48
4.2.4 Total Dissolved Solids (TDS).....	50
4.2.5 Biological Oxygen Demand (BOD ₅)	50
4.2.6 Chemical Oxygen Demand (COD).....	52
4.2.7 Electrical Conductivity (EC).....	53
4.2.8 Heavy metals in the Effluents	54
4.2.8.1 Chromium (Cr).....	55
4.2.8.2 Iron (Fe)	56
4.2.8.3 Manganese (Mn)	57
4.2.8.4 Nickel (Ni)	57
4.2.8.5 Copper (Cu)	58
4.2.8.6 Cadmium (Cd)	59
4.2.8.7 Zinc (Zn)	59
4.2.8.8 Lead (Pb).....	60
4.2.9 Major Anionic Parameters in the Effluents	61
4.2.9.1 Chloride ion (Cl ⁻)	61
4.2.9.2 Nitrate ion (NO ₃ ⁻).....	62
4.2.9.3 Bicarbonate ion (HCO ₃ ⁻).....	63
4.2.9.4 Sulfate ion (SO ₄ ²⁻).....	64
4.2.9.5 Phosphate ion (PO ₄ ³⁻).....	64
4.2.10 Total organic carbon (TOC).....	65

4.3 Photocatalytic decomposition of methylene blue	66
4.3.1 Effect of initial MB concentration	66
4.3.2 Effect of catalyst	68
4.3.3 Effect of irradiation time	69
4.3.4 Photodegradation kinetics of MB	70
4.3.5 Effect of pH	72
4.3.6 Effect of catalyst concentration	74
4.3.7 Effect of oxidizing agent (H ₂ O ₂) dose	75
4.3.8 Mineralization of the dye	76
4.3.9 Optimized parameters for photocatalytic degradation of MB	77
4.4 Photocatalytic decomposition of Silk Industry Effluent, Rajshahi-1	
(SIER-1)	79
4.4.1 Effect of initial effluent concentration	79
4.4.2 Effect of catalyst	80
4.4.3 Comparison among decomposition processes	81
4.4.4 Effect of irradiation time	83
4.4.5 Photodegradation kinetics of SIER-1.....	84
4.4.6 Effect of pH.....	86
4.4.7 Effect of catalyst concentration	87
4.4.8 Effect of oxidizing agent (H ₂ O ₂) dose	88
4.4.9 Mineralization of SIER-1	89
4.4.10 Optimized parameters for the photodegradation of SIER-1	90
4.5 Photocatalytic decomposition of Silk Industry Effluent, Rajshahi-2	
(SIER-2)	92
4.5.1 Effect of initial effluent concentration	92
4.5.2 Effect of catalyst	93
4.5.3 Comparison among decomposition processes	94
4.5.4 Effect of irradiation time	96
4.5.5 Photodegradation kinetics of SIER-2.....	97
4.5.6 Effect of pH.....	99
4.5.7 Effect of catalyst concentration	100
4.5.8 Effect of oxidizing agent (H ₂ O ₂) dose	101

4.5.9 Mineralization of SIER-2	103
4.5.10 Optimized parameters for the photodegradation of SIER-2	104
4.6 Photocatalytic decomposition of Yarn Dyeing Industry Effluent, Sirajganj (YDIES).....	105
4.6.1 Effect of initial effluent concentration	105
4.6.2 Effect of catalyst	106
4.6.3 Effect of irradiation time.....	107
4.6.4 Photodegradation kinetics of YDIES.....	109
4.6.5 Effect of pH.....	110
4.6.6 Effect of catalyst concentration	112
4.6.7 Effect of oxidizing agent (H ₂ O ₂) dose	113
4.6.8 Mineralization of YDIES	114
4.6.9 Optimized parameters for photocatalytic degradation of YDIES	115
4.7 Comparative studies	116
CONCLUSION	121-125
REFERENCES	126-158
APPENDICES	159-167

List of Figures

Figure No.		Page No.
Figure 3.1	Study Area	21
Figure 3.2	Schematic Diagram of photocatalytic reactor	39
Figure 3.3	Valence and conduction band positions in metal, semiconductor, and insulator	41
Figure 3.4	Mechanism of photocatalytic degradation	42
Figure 4.1	Comparisons among TSS values of SIER-1, SIER-2, and YDIES	49
Figure 4.2	Comparisons among TDS, COD, and BOD of SIER-1, SIER-2, and YDIES	51
Figure 4.3	Comparisons among EC values of SIER-1, SIER-2, and YDIES	53
Figure 4.4	Effect of initial dye concentrations on % of decomposition of MB	67
Figure 4.5	Effect of catalyst on % of decomposition of MB	68
Figure 4.6	Effect of irradiation time on % of decomposition of MB by a) single catalysts and b) mixed catalyst	69
Figure 4.7	Photocatalytic degradation of MB	71
Figure 4.8	Kinetics of photodegradation of MB	72
Figure 4.9	Effect of pH on % of decomposition of 40 ppm MB solution	73
Figure 4.10	Effect of catalyst concentration on % of decomposition of MB	75
Figure 4.11	Effect of H ₂ O ₂ dose on % of decomposition of MB	76

Figure 4.12	Mineralization of 40 ppm MB by photocatalytic treatment	77
Figure 4.13	Effect of initial effluent concentrations on % of decomposition of SIER-1	80
Figure 4.14	Effect of catalyst on % of decomposition of SIER-1	81
Figure 4.15	Comparison among various decomposition processes on 60% SIER-1	82
Figure 4.16	Effect of irradiation time on % of decomposition of SIER-1 by a) single catalysts and b) mixed catalyst.	83
Figure 4.17	Photocatalytic degradation of SIER-1	84
Figure 4.18	Kinetics of photodegradation of SIER-1	85
Figure 4.19	Effect of pH on % of decomposition of 60% SIER-1	86
Figure 4.20	Effect of catalyst concentration on % of decomposition of SIER-1	88
Figure 4.21	Effect of H ₂ O ₂ dose on % of decomposition of SIER-1	89
Figure 4.22	Effect of initial effluent concentrations on % of decomposition of SIER-2	93
Figure 4.23	Effect of catalyst on % of decomposition of SIER-2	94
Figure 4.24	Comparison among different decomposition processes on SIER-2	95
Figure 4.25	Effect of irradiation time on % of decomposition of SIER-2 by a) single catalysts and b) mixed catalyst	96
Figure 4.26	Photocatalytic degradation of SIER-2	97
Figure 4.27	Kinetics of photodegradation of SIER-2	98
Figure 4.28	Effect of pH on % of decomposition of 60% SIER-2	99

Figure 4.29	Effect of catalyst concentration on % of decomposition of SIER-2	101
Figure 4.30	Effect of H ₂ O ₂ dose on % of decomposition of SIER-2	102
Figure 4.31	Effect of effluent concentrations on % of decomposition of YDIES	106
Figure 4.32	Effect of catalyst on % of decomposition of YDIES	107
Figure 4.33	Effect of irradiation time on % of decomposition of YDIES by a) single catalysts and b) mixed catalyst.	108
Figure 4.34	Photocatalytic degradation of YDIES	109
Figure 4.35	Kinetics of photodegradation of YDIES	110
Figure 4.36	Effect of pH on % of decomposition of 50% YDIES	111
Figure 4.37	Effect of catalyst concentration on % of decomposition of YDIES	113
Figure 4.38	Effect of H ₂ O ₂ dose on % of decomposition of YDIES	114
Figure 4.39	Flow diagram of a novel approach for combination of photocatalytic decomposition of textile dyeing effluent treatment plant	120

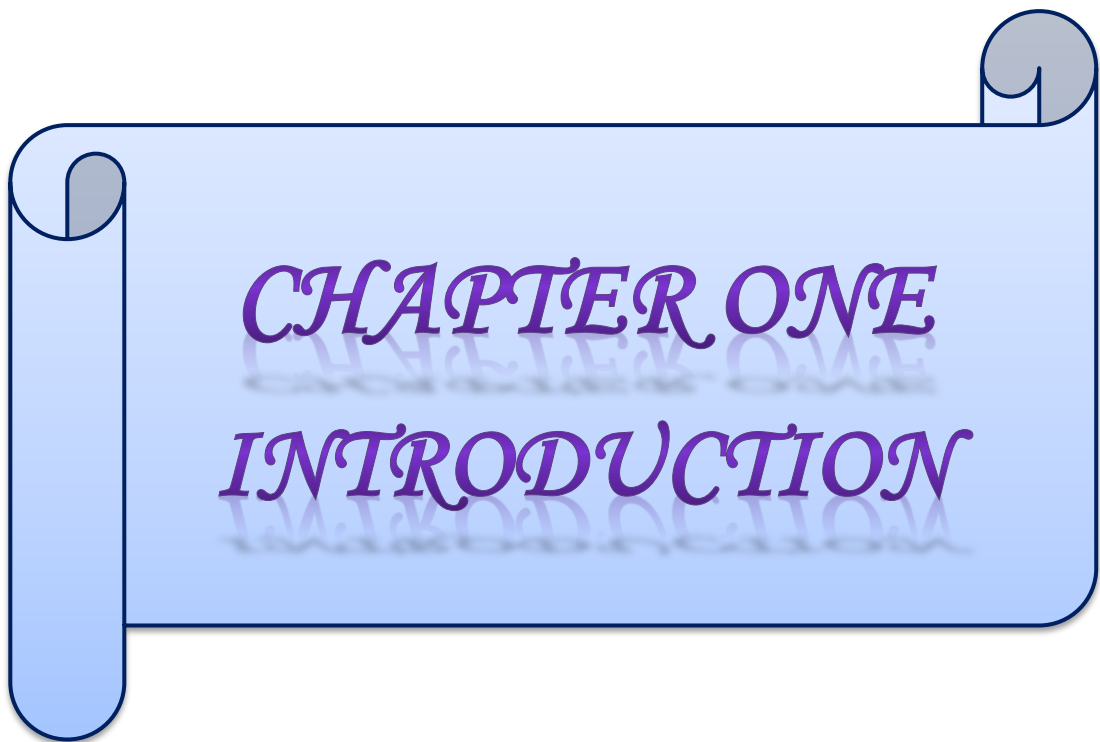
List of Tables

Table No.		Page No.
Table 3.1	Main characteristics of methylene blue	22
Table 3.2	Band gap energies of different Photocatalysts	42
Table 4.1	pH and DO of three textile industries effluents of Rajshahi and Sirajganj districts	48
Table 4.2	Major physicochemical parameters of three textile industries effluents of Rajshahi and Sirajganj districts at a glance	54
Table 4.3	Concentrations of heavy metals in the three textile industries effluents of Rajshahi and Sirajganj districts.	57
Table 4.4	Concentrations of anionic parameters in the three textile industries effluents of Rajshahi and Sirajganj districts.	62
Table 4.5	TOC values of Effluents of the three textile industries' effluents of Rajshahi and Sirajganj districts.	65
Table 4.6	Values of optimized parameters for the photocatalytic degradation of 40 ppm MB solution	78
Table 4.7	Reduction in TOC and COD of SIER-1 by photocatalytic treatment at optimized conditions	90
Table 4.8	Optimized parameters for the photocatalytic degradation of 60% SIER-1	91
Table 4.9	Reduction in TOC and COD of SIER-2 by photocatalytic treatment at optimized conditions	103
Table 4.10	Optimized parameters for the photocatalytic degradation of 60% SIER-2	104
Table 4.11	Reduction in TOC and COD of YDIES by photocatalytic treatment at optimized conditions	115

Table 4.12	Optimized parameters for the photocatalytic degradation of 50% YDIES	116
Table 4.13	Comparison of optimized parameters for photocatalytic degradation of MB, SIER-1, SIER-2, YDIES	116
Table 4.14	Comparison of photocatalytic degradation of MB and other dyes	117
Table 4.15	Comparison of photocatalytic degradation of SIER-1, SIER-2, YDIES and other effluents/mixture of dyes	119

List of Abbreviations

AAS- Atomic Absorption Spectroscopy
ADMI- American Dye Manufacturers Institute
AEPA- Australian Environmental Protection Authority
AOP- Advanced Oxidation Process
APHA- American Public Health Association
BOD- Biological Oxygen Demand
BSCIC- Bangladesh Small and Cottage Industries Corporation
BTMA- Bangladesh Textile Mills Association
COD- Chemical Oxygen Demand
DEPZ- Dhaka Export Processing Zone
DND- Dhaka- Narayanganj- Demra
DO- Dissolved Oxygen
DoE- Department of Environment
EC- Electrical Conductivity
ENRAC- Environment and Resource Analysis Center
EPA- Environmental Protection Agency
ETP- Effluent Treatment Plants
FTIR- Fourier-transform Infrared Spectroscopy
HDL- High Density Lipoprotein
HTCO- High-Temperature Catalytic Oxidation
IC- Inorganic Carbon
IES- Institute of Environmental Science
IUPAC- International Union of Pure and Applied Chemistry
MB- Methylene Blue
MO- Methyl Orange
NDIR- Non-dispersive Infrared
NGO- Non-governmental Organization
NHE- Normal Hydrogen Electrode
RB- Reactive Black
RG- Reactive Green
RU- Rajshahi University
RY- Reactive Yellow
SIER- Silk Industry Effluent, Rajshahi
TC- Total Carbon
TDS- Total Suspended Solids
TEL- Tetraethyl lead
TIB- Transparency International Bangladesh
TOC- Total Organic Carbon
TSS- Total Dissolved Solids
USD- United States Dollar
WHO- World Health Organization
WIN- Water Integrity Network
WWF- World Wildlife Fund
YDIES- Yarn Dyeing Industry Effluent, Sirajganj



CHAPTER ONE
INTRODUCTION

INTRODUCTION

The textile industry is one of the foremost pollutant discharging industries in the world. According to surveys, about 5% of all landfill areas are occupied by textile waste materials. Other than, 20% of all fresh water gets polluted by textile dyeing industries (Fibre2Fashion, 2012). Pollutants discharged by these industries are ceaselessly doing incredible harm to the environment all over the world. Textile fabricating units discharge hazardous waste into adjacent surface water bodies, land, and air. As per the Bangladesh Textile Mills Association (BTMA), the number of yarn and fabrics manufacturing mills in Bangladesh is 430 and 802 respectively. And also there are 244 dyeing-printing-finishing mills which are the most pollution generating industries in this sector (Dhaka Tribune, 7th January 2019). Most textile wastewaters contain a significant portion of unfixed dyes. It was evaluated that around 15% of the overall world dye production remained unused during the dyeing process and released with textile effluents. (Vautier *et al.*, 2001).

1.1 Significance of work

The discharge of effluent from textile industries into natural environments is harmful to aquatic life as well as mutagenic to humans. Tang and An (1995) reported that textile industries use more than ten thousand dyes and pigments worldwide under different trade names and every year around 280,000 tons of unfixed dyes are released as effluents (Hsueh *et al.*, 2005). The main compositions of textile dyeing effluents include organic chemicals of dyes and pigments, of which azo and anthraquinone dyes are most common (Kansal *et al.*, 2007; Tang and An, 1995). Huge amounts of wastewater are produced at dyeing and finishing units of textile industries, which are deeply colored and contain a high concentration of organic compounds (Maas *et al.*, 2005). These wastewaters are toxic, non-biodegradable and difficult to treat via classical methods. Dyes hamper aquatic photosynthesis process by strongly absorbing sunlight and seriously affecting the total ecosystem (Slokar *et al.*, 1998). These effluents increase BOD and COD, inhibit plant growth in water bodies, insert the food cycle and cause a severe ecological imbalance (Catanho *et al.*, 2006; Peralta-Zamora

et al., 1999). These are often toxic, mutagenic, and carcinogenic to living beings and have prolonged half-life, which increases the possibility of bioaccumulation (Zainal *et al.*, 2005; Kunz *et al.*, 2002). Dyes are highly persistent in environments because they are produced with great chemical and photolytic stability. Dyes also can cause severe damage to human beings, such as disturb or failure of the liver, kidney, and brain functions, reproductive and central nervous systems etc. (Salleh *et al.*, 2011). Approximately 40 % of dye chemicals utilized around the world contain naturally bound chlorine, which may be a carcinogen. The vapor of these chemicals may be mixed with the air and human breath or, these may absorb through human skin. These may exhibit allergic reactions and adversely affect children even not yet born. The normal physiological and biochemical functions of human body such as osmoregulation, respiration, reproduction etc. can be disturbed by this pollution, which ultimately lead to mortality. Additionally, high concentrations of non-biodegradable heavy metals may be present often in these textile industry effluents (Catanho *et al.*, 2006). They form organometallic compounds and gather in essential body organs in course of time, which is followed by different indications of illnesses. So, untreated or partially treated effluents of textile dyeing industries can be detrimental to both aquatic and terrestrial living beings because those can adversely affect the natural ecosystem and health issues (Khan and Malik, 2014). In this manner, the improvement of efficient and secure treatment process of textile dyeing effluents is a crying need for keeping up pollution free environment.

There are many pre-treatment and post-treatment procedures in practice to eliminate the color from dye-containing effluents so that the environmental regulatory requirements can be met up. These procedures may be physical, chemical, or biological (Robinson *et al.*, 2001; Tünay *et al.*, 1996). Physicochemical techniques mainly include filtration, coagulation and flocculation, sedimentation, adsorption, ion exchange, activated carbon treatment, ultrasonic mineralization etc. Biological techniques covers bacterial and fungal biosorption; aerobic and anaerobic biodegradation; combined anaerobic/aerobic treatment processes etc. The factors which determine the success of any treatment technique include wastewater composition, required chemicals costs, operation costs, and environmental fate etc.

Since, in most cases single technique fails to achieve complete decolorization, a combination of different techniques is often practiced for the treatment of textile dyeing effluents. However, these treatment technologies are non-destructive because in these techniques the non-biodegradable compounds are converted into sludge, which causes a novel secondary pollution that needs to be handled further (Arslan *et al.*, 2000; Stock *et al.*, 2000). A report stated that due to the biorecalcitrant nature of these dyes, most of them are only adsorbed on the sludge and not degraded (Sauer *et al.*, 2002). Considering these problems, there has been a lot of interest in the use of advanced oxidation processes (AOPs) to degrade the dyes completely. AOPs generally operate by producing reactive species like hydroxyl radicals, which rapidly and non-selectively oxidize a wide range of organic pollutants. (Das *et al* 1999; Yang *et al* 1998). In a broad sense, AOPs are a series of chemical treatment processes that oxidize organic matter in wastewater by reacting with hydroxyl radicals ($\cdot\text{OH}$) to eliminate them. Photocatalytic decomposition is one type of AOPs. In this research work, some selected textile effluents were photocatalytically decomposed to investigate the effects of various process parameters like initial effluent concentration, catalyst dose, reaction time, pH, and oxidizing agent dose etc.

1.2 Statement of problems

This study was initiated to evaluate the photocatalytic degradation efficiencies of some photocatalysts on some selected textile effluents in the BSCIC (Bangladesh Small and Cottage Industries Corporation) area in Rajshahi. The BSCIC in Rajshahi City comprises of more than 200 industries of different types like silk, textile, aluminum, automobile workshop, food processing, packaging, pharmaceuticals, etc. Among those there are about 20 silk and textile industries of small and large scale. There are lots of textile dyeing industries in several Upazilas of Sirajganj district also. These industries generate large amounts of liquid waste, especially dyeing effluents, which are falling through small open drains into the main drain and eventually into nearby surface water bodies. These untreated effluents contain highly concentrated colored and organic matter and contaminate soil and natural water, impede photosynthesis of aquatic plants, disturb the whole aquatic ecosystem and food chain, and thus cause a serious environmental hazard.

1.3 Research gaps

There are so many research works on photocatalytic degradation of various synthetic dyes that are frequently used in textile dyeing industries. But there are very few research reports on textile dyeing effluents regarding photocatalytic degradation. Although photocatalytic decomposition using UV radiation is an advanced and effective technology for non-biodegradable pollution control, the use of this technology has not yet been practiced in textile mills and other industries in Bangladesh. Some of these industries operate ETPs for the effluent treatment, which are still using traditional technologies like adsorption, flocculation, coagulation, sedimentation, activated carbon treatment etc. There is no detailed research so far that has been done on the treatment techniques as well as photocatalytic degradation of textile effluents of the BSCIC industrial area, Rajshahi, and those of Shirajganj District. This study evaluated the photocatalytic degradation efficiencies of some catalysts on selected textile effluents in the BSCIC area in Rajshahi.

It is notable that, photocatalytic decomposition is not a self-sufficient treatment process for textile effluents but must be an auxiliary process. Since the textile industries use a broad variety of colorants in their dyeing operations, the effluents produce a mixture of dyestuffs. When many dyes of different functional groups are present in one effluent mixture, the rate of removal and degree of decolorization may be affected, making the removal process more difficult. Moreover, the wide spread use of photocatalysts for large-scale water treatment is uneconomical. The main drawback that prevents this method from progressing is the need for a time-consuming and expensive filtration step to remove thin catalyst particles and to recycle those.

1.4 Objectives of this research

The textile dyeing industries of the BSCIC, Rajshahi, and Sirajganj districts discharge toxic and hazardous effluent into the adjacent water bodies causing severe water pollution. There is a pressing need to control pollution with eco-friendly green technologies. The main objective of the study was to reduce the pollutants from

Chapter One : Introduction

discharged textile dyeing effluents using UV-photocatalytic irradiation. To achieve the main objective, there were some specific objectives:-

1. To characterize some selected textile effluents to understand their pollution level.
2. To optimize the process parameters of the photocatalytic decomposition for achieving the best decomposition conditions.
3. To study the kinetics of the photocatalytic decomposition reactions.
4. To evaluate the photocatalytic decomposition efficiency by assessing the COD and TOC levels of the effluents before and after treatment.



CHAPTER TWO
LITERATURE REVIEW

LITERATURE REVIEW

A literature review is a critical study of established information on a specific topic, including hypotheses, methodologies, empirical results, criticisms, assessments, and evaluations. It entails a critical review that recognizes comparisons and discrepancies between current literature and the research in progress. It reviews what has already been studied on a given subject. As a consequence, based on established knowledge, a creative idea and concept for further research can be developed. It is essential to do a careful and thorough literature review for conducting a good research. It is basic homework that is done vigilantly in all research papers. It is not only the past literature surveys on the relevant topic, but it also appraises, encapsulates, compares, and correlates various scholarly books, articles, and other relevant sources that are related to the current research. This literature review was carried out to obtain a better understanding of the current status of textile industrial effluents in relation to the environment, as well as their characterization to assess pollution levels. The study conducted a detailed literature review based on different articles, books, internet, and peer-reviewed national and international journals of high impact factors published within about the last 20 years.

The water used to make commercial products in industrial activities in different phases of production is called industrial wastewater or effluent. Once this process water has been used, it is considered wastewater and required to be treated before it is released into any water bodies. Textile industrial sectors, like many others, have a direct association with environmental concerns that must be taken into account. The main reason is that chemical processing of the textile industries contributes to about 70% of pollution. It is well known that these textile mills use a huge volume of water in a series of production steps such as sizing, scouring, bleaching, dyeing, printing, finishing, and ultimately washing. The textile dyeing industries discharged a large volume of wastewater containing a variety of pollutants. Special attention must be paid to these streams of water because they affect the aquatic eco-system in a variety of ways, including depletion of DO content and the settlement of suspended substances in anaerobic conditions. These effluents produced in different steps exceed

the permissible limit in maximum cases and thus are highly polluted and dangerous. In this chapter, an effort has been made to represent a brief review of research information concerning the sources of textile effluents, their characteristics, and adverse effect on the environment and traditional and advanced treatment processes of these effluents. In this regard, Advanced Oxidation Processes (AOPs) and photocatalytic decomposition have been discussed in detail.

2.1 Textile effluents

The textile industry, with its dye-containing wastewaters, is one of the major causes of serious pollution problems around the world. In fact, 45 % of textile effluents are produced in preparatory processing, 33 % in dyeing, and 22 % are reprocessed in finishing, according to a realistic estimate. (Fibre2Fashion, 2006). Several reports stated that there are more than ten thousand different textile dyes commercially available worldwide, with an approximate annual production of 7×10^5 metric tons, 30% of which are used in excess of 1,000 tons per year (Baban *et al.*, 2010; Robinson *et al.*, 2001; Solomon *et al.*, 2009). During the dyeing process, 10-25 % of textile dyes are lost, and 2-20 % is directly discharged as aqueous effluents in the environment. Most of these dyes are recalcitrant, especially the azo dyes (N=N group) are of great environmental concern. These dyes account for about 60-70% of all dyes used in food and textile production. Olukanni *et al.* (2009) reported that at the time of manufacture and application around 2- 50% of these dyes are lost with effluents.

O'Neill *et al.* (1999) and Georgiou *et al.* (2002) stated that the use of significant quantities of dyestuffs during the dyeing stages of the textile manufacturing process is the key source of color in textile industry effluent. Significant dye residuals are often observed in the final dye house waste water as hydrolyzed or unfixed forms due to inefficient dyeing processes. (Yonar *et al.*, 2005). Sobana and Swaminathan (2007) stated that the most important type of synthetic organic dyes used in the textile industry is azo dyes, which are therefore also common environmental pollutants. They are manufactured in large quantities and released into the environment during their production processes. Walker and Weatherley (1997) reported that around 10,000 different dyes are produced all over the world, and the textile industry uses

approximately 8×10^5 tons of synthetic dyes. Wijannarong *et al.* (2013) and Gupta *et al.* (2012) reported that in textile industries 93% of the consumed water finally appears as colored effluents due to the use of highly concentrated organic dye compounds and heavy metals. Several reports on water consumption in textile industries are based on different production stages of wet processing and the type of textile produced (Eswaramoorthi *et al.*, 2008; Ntuli *et al.*, 2009). As a result of different processes in textile manufacturing, considerable amounts of polluted water are released. All dyes that are added to fabrics during the dyeing process are not set on them. A part of these dyes still remains unattached to the fabrics and is washed out. Hence, high concentration of these unfixed dyes is often observed in the textile effluents (Hassaan and El Nemr, 2017).

2.2 Textile industrial effluents in Bangladesh

Hossain *et al.* (2018) reported that the textile sector accounts for 82 % of the country's total export earnings, which is about 28 billion dollars annually. The ready-made garment (RMG) market being the major segment in the textile industry is expected to reach 50 billion dollars per year by 2021. But sad fact is that untreated effluents from these textile industries have been discharged into the nearby water bodies like ponds, canals, rivers etc. outside the city areas of Saver, Gazipur, Ashulia, Tongi etc. (Belal *et al.*, 2015). According to the Department of Inspection for Factories and Establishments, Dhaka has about 3000 garment factories. In 2016, textile dyeing effluent was reported to be about 217 million m^3 in Bangladesh, containing a broad range of pollutants, and will cross 349 million m^3 by 2021 if typical dyeing practices are continued (Hossain *et al.*, 2018). There are approximately 1,700 washing, dyeing, and finishing factories in Bangladesh producing export quality fabrics (Hossain, 2019). These industries are mainly located around Dhaka, Chittagong, and Mymensingh, Narayanganj and Gazipur districts. Factories are almost always constructed near water bodies like canals or rivers. One of the country's main textile belts is the Konabari Industrial Cluster in Gazipur. There are 28 washing, dyeing, and finishing units here generating 51,000 m^3 of wastewater daily, with the 5 largest units liable for 60% of the total run-off.

An NGO working for environmental protection, Water Integrity Network (WIN) found that untreated effluent streams are very often released into surrounding areas, irrigation channels, or ponds. The discharge flows into the Turag River, then downstream to the Buriganga and Shitalakhsya Rivers, polluting the water severely. The volume of water used in the industry varies significantly, depending on the factory's particular procedures, the equipment used, and the current management structure. The most water is used to produce cotton yarn and cloth. The largest quantity of water is required in cotton yarn and fabric manufacturing industries. Textile production in Bangladesh is extremely water intensive consuming 250 –300 liters of water for each kg of fabric production which is equivalent to daily water use for two people and far exceeding (about 5 times) the international best practice (Restiani, 2016). Approximately 300 tons of water is consumed for the production of 1 ton of cloth. Approximately 80 - 85% is ultimately discharged as wastewater. According to the World Wildlife Fund (WWF), it can spend 2,700 liters of water to produce the cotton yarn required to weave a single T-shirt.

2.3 Characteristics of textile effluents

Textile industrial effluents usually contain high quantities of recalcitrant chemicals, both organic and inorganic, and are distinguished by high COD, BOD, and TOC values, higher concentrations of dissolved solids, surfactants, oil, fluctuating temperature, pH, and probably heavy metals (e.g. Pb, Cu, Cr, Ni, etc.) and acute color. (Grau, 1991; Solmaz *et al.*, 2009). Textile dyes are a class of organic compounds that are generally considered as pollutants and are found in wastewaters as a result of chemical textile finishing processes. (Suteu *et al.*, 2009). Multiple dyes from various chemical classes may be used in a single dyeing process, resulting in a complex wastewater. (Correia *et al.*, 1994; Zaharia *et al.*, 2009). Anjaneyulu *et al.* (2005) argued that because of their complex structures, synthetic roots, and recalcitrant nature, as well as the presence of non-biodegradable compounds, textile dyes must be eliminated from industrial effluents before being disposed of into hydrological systems. Hasani *et al.* (2008) observed that textile wastewater is a highly complex and variable mixture of many polluting substances, including dyes, which trigger color and organic load, upsetting the overall ecological balance of the receiving water

bodies. Kansal *et al.* (2007) reported that colored commercial dye chemicals make up the bulk of the textile effluents. The textile industry produces wastewaters of great chemical variety, diversity, and volume due to the use of broad range of fabrics, dyes, process aids, and finishing products (Bizani *et al.*, 2006; Secula *et al.*, 2008). Blomqvist (1996) reported that some textile effluents are found to contain inorganic chemicals like HCl, NaOCl, NaOH, NaS, which are capable of being poisonous to marine lives. As per the report of AEPA (Australian Environmental Protection Authority, 1998), textile industrial effluents from different stages of operations are characterized by higher values of BOD, COD, dissolved solids (DS), and suspended solids (SS). In the case of sizing and desizing units, high alkalinity and SS for bleaching units, and high pH, low BOD, and high DS for mercerizing units. In the case of dyeing units, the effluents usually tend to be strongly colored with the presence of heavy metals and with high BOD and DS but low SS.

2.4 Adverse effects of textile effluents on environment

Synthetic dyes are a major environmental issue because of their frequent use and low removal rate during aerobic effluent treatment. Suteu *et al.* (2009) and Zaharia *et al.* (2009) described that dye-containing effluents are unacceptable not only because of their color, but also because many of their breakdown products like benzidine, naphthalene, and other aromatic compounds are poisonous, carcinogenic, or mutagenic to living beings. Xu *et al.* (2005) stated that the color of wastewater is aesthetically unappealing to marine life, reducing water oxygenation and damaging the aquatic environment and food chain. The dyes in spent dye baths from textile factories are non-biodegradable, posing a significant environmental risk. These dyes may remain in nature for a long time if they aren't handled properly. For example, the hydrolyzed Reactive Blue 19 has a half-life of about 46 years at pH 7 and 25°C (Chequer *et al.*, 2013).

Maas *et al.* (2005) stated that textile dyeing and finishing processes generate significant volumes of deeply colored wastewater with a high concentration of organic matter, which is difficult to handle using conventional methods. Slokar *et al.* (1998) described that apart from the aesthetic issues that colored effluents cause when

they enter natural water currents, dyes hamper aquatic photosynthesis process by strongly absorbing sunlight and seriously affecting the total ecosystem. Color is one of the most visible indications of water contamination, and heavily colored effluents containing dyes can be harmful to the receiving bodies. (Saltabas *et al.*, 2012; Sousa *et al.*, 2012). Because of their widespread usage, especially in the textile industry, the possible formation of toxic aromatic amine intermediates under anoxic conditions, and resistance to aerobic wastewater treatment, azo-dyes are of particular concern. (Aber and Esfahlan, 2011; Wang *et al.*, 2008b). Dyeing effluent may alter the pH, increases the BOD and COD also (Duran and Esposito, 2000; Mester and Tien, 2000; Wu *et al.*, 2011). Olukanni *et al.* (2006) reported that these dyes may persist in the environment for a long time if they are not properly handled. Minussi *et al.* (2001) and Gharbani *et al.* (2008) stated that the largest group of synthetic dyes is azo dyes giving in a wide range of colors and structures. Even at low concentrations, their tolerance to biological and chemical breakdown renders them very much harmful to the environment. (Sahel *et al.*, 2007). Because of their non-biodegradability and possible carcinogenic nature, organic pollutants such as dyes, surfactants, pesticides, and other chemicals in the hydrosphere are of particular concern for freshwater, coastal, and marine ecosystems. (Amini *et al.*, 2011; Atchariyawut *et al.*, 2009; Bulut and Aydin, 2006; Demirbas *et al.*, 2002; Fang *et al.*, 2004; Li *et al.*, 2008; Mahmoodi and Arami, 2006; 2008; 2009; 2010 and Mozia *et al.*, 2008). The major concern with dyes is their aesthetic character at the discharge point for the visibility of the receiving waters (Slokar *et al.*, 1998).

Water Integrity Network (WIN) and Transparency International Bangladesh (TIB) conducted joint research on the use and feasibility of Effluent Treatment Plants (ETPs) in Bangladesh's garment industry and released an article in May 2017. In that article, Haque and ENRAC (Environment and Resource Analysis Center) team reported that approximately 67% of respondents in the Shanirvar Dhamshona Union of Dhaka District and 88% in Kanchpur Union of Tangail District said that textile industry pollution has negatively affected their income. Around 25% of farmers and 4% of fishermen in Shanirvar Dhamshona Union said that because the textile industry began operating in their area, agricultural production capacity and fish availability decreased.

2.5 Treatment processes for textile effluents:

The treatment of textile effluents is always related to decolorization process in terms of the local environmental quality criteria and guidelines. To decolorize textile effluents, a number of physical, biological, and chemical processes are used, which include adsorption, coagulation, flocculation, membrane filtration, ozonation, electrochemical, radiolysis, bacterial, algal, fungal, and advanced oxidation processes (AOPs) etc. (Chaudhari *et al.*, 2011; Ince and Tezcanh, 1999; Kannan and Sundaram, 2001; Rai *et al.*, 2005; Solmaz *et al.*, 2009 and Wojnarovits and Takacs, 2008).

2.5.1 Traditional treatment processes and their drawbacks

Many researchers suggest different physicochemical processes such as activated carbon adsorption, flocculation, reverse osmosis, membrane processes, ion exchange, and ultra-filtration to isolate color from textile effluents. (Robinson *et al.*, 2001; Georgiou *et al.*, 2002). These physicochemical treatment systems are only capable of shifting pollutants from one state to another, but these cannot separate them completely from the effluent. Erswell *et al.* (1988) reported that many scientists are currently investigating the recovery and reuse of certain and useful chemical compounds, which are released with textile effluents. Gümüş and Akbal (2011) described that adsorption, flocculation, reverse osmosis, and ultra-filtration etc. are non-destructive physicochemical processes that simply transfer organic compounds from liquid to the solid phase, resulting in a novel pollution. As a result, cost-effective regeneration of adsorbent materials and solid waste management become necessary. Chemical treatment with strong oxidants like chlorine or ozone has shown better results, but it is not cost-effective due to the large doses needed. At this point, the AOPs have distinct advantages over traditional treatment options because they can decompose non-biodegradable organic components and mitigate the need to dispose of residual sludge. Aksu (2005) found that biological methods can eliminate a wide variety of dyes by bacterial and fungal degradation under aerobic or anaerobic conditions. However, due to the susceptibility of azo dyes to aerobic degradation as well as the formation of carcinogenic aromatic amines, these treatment methods have proven ineffective (Habibi *et al.*, 2005; Yang *et al.*, 2004). Traditional biological

treatment techniques for decolorization and degradation of dyeing effluents are not much successful due to the high level of aromatics present in dye molecules and the stability of modern dyes.

The activated sludge processes, as well as their improved forms, are the most common treatment methods for textile industrial effluents. In most situations, the activated sludge process is combined with physical and chemical processes (Vandevivere *et al.*, 1998; Uygur and Kok, 1999). But Venceslau *et al.* (1994) and Willmott *et al.* (1998) found that the activated sludge process and its adapted variants, as well as combinations of this process with physical or chemical processes, are ineffective for the treatment of dyeing waste waters. In addition, most dyes are only adsorbed on the sludge but are not degraded by these processes (Konstantinou and Albanis, 2004; Sohrabi and Ghavami, 2008). So far, a considerable number of researches have been performed on the photocatalytic degradation of model dyes under UV or solar radiation. (Li and Zhang, 1996; Poulios and Tsachpinis, 1999; da Silva and Faria, 2003; Muruganandham *et al.*, 2006; Khataee *et al.*, 2010; Soutsas *et al.*, 2010; Gümüş and Akbal, 2011). However, there are relatively few studies regarding the photocatalytic degradation of real or simulated dyeing effluents (Pekakis *et al.*, 2006; Rupa *et al.*, 2011).

The combination of light and catalysts has proven very effective for water purification. Pal and Mazumdar (1974) investigated the photoreduction of methylene blue in the presence of various organic and bimolecular, spectrophotometrically, and potentiometrically. Also, Kang *et al.* (2003) treated the textile effluents by H₂O₂/ UV oxidation combined with reverse osmosis separation for reuse. Singh and Kulkarni (2012) observed 61% degradation of azo dyes in textile wastewater by photocatalytic treatment using aerioxide as a catalyst. Gümüş and Akbal (2011) conducted photodegradation experiments on textile wastewater and noticed that acidic conditions raised the percentage of degradation. They observed that at pH 3.0, 3 g/L catalyst loading, and 120 minutes of treatment time, the decolorization and degradation efficiencies for textile wastewater were 97.8% and 84.9 percent, respectively.

2.5.2 Advanced oxidation processes (AOPs):

Advanced Oxidation Processes (AOPs) are known as the processes involving the formation and use of relatively non-selective free hydroxyl radicals (OH^\bullet) in plentiful quantities to oxidize the majority of the non-biodegradable chemicals present in the effluent water (Gogate and Pandit, 2004; Ledakowicz *et al.*, 2001). After the fluorine radical, OH^\bullet radicals have the highest oxidation potential ($E^0 = 2.8 \text{ V}$) as compared to a normal hydrogen electrode (NHE). But, because of its high toxicity, fluorine cannot be used for wastewater treatment in spite of being the strongest oxidant (Oxidation potential, $E^0 = 3.06 \text{ V}$). For these reasons, most scientists and technology developers are interested in the generation of hydroxyl radicals including AOPs. The short mechanism of AOPs involves two steps: (a) the formation of hydroxyl radicals, (b) oxidative reaction of organic molecules by these radicals to convert them into smaller molecules like CO_2 and H_2O (Azbar *et al.*, 2005). The advantages of these processes over other chemical and biological processes is that they neither transfer pollutants from one phase to the other nor produce massive amounts of hazardous sludge (Lucarelli *et al.*, 2000; Annadurai *et al.*, 2003 and Ince *et al.*, 2000). Also, those involve ambient conditions, low expenses and low level of energy consumption during the process. There are two types of AOPs: (1) non-photochemical AOPs and (2) photochemical AOPs.

2.5.2.1 Non-photochemical AOPs

Examples of non-photochemical AOPs are (1) ozonation, (2) ozone /hydrogen peroxide, (3) Fenton process, (4) electrochemical oxidation, (5) supercritical water oxidation, (6) cavitation, (7) electrical discharge-based nonthermal plasma, (8) gamma-ray, (9) x-ray, and (10) electron beam etc. Among those, ozonation, ozone/ H_2O_2 , and Fenton process are frequently applied and examined processes for textile effluent treatment.

2.5.2.2 Photochemical AOPs

Photochemical AOPs include (1) vacuum UV photolysis, (2) UV/hydrogen peroxide, (3) UV/ozone, (4) UV/ozone/hydrogen peroxide, (5) photo-Fenton, etc. These are homogenous photochemical AOPs. In this class, there are heterogeneous AOPs also,

for example, photocatalysis, etc. Most of the complex chemicals present in effluents can be oxidized into simpler, non-toxic degraded products by AOPs (Galindo *et al.*, 2000; 2001). Kestioğlu *et al.* (2005) and Mandal *et al.* (2004) showed that the formation of highly reactive free radicals can be achieved by using $\text{TiO}_2/\text{H}_2\text{O}_2$, UV/O_3 , $\text{UV}/\text{H}_2\text{O}_2$, $\text{Fe}^{2+}/\text{H}_2\text{O}_2$, etc. Among these processes, heterogeneous photocatalysis was reported to be an emerging destructive technology that results in the complete mineralization of most organic contaminants (Guillard *et al.*, 2003). Azbar *et al.* (2004) reported that the heterogeneous photocatalytic oxidation processes have been extensively used in the literature for the degradation of dyes. Photocatalytic treatments are based on in situ generations of highly reactive hydroxyl radicals. According to Azbar *et al.* (2004), heterogeneous photocatalytic oxidation processes for dye degradation have been most commonly investigated by different researchers. Legrini *et al.* (1993) and Schivello (1997) observed that photolytically induced oxidation with ozone (UV/O_3) or hydrogen peroxide ($\text{UV}/\text{H}_2\text{O}_2$), known as homogeneous photocatalysis, was found to be expensive for industrial wastewater treatment. Pignatello *et al.* (2006) showed that use of metal salt Fe (II) as a Fenton's reagent needs pH control and results in sludge formation, which can cause waste disposal issues. Aleboyeh *et al.* (2003) observed that among the various AOPs heterogeneous photocatalysis with a metal oxide semiconductor as catalyst was found to be very effective for the degradation of organic pollutants and bio-resistant organic contaminants from industrial effluents. Gupta *et al.* (2012) stated that techniques such as Fenton's reagent oxidation UV photolysis, photocatalysis, and sonolysis can degrade organic pollutants at room temperature and pressure. The adaptability of AOPs lies in the fact that OH^\bullet radicals can be produced in a variety of ways. Kestioğlu *et al.* (2005) reported that AOPs have a number of distinct advantages over traditional treatment approaches, including the ability to remove non-biodegradable organic components and no residual sludge disposal problems.

Many researchers perform extensive investigation on the photodegradation of commercial dyes all over the world. Kansal *et al.* (2007) performed experiments in which they irradiated aqueous solutions of the dyes Methyl Orange and Reactive Green 6 and more than 90% decolorization was achieved by the photocatalyst, ZnO.

Each dye reacted differently to the photocatalytic system while the pH, catalyst doses, and dye concentration were varied (Teh and Mohamed, 2011). They discovered that incorporating foreign species into the TiO₂ matrix can boost up the catalyst's efficiency. The photocatalytic behavior of TiO₂ on the photodecomposition of methylene blue was studied, and it was observed that the degradation of MB varied from 80%-92% (Kasanen *et al.*, 2011 and Syoufian *et al.*, 2007). The study of Qamar *et al.* (2005a) reported that the photocatalytic decomposition of two dyes chomotrope 2 and Bandamido black 10B by TiO₂ is greatly affected by pH, catalyst doses, and reaction enhancer like H₂O₂. They suggested conducting more research using actual textile effluent to determine the best conditions for degradation. Bizani *et al.* (2006) published their results on the photodegradation of two industrial azo-dyes in the presence of TiO₂, as well as the efficacy of their system in actual textile effluent. They found that the color had been entirely removed within 6 (six) hours of treatment and parameters like pH, H₂O₂ doses etc. played an important role in enhancing the degradation.

Jain and Shrivastava (2008) reported that photodegradation of a dye named Cyanosine by TiO₂ is faster at a pH of 8, temperature of +30 °C, and in the presence of H₂O₂. Other research has found that UV-TiO₂ degradation of commercial dyes such as Rhodamine B, Acid Blue 40, Simple Yellow 15, Direct Blue 160, and Reactive Red 120 was successful under optimum conditions, but adding H₂O₂ had no significant effect on degradation percentages (Aguedach *et al.*, 2005; Kansal *et al.*, 2007). Other researchers reported that photodegradation of azo dyes like Reactive Yellow 145, Reactive Black 5 and Chrysoidine was effective at acidic conditions (Rupa *et al.*, 2011; Aguedach *et al.*, 2005; Tang and Chen, 2004). Qamar *et al.* (2005b) and Zayani *et al.* (2009), on the other hand, found kinetic dependency on catalyst loading, pH, and H₂O₂ loading. Bansal and Sud (2011) used TiO₂ and ZnO to study the photodegradation of Procion Blue dye from a real effluent and they claimed that ZnO was the more efficient catalyst at pH 7, which was the pH of industrial effluent discharge. Many researchers have investigated the photodegradation of organic and inorganic pollutants of dyes using photocatalysts such as TiO₂, ZnO, and H₂O₂ in the last two decades, and it is expected that photocatalysis will be the most successful

technique for treating textile wastewater in the future (Prieto *et al.*, 2005). However, there were conflicting reports on the suitability and efficiency of semi-conductors. Just a few studies were done on real textile wastewater, and the majority of the research works were done on an aqueous solution of the dyes prepared in laboratories. Again, sufficient knowledge about the semiconductors like TiO₂ and ZnO, or their combined effect on real textile waste water is still not gained.

According to Grzechulska and Morawski (2002) removal of color from effluent is sometimes more urgent than the removal of other organic colorless compounds. Alkhateeb *et al.* (2005) have reported that since TiO₂ and ZnO have strong photocatalytic properties, both catalysts have been suggested as potential substrates for photodegradation of industrial wastewater. Hence, the focus of this research was on the decolorization of selected textile effluents collected from local industries using TiO₂, ZnO, and Fe₂O₃ with UV light irradiation at constant temperature but at different pH. The main disadvantage that prevents this method from development is the need for a difficult and expensive filtration step to remove thin catalyst particles and to recycle those. Alternatively, some works immobilize catalysts on a suitable supporting material, such as quartz, silica, various forms of glass, ceramics, activated carbon, zeolites, glass fibers, stainless steel, etc. which eliminates the catalyst removal step (Lachheb *et al.*, 2002 and Guillard *et al.*, 2003).

2.6 Catalyst and photocatalyst

A catalyst is a material that can speed up or slow down a reaction by engaging in it but without being consumed. A photocatalyst is a material that uses light energy to produce catalytic activity. The key difference between them is that a traditional catalyst is activated by heat, while a photocatalyst is activated by photons of sufficient energy. The prefix "Photo" (phos: Light) and the word "Catalysis" make up the word photocatalysis, which is of Greek origin (Katalyo: brake apart, decompose). The term photocatalysis describes a process in which light is used to stimulate a substance for catalytic activity. Photocatalysts are specific materials which modify the rate of a reaction without being involved itself in chemical transformation using energy from any radiation (Kondarides, 2010).

The discovery of the Honda-Fujishima effect contributed to the realization of the semiconductor TiO₂'s oxidation and reduction ability as a photocatalyst. Photoinduced decomposition of water on TiO₂ electrodes was first reported by Fujishima *et al.* (1972). There has been a growing interest in environmental applications since Frank and Bard first explored the possibilities of using TiO₂ to decompose cyanide in water in 1977. TiO₂ has been successfully used to decompose recalcitrant pollutants in industrial wastewater in recent years. TiO₂ is a very effective photocatalyst due to its specific properties such as high photochemical and photocatalytic reactivity, insoluble nature, low cost, low toxicity, reusability, and photo-stability. (Yeber *et al.*, 2000; Fujishima *et al.*, 2000). ZnO is considered to be a suitable alternative to TiO₂ since its photo degradation mechanism is very similar to TiO₂ (Tang and Huang, 1995). ZnO is an n-type semiconductor and has a wide band gap of 3.37 eV compared to TiO₂ (E_{bg} anatase = 3.2 eV) and a large exciton binding energy of 60 meV, making it another attractive photocatalyst. ZnO has gotten a lot of attention because of its high photosensitivity and capability to generate sufficient quantity of hydroxyl radicals by which various pollutants can be degraded. Furthermore, some research reports have shown that ZnO is more effective than TiO₂. The most important advantage of ZnO over TiO₂ is that it absorbs a greater portion of the solar spectrum (Behnajady *et al.*, 2006; Khodja *et al.*, 2001; Lizama *et al.*, 2002; Gouvea *et al.*, 2000). Besides, many compounds of iron like Fe(III) oxides (α -Fe₂O₃, γ -Fe₂O₃ etc.), oxyhydroxides (α -FeOOH, β -FeOOH, and γ -FeOOH) have also drawn attention to the scientists for their special photocatalytic properties to oxidize organic pollutants (Leland and Bard, 1987). Many research on the photochemical properties and potential applications of various Fe(III) species have been performed over the last 50 years.

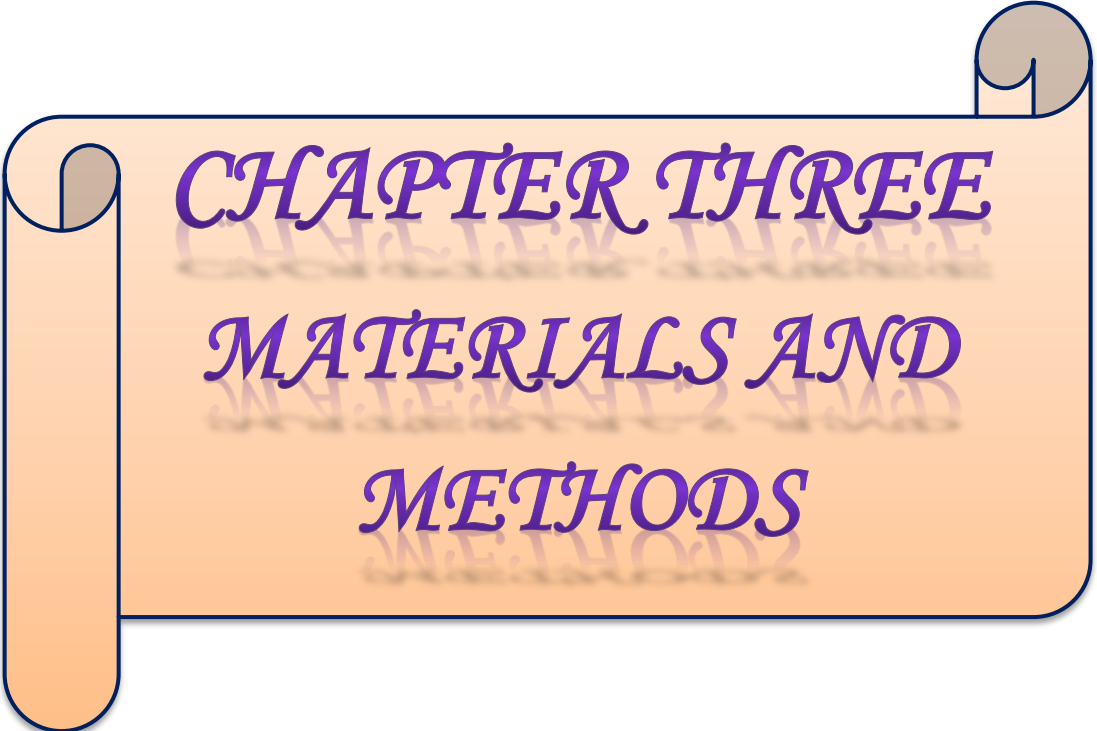
2.7 Factors affecting photodegradation efficiency

The oxidation rates and performance of photocatalytic degradation processes are highly dependent on a variety of operational parameters. The significance of these operational parameters has been mentioned in several studies. Kumar and Pandey (2017); Reza *et al.* (2017) and Gnanaprakasam *et al.* (2015) discussed the factors affecting the degradation performance of photocatalysts. These include effects of type of catalysts, catalyst loading, pH, reaction temperature, dye concentration, nature of pollutants, inorganic ions, light source, size and structure of the photocatalyst, H₂O₂ concentration, and doping etc.

2.8 Degradation of textile effluent by photocatalysts

Many scientists have attempted to investigate the photocatalytic behavior of various semiconductors such as TiO₂, SnO₂, CdS, ZnO, and so on. (Vinodgopal and Kamat, 1995; Neppolian *et al.*, 2002a; Lathasree *et al.*, 2004; and Akyol *et al.*, 2004). For some commercial azo-dyes, ZnO is reported appropriate and for some, TiO₂ (Daneshvar *et al.*, 2003). Photocatalytic degradation of various dye groups has been a subject of research and is stated by many researchers (Poulios and Tsachpinis, 1999 and Yang *et al.*, 2004). Factors influencing the degradation rate of aqueous systems have been studied such as the effect of pH, initial dye concentration, catalyst loading, oxidizing agent dose, UV intensity, etc. The experimental results of Ram *et al.* (2012) indicated that at optimum conditions (100 ppm dye, pH 7.8, TiO₂ dose 0.5g/L, UV strength 25 W/m², and period 3.5h), 83.6 % of the reactive Procion Yellow dye was degraded. In the presence of UV light and at natural pH, the solar photocatalytic method appears to be a suitable alternative to TiO₂.

The majority of the experiments were performed on an aqueous solution of dyes widely used in textile dyeing industries, with only a few studies conducted on actual textile effluents. In Bangladesh's rapidly developing economy, the textile and clothing industries provide a single source of growth. With the expansion of these industries, environmental pollution has also increased by their effluents up to an alarming level. Although photocatalytic decomposition is an advanced and effective technology for the control of non-biodegradable pollution caused by textile effluents, the technology is not so familiar in Bangladesh as well as the use of this technology has not yet been practiced by textile mills and other industries here. Moreover, there is no research work so far has been reported on the treatment techniques as well as photocatalytic degradation of textile effluents in the country. There is no research study on silk textile dyeing effluents of the BSCIC industrial area, Rajshahi, and cotton textile dyeing effluents of Shirajgang area in particular. The present research work focused on the photocatalytic decomposition of selected textile industrial effluents using TiO₂, ZnO, and Fe₂O₃ as catalysts. The materials and methods of the study are discussed in the next chapter.



CHAPTER THREE
MATERIALS AND
METHODS

MATERIALS AND METHODS

The materials used for the present study and the methods adopted for carrying out the experimental work is discussed in this chapter. The effluents samples were collected, analyzed, and treated using photocatalytic degradation in the laboratory through experiments. The effluents sample analysis results were compared with the industrial wastewater discharge quality standard. This research work was carried out at the Water Resource Lab in the Institute of Environmental Science (IES), University of Rajshahi, Bangladesh. Some physicochemical parameters of the textile effluents were analyzed in the Central Science Laboratory, University of Rajshahi, BCSIR Lab of Rajshahi, and Dhaka, Bangladesh. All experiments were performed very carefully with three replicates using the standard methods of analysis. The study analyzed the effluent samples before and after the treatment using several analytical methods, including gravimetric, colorimetric, and spectrophotometric. The detailed analytical techniques of effluent samples and the data were analyzed in this study are discussed in this chapter.

3.1 Study area

Two effluent samples were collected from Bangladesh Small and Cottage Industries Corporation (BSCIC) industrial area, Rajshahi is Bangladesh's fourth-largest city, situated between 24°21' and 24°25' north latitudes and 88°32' and 88°40' east longitudes. The city is surrounded by two large rivers, the Padma and the Barnai. The Padma runs along the city's southern side, and the Barnai is about 6 kilometers away on the city's northern edge. The wastewater generated in the city area falls either directly in the Padma or Barnai river through some open channels via the Beels. Thus, the Padma and the Barnai are directly polluted by the wastewaters of the city. The BSCIC industrial estate is situated at Sapura, 2 km away from the north of downtown Rajshahi City and very closed to the Rajshahi Cantonment. about 191 industries of various kinds such as silk, dyeing, plastic, chemicals, textile, aluminum, biscuit and bread factories, automobile workshop, etc. are situated here occupying 96.63 acre land. The textile dyeing industries of BSCIC, Rajshahi consume huge quantities of

Chapter Three : Materials and Methods

water and produce large volumes of wastewater in different steps during the dyeing and printing process, which ultimately falls in the Padma or Barnai River.

The place Pipulbaria is situated in Sadar Upazila of Sirajganj District. Its geographical coordinates are $23^{\circ} 44' 0''$ north, $89^{\circ} 26' 0''$ east. The effluent collected from this location was from a cotton yarn dyeing industry. There are many textile dyeing industries in this area. These industries generate large amounts of effluents every day which are being disposed into the surrounding areas, agricultural fields, irrigation channels, and surface water, ultimately entering the river Jamuna. As a result, a significant number of villagers in Sirajganj district are now at risk due to pollution.

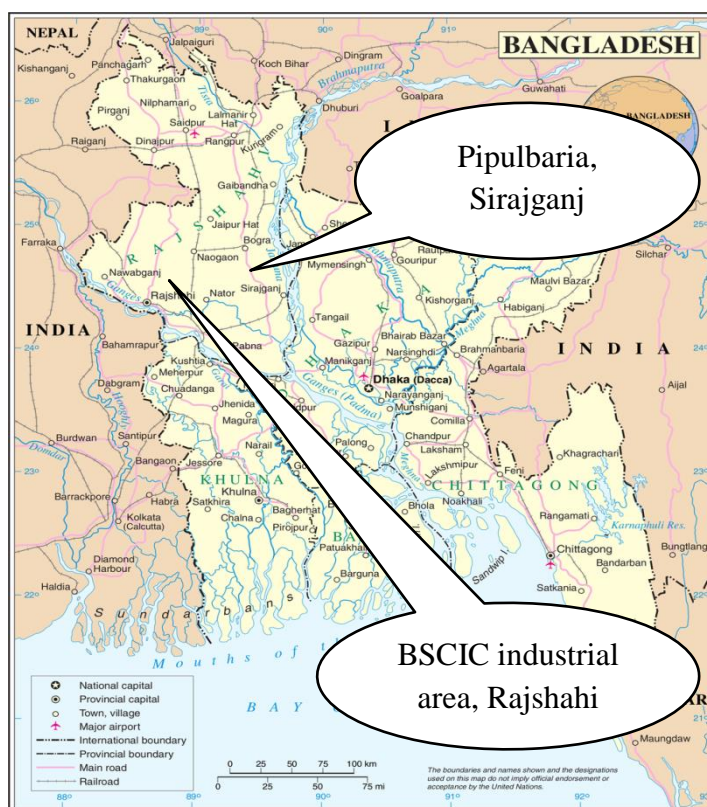


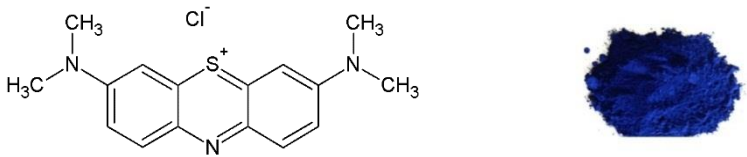
Figure 3.1 Study Area

3.2 Sample types

Mainly two types of samples were used for this study, viz., (1) synthetic dye effluent sample and (2) textile dyeing effluent samples. This research was mainly related to examine the photocatalytic decomposition of real textile dyeing effluents. But before the experiment with real effluents, a synthetic dye solution was studied for

photocatalytic decomposition to gather knowledge and experience on the research work. To prepare synthetic dye effluent methylene blue was chosen which is a cationic dye and is categorized as one of the dyes in the textile industry, which contaminates the aquatic environment. It is a heterocyclic aromatic chemical compound with a molecular formula $C_{16}H_{18}N_3S$ and a molecular weight of 319.85 g/mol. The chemical structure and physical properties of methylene blue are given in Table 3.1. A total of three textile dyeing effluent samples were collected, two of them were from the two silk industries of the BSCIC industrial area, Rajshahi, and the other was from a cotton yarn dyeing industry, Pipulbaria, Sirajganj.

Table 3.1 Main characteristics of methylene blue

Name of dye	Methylene Blue
Synonym	Methylthionine chloride
IUPAC	3,7-bis(dimethylamino)phenothiazin-5-ium chloride or, [7-(dimethylamino)phenothiazin-3-ylidene]-dimethylazanum;chloride
Colour index	C.I. 52015
Molecular formula	$C_{16}H_{18}ClN_3S$.
Molecular weight	319.851 g/mol
λ_{max}	662, 614, and 292 nm
Structure	

3.3 Sample collection

Three textile industrial collected samples were named Silk Industry Effluent, Rajshahi-1 (SIER-1), Silk Industry Effluent, Rajshahi-2 (SIER-2), and Yarn Dyeing Industry Effluent, Sirajganj (YDIES) respectively. These effluent samples were collected separately in 5 liter PET plastic bottles, which were pre-washed with dilute HCl and rinsed three to four times with distilled water. Wastewater was taken directly from the outlet of those industries. As the effluents were colored and measurement of color was one of the major experimental parameters, the effluent samples were wrapped in aluminum foil paper so that they could not be naturally degraded slowly

by light. Samples were labeled, sealed, and transported to the laboratory and stored in a cold and dry place until the experiments were done. These were analyzed according to the standard procedures stated in the American Public Health Association (APHA, 2017). In some cases, the samples were filtered to remove suspended impurities and foreign matters. Some of the effluents were very much concentrated and were not feasible for photocatalytic degradation experiments. The effluents were appropriately diluted with distilled water to use for a particular purpose.

3.4 Sample analysis

The analyzed physicochemical parameters for these effluent samples included pH, EC, DO, TDS, TSS, COD, BOD, TOC, heavy metals, and anions. To prevent further contamination, EC, pH and DO were determined immediately after the samples were obtained. TDS, TSS, COD, and BOD were determined according to the methods, which are discussed below. To ensure accuracy and consistency, all experiments were performed in triplicate, and all reagents used in this analysis were analytical grade chemicals.

3.4.1 pH, EC, and DO

pH, EC, DO were measured by pH meter and EC meter (EC-210, HANNA, Italy), DO meter respectively just after sample collection.

3.4.2 Total suspended solids (TSS)

At first, a Whatman 42 filter paper was dried in an oven at 105°C for 24 hours and then allowed to cool and weighed. Then 100 mL of effluent sample was filtered through the oven-dried filter paper, and it was allowed to dry in an oven at 105°C for 24 hours. Then the filter paper was cooled and weighed. The cooling and heating process was repeated until a constant weight was obtained.

$$\text{Total Suspended Solids (TSS, mg/L)} = \frac{(A - B) \times 1000000}{V}$$

Where,

A= final weight of filter paper (after filtration) in gram

B = initial weight of filter paper (before filtration) in gram

V = volume (mL) of water sample taken = 100mL

3.4.3 Total dissolved solids (TDS)

At first, a 150 mL Pyrex beaker was taken and dried in an oven at 105°C for 24 hours. Then it was allowed to cool and weighed. 100 mL of effluent sample was filtered through an oven-dried Whatman 42 filter paper into the above beaker and evaporated to dry at 105°C for 24 hours. Then the beaker was allowed to cool and its weight was recorded. The heating and cooling process was repeated until a constant weight was obtained.

$$\text{Total Dissolved Solids (TDS, mg/L)} = \frac{(A - B) \times 1000000}{V}$$

Where,

A = final weight of beaker (after filtration) in gram

B = initial weight of beaker (before filtration) in gram

V = volume (mL) of water sample taken = 100mL

3.4.4 Determination of biochemical oxygen demand (BOD₅)

BOD is the most common and widely used test for evaluating the amount of organic matter in wastewater samples. BOD is based on the principle that if there is adequate oxygen, aerobic biological decomposition (i.e., the stabilization of organic waste) by microorganisms will occur until all of the waste has been consumed. The BOD test is also known as the "BOD₅" test because it is based on a precise calculation of DO (dissolved oxygen) at the start and end of a five-day period in which the sample is held in dark, incubated conditions (i.e., 20°C or 68°F).

Apparatus and reagents:

- a. BOD₅ bottles (glass-stoppered bottles)
- b. BOD₅ incubator having temperature control at 20 °C.
- c. Phosphate buffer: Dissolve 0.85 g KH₂PO₄, 2.175g K₂HPO₄, 3.34g Na₂HPO₄. 7H₂O, and 0.17 g NH₄Cl in distilled water to prepare 100 mL solution.
- d. Magnesium sulfate solution: 8.25 g MgSO₄.7H₂O/ 100 mL.

Chapter Three : Materials and Methods

e. Calcium chloride solution: 2.75g anhydrous CaCl₂ /100 mL.

f. Ferric chloride solution: 0.025g FeCl₃.6H₂O/100 mL.

Procedure:

(i) Bubble compressed air in distilled water for 30 minutes- this is then called dilution water.

(ii) In a liter of dilution water add 1c.c. each of phosphate buffer, MgSO₄, CaCl₂, and FeCl₃ solution and mix well.

(iii) Neutralize the water sample to pH 7.

(iv) The dissolved oxygen of the sample may not be sufficient for the oxidation of biologically degradable organic matter so that the sample is mixed with a known volume of dilution water which is rich in oxygen.

(v) Carry out dilution in a large trough or bucket and mix well.

(vi) Fill two sets I and II of BOD₅ bottles.

(vii) Determine the dissolved oxygen in the sample bottles of the set I immediately

(viii) Determine the dissolved oxygen in the sample bottles of the set II after keeping the bottles in a BOD₅ incubator at 20 C for 5 days.

Calculation:

$$\text{BOD}_5, \text{ mg/L} = (D_0 - D_5) \times \text{dilution factor}$$

Where, D_0 = concentration of the dissolved oxygen in the sample.

D_5 = concentration of the dissolved oxygen after incubation for 5 days.

3.4.5 Determination of chemical oxygen demand (COD)

Chemical Oxygen Demand (COD) means the amount of oxygen required for the oxidation of oxidizable organic matter by a strong oxidizing agent. For COD determination, potassium dichromate in presence of H₂SO₄ is generally used as an oxidizing agent. The water sample is refluxed with K₂Cr₂O₇ and concentrated H₂SO₄

Chapter Three : Materials and Methods

in presence of HgSO_4 and Ag_2SO_4 (catalysts). The residual dichromate is titrated back with a standard solution of ferrous ammonium sulfate using ferroin as an indicator.

Reagents:

- a. 0.25 N $\text{K}_2\text{Cr}_2\text{O}_7$: 6.125g of dried $\text{K}_2\text{Cr}_2\text{O}_7$ was dissolved in distilled water and made up the volume to 500 mL.
- b. 0.1N ferrous ammonium sulfate: The solution was standardized with standard $\text{K}_2\text{Cr}_2\text{O}_7$ solution.
- c. Ferroin indicator solution: 1.485g of 1,10 -phenanthroline and 0.695g of ferrous sulfate were dissolved in distilled water and diluted to make 100 ml solution.
- d. Concentrated H_2SO_4 (sp. gr. 1.84).
- e. Solid HgSO_4 and Ag_2SO_4 .

Procedure:

- (i) Introduce 20 mL of the water sample in a 250 mL round bottom flask with a ground glass joint for fixing a reflux condenser.
- (ii) Add 10 mL of 0.25 N $\text{K}_2\text{Cr}_2\text{O}_7$, a pinch of HgSO_4 , and Ag_2SO_4 and 20 mL of H_2SO_4 . Reflux for 2-3 hours.
- (iii) Cool, dilute, and titrate with 0.1N ferrous ammonium sulfate solution using ferroin as indicator until color changes from blue to red.
- (iv) Run a blank also.

Calculation:

$$\text{COD, (mg/L)} = \frac{(A-B) \times N \times 1000 \times 8}{V}$$

Where,

A = Volume of ferrous ammonium sulfate for blank, mL

B = Volume of ferrous ammonium sulfate for sample, mL

N= normality of ferrous ammonium sulfate used.

V= volume of the sample taken, mL

3.4.6 Estimation of heavy metals

The concentration of major heavy metals like Cr, Mn, Fe, Cd, Zn, and Pb in the textile effluents was analyzed by an Atomic Absorption Spectrophotometer (AAS, Model: Shimadzu AA-6800). The detailed procedures are described below:

Sample preparation:

A 75 mL effluent sample was taken in a 250 mL beaker and added 2 mL of concentrated HNO₃ and 3 mL of concentrated HCl to it and then mixed well. The beaker was heated at 90-95°C in an oven until the volume was reduced to 10-15 mL. Then, it was removed from the oven and allowed to cool. Finally, the volume was made up to 20 mL with distilled water. This mixture was then analyzed by AAS for the determination of heavy metals already mentioned.

3.4.6.1 Iron (Fe)

Apparatus: AAS wavelength at 248.3 nm with 0.7 nm slit.

Reagent:

1000 mg/L standard solution of iron ion was prepared by exactly taking 4.980 g of analytically pure (99%) FeSO₄ · 7H₂O in a 1000 mL volumetric flask and then added distilled water slowly and shaken well and finally made up to the mark with distilled water.

Standard curve:

The proportions of 0.5, 1.0, and 2.0 mL Fe ion contained standard solutions were taken in three different 1000 mL volumetric flasks and gradually added distilled water and thoroughly shaken, and finally made up to the mark with distilled water. The absorbance of the water samples was determined by an AAS. A standard curve was made by plotting the absorbance against the concentration (Figure 1.3 in Appendix-1).

Calculation:

Iron (Fe, mg/L) = Concentration of Fe (mg/L) from standard curve × dilution factor.

3.4.6.2 Chromium (Cr)

Apparatus: AAS wavelength at 248.3 nm with 0.7 nm slit.

Reagents:

a. 1000 mg/L standard solution

The standard solution for chromium ion was prepared by exactly taking 2.8290 g of analytically pure potassium dichromate ($K_2Cr_2O_7$) in a 1000 mL volumetric flask. Then 5 ml of sulfuric acid was added to it and added slowly distilled water and shaken well and finally made up to the mark with distilled water.

b. Chromium standard solution corresponding to 10 mg/L of chromium

10 ml of the chromium stock solution was taken into a 1000 ml volumetric flask by pipette. 20 ml of nitric acid was added, filled to the mark with water, and mixed well.

c. Chromium standard solution corresponding to 0.4 mg/L of chromium

A 20 ml of the chromium standard solution was taken into a 500 ml volumetric flask by pipette. 10 ml of nitric acid was added, filled to the mark with water, and mixed well. This solution was prepared on the day of use.

Standard curve:

The proportions of 0.5, 1.0, and 2.0 mL Cr ion contained standard solutions were taken in three different 1000 mL volumetric flasks and gradually added distilled water and thoroughly shaken, and finally made up to the mark with distilled water. The absorbance of the water samples was determined by an AAS. A standard curve was made by plotting the absorbance against the concentration (Figure 1.1 in Appendix-1).

Calculation:

Chromium (Cr, mg/L) = Conc. of Cr (mg/L) from standard curve \times dilution factor.

3.4.6.3 Manganese (Mn)

Apparatus: AAS wavelength at 279.48 nm with 0.2 nm slit.

Reagent:

A 1000 mg/L standard solution of manganese ion was prepared by exactly taking 3.070 g of analytically pure (99%) $\text{MnSO}_4 \cdot 10\text{H}_2\text{O}$ in a 1000 mL volumetric flask, and added distilled water slowly and shaken well. Finally, it was made up to the mark with distilled water.

Suppressing agent:

The solution of 2% calcium was prepared by exactly taking 2 g of CaCO_3 in a 100 mL volumetric flask, and added 3mL of 1M HCl to it. Then it was dissolved by distilled water slowly, made up to the mark with distilled water gradually, and shaken well. Then 10 mL of 2% CaCO_3 solution was taken and diluted to 100 mL with distilled water to make the final concentration of 0.2% CaCO_3 . This solution was used for maintenance in every standard and sample.

Standard curve:

The proportions of 1.0, 3.0, and 5.0 mL Mn ion contained standard solutions were taken in three different 1000 mL volumetric flasks, and distilled water was gradually added, and thoroughly shaken, and finally made up to the mark with distilled water. The absorbance of the water samples was determined by an AAS. A standard curve was made by plotting the absorbance against the concentration (Figure 1.2 in Appendix-1).

Calculation:

Manganese (Mn, mg/L) = Concentration of Mn (mg/L) from standard curve \times dilution factor.

3.4.6.4 Cadmium (Cd)

Apparatus: AAS wavelength at 228.80 nm with 0.7 nm slit.

Reagent:

A 1000 mg/L standard solution of manganese ion was prepared by exactly taking 2.282 g of analytically pure (99%) $3\text{CdSO}_4 \cdot 8\text{H}_2\text{O}$ in a 1000 mL volumetric flask, and

added distilled water slowly and shaken well. Finally, it was made up to the mark with distilled water.

Standard curve:

The proportions of 0.1, 0.2, and 0.4 mL Cd ion contained standard solutions were taken in three different 1000 mL volumetric flasks, and distilled water was gradually added and thoroughly shaken, and finally made up to the mark with distilled water. The absorbance of the water samples was determined by AAS. A standard curve was made by plotting the absorbance against the concentration (Figure 1.7 in Appendix-1).

Calculation:

Cadmium (Cd, mg/L) = Concentration of Cd (mg/L) from standard curve × dilution factor.

3.4.6.5 Zinc (Zn)

Apparatus: AAS wavelength at 213.86 nm with 0.7 nm slit.

Reagent:

1000 mg/L standard solution of zinc ion was prepared by exactly taking 4.980 g of analytically pure (99%) ZnSO₄ ·7H₂O in a 1000 mL volumetric flask, and added distilled water slowly, and shaken well. Finally, it was made up to the mark with distilled water.

Standard curve:

The proportions of 0.1, 0.2, and 0.4, mL Zn ion contained standard solutions were taken in three different 1000mL volumetric flasks, and distilled water was gradually added and thoroughly shaken, and finally made up to the mark with distilled water. The absorbance of the water samples was determined by AAS. A standard curve was made by plotting the absorbance against the concentration (Figure 1.6 in Appendix-1).

Calculation:

Zinc (Zn, mg/L) = Concentration of Zn (mg/L) from standard curve × dilution factor.

3.4.6.6 Lead (Pb)

Apparatus: AAS wavelength at 283.31 nm with 0.7 nm slit.

Reagent:

1000 mg/L standard solution of lead ion was prepared by exactly taking 1.599 g of analytically pure (99%) $\text{Pb}(\text{NO}_3)_2$ in a 1000 mL volumetric flask, and added distilled water slowly and shaken well. Finally, it was made up to the mark with distilled water.

Standard curve:

The proportions of 2.5, 5, and 10 mL Pb ion contained standard solutions were taken in three different 1000mL volumetric flasks, and distilled water was gradually added and thoroughly shaken, and finally made up to the mark with distilled water. The absorbance of the water samples was determined by AAS. A standard curve was made by plotting the absorbance against the concentration (Figure 1.8 in Appendix-1).

Calculation:

Lead (Pb, mg/L) = Concentration of Pb (mg/L) from standard curve \times dilution factor.

3.4.6.7 Copper (Cu)

Apparatus: AAS wavelength at 324.75 nm with 0.7 nm slit.

Reagent:

1000 mg/L standard solution of copper ion was prepared by exactly taking exactly 3.93 g of analytically pure (99%) $\text{CuSO}_4 \cdot 5\text{H}_2\text{O}$ in a 1000 mL volumetric flask, and added distilled water slowly and shaken well. Finally, it was made up to the mark with distilled water.

Standard curve:

The proportions of 0.5, 1.0, and 2.0 mL Cu ion contained standard solutions were taken in three different 1000 mL volumetric flasks, and gradually added distilled water and thoroughly shaken, and finally made up to the mark with distilled water. The absorbance of the water samples was determined by an AAS. A standard curve

was made by plotting the absorbance against the concentration (Figure 1.5 in Appendix-1).

Calculation:

Copper (Cu, mg/L) = Concentration of Cu (mg/L) from standard curve × dilution factor.

3.4.7 Estimation of major anions

3.4.7.1 Chloride ion (Cl⁻)

The chloride ion (Cl⁻) in the effluent samples was determined using the AgNO₃ titration method, which was as follows:

Reagents:

- a. K₂CrO₄ indicator and 0.0141N AgNO₃.
- b. **Preparation of 5% K₂CrO₄ indicator:** 5g K₂CrO₄ was taken in a 100 mL volumetric flask, and dissolved by 50 mL distilled water. Then 0.0141N AgNO₃ was added drop-wise in the K₂CrO₄ containing volumetric flask until the first permanent red precipitate was produced. The solution was filtered, diluted by distilled water slowly and finally made up to the mark.
- c. **Preparation of 0.0141N AgNO₃:** 2.397g of AgNO₃ was weighed out, transferred to a 1000 mL volumetric flask, and made up to the mark with distilled water gradually. The resulting solution was 0.0141 N. The solution was standardized against NaCl. Reagent-grade NaCl was dried overnight and cooled at room temperature. 0.25 g portions of NaCl were weighed into Erlenmeyer flasks and it was dissolved by distilled water. Finally, it was diluted up to mark of 100 mL by distilled water. To adjust the pH of the solutions, small quantities of NaHCO₃ were added until effervescence ceased. About 2 mL of K₂CrO₄ was added and the solution was titrated to the first permanent appearance of red K₂CrO₄.

Procedure:

At first 100mL of effluent sample was filtered and taken in a 250 mL conical flask. 1 mL of K₂CrO₄ indicator was added to the flask and shaken slowly. Then the sample

was titrated with 0.0141 N AgNO₃ until the brick red color was arrived indicating the endpoint. The volume of 0.0141N AgNO₃ used for titration was noted.

Calculation:

$$\text{Chloride (Cl}^-, \text{ mg/L)} = \frac{(A \times N)}{V} \times 35450$$

Where, A = mL of 0.0141N AgNO₃ used for titration from burette

N = normality of AgNO₃ = 0.0141N

V = volume of water sample taken = 100 mL

3.4.7.2 Nitrate ion (NO₃⁻)

The nitrate ion (NO₃⁻) in the effluent sample was determined using a UV spectrophotometric method, which is described below:

Apparatus: UV-Spectrophotometer wavelength at 220 and 275 nm silt with matched silica cells of 1 cm.

Reagents:

- a. Nitrate-free water:** Double distilled water was used to prepare all solutions and dilutions.
- b. Stock nitrate solution:** Potassium nitrate (KNO₃) was dried in an oven at 105°C for 24 hours. 0.7218 g KNO₃ was weighed out and it was transferred to a 1000 mL volumetric flask, and made up to the mark with distilled water gradually, where 1 mL = 100 µg NO₃-N.
- c. Intermediate nitrate solution:** 100 mL stock nitrate solution was taken in a 1000mL volumetric flask, and distilled water was added gradually and finally made up to the mark where 1 mL = 10 µg NO₃-N. 2 mL CHCl₃ was used per litter solution to preserve it for at least 6 months.
- d. 1N Hydrochloric acid (HCl) solution:** 83 mL of concentrated HCl was measured and transferred to in a 1000mL volumetric flask and finally made up to the mark 1000 mL by distilled water gradually.

Procedure:

- i. Treatment of sample:** 1 mL of 1 N HCl solution was mixed thoroughly in 50 mL clear sample and filtered.
- ii. Preparation of standard curve:** The proportions of 0.50, 1.0, and 2.0 mL intermediate nitrate solutions were taken in three different 1000mL volumetric flasks, and distilled water was gradually added and thoroughly shaken, and finally made up to the mark by distilled water. The absorbance of the water samples was determined by a UV Spectrophotometer. A standard curve was made by plotting the absorbance against the concentration (Figure-2.1 in Appendix-2).
- iii. Spectrophotometric measurement:** The absorbance was read against distilled water set zero absorbance. A wavelength of 220 nm was used to obtain NO_3^- reading and a wavelength of 275 nm used to determine interference due to dissolved organic matter.

Calculation:

The estimation of $\text{NO}_3\text{-N}$ was measured using a UV-Spectrophotometer at two wavelengths i.e., 275 and 220. The absorbance for samples and standard solutions were taken at two wavelengths and the absorbance reading at 275nm was subtracted from the reading at 220nm for each sample and standard solution.

$$\text{Nitrate-Nitrogen (NO}_3\text{-N mg/L)} = \frac{\mu\text{gNO}_3\text{-N from standard curve}}{\text{Volume (mL) of sample taken}}$$

$$\text{Nitrate (NO}_3^- \text{ mg/L)} = (\text{NO}_3\text{-N}) \times 4.429$$

3.4.7.3 Bicarbonate ion (HCO_3^-)

The bicarbonate ion (HCO_3^-) in the effluent samples was determined using the titration method, which is described below:

Reagents: Phenolphthalein indicator, methyl orange indicator and 0.1N HCl.

Procedure:

100 mL of effluent sample was taken in a 250 mL conical flask and 2 drops of methyl orange indicator was added and shaken gradually. The sample was then titrated with

0.1N HCl until the color changed to orange, which indicated the endpoint. The volume (mL) of the acid 0.1N HCl from the burette used for the titration was noted.

Calculation:

$$\text{Bicarbonate ion (HCO}_3^- \text{, mg/L)} = \frac{A \times N \times 1000 \times 50}{V}$$

Where, A = ml of HCl used for titration with methyl orange indicator

N = normality of HCl = 0.1N HCl

V = volume of water sample taken = 100mL

3.4.7.4 Sulfate ion (SO₄²⁻)

The sulfate ion (SO₄²⁻) in the effluent samples was determined using a UV spectrophotometric method, which is described below:

Apparatus: UV-Spectrophotometer wavelength at 420 nm silt.

Reagent:

- a. Buffer solution:** The solution of buffer was prepared by taking exactly 30g of MgCl₂.6H₂O, 5g sodium acetate (CH₃COONa.3H₂O), 0.111g sodium sulfate (Na₂SO₄) and 20 mL acetic acid in a 1000 mL volumetric flask. Then it was dissolved with the distilled water and shaken well. Finally, it was made up to the mark with distilled water.
- b. Barium chloride:** BaCl₂ crystal 20 to 30 mesh was used to made uniform turbidity.
- c. Standard sulfate solution:** The standard sulfate solution was prepared by weighed out exactly 0.1479g anhydrous Na₂SO₄ and it was taken in a 1000 mL volumetric flask. Then it was dissolved with the distilled water and shaken well. Finally, it was made up to the mark with distilled water, where 1 mL = 100 μg sulfate (SO₄²⁻).

Procedure:

- i. Formation of barium sulfate turbidity:** 100 mL effluent sample was taken in a 250 mL Erlenmeyer flask and 20 mL buffer solution was added and mixed with

stirring apparatus. At the time of stirring a spoonful of BaCl_2 crystals was added and the solution was stirred for 1 minute.

ii. Measurement of turbidity: After stirring solution was poured in absorption cell and turbidity was measured within 5 minutes.

iii. Preparation of standard curve: The proportions of 2, 4, 6, 8, and 10 mg/L of Na_2SO_4 solutions were taken in four different 1000 mL volumetric flasks, and distilled water was gradually added and thoroughly shaken, and finally made up to the mark with distilled water. The absorbance of the water samples was determined using a UV Spectrophotometer. A standard curve was made by plotting the absorbance against the concentration (Figure-2.2 in Appendix-2).

Calculation:

Sulfate (SO_4^{2-} , mg/L) = Concentration of SO_4^{2-} (mg/L) from standard curve \times dilution factor.

3.4.7.5 Phosphate ion (PO_4^{3-})

The phosphate ion (PO_4^{3-}) in the effluent samples was determined using a UV spectrophotometric method, which is described below:

Reagent:

a. Ammonium metavanadate (NH_4VO_3) solution: 2.5 g of – was taken in a 1000 mL volumetric flask in which 20 mL of concentrated HNO_3 was added. After filtration the mixture was diluted with distilled water and it was made up to the mark.

b. Ammonium heptamolibdate solution: 5g of $(\text{NH}_4)_6\text{Mo}_7\text{O}_{24}\cdot 4\text{H}_2\text{O}$ was taken in a 100 mL volumetric flask and diluted up to the mark with distilled water.

c. Sulphuric Acid: 1:6 H_2SO_4 was prepared and kept in a glass bottle.

d. Standard phosphate solution: Exactly 0.4391g KH_2PO_4 was taken in a 100 mL volumetric flask and dissolved in distilled water through continuous shaking and finally made up to the mark with distilled water. 10 mL of this solution was transferred to a 100 mL volumetric flask, and made up to the mark with distilled water (here, 1 mL solution = 100 mg PO_4^{3-}).

Procedure:

Standard curve:

A proportion of 0.5, 1, 2, 4, and 8 mL intermediate phosphate solutions were taken in 5 separate 100 mL volumetric flasks. Distilled water was added to the flasks gradually and thoroughly shaken, and finally made up to the mark. 2 mL standard sample, 5 mL NH_4VO_3 solution, 5 mL $(\text{NH}_4)_6\text{Mo}_7\text{O}_{24}\cdot 4\text{H}_2\text{O}$ solution and 5 mL H_2SO_4 were taken in a 50 mL volumetric flask. The absorbance was read against distilled water previously set at zero absorbance. A wavelength of 450 nm was used to obtain PO_4^{3-} ion absorbance. (A standard curve was made by plotting the absorbance against the concentration (Figure-2.3 in Appendix-2))

Calculation:

Phosphate (PO_4^{3-} , mg/L) = Concentration of PO_4^{3-} (mg/L) from standard curve \times dilution factor.

3.4.8 Determination of total organic carbon (TOC)

Total Organic Carbon (TOC) is a simple method for detecting organic carbon and expressing the amount of carbon detected. It is a non-specific method unable to distinguish between various organic species and only indicates that organic carbon compounds are present.

Principle and procedure of the method

In the present study standard methods 5310 B was used for TOC determination, which describes the procedure and requirements for analysis by high-temperature catalytic oxidation (HTCO) with non-dispersive infrared (NDIR) detection. Inorganic carbons (the carbonate, bicarbonate and dissolved CO_2) are always present in any water sample. In most water samples, the inorganic carbon fraction is many times greater than the organic carbon fraction. Eliminating or compensating for inorganic carbon interferences is essential for determinations of both TC and TOC. The half of the sample is injected into a chamber where it is acidified to turn all of the inorganic carbon into CO_2 . This is then sent to a detector for measurement of total IC. The other half of the sample is injected into a combustion chamber which is combusted at high

temperature. Here all the carbon reacts with oxygen, forming CO₂. It's then flushed into a cooling chamber and finally into a detector for total carbon measurement. Here the sample is homogenized and diluted as necessary, and a micro portion is injected into a heated reaction chamber packed with an oxidative catalyst such as cobalt oxide, platinum catalyst or barium chromate. Water vaporizes, and organic carbon compounds are oxidized to CO₂ and H₂O. The CO₂ is transported in the carrier-gas stream and is measured by means of a non-dispersive IR analyzer. By Subtracting total inorganic carbon from total carbon, the amount of total organic carbon is determined.

3.5 Photocatalytic treatment of effluent samples

The photocatalytic decomposition efficiency of three photocatalysts TiO₂, ZnO, Fe₂O₃, and their combination on methylene blue and three real effluents under UV irradiation was assessed. The effects of various process parameters were analyzed so that those can be optimized. The decomposition efficiency of the photocatalysts was measured in terms of decrease in effluent concentration, which was determined spectrophotometrically.

3.5.1 Variable parameters

The effects of variation of the following parameters on the photocatalytic decomposition of the effluents were studied:-

1. Initial dye solution concentration
2. Catalyst type
3. Reaction time
4. pH
5. Catalyst dose
6. Oxidizing agent dose

3.5.2 Photocatalytic reactor

A photocatalytic reactor was designed to perform catalytic degradation experiments in a wooden chamber equipped with a 15w UV light (model-PHILIPS TUV 15W G15 T8 UVC) as an illumination source. The size of the box was 4 feet long, 2.5 feet high

and 2 feet wide. The degradation process was carried out in a 250 mL glass beaker kept on a magnetic stirrer inside the UV-chamber. The magnetic stirrer was set at a constant speed.

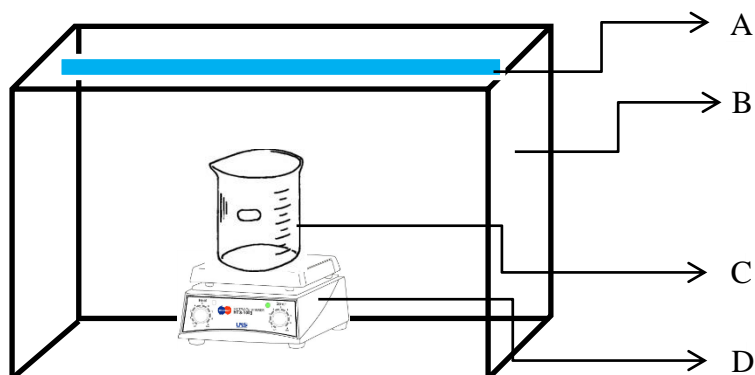


Figure 3.2 Schematic Diagram of photocatalytic reactor

[A- UV lamp, B- Wooden box, C- 250 ml Pyrex glass beaker, D- Magnetic stirrer]

3.5.3 Photocatalytic decomposition Process

Firstly, the bulk solution of the effluent sample was prepared in a 1000 ml volumetric flask, and further experiments were done taking 50 ml effluent from the bulk for each experiment. As molecular weight is known several ppm level solutions were prepared in the case of methylene blue. The photocatalytic activity of TiO_2 , ZnO and Fe_2O_3 was studied for the degradation of the effluents collected from three (3) textile dyeing industries and for methylene blue solution. The photocatalytic reaction system included a 250 mL glass beaker, which was set on a magnetic stirrer running at constant speed inside the UV-chamber (section 3.5.2). All photocatalytic tests were performed at room temperature. At first, 50 mL of effluent solution was taken in the beaker and a certain amount of catalyst was added. The pH of the solution was fixed at the desired value by adding the required amount of NaOH or HCl standard solutions. The beaker was then placed on the magnetic stirrer inside the UV-chamber and the effluent was stirred in dark for half an hour to achieve heterogeneous equilibrium. To enhance the photocatalytic degradation hydrogen peroxide (30%) was used as an oxidizing agent. Afterward, the effluent was photocatalytically decomposed for a certain time under the UV light.

3.5.4 Assessment of decomposed effluents

At the end of the experiment, the beaker was taken away from the chamber. A small portion of the decomposed effluent was then transferred to falcon tubes and centrifuged at a high-speed of about 1000 rpm for decanting the suspended catalyst particles. To study the effect of irradiation time on photodegradation efficiency this step was done every hour during the experimental run also. In those cases, the aliquot was taken out with the help of a syringe at certain time intervals. 5/6 ml of the centrifuged effluent was then carefully withdrawn with a syringe and examined by a UV spectrophotometer (UVmini-1240, SHIMADZU) for measuring the absorbance of the decomposed effluent at its λ_{\max} , which was measured earlier. A calibration curve was prepared before the experiments based on the respective λ_{\max} of the effluents. For the calibration curve, several samples of very low concentration were prepared in a 50 ml volumetric flask. Now the value of the absorbance was plotted on the calibration curve to calculate the concentration of the decomposed effluent. The percentage of decomposition or decolorization efficiency was calculated using the following equation-

% of decomposition

$$= \frac{\text{Initial effluent's conc.} - \text{Decomposed effluent's conc}}{\text{Initial effluent's conc.}} \times 100$$

$$\text{i.e., \% of decomposition} = \frac{C_0 - C}{C_0} \times 100$$

Where, C_0 = Concentration of Initial effluent

C = Concentration of effluent after decomposition.

Similar experiments were performed varying initial dye concentration, catalyst type, catalyst concentration, oxidizing agent, pH value, reaction time, etc. on the percentage of decomposition to find the optimum conditions. The results were compared among the degradation efficiencies of catalytic, photolytic and photocatalytic processes. The decomposition of the effluents was also evaluated in terms of COD and TOC before and after photocatalytic treatment.

3.6 Photocatalytic reaction mechanisms

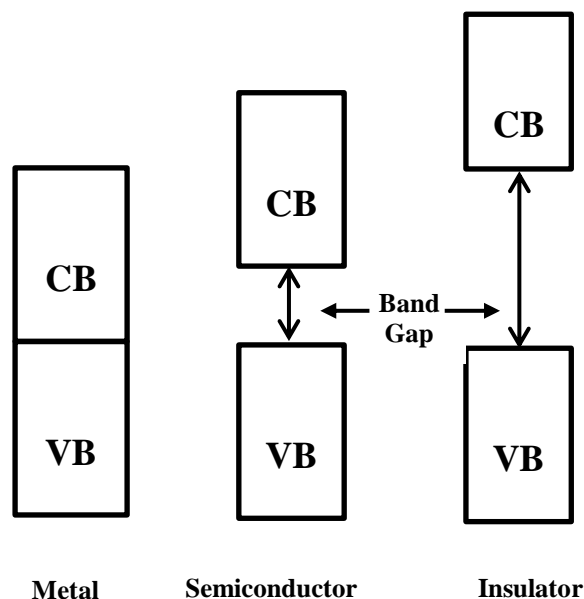


Figure 3.3 Valence and conduction band positions in metal, semiconductor, and insulator

In a photocatalytic reaction, two or three phases are involved—a light source and a semiconductor material are used to initiate the photoreaction, and the catalyst system can carry out oxidation and reduction reactions simultaneously using a long wavelength, UV light, as well as sunlight. The absorption of light excites electrons from the valance band to the conduction band in a photocatalytic reaction. There is no band difference in metals since the valance and conduction bands are fused together. As a consequence, depending on the band location, either reduction or oxidation can occur. However, since the band gap in insulators is too high, the excitation process requires a lot of energy. Semiconductors are the materials that have conductivities that fall somewhere between metals and insulators. Their band gap (E_{bg}), which is the energy gap between the valance band (highest occupied band) and conduction band (lowest unoccupied band), is between that of metals and insulators (Rajesh, 2011).

3.6.1 Photocatalysts

The process parameters including initial effluent concentration, pH, irradiation time, catalyst and oxidizing agent concentration were optimized using three commercial photocatalysts, i.e., TiO_2 , ZnO , and Fe_2O_3 and their mixtures. Mixed catalysts were

used as follows: TiO₂ + ZnO (1:1), TiO₂ + Fe₂O₃ (1:1), ZnO + Fe₂O₃ (1:1) and TiO₂ + ZnO + Fe₂O₃ (1:1:1). TiO₂ was used having a surface area of 50 m²/g and a particle size of 11 nm as per the information provided by the manufacturer. The band gap energies of common photocatalysts are shown in Table 3.1 (Mahlambi *et al.*, 2015).

Table 3.2 Band gap energies of different Photocatalysts

Photocatalyst	Band gap energy(eV)	Photocatalyst	Band gap energy(eV)
Si	1.1	SiC	3.0
WSe ₂	1.2	TiO ₂ rutile	3.02
α- Fe ₂ O ₃	2.2	Fe₂O₃	3.1
CdS	2.4	TiO₂ anatase	3.2
NaBiO ₃	2.62	ZnO	3.2
V ₂ O ₅	2.7	SrTiO ₃	3.4
WO ₃	2.8	ZnS	3.7

3.6.2 Band gap (E_{bg})

Semiconductors have two distinct energy bands: the low-energy valence band (h⁺_{VB}) and the high-energy conduction band (e⁻_{CB}). Each band is made up of a number of energy levels where electrons can reside. Within each energy band, the separation between energy levels is minimal, and they basically form a continuous spectrum. The energy separation between the valence and conduction bands is called the band gap (Sonwane and Mahajan, 2016). Band gap extends from the top of the filled valence band to the bottom of the vacant conduction band of a semiconductor.

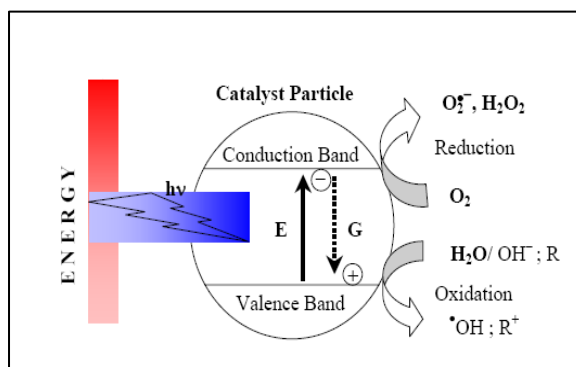


Figure 3.4 Mechanism of photocatalytic degradation

If a photon with energy same to or greater than the semiconductor's band gap is absorbed, an electron from the valence band is excited to the conduction band; meanwhile a positive hole is generated in the valence band. The ultimate fate of the process is to occur reactions between the agitated electrons with oxidants to give reduced products, as well as reactions between the created holes with reductants to produce oxidized products. These redox reactions take place at semiconductor's surface due to the generation of positive holes and electrons.

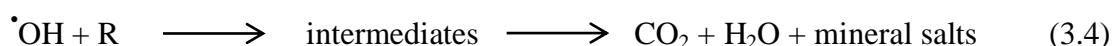
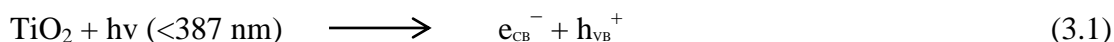
3.6.3 Photocatalytic reactions

One of the most common photocatalytic reactions is heterogeneous photocatalysis, which is based on the absorption of photons with energies equal to or higher than the semiconductor's band gap energy, resulting in electron excitation and a charge separation cases. The following mechanism is widely recognized, which accounts for the photodegradation of organic compounds by oxidation. Attia *et al.* (2008) explained that when a photocatalyst is irradiated with a photon whose energy is equal to or greater than the band gap energy of the photocatalyst, an electron/hole (e^-/h^+) pair is generated. Here free electron is produced in the empty conduction band (e^-_{CB}), creating an electron gap or positive hole in the valence band (h^+_{VB}) (Equation 3.1). These h^+_{VB} and e^-_{CB} are strong oxidizing and reducing species, respectively. If these charges can be kept separated, the electrons and holes may migrate to or near the catalyst surface where they take part in redox reactions with adsorbed species. In photocatalytic oxidation processes, hydroxyl radicals ($OH\bullet$) and superoxide radical anions ($O_2^{\bullet-}$) are thought to be the main oxidizing agents.

The h^+_{VB} can also oxidize organic compounds by forming hydroxyl radicals by reacting with adsorbed water molecules. The positive holes, h^+_{VB} can directly react with organic compounds occurring their oxidation to produce CO_2 , H_2O etc. as degradation end products (Equation 3.2) (Thiruvengkatachari *et al.*, 2008). The h^+_{VB} can also oxidize organic compounds by hydroxyl radicals ($\bullet OH$), which are formed by reacting with adsorbed water molecules (Equation 3.3). Hydroxyl radical has the second highest oxidation potential (2.80 V), which is only slightly less than that of the strongest oxidant, fluorine. Due to electrophilic nature, hydroxyl radicals are very

reactive, strong oxidizer and non-selective to all types of organic pollutants. They are able to oxidize organic compounds in solution and almost completely degrade all electron rich contaminants into harmless compounds like CO₂, H₂O, or HCl etc. (Konstantinou and Albanis 2004, Tayade *et al.*, 2009) (Equation 3.4).

can non-selectively oxidize almost all electron rich organic molecules



Here R represents the dye molecules/organic compounds.

In addition, Okamoto *et al.* (1985) pointed out that the rate-determining step of the photocatalytic reactions could be the formation of hydroxyl radicals ($\cdot\text{OH}$), since they react very rapidly with aromatic ring compounds.

3.7 Equipment and instruments

A brief description of the equipment and instruments used in this research work is given below:

3.7.1 Centrifuge machine

A high-speed Centrifuge machine (Model: TG16-WS) was used for removing suspended catalyst particles from the treated effluents. It was a microprocessor-based benchtop high speed medium capacity centrifuge machine, with a rotor, and user-friendly operational panel.

3.7.2 Electric oven

It was used for drying glass made apparatus used in different treatment and characterization experiments of the effluent/dye solution. It was also used for the preparation of samples and reagents before the COD test and heavy metal analysis of the effluents.

3.7.3 UV-Vis spectrophotometer for colour measurement

Color concentration measurement is another significant feature of most wastewater analyses. Color content of water and wastewater samples can be determined with four different standard methods (Greenberg *et al.*, 1992)-

- (i) Platinum-Cobalt or Visual Comparison Method,
- (ii) Spectrophotometric Method,
- (iii) Tristimulus Filter Method, and
- (iv) ADMI Tristimulus Filter Method.

Pt-Co method is useful for measuring color of potable water and of water in which color is due to naturally occurring materials. It is not suitable for highly colored industrial wastewaters. In Tristimulus Filter Method is applicable to potable and surface waters and to wastewaters, both domestic and industrial. ADMI Tristimulus Filter Method is an extension of Tristimulus Method. By this method a measure of the sample color, independent of hue, may be obtained.

Spectrophotometric method for colour measurement is applicable to potable and surface waters and to wastewaters, both domestic and industrial. In the present study, the spectrophotometric method was used for color concentration determination. For this purpose, an UV-visible Spectrophotometer (UV mini-1240; SHIMADZU) was used for recording the spectrum and absorbance of the effluents before and after photocatalytic treatment.

3.7.4 Atomic absorption spectrophotometer (AAS)

The study used an atomic absorption spectrophotometer (Model: Shimadzu AA-6800) to detect the heavy metals in the dyeing effluents.

3.7.5 TOC analyzer

Machine Name: Total Organic Carbon analyser, Model No: TOC-V CPN, Manufacturer: SHIMADZU, Japan.



CHAPTER FOUR
RESULTS AND DISCUSSION

RESULTS AND DISCUSSION

4.1 Introduction

This chapter deals with the studies of photocatalytic decomposition under various conditions for three selected textile industrial dyeing effluents as well as synthetic organic dye methylene blue to derive the best photocatalytic activity from all possible combination effects. Two effluents were collected from two silk industries at the BSCIC industrial estate of Rajshahi and another was collected from a small yarn dyeing industry at Pipulbaria in Sirajganj district, Bangladesh. These effluent samples were named SIER-1 (Silk Industry Effluent, Rajshahi-1), SIER-2 (Silk Industry Effluent, Rajshahi-2), and YDIES (Yarn Dyeing Industry Effluent, Sirajganj). Firstly characterization of these effluents was studied by measuring the major physicochemical parameters. The photocatalytic activity of three catalysts TiO_2 , ZnO , and Fe_2O_3 in an aqueous solution was assessed for the degradation of dyeing effluents under UV irradiation. The various process parameters like catalyst dose, pH, initial dye concentration, reaction time, and oxidizing agent dose were analyzed. An attempt has also been made to explore the possibility of utilizing a mixed catalyst system for photocatalytic degradation. The photocatalytic degradation efficiency was measured spectrophotometrically. The mineralization of the effluents was measured by reduction in COD and TOC. Furthermore, the photocatalytic decomposition reaction kinetics was studied.

4.2 Characterization of the effluents

The effluents of two silk industries of Rajshahi and one of Sirajganj district were analyzed to find the major physicochemical parameters. The effluent samples were analyzed for some major physicochemical parameters like pH, EC, TDS, TSS, DO, COD, BOD, TOC, etc. Besides these the concentration of some anions (Cl^- , HCO_3^- , SO_4^{2-} , and NO_3^-) and major heavy metals (Cr, Mn, Fe, Co, Ni, Cu, Zn, Pb, and Cd) were also estimated. These physicochemical parameters represent the pollution status of an effluent.

4.2.1 pH

The majority of aquatic organisms prefer a pH range of 6.5-8.0, though some can live in water with pH levels outside of this range (Addy *et al.*, 2004). If pH levels exist beyond this range it can affect aquatic systems and reduce hatching and survival rates. The pH values of the effluents were 6.7, 6.8, and 7.8 for SIER-1, SIER-2, and YDIES, respectively (Table 4.1) indicating that all pH values were almost around neutral. The pH levels of all the effluents were within permissible limits of the Department of Environment, Bangladesh (DoE, BD) standards (6.5–8). This may be due to the usage of H₂O₂ and NaOH as bleaching and kier agents in textile dyeing industries, which almost neutralize each other (Islam *et al.*, 2011). Slightly higher pH in YDIES appeared which may be due to the presence of chemicals like NaOCl, NaOH, Na₂SiO₃, surfactants, sodium phosphate, etc. (Sultana *et al.*, 2009). Excessive pH levels typically increase the solubility of elements and complex compounds, making harmful chemicals more mobile and raising the risk of absorption by aquatic organisms. It also influences the other properties of the water body, organism's activity, and potency of toxic substances present in the aquatic environment. Excessive pH is hazardous to aquatic life like fish and microorganisms, etc. (Yusuff and Sonibare, 2004; Rouse, 1979).

A similar study showed that the pH of textile effluent samples varied from 6.70 to 8.10 (Islam and Mostafa, 2020). Joshi and Shrivastava (2015) conducted a study on the printing and dyeing effluent samples in Maharashtra state, India, and observed the pH value within the range of 7.52 to 9.42 which supports the present findings. A similar study showed that the pH of a composite textile industry wastewater was 7 to 9 (Al-Kdasi *et al.*, 2004).

4.2.2 Dissolved oxygen (DO)

Oxygen is essential to all forms of aquatic life including those organisms responsible for the self-purification processes in natural waters. The presence of oxygen in water is a positive sign of a healthy water body but the absence of it is a signal of severe pollution. Oxygen gets into the water by diffusion from the atmosphere, aeration of the water as it tumbles over rocks and waterfalls, and as a product of photosynthesis.

Chapter Four : Results and Discussion

The DO values of the effluents were 2.8, 2.4, and 3.2 mg/L for SIER-1, SIER-2, and YDIES, respectively (Table 4.1). The DoE, BD standard ranges from 4.5 to 8 mg/L, which indicated that there is a depletion of necessary oxygen in the water. This may occur when there is an increase in nutrients and organic materials from industrial wastewater, sewage discharges, and runoff from the land. The DO value of an effluent depends on its physical, chemical, and biological properties. Cox (2003) stated that aquatic animals are forced to alter their breathing habits or lower their activities if DO concentration decreases. Sultana *et al.* (2009) observed that the average DO value of the textile dyeing effluents in Narayanganj industrial area, Bangladesh was 2.36 mg/L which is similar to the present study. Another research work on the textile dyeing effluents at Dhaka- Narayanganj- Demra (DND) areas, Bangladesh observed DO concentration of the effluents ranged from 3.24 to 6.38 mg/L, which was some extent higher than the present results (Ahmed *et al.*, 2019). However, all the effluent samples contained 50% or lower DO than the standard value indicating high water pollution.

Table 4.1 pH and DO of three textile industries effluents of Rajshahi and Sirajganj districts.

Parameters	SIER-1	SIER-2	YDIES	*DoE, BD Standard
pH	6.7	6.8	7.8	6.5-8
DO(mg/L)	2.8	2.4	3.2	4.5-8

*DoE, BD = Department of Environment, Bangladesh

4.2.3 Total suspended solids (TSS)

The TSS is composed of clay, algae, bacteria, and decomposed organic particles (Casey, 1997). These solids may be originated from man-made wastes or natural sources including anything drifting or floating in the water from sediment, silt, and sand to plankton and algae. The TSS values of the effluents were 1990, 850, and, 2135 mg/L for SIER-1, SIER-2, and YDIES, respectively (Figure 4.1), which were 5.7 to 14.2 times higher than the DoE, BD standard value (150 mg/ L). Total suspended solids are a significant factor in observing water clarity. The more solids present in the water, the less clear the water will be (Langland and Cronin, 2003). TSS of textile effluent includes various types of organic and mineral particles suspended in

the water. The high value of TSS increases sedimentation rates and turbidity level of water, create sludge deposits, thereby influencing the oxygen-demand and reducing photosynthesis (Bash *et al.*, 2001). It is also responsible for pollutant transport; and an increase in the levels of pathogens and contaminants, thus distressing the food chain of aquatic biota (Giller *et al.*, 1998). Hence, it has to be reduced before discarded into the effluents. Sultana *et al.* (2009) conducted research on the effluents of the textile dyeing industries of the Narayanganj industrial area and observed that the TSS value varied from 736 to 1960 mg/L and the average value was found to be 1123 mg/L. Ahmed *et al.* (2019) also studied the textile effluents of the DND area, Bangladesh, and observed that TSS varied from a range of 29-658 mg/L. Another research on three textile effluents of Narsingdi, Rajshahi, and Gazipur District, Bangladesh showed that TSS varied from 233 to 401 mg/L which was lower than the present findings (Islam and Mostafa, 2020). The observed TSS values of the effluents were higher than those of Narayanganj and the DND industrial areas as well as those observed by Islam and Mostafa (2020) indicating highly polluted effluents.

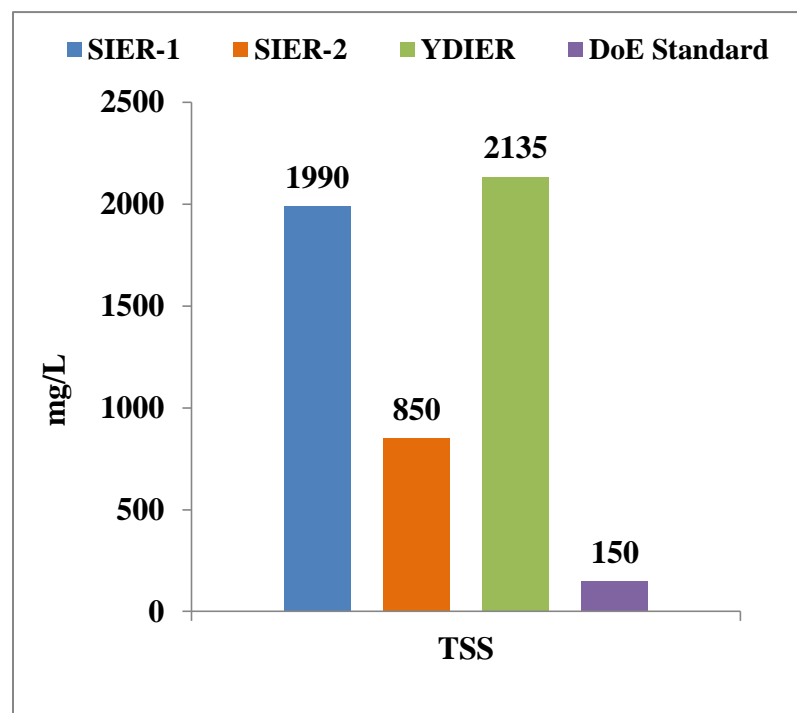


Figure 4.1 Comparisons among TSS values of SIER-1, SIER-2, and YDIES

4.2.4 Total dissolved solids (TDS)

TDS in textile dyeing effluent includes various salts like chloride, phosphates, carbonates, bicarbonates, and nitrates of calcium, sodium, potassium, magnesium, manganese, and other particles (Patel and Parikh, 2013). The TDS values of the effluents were 11970, 7344, and 2565 mg/L for SIER-1, SIER-2, and YDIES, respectively (Figure 4.2). The results were about 1.2 to 5.7 times greater than the DoE, BD standard (2100 mg/L). Water with high TDS is unpalatable and potentially harmful for health and the environment (Hussain and Rao, 2013). TDS concentrations are found to vary within a wide range depending on the type of effluents, which again depend on the type of operating processes in the textile plants and the total production. Sultana *et al.* (2009) observed that the TDS values of the effluents in Narayanganj industrial area lied between 391 to 46700 mg/L and the average value was found 10283 mg/L, which was 3 to 7 times higher than the DoE, BD standard. A similar study showed the TDS in the textile effluents collected from eight industries varied from 246 to 8180 mg/L (Ahmed *et al.* 2019). A study conducted by Islam and Mostafa, (2020) on three textile effluents of Narsingdi, Rajshahi, and Gazipur District, Bangladesh illustrated that the TDS concentrations were 3778, 2937.5, and 3350 mg/L, respectively, which were lower than the present study results. However, the TDS results of the effluents showed that the effluents were moderately polluted. The study observed that the high TDS value of effluent was not desirable because the high content of dissolved solids elevates the density of water, influences osmoregulation of freshwater organisms and also, reduced the solubility of gases and utility of water for drinking, irrigational, and industrial purposes.

4.2.5 Biological oxygen demand (BOD₅)

Measurement of the oxidizable organic matter in wastewater is usually achieved by determining a 5-day biological oxygen demand (BOD₅), the chemical oxygen demand (COD), and total organic carbon (TOC). BOD₅ is an important water quality parameter since it provides a biological index to assess the effect of discharge water on the environment. It is useful for determining approximately how much oxygen will consume by the organic matter in the effluent and is therefore important when estimating the size of the ETP needed. The BOD values of the effluents were 969,

1369, and 875 mg/L for SIER-1, SIER-2, and YDIES, respectively (Figure 4.2), which were 17 to 27 times higher than the DoE, BD standard value (50 mg/ L). Higher BOD values indicate depletion of dissolved oxygen in aquatic life. Effluents from textile industries with high nutrient concentration may result in eutrophication, which interferes with drinking and recreational water supplies (Panswad *et al.*, 2016). Excessive BOD is harmful to aquatic animals like fish and microorganisms. It also causes a bad taste in the drinking water. Textile industries released a lot of biochemical oxygen demanding wastes. Momtaz *et al.* (2012) observed that 12 to 18 times higher BOD₅ values than the DoE, BD standard for the effluents of the Dhaka Export Processing Zone (DEPZ) industrial area. Another study on three textile effluents of Narsingdi, Rajshahi, and Gazipur District, Bangladesh showed that BOD values were 272, 117, and 197mg/L, respectively which were lower than the present findings (Islam and Mostafa, 2020). Another research report showed that the BOD₅ varied from 770 to 5000 mg/L with an average value of 2040 mg/L (Ntuli *et al.*, 2009). The present study results for BOD₅ showed comparatively worse conditions than those observed by Momtaz *et al.* (2012) and Islam and Mostafa (2020) but better than those found by Ntuli *et al.* (2009) indicating moderate to highly polluted industrial area.

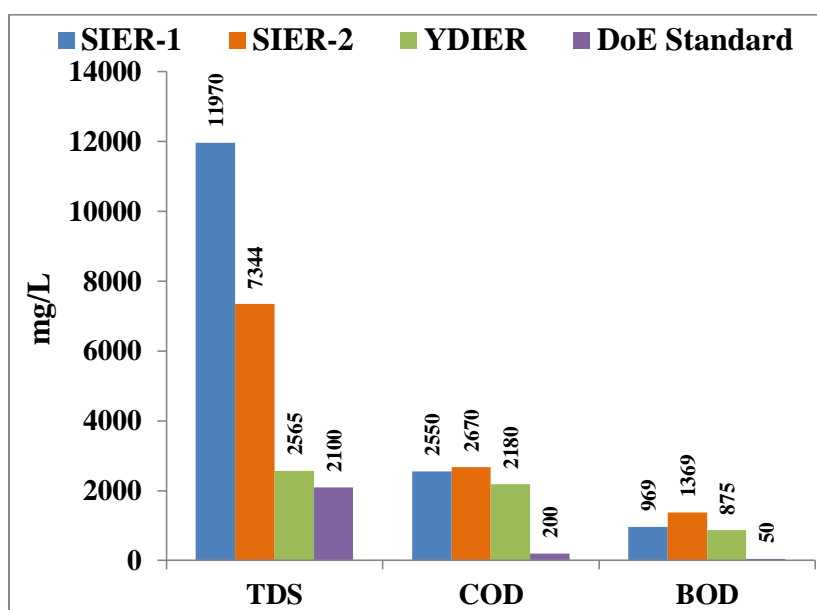


Figure 4.2 Comparisons among TDS, COD, and BOD of SIER-1, SIER-2, and YDIES

4.2.6 Chemical oxygen demand (COD)

COD is a measure of the oxygen equivalent of the organic matter in a water sample that is susceptible to oxidation by a strong chemical oxidant. The COD is widely used as a measure of the susceptibility to oxidation of the organic and inorganic materials present in water bodies and the municipal and industrial wastewater (Jain and Singh, 2003). It is also a measure of water and wastewater quality and is determined by adding dichromate in an acid solution of the wastewater. The COD values of the effluents were 2550, 2670, and 2180 mg/L for SIER-1, SIER-2, and YDIES, respectively (Figure 4.2). These values were about 11 to 13 times higher than the DoE, BD standard (200 mg/L) indicating high pollution. It is noticeable that the COD values of the effluents were significantly higher than their BOD values. Higher COD values were due to the presence of oxidizable compounds, which are used in various steps of textile dyeing processes. The study observed that chemical pollution was more acute rather than biological pollution in those textile industries. COD is often used as a substitute for BOD as it only takes a few hrs not five days to determine. The higher level of COD indicates the toxicity of the effluents and the existence of a huge quantity of biologically resistant organic substances (Yusuff and Sonibare, 2004; Geetha *et al.*, 2008). Textile industries release a lot of chemical oxygen demanding wastes. Joshi and Shrivastava, (2015) observed that the COD values of some printing and dyeing effluents samples in Maharashtra state, India varied from 412 to 1240 mg/L. Another research result also supports the present observation, which found that the COD values of textile effluents of Narsingdi Sadar industrial area, Bangladesh varied from 810.6 to 1430.4 mg/L (Kanan *et al.*, 2014). A report showed that the COD concentrations of three textile industries effluents of Narsingdi, Rajshahi, and Gazipur District, Bangladesh Islam and Mostafa, (2020) observed that the COD were 784, 340, and 512 mg/L, respectively, which were much lower than the present study results. The COD results of the effluents indicated that the effluents were highly polluted. BOD and COD are correlated to DO. The results of BOD and COD of the effluents (Table 4.2) also support the DO values. The higher BOD and COD values mean the lower oxygen content in the effluents, i.e., lower DO values.

4.2.7 Electrical conductivity (EC)

EC is important for the measurement of the dissolved materials in an aqueous solution, which relates to the ability to conduct electrical current through it. EC is usually used for indicating the total concentration of the ionized constituents of water. It is an indirect measure of the ions or the charge carrying species in the effluents under the measurement conditions. The EC values of the effluents were 17370, 11445, and 4845 $\mu\text{S}/\text{cm}$ for SIER-1, SIER-2, and YDIERS, respectively (Figure 4.3). The values were about 4 to 14 times higher than that of the DoE, BD standards (1200 $\mu\text{S}/\text{cm}$). It indicated that the effluents contained huge amounts of ionic substances that were released from the textile industries in the studied area. The EC of the textile wastewater depends on the quantity and type of textile production processes. Such a high value of EC is not suitable for aquatic life and irrigation purposes. It caused an increase in the osmotic pressure of soil solutions and harm to absorb the ability of the water and nutrients of plants (Tatawat and Chandel, 2008).

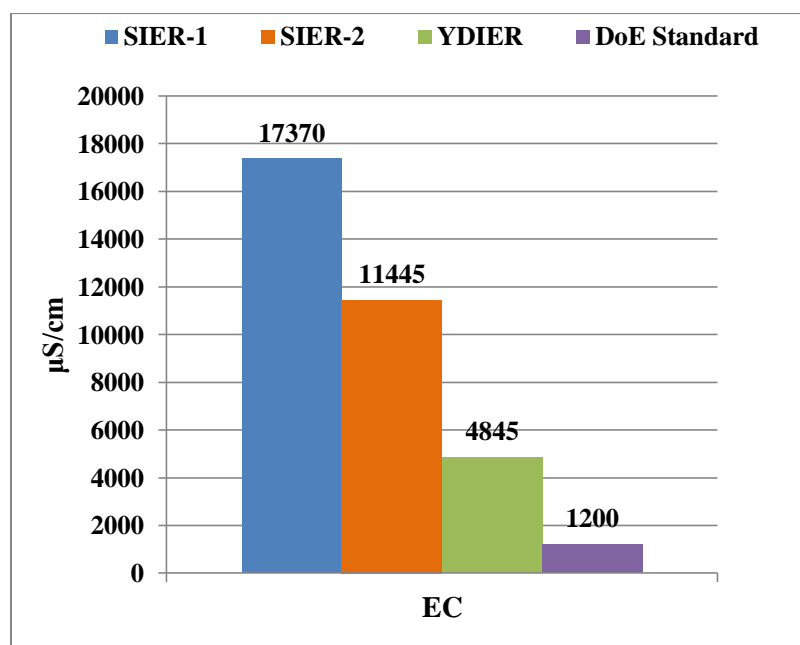


Figure 4.3 Comparisons among EC values of SIER-1, SIER-2, and YDIERS

A study conducted by Sultana *et al.* (2009) on the effluents of textile dyeing industries inside the DND embankment, Narayanganj and they found EC values ranging from 795 to 60200 $\mu\text{S}/\text{cm}$ with an average of 14109.56 $\mu\text{S}/\text{cm}$. Another study on three textile effluents of Narsingdi, Rajshahi, and Gazipur District, Bangladesh showed that

EC values were 5640, 4590, and 4150 $\mu\text{S}/\text{cm}$, respectively which was lower than the present findings (Islam and Mostafa, 2020). The higher value of EC might be due to the excessive use of dyes and other chemicals used for fixing those on fabrics. However, Tariq *et al.* (2008) illustrated that the EC value of several industrial effluents of Hayatabad industrial estate, Peshawar, Pakistan, were ranged from 288 to 1920 mg/L with a mean value of 682.4 mg/L.

The values were much lower than those of the present study. So, it can be said that the effluents were greatly polluted based on the EC status. Table 4.2 represents the major physicochemical parameters of the effluents of the present research work at a glance.

Table 4.2 Major physicochemical parameters of three textile industries effluents of Rajshahi and Sirajganj districts at a glance

Parameters	Observed Value			DoE, BD Standard
	SIER-1	SIER-2	YDIES	
pH	6.7	6.8	7.8	6.5-8
EC($\mu\text{S}/\text{cm}$)	17370	11445	4845	1200
TDS(mg/L)	11970	7344	2565	2100
TSS(mg/L)	1990	850	2135	150
DO(mg/L)	2.8	2.4	3.2	4.5-8
COD(mg/L)	2550	2670	2180	200
BOD(mg/L)	969	1369	875	50

4.2.8 Heavy metals in the effluents

Heavy metals are also referred to as trace elements and are the metallic elements of the periodic table (Salem *et al.*, 2000). The most common toxic heavy metals in wastewater include arsenic, lead, mercury, cadmium, chromium, copper, nickel, silver, and zinc. In the present study, eight (8) heavy metals named Cr, Mn, Fe, Ni, Cu, Zn, Pb, and Cd in the three textile effluent samples were analyzed. The analysis results and respective DoE, BD standards are illustrated in Table 4.3, which shows that the concentrations of most of the heavy metals such as Mn, Fe, Ni, Cu, Zn, and

Cd were within the permissible limit of the DoE, BD standard (2003). It suggested that these textile dyeing industries used organic dyes instead of heavy metal pigment dyes (Momtaz *et al.*, 2012). Some heavy metals are either essential nutrients (typically iron, cobalt, and zinc), or relatively harmless (such as ruthenium, silver, and indium), but can be toxic in larger amounts or certain forms. Other heavy metals such as cadmium, mercury, and lead are highly poisonous. From the eco-toxicological point of view, the most dangerous metals are mercury, lead, chromium (VI), and cadmium (Baysal *et al.*, 2013). The release of high amounts of heavy metals into water bodies creates serious health and environmental problems that may lead to an upsurge in wastewater treatment costs. The two main sources of heavy metals in wastewater are natural and human. The natural factors include soil erosion, volcanic activities, urban runoffs, and aerosols particulate while the human factors include metal finishing and electroplating processes, agricultural runoff, mining extraction operations, textile industries, and nuclear power (Akpor *et al.*, 2014). The textile industries are indicated to be major sources of heavy metal pollutants in water. This is said to mostly originate from the dyeing process, which is a major process in such industries. The compounds used for these dyeing processes include copper, chromium, nickel, and lead which are very toxic and carcinogenic.

4.2.8.1 Chromium (Cr)

Chromium (Cr) presents in nature chiefly in two oxidation states, Cr (III) and Cr (VI). Both chromium (III) and (VI) are dangerous to human health, mainly for the people who work in the leather, steel, and textile industries. But Cr (III) is relatively less toxic and is required as a trace element by animals, whereas Cr (VI) exhibits carcinogenic properties (Aranda *et al.*, 2010). In the present study, the concentrations of Cr were 0.5842, 0.08, and 0.0027 mg/L for the effluents of SIER-1, SIER-2, and YDIES, respectively (Table 4.3). In the case of Cr content, only the effluent of Silk Industry-1, BSCIC, Rajshahi slightly exceeded the permissible limit of the DoE, BD standard, 2003 (0.5 mg/L). This result suggested that this industry might use chromium-containing compounds such as a chrome agent in dyeing processes. Chromium, Cr (VI) oxidation state is responsible for lung cancer, nasal irritation, nasal ulcer, hypersensitivity reactions, and contact dermatitis when entered into

human bodies via dermal and inhalation routes (Shrivastava *et al.*, 2002). A similar study on three textile effluents of Narsingdi, Rajshahi, and Gazipur District, Bangladesh; Islam and Mostafa (2020) observed Cr concentrations as 0.1334, 0.0320, and 0.0355 mg/L, respectively, which supports the present study results. Another research report showed that the concentration of Cr was varied from 0.21 to 1.91 mg/L, found in a study on the printing and dyeing effluents in Maharashtra state, India (Joshi and Shrivastava, 2015). So, it can be stated that the effluents of the present study were almost free of chromium pollution based on Cr concentrations.

4.2.8.2 Iron (Fe)

Iron (Fe) is one of the most abundant trace elements found in the earth's crust. The sources of Fe in textile effluents are the different types of dyes used in the textile and silk industries. This heavy metal may form complexes with organic acids, esters, and some heterocyclic compounds. The concentrations of Fe in the effluents were 1.509, 1.949, and 0.0947 mg/L for SIER-1, SIER-2, and YDIES, respectively (Table 4.3) indicating that all values were within the permissible limit of the DoE, BD standard, 2003 (2.0 mg/L). The presence of a high concentration of Fe may increase the hazard of pathogenic organisms as most of these organisms need Fe for their growth. Overdosing of Fe is potentially hazardous and plays a vital role in causing diabetes anemia and hemochromatosis lung and heart disease (Sobana and Swaminathan, 2007). Similar results were found by Ahmed *et al.* (2019) from a study on the textile effluents of the D.N.D area, Bangladesh, where the concentrations of Fe varied from 0.238 to 1.45 mg/L. Lokhande *et al.* (2011) conducted a study on the textile effluents of Taloja industrial estate of Mumbai, India in which they observed the mean concentration of Fe was 12.8 mg/L which was much higher than the present study results. Another research on three textile effluents of Narsingdi, Rajshahi, and Gazipur District, Bangladesh showed that the Fe concentrations were 4.2826, 3.6188, and 2.8911 mg/L, respectively, which were also higher than the present findings. So, it is evident that the effluents of the present study were free of iron pollution based on Fe concentrations.

4.2.8.3 Manganese (Mn)

Manganese (Mn) is reported to be exigent in every animal species studied (Goldhaber, 2003). The concentrations of Mn of the effluents were 0.7966, 0.945, and 0.08 mg/L found in SIER-1, SIER-2, and YDIES, respectively (Table 4.3). The results indicated that all the effluents had Mn concentration within the permissible limit of the DoE, BD standard, 2003 (5.0 mg/L). A study conducted in Greece reported that individuals who consumed drinking water containing more than 1.8 mg/L Mn, exhibited neurologic symptoms that are similar to Parkinson's disease (Kondakis *et al.*, 1989). Hallucinations, memory impairment, disorientation, and emotional instability are also caused by Mn overdose (Gupta and Gupta, 1998). Research work conducted by Islam *et al.* (2016) showed that the Mn concentration in the effluents of Kumarkhali textile and BSCIC industrial areas, Kushtia, Bangladesh varied from 0.68 to 0.72 mg/L which are very much similar to the present study results. In similar research with three textile effluents of Narsingdi, Rajshahi, and Gazipur District, Bangladesh Islam and Mostafa (2020) stated that the Mn concentrations were 0.1977, 0.1722, and 0.4119 mg/L, respectively, which supports the present study results. So, it is evident that the effluents of the present research were free of manganese pollution.

Table 4.3 Concentrations of heavy metals in the three textile industries effluents of Rajshahi and Sirajganj districts.

Sample	Cr (mg/l)	Fe (mg/l)	Mn (mg/l)	Ni (mg/l)	Cu (mg/l)	Zn (mg/l)	Pb (mg/l)	Cd (mg/l)
SIER-1	0.5842	1.509	0.7966	0.263	0.0066	0.0058	0.31	0.00
SIER-2	0.08	1.949	0.945	0.274	0.016	0.028	0.725	0.021
YDIES	0.0027	0.0947	0.08	0.015	0.0029	0.0066	0.0085	0.0015
DoE, BD Standard (for effluent discharge)	0.50	2.00	5.00	1.00	0.50	5.00	0.10	0.05

4.2.8.4 Nickel (Ni)

Nickel (Ni) is a naturally occurring element widely used in many industrial applications. It is a nutritionally essential trace element for humans as well as other animal species and plants but is toxic when in high concentrations (Hasan *et al.*,

2019). The concentrations of Ni in the effluents were 0.263, 0.274, and 0.015 mg/L for SIER-1, SIER-2, and YDIES, respectively (Table 4.3) which indicates all values were within the permissible limit of the DoE, BD standard, 2003 (1.0 mg/L). Nickel can be present in wastewater as a result of human activities. Sources of nickel in wastewater include ship cruise effluents, industrial applications, and the chemical industry (Baysal *et al.*, 2013). Higher Ni concentration is responsible for asthma, conjunctivitis, inflammatory reactions to nickel-containing prostheses, and implants (Nielsen *et al.*, 1999). Moreover, nickel compounds can cause cancer (Bal *et al.*, 2000). Manekar *et al.* (2014) conducted a study on the effluents of the textile park located in western India observed that the Ni concentration varied from 0.08 to 0.3 mg/L which were much similar to the present study results. Another research report on the printing and dyeing effluent samples in Maharashtra state, India showed some extent higher concentration of Ni where it varied from 0.33 to 0.72 mg/L (Joshi and Shrivastava, 2015). So, it can be said that the effluents of the present study were free of nickel pollution based on Ni concentrations.

4.2.8.5 Copper (Cu)

Copper is an indispensable trace element that shows a significant role in the biochemistry of all living organisms and essential for human health (Bremner and Beattie, 1990). Although humans can handle proportionally large concentrations of copper, too much of it can still cause eminent health problems (Baysal *et al.*, 2013). The concentrations of Cu in the effluents were 0.0066, 0.016, and 0.0029 mg/L for SIER-1, SIER-2, and YDIES, respectively (Table 4.3) indicating that all the values were within the permissible limit of the DoE, BD standard, 2003 (0.5 mg/L). Excess copper accumulation leads to copper toxicosis which results in hepatic cirrhosis, hemolytic anemia, and degeneration of the basal ganglia (Harris and Gitlin, 1996). Nearly similar results were found by Ahmed *et al.* (2019) from a study on the textile effluents of the D.N.D area, Bangladesh where the concentrations of Cu varied from 0.034 to 0.105 mg/L. Manekar *et al.* (2014) conducted research work on the textile effluents in western India observed that Cu concentrations varied from 0.03 to 0.04 mg/L which also supports the present study results. Another research report on textile effluents of Narsingdi, Rajshahi, and Gazipur District, Bangladesh showed that the Cu

concentrations were 0.0479, 0.0790, and 0.0470 mg/L, respectively, which were higher than those of present findings (Islam and Mostafa, 2020). So, based on Cu concentrations, it can be said that the effluents of the present study were free of copper pollution.

4.2.8.6 Cadmium (Cd)

Cadmium (Cd) is considered a very toxic trace metal because of its extremely long half-life (Baysal *et al.*, 2013). Together with Hg and Pb, Cd is one of the big three heavy metal poisons and is not known for any essential biological function. The concentrations of Cd in the effluents were 0.00, 0.021, and 0.0015 mg/L for SIER-1, SIER-2, and YDIES, respectively (Table 4.3) indicating that the Cd concentration in all the effluents was within the permissible limit of the DoE, BD standard, 2003 (0.05 mg/L). Vegetables and fruits contained a high concentration of trace elements like cadmium, copper, and lead increases the probability of upper gastrointestinal cancer (Türkdoğan *et al.*, 2003). Long-term consumption of cadmium increases the rate of kidney failure, softening of bones (Ahmed *et al.*, 2015; Imed *et al.*, 2008), and prostate cancer (Gray, 2005). Food intake and tobacco smoking are the main routes by which Cd enters the body (Manahan, 2002). A recent study showed that the mean concentration of Cd was almost five times higher (0.014 mg/L) than the WHO limit in the tube well water in Rajshahi city (Mostafa *et al.*, 2017). Another study conducted by Joshi and Shrivastava (2015) illustrated that Cd concentration was detected in the range of 0.014-0.56 mg/L in printing and dyeing effluents of Maharashtra state, India. The observations of the studies were similar to the present findings. It may be said that the effluents of the present study were free of cadmium pollution based on the detected concentration of Cd.

4.2.8.7 Zinc (Zn)

Zinc (Zn) is a trace element that essential for human health and its shortages can cause birth defects (Wuana and Okieimen, 2011). Zn is one of the essential micronutrients, which takes part in plant physiological functions and showed beneficial effects on plant growth. But, water may be polluted with large quantities of Zn present in the wastewater of industrial plants. The study results showed that the Zn

concentration in the effluents was 0.0058, 0.028, and 0.0066 mg/L for SIER-1, SIER-2, and YDIES, respectively (Table 4.3) indicated that the Zn concentration of all the effluents was within the permissible limit of the DoE, BD standard, 2003 (5.0 mg/L). Some fish can accumulate Zn in their bodies when they live in Zn-contaminated waterways. When Zn enters the bodies of these fish, it can able to biomagnify up the food chain (Wuana and Okieimen, 2011). Ingestion of acute zinc can cause vomiting, diarrhea, neurological damage ("Zn shakes") (Gupta and Gupta, 1998) and chronic exposure to Zn is responsible for depressing Cu utilization (Sandstead, 1978), Fe deficiency, lowered levels of HDL cholesterol (Hooper, 1980). Research work on the textile dyeing effluents at the D.N.D area, Bangladesh observed that Zn concentration of textile effluents was ranged from 0.021 to 0.204 mg/ L, which was to some extent higher than the present results (Ahmed *et al.*, 2019). Another study conducted by Islam and Mostafa (2020) observed That the Zn concentrations of three textile effluents of Narsingdi, Rajshahi, and Gazipur District, Bangladesh were 0.2585, 0.2047, and 0.1648 mg/L, respectively, which were also higher than the present findings. Another study conducted by Lokhande *et al.* (2011) illustrated that the mean concentration of Zn was found as 27.1 mg/L found in the textile effluents collected from the Taloja industrial estate of Mumbai, India that were much higher than the present study results. The study results found that Zn concentration in the effluents has no threat to the environment.

4.2.8.8 Lead (Pb)

Lead is one of the oldest metals known to man and discharged in the surface water through paints, solders, pipes, building material, gasoline, etc. (Wuana and Okieimen, 2011). The most stable forms of lead are Pb (II) and lead-hydroxy complexes. Lead is not an essential element, but a well-known metal toxicant, and its effects were more extensively reviewed than the effects of other heavy metals. In the present study, Pb concentration was 0.31, 0.725, and 0.0085 mg/L found for the effluents of SIER-1, SIER-2, and YDIES, respectively (Table 4.3). Here the SIER-1 exceeded the permissible limit of the DoE, BD standard, 2003(0.1 mg/L) by nearly 3 times, and SIER-2 exceeded the permissible limit by more than 7 times. However, the concentration of Pb in the effluent of YDIES was within the permissible limit of the

DoE, BD standard. This may be due to the use of Pb-bearing dyes and other chemicals by the relevant textile industries. The toxicities and environmental effects of organo-lead compounds are particularly noteworthy because of the former widespread use and distribution of tetraethyl lead (TEL) as a gasoline additive (Wuana and Okieimen, 2011). Lead can cause serious injury to the brain, nervous systems, red blood cells, and kidneys (Baldwin and Marshall, 1999). Exposure to lead produces various deleterious effects on the hematopoietic, renal, reproductive, and central nervous systems, mainly through increased oxidative stress (Flora *et al.*, 2012). Research conducted by Islam *et al.* (2016) showed that the Pb concentration in the effluents of Kumarkhali textile and the BSCIC industrial areas, Kushtia, Bangladesh were varied from 0.0045 to 0.0085 mg/L, which were very much similar to the Pb concentration of YDIES of the present study. Another research report on textile effluents of Narsingdi, Rajshahi, and Gazipur District, Bangladesh showed that the Pb concentrations were 0.0621 0.0086 0.2900 mg/L, respectively, which were lower than those of present findings (Islam and Mostafa, 2020). Another study conducted by Manekar *et al.* (2014) on the effluents of the textile park located in western India observed Pb concentration varied from 0.11 to 0.12 mg/L which also supports the present study results. Concerning Pb concentration in the textile effluents, it can be said that the water bodies of the areas would not be caused harm to the environment.

4.2.9 Major anionic parameters in the effluents

The concentrations of five anions (Cl^- , HCO_3^- , NO_3^- , SO_4^{2-} , and PO_4^{3-}) in the effluents were measured. The analysis results and respective DoE, BD standards are illustrated in Table 4.4.

4.2.9.1 Chloride ion (Cl^-)

The different types of textile and dyeing effluents contain bleach liquor, which is quite toxic due to the presence of Cl^- ion and a minor quantity may prove lethal to fish (Sultana *et al.*, 2009). The concentrations of Cl^- ion of the effluents were found to be 1392, 845, and 296.5 mg/L for SIER-1, SIER-2, and YDIES, respectively (Table 4.4) indicated that two effluent samples exceeded the DoE, BD standard limits (150-600 mg/L) by several times. The most common toxicity is from chloride in irrigation

Chapter Four : Results and Discussion

water. Chloride is not adsorbed by soils, therefore it moves readily with the soil-water. Thus the crops uptake and accumulate chlorides in the leaves. If the chloride concentration in the leaves exceeds the tolerance of the crop, injury symptoms develop such as leaf burn or drying of leaf tissue (Ayers and Westcot, 1985). Research report showed a much higher concentration of Cl^- ion, which varied from 1035 to 69494 mg/L in textile dyeing effluents of Narayanganj area, Bangladesh (Sultana *et al.*, 2009). Another research report on the printing and dyeing effluent samples in Maharashtra state, India showed that the Cl^- concentration ranging from 834 to 3252 mg/L (Joshi and Shrivastava, 2015). A similar study on three textile effluents of Narsingdi, Rajshahi, and Gazipur district, Bangladesh showed that the chloride contents of textile dyeing effluents were 654.95, 337.96, and 126.74 mg/L, respectively (Islam and Mostafa, 2020). However, the concentration of Cl^- ion of the effluents under the present research was lower than the results indicating comparatively less chloride pollution in those areas. The present study results for Cl^- concentration showed comparatively worse conditions than those observed by Islam and Mostafa (2020) but better than those found by Joshi and Shrivastava, (2015) and Sultana *et al.* (2009) indicating less chloride pollution in those areas.

Table 4.4 Concentrations of anionic parameters in the three textile industries effluents of Rajshahi and Sirajganj districts.

Parameters	Observed Value (mg/L)			DoE, BD Standard (for effluent discharge) (mg/L)
	SIER-1	SIER-2	YDIES	
Cl^-	1392	845	296.5	150-600
NO_3^-	27.45	32.2	6.7	10
HCO_3^-	908	1063	534	300
SO_4^{2-}	3820	1595	810	400
PO_4^{3-}	33.5	2.08	9.4	25

4.2.9.2 Nitrate ion (NO_3^-)

NO_3^- is one of the important nutrients for the growth of algae and it helps to accelerate eutrophication. Agricultural activities, industrial wastes, and domestic wastes are the important sources of NO_3^- ion (Sultana *et al.*, 2009). The concentration of NO_3^- , which is another important inorganic anion of the effluents, was found to be 27.45,

32.7, and 6.7 mg/L for SIER-1, SIER-2, and YDIES, respectively (Table 4.4). It indicates that the concentrations of NO_3^- ion of SIER-1 and SIER-2 exceeded the DoE, BD standard (10 mg/L) limits by several times, which may be due to the continuous discharge of combined industrial waste. NO_3^- is responsible for surface water as well as groundwater contamination and nitrification of water resources lead to potentially serious health effects (Patel, 2016). Nitrate is a common surface water and groundwater contaminant that can cause health problems in infants and animals, as well as the eutrophication of water bodies (Fennessy and Cronk, 1997). Bacterial conversion of the relatively innocuous nitrate ion to nitrite can lead to the development of Methemoglobinemia, which can be the cause of infant death (Winton *et al.*, 1971). In a study, Sultana *et al.* (2009) observed higher concentrations of NO_3^- ion, which was 108.87 mg/L on an average. Another research report showed that the average NO_3^- concentration in the water samples of the area ranged from 2.86 to 5.65 mg/L (Momtaz *et al.*, 2012). However, the concentrations of NO_3^- ion of the effluents were higher than those of the last reported results indicating comparatively moderate nitrate pollution in those areas.

4.2.9.3 Bicarbonate ion (HCO_3^-)

HCO_3^- is the most abundant anion and ionic species in water and therefore has a dominating role in electrical conductivity. It is a simple single carbon molecule that plays surprisingly vital roles in diverse biological processes (Casey, 2006). It is associated with the hardness of water and usually expressed as milligrams of calcium carbonate per liter (WHO, 2011). The concentrations of HCO_3^- in the effluents observed were 908, 1063, and 534 mg/L for SIER-1, SIER-2, and YDIES, respectively (Table 4.4), which were about 2 to 3 times higher than the DoE, BD standard (300 mg/L). HCO_3^- exposures to aquatic organisms can result in toxic effects as concentrations approach a critical threshold (Harper *et al.*, 2014). The sensitivity of aquatic organisms to HCO_3^- is variable. Some fish such as catfish, rainbow trout, and bluegill and macro invertebrates such as chironomidae, crayfish, and many others are tolerant of HCO_3^- (Bringolf *et al.*, 2005). Research conducted on the printing and dyeing effluents in Maharashtra state, India by Joshi and Shrivastava (2015) observed the HCO_3^- ion concentrations within the range of 322 to 1162 mg/L, which is similar

to the present findings. In similar research with three textile effluents, Islam and Mostafa, (2020) stated that the bicarbonate ion concentrations were 654.95, 337.96, and 126.74 mg/L. However, the concentration of HCO_3^- ion of the effluents under the present research was much higher than the DoE, BD standard indicating comparatively higher water pollution in those areas.

4.2.9.4 Sulfate ion (SO_4^{2-})

Sulfate is an important anion imparting hardness to the water. It may transform sulfur or hydrogen supplied depending largely upon the redox potential of the water (Sultana *et al.*, 2009). The concentrations of SO_4^{2-} ion of the effluents were 3820, 1595, and 810 mg/L for SIER-1, SIER-2, and YDIES, respectively (Table 4.4) which are about 2 to 10 times than the DoE, BD standard (400 mg/L). Higher SO_4^{2-} concentration may cause a mild laxative effect along with slightly looser and heavier stools and may lead to diarrhea (Heizer *et al.*, 1997). A similar study conducted by Sultana *et al.* (2009) observed much higher concentrations of SO_4^{2-} ion of the effluents in the Narayanganj industrial area, which lied between 0.27 to 90502 mg/L, and the average value was found 14964 mg/L. Another research on three textile effluents of Narsingdi, Rajshahi, and Gazipur District, Bangladesh showed that the SO_4^{2-} concentrations varied from 434 to 638 mg/L, which was similar to the present findings (Islam and Mostafa, 2020). The concentration of SO_4^{2-} ion of the effluents of the present study was much higher than the DoE, BD standard as well as those observed by Islam and Mostafa, (2020) indicating moderate to high sulfate pollution in those areas.

4.2.9.5 Phosphate ion (PO_4^{3-})

Phosphate is generally the limiting nutrient for algal growth and controls the primary productivity of the water body (Sultana *et al.*, 2009). The concentrations of PO_4^{3-} ion of the effluents were 33.5, 2.08, and 9.4 mg/L for SIER-1, SIER-2, and YDIES, respectively (Table 4.4) which are almost within the DoE, BD standard (25 mg/L). PO_4^{3-} in water bodies can cause eutrophication, hence its amount should be low (Zhang *et al.*, 2011). High levels of phosphate may originate from municipal wastewater discharges since it is an important component of detergents. Therefore, the measurement of phosphate is of considerable importance. In a similar study, Sultana *et al.* (2009) observed much higher concentrations of PO_4^{3-} ion which varied

from 191.30 to 5969.03 mg/L with an average value of 1737.89 mg/L. So, based on PO_4^{3-} ion concentrations of the effluents, it can be stated that the effluents were almost free of phosphate pollution.

4.2.10 Total organic carbon (TOC)

Total organic carbon (TOC) is useful to measure the sum of all organic carbon in the compounds of a sample. The results showed that the TOC values of the effluents were 41.6, 833, 874, and 710 mg/L found for MB solution (40 mg/L), SIER-1, SIER-2, and YDIES, respectively (Table 4.5). TOC has a wide range of applications including checking the water quality. Industries that discharge liquid waste into a surface water body are required to monitor TOC levels. Depending on regulatory compliance and territory typical TOC values in drinking water may range up to 25 ppm (Edition, 2011). But there is no standard limit of TOC for industrial effluent discharge. However, measured TOC values for the effluents under the present study are shown in Table 4.5

Table 4.5 TOC values of Effluents of the three textile industries' effluents of Rajshahi and Sirajganj districts.

Untreated Effluent	TOC (mg/L)
Methylene Blue Solution, 40 ppm	41.6
SIER-1	833
SIER-2	874
YDIES	710

Tomei *et al.* (2016) studied the wastewater originated from dyeing bath of textile factory located in the textile industrial district of Como, Italy, observed average TOC value as 158 mg/L. Another research work on textile effluents from the rinsing step of a denim textile industry in Mexico reported that the TOC value was 84.92 mg/L (Almazán-Sánchez *et al.*, 2016). Syafalni *et al.* (2012) studied the dye wastewater of Penfabric Mill 3, Penang, Malaysia illustrated that the TOC value ranged from 74 to 534 mg/L. However, Singh *et al.* (2013) conducted a study on seven woven and knit textile mills of finishing industries in Punjab, India, and found some extent higher value of TOC as 101–7784 mg/L.

4.3 Photocatalytic decomposition of methylene blue

A synthetic dye solution of methylene blue (MB) was considered as a synthetic dye effluent for the photocatalytic decomposition reactions before starting the study with textile dyeing effluents. MB is a cationic thiazine dye employed by textile industries very frequently and a common ingredient in wastewater from textile mills. It is a heterocyclic aromatic chemical compound with a molecular formula $C_{16}H_{18}ClN_3S$ and λ_{max} values at 662, 614, and 292 nm. It contains three mesomeric structures in which the positive charge can be placed either on the amine nitrogen atom or the sulfur atom. The photocatalytic degradation of MB in an aqueous solution was carried out using different catalysts under UV irradiation in a batch-type reactor. Before illumination, the suspensions were stirred at a dark place for 30 min to reach an adsorption-desorption equilibrium between the photocatalyst and dye molecules. An attempt was made to optimize the process parameters including initial dye concentration, pH, reaction time, catalyst type, and catalyst concentration for the degradation of the dye using three commercial photocatalysts, i.e., TiO_2 , ZnO , and Fe_2O_3 and their combinations. The effect of the oxidizing agent, i.e., H_2O_2 was also studied. The results are presented in the subsequent Tables and Figures and discussed as well.

4.3.1 Effect of initial MB concentration

Dye concentration is a very important parameter in photocatalytic degradation. The effect of different concentrations of MB solution viz., 20, 30, 40, 50, and 60 mg/L on their photocatalytic decomposition for 2 hrs at pH 6 (normal pH of MB solution) was investigated using TiO_2 as the catalyst. The results are presented in Figure 4.4. The results showed that the percentage of photocatalytic decomposition decreases with increasing the dye concentrations. A similar observation was made for the photocatalytic oxidation of other dyes (Davis *et al.*, 1994). The maximum decomposition was about 90% found in 20 ppm dye concentration. The study suggested that the increased dye concentration prevent penetrating the incident light into the lower parts and thus reduced the desired light intensity to reach the semiconducting particles. Hence, a decrease in the photocatalytic degradation of the

dye occurred. This observation was supported by Ameta *et al.* (2013). This study also observed that the higher is the dye concentration, the higher is the amount of dye adsorbed on the catalytic surface, thus reduce the photocatalytic activity.

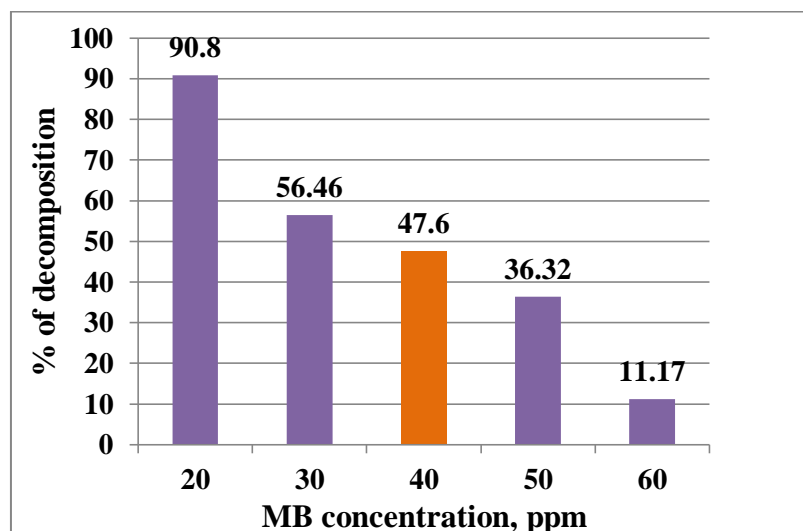


Figure 4.4 Effect of initial dye concentrations on % of decomposition

(Catalyst = TiO₂, Catalyst conc. = 200 ppm, pH = 6.0, Reaction time = 2 hrs, H₂O₂ = 300 ppm)

The increase in dye concentration also decreases the path length of photons entering the dye solution. The rate of degradation is related to the formation of OH radicals, a critical species in the degradation process (see Eq. 4, sec. 3.6.3). Hydroxyl radicals are non-selective, strong oxidizers, and very reactive. The free radicals are able to oxidize organic compounds in solution and almost completely degrade contaminants (Konstantinou and Albanis, 2004). The photocatalytic degradation of aromatic compounds happens through the hydroxylation by hydroxyl radicals (Almquist *et al.*, 2003). The hydroxyl radicals are formed through the reaction of holes with adsorbed OH⁻ and water. If we assume that the positions of adsorbed OH radicals are replaced by dye ions (dye⁻) then the generation of OH radicals will be reduced due to the reduced number of active sites available for the generation of OH radicals. However, although 20 and 30 ppm MB solutions were better degraded than others, 40 ppm solution was selected for the optimization of other parameters.

4.3.2 Effect of catalyst

The effect of different photocatalysts like TiO_2 , ZnO , Fe_2O_3 , and their mixtures on the decomposition of 40 ppm MB solution was examined. The comparison of the efficiency of these catalysts is important since they have commercial prices.

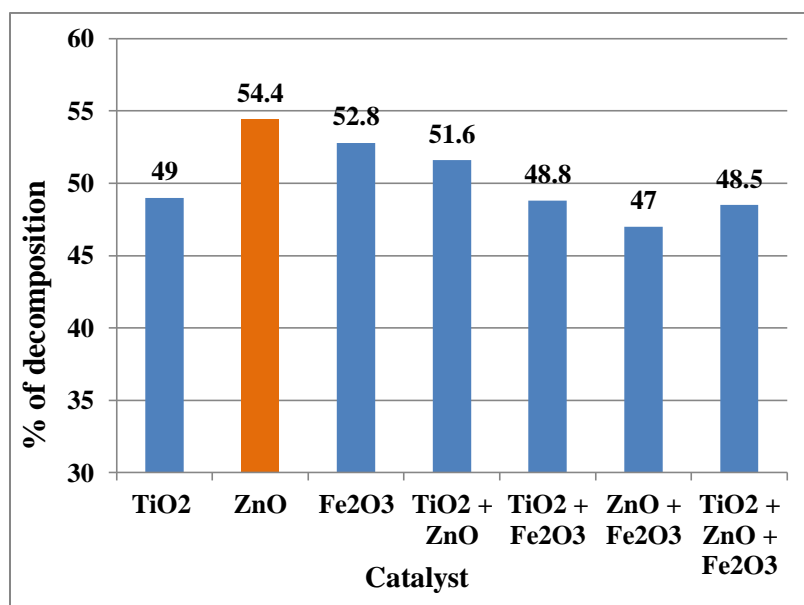


Figure 4.5 Effect of catalyst on % of decomposition of MB

(Effluent conc. = 40 ppm, Catalyst conc. = 200 ppm, pH = 6, Reaction time = 2 hrs, H_2O_2 = 300 ppm)

The maximum 54.4 % of degradation of the dye solution was achieved by the catalyst ZnO . However, catalyst Fe_2O_3 and the mixed catalysts $\text{TiO}_2 + \text{ZnO}$ (1:1) showed the degradation of about 52.2 and 51.6%, respectively. TiO_2 alone showed comparatively lower degradation of 49% under the same conditions. The study observed that a single catalyst was more efficient than a mixed one in most of the photocatalytic degradation of MB. The photocatalytic decomposition efficiency after 2 hrs of irradiation was following the order: $\text{ZnO} > \text{Fe}_2\text{O}_3 > (\text{TiO}_2 + \text{ZnO}) > \text{TiO}_2 > (\text{TiO}_2 + \text{Fe}_2\text{O}_3) > (\text{TiO}_2 + \text{ZnO} + \text{Fe}_2\text{O}_3) > (\text{ZnO} + \text{Fe}_2\text{O}_3)$ (Figure 4.5). Hussein and Abass, (2010) conducted a study on the photocatalytic decomposition of textile effluents by TiO_2 (rutile), TiO_2 (anatase), and ZnO catalysts. The results showed the order: $\text{ZnO} > \text{TiO}_2$ (anatase) $> \text{TiO}_2$ (rutile). Another research showed that ZnO performed better photocatalyst compared to TiO_2 for the degradation of MB (Mohabansi *et al.*, 2011). A report showed that the nanostructured Fe/FeS powder degraded about 50% of the dye in 3 hrs 20 minutes of irradiation (Esmaili *et al.*, 2018). This study showed a

comparatively better result where 54.4 % degradation of the dye solution was achieved by the catalyst ZnO within 2 hrs. The study observed that the extent of degradation by photocatalysts varies among different dyes, and it was related to the nature of both the dyes and catalysts. Figure 4.5 shows that ZnO was the most efficient catalyst for the photocatalytic degradation of MB. Hence, ZnO was selected as a photocatalyst for the optimization of different parameters.

4.3.3 Effect of irradiation time

The effect of irradiation time on photodegradation efficiency of different catalysts was studied for the decomposition of MB for different periods up to 8 hrs under UV light. The study results showed the influence of the irradiation time on the decomposition percentage in Figure 4.6). The decomposition percentage sharply increased with the increase of time within six (6) hrs and then slowly increased up to 8 hrs tending to reach equilibrium. All the three catalysts and their mixtures showed similar behavior. This trend was observed by other researchers. Salama *et al.* (2018) stated that the number of active sites on the photocatalyst surface remained high at the beginning of photoreaction and as a result, a greater degradation rate was achieved.

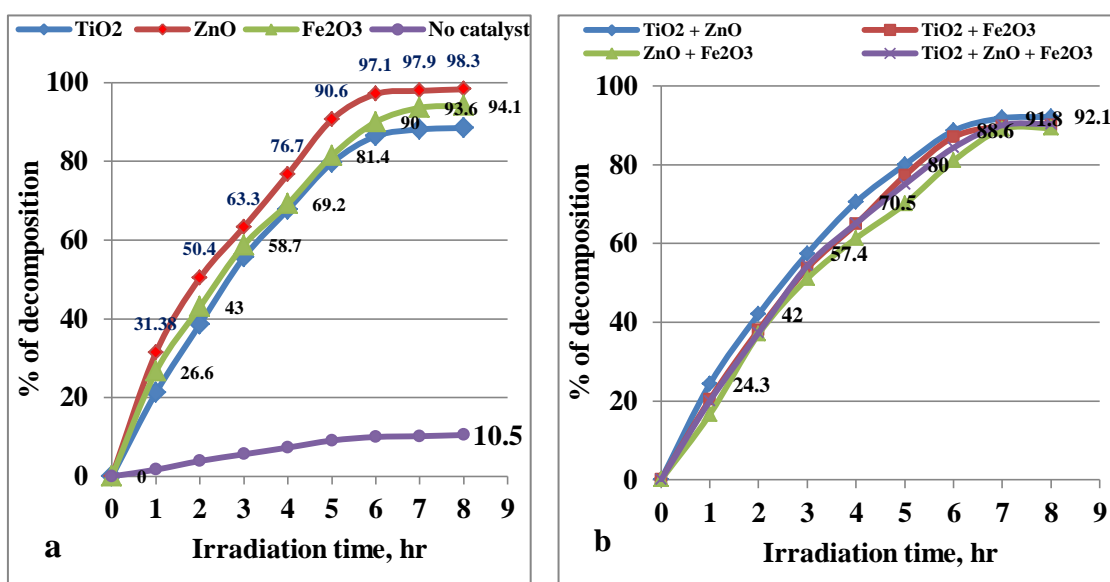


Figure 4.6 Effect of irradiation time on % of decomposition of MB by a) single catalysts and b) mixed catalyst.

(Dye conc. = 40 ppm, Catalyst conc. = 200 ppm, pH = 6.0, H₂O₂ = 300 ppm)

The difficulty in reacting short-chain aliphatics with •OH radicals, as well as the short lifetime of photocatalysts due to active site deactivation by strong by-products deposition, account for the slow rate of degradation after a certain time limit. (Kumar and Pandey, 2017).

The dye degradation rate was decreased after six (6) hrs of irradiation due to fewer hydroxyl radicals in low concentrated dye solution (Alalm *et al.*, 2015). Similar results were observed by the other two individual studies (Ghasemi *et al.* 2016; Che Ramli *et al.*, 2014). In the absence of any catalyst, the photolytic degradation was only 10.5% achieved after eight (8) hrs of irradiation indicated that without a catalyst the degradation was negligible as shown in Fig 4.6a. So, both UV light and catalyst are essential for the effective degradation of the dye. The mixed catalyst was unable to show better degradation in 8 hrs of irradiation time (Figure 4.6b). It is also noticeable that about 63.3% decomposition was achieved with ZnO for 3 hrs reaction time, and further reaction gave more decomposition (Fig 4.6a). But for any reaction on a commercial basis time is an important factor. Because, on an industrial scale, continuing the effluent treatment process over a longer period is costly and troublesome. Therefore, it is beneficial for improving degradation efficiency by changing other parameters. Hence, the study considered the degradation experiments would be carried out for three (3) hrs to make the process more feasible from an economic point of view. Thus the next experiments were carried out for a three (3) hrs of irradiation to optimize the rest of the parameters.

4.3.4 Photodegradation kinetics of MB

Chemical kinetics is the branch of physical chemistry concerned with understanding the rates of chemical reactions. Kinetic studies are of fundamental importance in any investigation of the reaction mechanism. By understanding how a reaction takes place, many processes can be improved. The change in concentration of the solution (C/C_0) is plotted as a function of irradiation time (C_0 = the initial concentration of the bulk solution, C = concentration at time t). Figure 4.7 shows that negligible degradation was observed without any photocatalyst in the presence of only UV light. However,

almost complete degradation of the dye was achieved within 8 hrs of irradiation in the presence of photocatalysts.

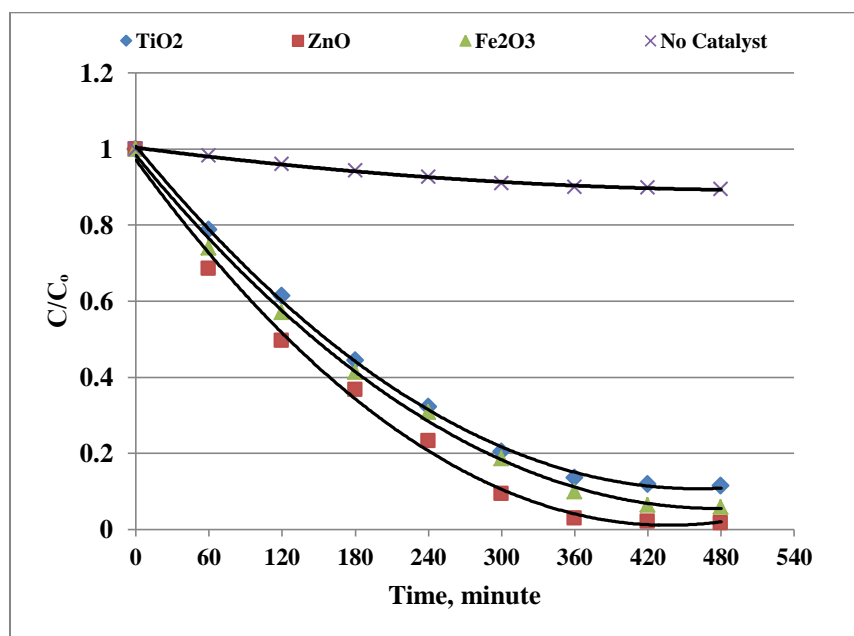


Figure 4.7 Photocatalytic degradation of MB

(Dye conc. = 40 ppm, Catalyst conc. = 200 ppm, pH = 6.0, H₂O₂ = 300 ppm)

The graphs of $\ln \frac{C_0}{C}$ versus time for photocatalytic reaction by ZnO, TiO₂, and Fe₂O₃ are shown in Figure 4.8 (almost straight line) from which the study found that the photocatalytic degradation of MB by different catalysts obeyed approximately pseudo-first-order kinetics. The correlation constant for the fitted lines were calculated to be $R^2 = 0.9992$, 0.9954 , and 0.9947 for Fe₂O₃, ZnO, and TiO₂, respectively indicating that the R^2 value fitted best for Fe₂O₃. The rate constants of the photodegradation reactions by Fe₂O₃, ZnO, and TiO₂ were calculated to be 4.88×10^{-3} , 5.89×10^{-3} , and $4.51 \times 10^{-3} \text{ min}^{-1}$, respectively. The photocatalytic degradation rate depends on the dye, its structure, and catalyst concentration, and pH of the medium (Abo-Farha, 2010). Houas *et al.* (2001) studied the photocatalytic degradation pathway of MB in water and observed similar results. Another research reported that the disappearance of a dye Reactive Yellow 17 in the solution followed approximately pseudo-first-order kinetics (Neppolian *et al.*, 2001).

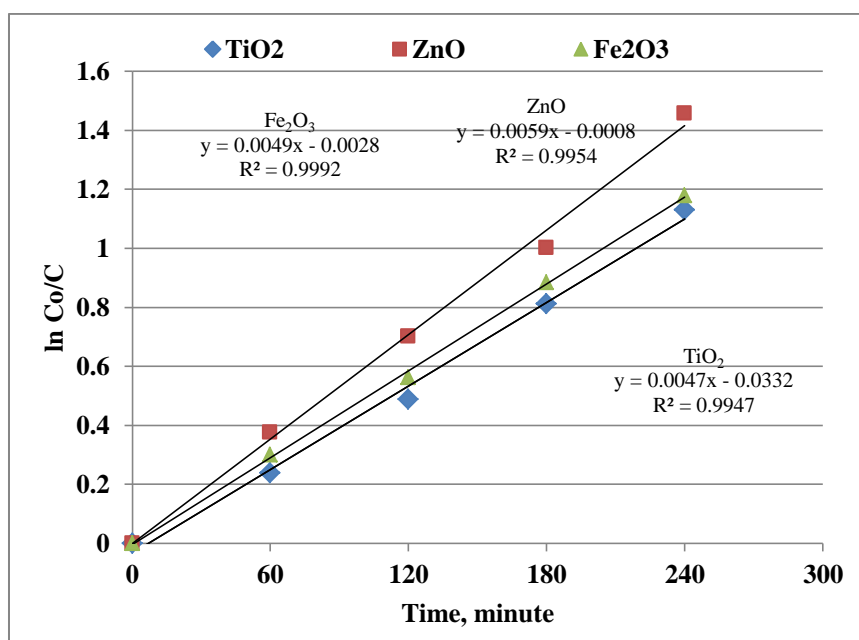


Figure 4.8 Kinetics of photodegradation of MB

4.3.5 Effect of pH

Different photocatalytic degradation experiments on 40 ppm MB solution were performed by ZnO at pH values of 4 to 10 for 3 hrs. The results are shown in Figure 4.9. The pH is an important parameter because it defines the surface charge properties of the catalyst, the size of aggregates produced, the charge of dye molecules, dye adsorption onto the catalyst surface, and the concentration of hydroxyl radicals in photocatalytic degradation. (Sakthivel *et al.*, 2003; Aguedach *et al.*, 2005).

It is extremely difficult to interpret the effects of pH on the efficiency of the photodegradation process. This is because dye degradation can be caused by three different reaction mechanisms: hydroxyl radical attack, direct oxidation by the positive hole, and direct reduction by the electron in the conducting band. The contribution of each depends on the substrate nature and pH (Tang *et al.*, 1997). The results revealed that the photodegradation efficiency decreases with the increase in pH. At low pH value (pH = 4) the photodegradation efficiency reached to 69.62%. When the pH value of MB dye solution was increased from 4 to 7, the photodegradation efficiency decreased to 54.2% at pH 7. This decrease by pH change can be attributed to the point of zero charges (pzc) of the photocatalyst. The pH value

at which the surface charge of a photocatalyst is zero is its pzc. It was reported that the pzc for ZnO is 8.0 (Daneshvar *et al.*, 2007), and so, ZnO surface is negative at pH values above 8.0 and positive at pH values below 8.0.

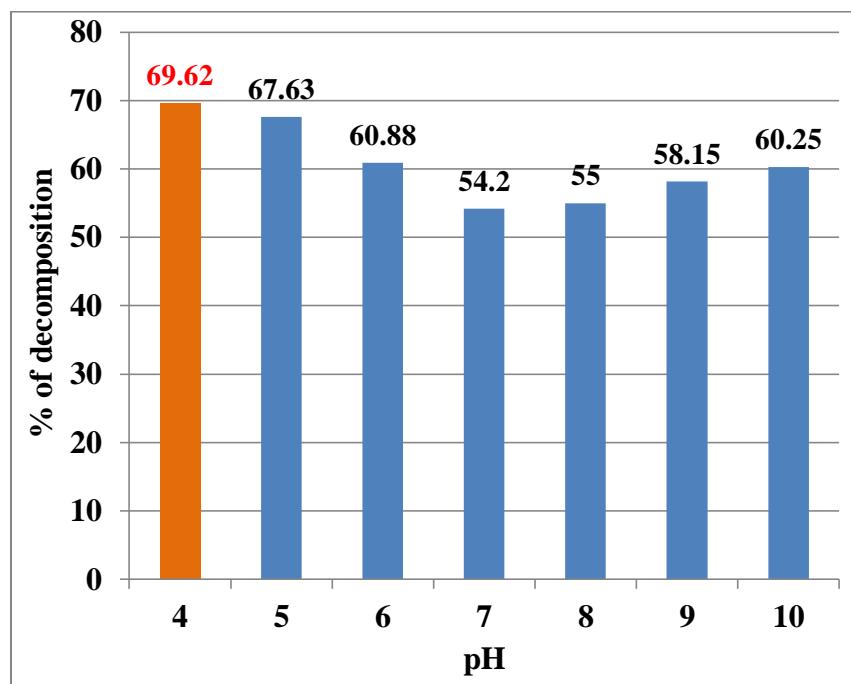


Figure 4.9 Effect of pH on % of decomposition of 40 ppm MB solution

(Catalyst = ZnO, Catalyst conc. = 200 ppm, Reaction time = 3 hrs, H₂O₂ = 300 ppm)

MB is negatively charged in an acidic medium, whereas ZnO is positively charged below pH 8.0. So an increase in pH value tends to change the surface charge of ZnO from positive to negative by adsorbing HO⁻ ions, which favors the formation of HO• (Wang *et al.*, 2007) and consequently, the photocatalytic activity decreased due to the increase of the electrostatic repulsion between ZnO and dye gradually. Besides, the increase of pH may increase the electron/hole (e⁻/h⁺) pairs recombination rate, which was generated earlier by the illumination of photocatalyst with photon and thus, decreased the photocatalytic activity (El-Bahy *et al.*, 2009). But further increases in pH value of MB solution to 10 lead to increases in photodegradation efficiency from 54.2% to 60.25%. The increase in degradation efficiency by pH can also be attributed to the pzc and the nature of the dyes. Since MB is a cationic dye, at pH values higher than 8.0, adsorption between the MB molecules and the catalyst surface increases during photodegradation. Another reason is the larger amount of OH⁻ available to

react with the H^+ on the ZnO surface resulting larger production of hydroxyl radicals for degradation. According to Ling *et al.* (2004), at basic pH electrostatic interactions between negative ZnO^- and MB cation leads to strong adsorption with a correspondingly high rate of degradation. Similar results were observed in photodegradation of 15 ppm MB by ferrite bismuth nanoparticles under sunlight irradiation, where pH 2.5 showed the best photodegradation efficiency (Soltani and Entezari, 2013). Hence, the optimal pH value for the photodegradation of MB was selected as 4 at which the positively charged ZnO and negatively charged MB molecules should readily attract each other, and photocatalytic degradation is maximal. Kansal *et al.* (2009) also found that the degradation of Reactive Black 5 and Reactive Orange 4 dyes was favored in acidic medium with TiO_2 .

4.3.6 Effect of catalyst concentration

The amount of catalyst is an important factor influencing the photodegradation process significantly. Hence, it is important to determine the optimum amount of the catalyst required to degrade the maximum amount of MB during the process. The effect of different concentrations of the catalyst, ZnO viz., 100, 200, 300, 400, and 500 ppm on the photocatalytic decomposition of 40 ppm MB was investigated. The degradation efficiency increased slightly to reach a maximum value of about 69.62% with an increase in catalyst dose from 100 ppm to 200 ppm (Figure 4.10). The reason is that increasing the number of active sites for photocatalytic reaction leads to higher production of OH^\bullet radicals up to the catalyst dose of 200 ppm. Therefore, a higher catalyst dose is expected to result in higher degradation efficiency. But no noticeable variation of degradation efficiency was observed at a catalytic dose of 300 ppm. When all the dye molecules were adsorbed on the catalyst surface no improvement is achieved by adding more catalysts. As the dose was further increased up to 500 ppm, the degradation efficiency decreased. This is probably because further increases in catalyst dose can reduce light penetration in dye solution (Nomikos *et al.*, 2014; Martínez *et al.*, 2011).

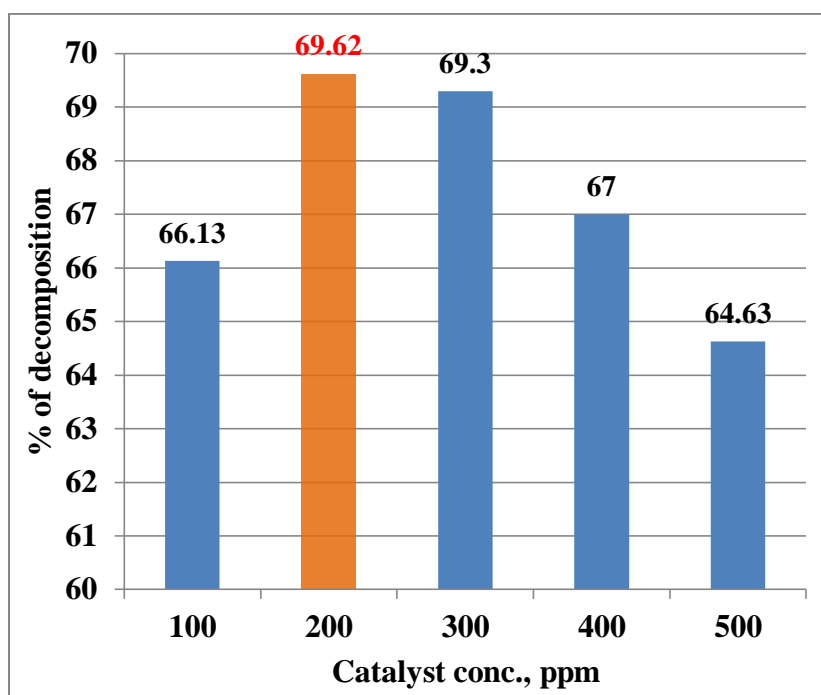


Figure 4.10 Effect of catalyst concentration on % of decomposition of MB

(Dye conc. = 40 ppm, Catalyst = ZnO, pH= 4, Reaction time = 3 hrs, H₂O₂ = 300 ppm)

Another reason behind this phenomenon is the catalyst-powder agglomeration and the subsequent decrease in the active surface sites (Tayeb and Hussein, 2015). Similar trends in photodegradation were observed by many other researchers (Esmaili *et al.*, 2018; Mohamed *et al.*, 2012). Therefore, a catalyst dose of 200 ppm was selected as the optimum for the photodegradation of 40 ppm MB.

4.3.7 Effect of oxidizing agent (H₂O₂) dose

In photocatalytic processes, oxidants such as H₂O₂ have major effects on degradation rates (Guettai and Amar, 2005; Madhu *et al.*, 2007). Different photocatalytic degradation experiments were carried out for varying H₂O₂ doses viz., 200, 300, 400, 500, 600, and 700 ppm in 40 ppm MB solution. The results are shown in Figure 4.11. An increase in the dose of H₂O₂ from 200 to 600 ppm increased the percentage of decomposition from 63.63% to 82.75 % in 3 hrs. A higher concentration of H₂O₂ liberated more hydroxyl free radicals which increased the dye decomposition percentage. However, a further increase in H₂O₂ loading up to 700 ppm no significant effect was observed on the percentage of decomposition. A higher concentration of H₂O₂ rendered reaction solution acidic resulting in reduced rates. This could be

because of an increase in the H₂O₂ concentration beyond certain limits does not increase the reaction rates as it tends to act as a hydroxyl radical scavenger instead of a free radical generator (Baxendale and Wilson, 1957; Guettai and Amar, 2005).

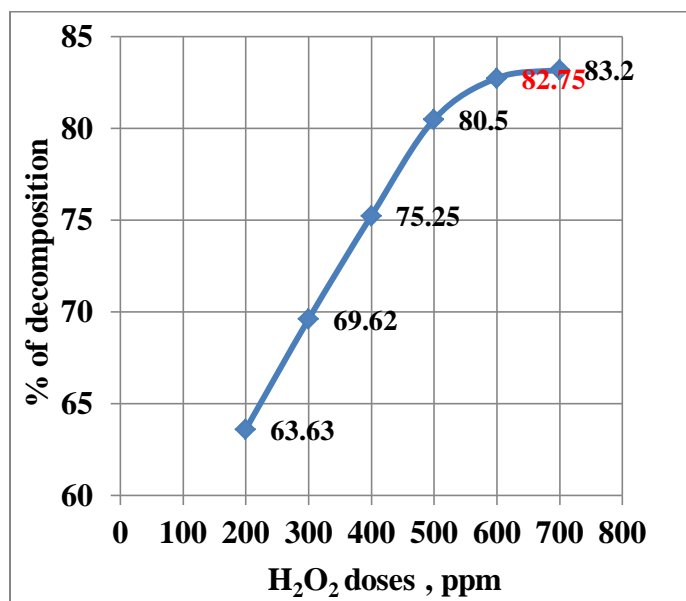


Figure 4.11 Effect of H₂O₂ dose on % of decomposition of MB

(Dye conc. = 40 ppm Catalyst = ZnO, Catalyst conc. = 200 ppm, pH= 4, Reaction time = 3 hrs)

Similar results were observed by Madhu *et al.* (2009) in a research work of photocatalytic degradation of MB using different concentrations of H₂O₂. Figure 4.11 infers that 600 ppm can be considered to be an optimum value of H₂O₂ loading for the discoloration in the presence of UV.

4.3.8 Mineralization of the dye

The mineralization of the 40 ppm MB solution was determined by measuring the TOC values before and after the photocatalytic treatment. Mineralization to a moderate extent of 44.71% was observed as the TOC value decreased from 41.6 to 23 mg/L after 3 hrs of photocatalytic treatment (Figure 4.12). However, other researchers observed higher TOC reduction in their study. For example, Bulc and Ojstršek, (2008) reported up to 89% of TOC reduction in dye-rich textile wastewater treatment by the constructed wetland. 80-82% of TOC reduction was reported in a review on the treatment of textile effluents (Ghaly *et al.*, 2014).

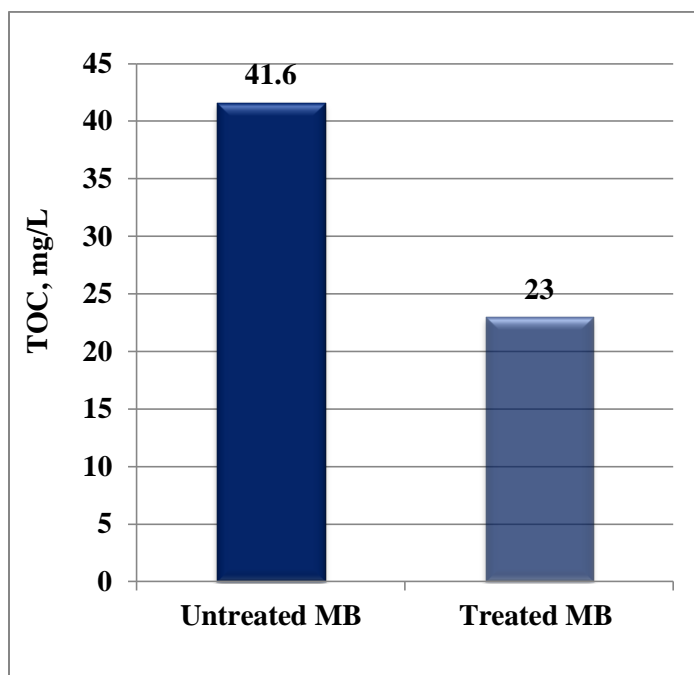


Figure 4.12 Mineralization of 40 ppm MB by photocatalytic treatment

(Catalyst = ZnO, Catalyst conc. = 200 ppm, pH= 4, Reaction time = 3 hrs, H₂O₂ = 600 ppm)

4.3.9 Optimized parameters for photocatalytic degradation of MB

The results of the present study showed that heterogeneous photocatalytic degradation of the dye MB can be efficiently carried out using ZnO catalyst under UV irradiation. Photodegradation was maximum in an acidic medium and the degradation efficiency depended upon the process parameters like catalyst concentration, dye concentration, irradiation time, and pH. The optimum catalyst dose for the degradation of 40 mg/L solutions of MB was 200 ppm of ZnO. TOC analysis of the dye under optimized conditions showed a 44.71% reduction in TOC after 3 hrs of irradiation. The optimized values are shown in Table 4.6. Maximum 82.75 % of decomposition of MB was achieved at the optimized parameters.

Table 4.6 Values of optimized parameters for the photocatalytic degradation of 40 ppm MB solution

Parameters	Optimized values
Catalyst	ZnO
Catalyst concentration	200 ppm
Irradiation time	3.0 hrs
pH	4.0
H ₂ O ₂ concentration	600 ppm
Maximum decomposition achieved = 82.75%	

4.4 Photocatalytic decomposition of Silk Industry Effluent, Rajshahi-1 (SIER-1)

Silk Industry Effluent, Rajshahi-1 (SIER-1) collected from the BSCIC industrial area, Rajshahi was blue and almost neutral (pH=6.7). SIER-1 was highly concentrated and it was difficult to measure the absorbance of the effluent in its original concentration. So for convenience and practical purposes, dilution was required to assess the concentration and degradation studies. The degradation efficiency of three photocatalysts namely, TiO₂, ZnO, and Fe₂O₃ was investigated for the treatment of the collected textile effluent under UV radiation. The effects of various process parameters, like initial effluent concentration, irradiation time, catalyst type and catalyst concentration, pH, and the oxidizing agent dose on the photocatalytic degradation efficiency were analyzed. The percentage of degradation of the effluent was evaluated in terms of reduction in absorbance measured by spectrophotometric methods. The decomposition of the effluents was also evaluated in terms of reduction in COD and TOC. The concentration of the effluent was estimated using the absorbance recorded on a UV-spectrophotometer at the λ_{max} 584 nm.

4.4.1 Effect of initial effluent concentration

The effect of initial concentrations of SIER-1 (40%, 60%, 80%, and 100%) on their photocatalytic decomposition by TiO₂ at pH 6.7 (effluent's normal pH) was investigated. The results are represented in Figure 4.13, which indicates that the percentage of photocatalytic decomposition decreases with increasing concentration of the effluents. An increase in the concentration of effluent from 40 % to 100 % reduces the percentage of decomposition from 58.95% to 32.74%. This behavior could be explained due to the coverage of the catalyst's active sites by dye molecules (Guettai and Amar, 2005). As the concentration of the dyeing effluent is increased, the dye molecules start acting as a filter for the incident UV radiation and they do not permit the desired light intensity to reach the catalyst surface and thus, result in a decrease in the percentage of photocatalytic degradation (Ameta *et al.*, 2013). Neppolian *et al.* (2002b) degraded reactive blue 4 dye in the presence of TiO₂ photocatalyst with a constant catalyst loading of 2 g/L. They observed that degradation decreased from 98% to 32% when initial dye concentration was increased from 0.0001 M to 0.0005

M, which supports the present study results. A similar observation was reported by Toor *et al.* (2006). However, although 40% SIER-1 showed better degradation than others, 60% SIER-1 solution was selected for the optimization of other parameters.

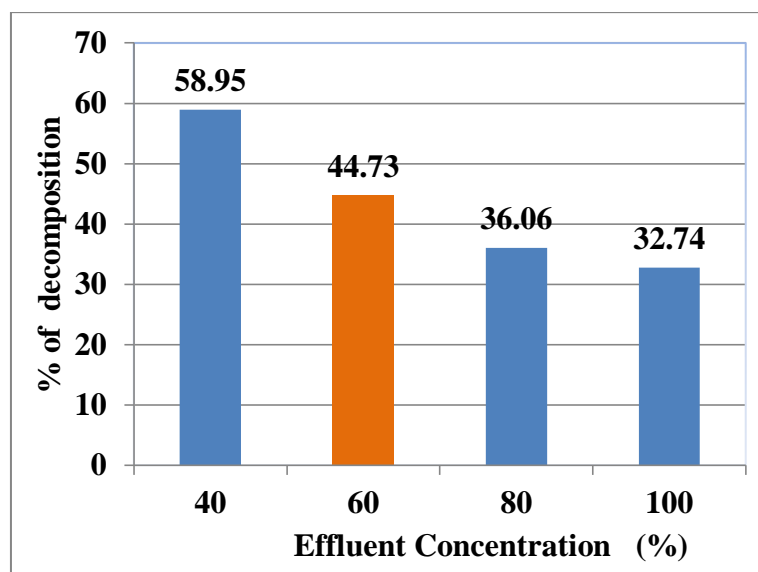


Figure 4.13 Effect of initial effluent concentrations on % of decomposition of SIER-1

(Catalyst = TiO₂, Catalyst conc. = 200 ppm, pH = 6.7, Reaction time = 2 hrs, H₂O₂ = 300 ppm)

4.4.2 Effect of catalyst

The photodegradation of SIER-1 with different catalysts like TiO₂, ZnO, Fe₂O₃, and their combinations under UV light irradiation for 3 hrs was studied. The maximum 58.9 % degradation of the effluent took place in the case of ZnO photocatalyst (Figure 4.14). The next better photodegradation efficiency was shown by the mixed catalyst ZnO+Fe₂O₃ (1:1), where 56.1% degradation of the effluent was achieved. In most cases, the degradation efficiency of single catalysts was higher than that of mixed catalysts. When TiO₂, ZnO, and Fe₂O₃ were used for 3 hrs under the same conditions 54.4%, 58.9%, and 49.2% of degradation occurred, respectively. The photodegradation efficiency of these catalysts after 3 hrs of irradiation was of the following trends: ZnO > (ZnO+Fe₂O₃) > TiO₂ > (TiO₂+ZnO) > (TiO₂+ZnO+Fe₂O₃) > Fe₂O₃ > (TiO₂+Fe₂O₃) > No catalyst. Hussein and Abass, (2010) studied the photocatalytic decolorization of textile industrial wastewater by TiO₂ (rutile), TiO₂ (anatase), and zinc oxide and observed that the efficiency in the following order: ZnO > TiO₂ (anatase) > TiO₂ (rutile). Mohabansi *et al.* (2011) also reported that ZnO was a

better alternative photocatalyst compared to TiO_2 for the degradation of MB. The mixture of Fe_2O_3 and TiO_2 has been reported to be less active than the original TiO_2 itself for the degradation of MB and other dyes (Crittenden *et al.*, 1997), which supports the present findings. The study observed that the efficiency of photodegradation of catalysts varies among different effluents and it depends on the nature of both effluents and catalysts. The effluent is almost resistant to self-photolysis as shown in Figure 4.14 that without any catalyst the photolytic degradation is only 9.6 %. It can be said that both UV light and catalyst were needed for effective degradation. From Figure 4.14 it can be assessed that ZnO was a more efficient catalyst than the others for the photocatalytic degradation of this particular effluent. Hence, ZnO was selected as the photocatalyst for the optimization of other parameters.

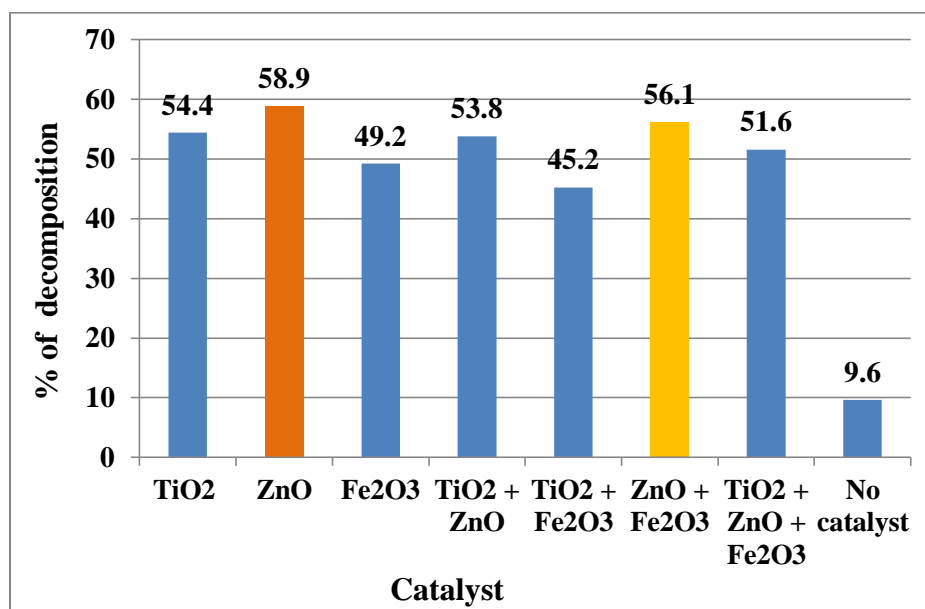


Figure 4.14 Effect of catalyst on % of decomposition of SIER-1

(Effluent conc. = 60%, Catalyst conc. = 200 ppm, pH = 6.7, Reaction time = 3 hrs, H_2O_2 = 300 ppm)

4.4.3 Comparison among decomposition processes

Comparison among various decomposition processes viz., catalytic, photolytic, and photocatalytic was observed to find the contribution and efficiency of each in the whole degradation process separately. Each process was carried out with or without H_2O_2 as the oxidizing agent. The photocatalyst, UV irradiation, and oxidizing agent

Chapter Four : Results and Discussion

are the major key players in the total decomposition process of effluent. The results are presented in Figure 4.15 shows the degradation efficiencies of these processes after 3 hrs of irradiation, and these follow the trends: photocatalytic (with H_2O_2) > photolytic (with H_2O_2) > photocatalytic (without H_2O_2) > catalytic (with H_2O_2) > catalytic (without H_2O_2) > with only H_2O_2 > photolytic (without H_2O_2). It is noticeable that the role of the oxidizing agent is very important in these decomposition processes as all the three processes without H_2O_2 showed poor performance. H_2O_2 increases the rate of hydroxyl radical formation, which is the main factor of dye decomposition (Guettai and Amar, 2005; Madhu *et al.*, 2007). Again, the single key players, i.e., photocatalyst, UV irradiation, and H_2O_2 achieved 10.9%, 9.61%, and 10.26% of decomposition, respectively, which proves that the contribution of each factor is almost equal in the whole degradation process. In the presence of ZnO without irradiation, slight decomposition was observed due to the adsorption of the dye on the surface of the catalyst. The study observed that these factors all together created a synergistic effect in the degradation process and thus the photocatalytic process with an oxidizing agent (H_2O_2) created the best decomposition result of 54.36%. Besides, the photolytic process with H_2O_2 also gave the second-best decomposition result of 48.6%.

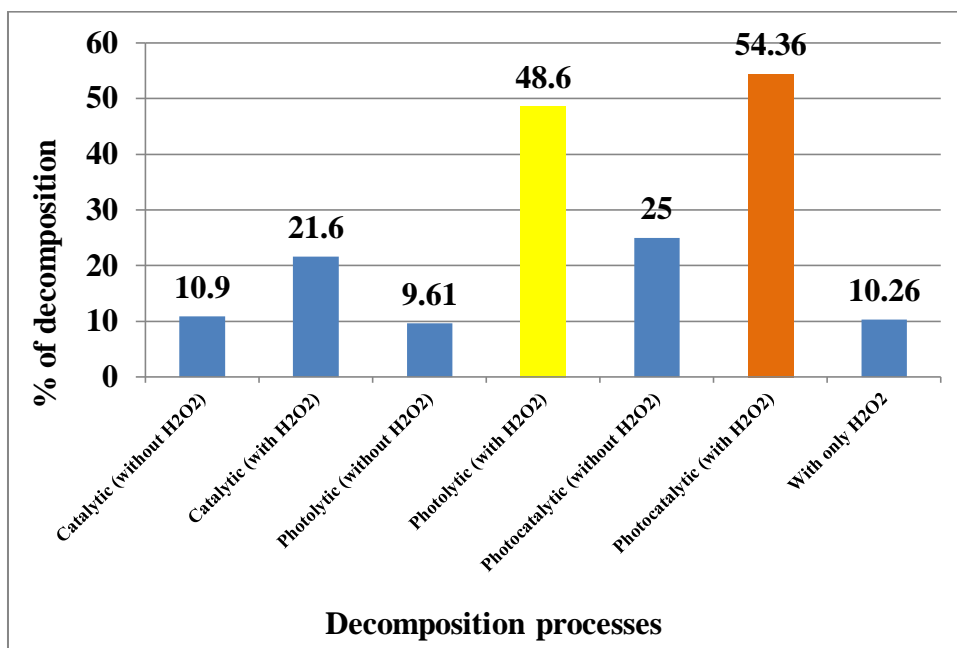


Figure 4.15 Comparison among various decomposition processes on 60% SIER-1

(Catalyst = ZnO, Catalyst conc. = 200 ppm, pH = 6.7, Reaction time = 3 hrs, H_2O_2 = 300 ppm)

4.4.4 Effect of irradiation time

The effect of irradiation time on the photocatalytic decomposition efficiency of different catalysts like TiO_2 , ZnO , Fe_2O_3 , and their combinations for SIER-1 was investigated for different periods up to 7 hrs under UV light. The results obtained are represented in Figure 4.16. The degradation increased from 25.2% at 1 hour to 79% at 7 hrs when ZnO was the photocatalyst. It was observed that during the first few hrs of reaction, the degradation rate was high, reaching 75.3 % for ZnO and 66.7% for TiO_2 after 5 hrs. Then, the degradation rate gradually decreased, reaching 79% for ZnO and 70.1% for TiO_2 after 7 hrs.

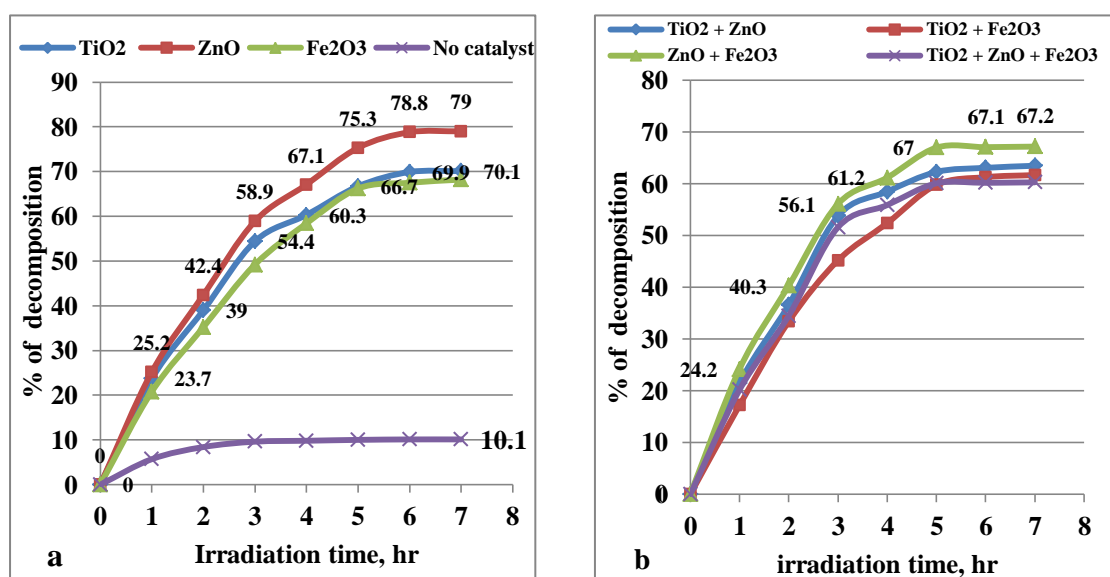


Figure 4.16 Effect of irradiation time on % of decomposition of SIER-1 by a) single catalysts and b) mixed catalyst. (Effluent conc. = 60%, Catalyst conc. = 200 ppm, pH = 6.7, H_2O_2 = 300 ppm)

This occurred because, in the beginning, the number of active sites on the catalyst surface remained high. As a result greater degradation rate was observed. The degradation rate was then gradually reduced because of catalyst consumption, i.e., reducing the active sites (Salama *et al.*, 2018). The study used TiO_2 for the photocatalytic decomposition of model textile wastewaters containing azo dyes where C.I Reactive Black 5 was degraded from 75% at 30 minutes to 93% at 120 minutes with 1 g/L of TiO_2 (Saggiaro *et al.*, 2011). The percentage of decomposition increases rapidly in the first few hrs of irradiation as the excitation of many electrons from the

valence to conduction bands of the photocatalysts generates lots of electron/hole (e^-/h^+) pairs in the photocatalyst surface, which are powerful for generating free radical oxidizers. Thereafter, there is a plateau that may result from the consumption of the catalyst (Alshabanat and AL-Anazy, 2018). Similar results were observed by other studies (Ghasemi *et al.* 2016; Che Ramli *et al.*, 2014). Beyond 5 hrs, the degradation didn't increase significantly. No better result was observed by the mixed catalyst for 7 hrs of irradiation time (Figure 4.16b). It is noticeable that for a 3 hrs reaction 58.9% decomposition was achieved and further reaction up to 7 hrs gave more decomposition. But for any industrial operation time is a factor and continuing any process over a longer period is cost-effective and less desirable. Therefore, it is wise to improve degradation efficiency by changing other parameters. Hence, the next experiments were carried out for 3 hrs of irradiation to optimize other parameters.

4.4.5 Photodegradation kinetics of SIER-1

Chemical kinetics is concerned with understanding the rates of chemical reactions. Kinetic studies are of fundamental importance in any investigation of the reaction mechanism. The results of photocatalysis of the textile effluent SIER-1 by different catalysts, i.e., TiO_2 , ZnO , and Fe_2O_3 and also without catalyst are shown in Figure 4.17.

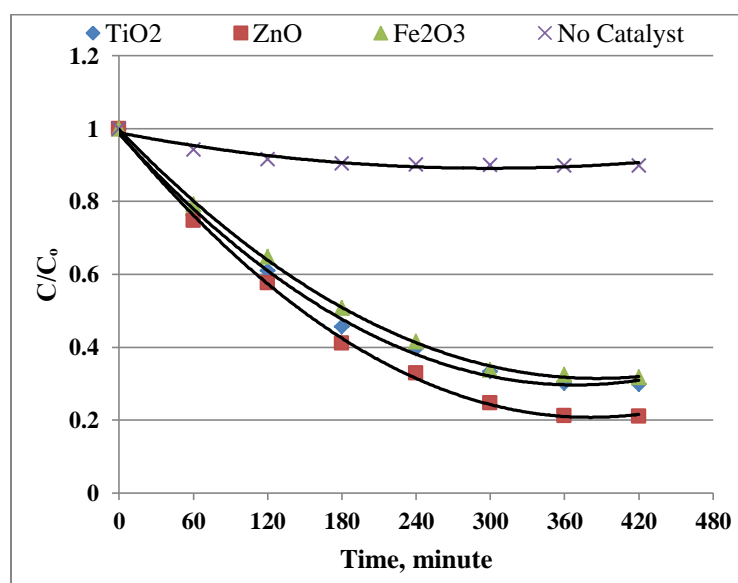


Figure 4.17 Photocatalytic degradation of SIER-1

(Effluent conc. = 60%, Catalyst conc. = 200 ppm, pH = 6.7, H_2O_2 = 300 ppm)

The change in concentration of the effluent (C/C_0) is plotted as a function of irradiation time (C_0 = the initial concentration of the bulk solution, C = concentration at time t). The study observed that both photocatalyst and a light source were necessary for the degradation reaction to occur. About 70-80% of the effluent degraded after 7 hrs of irradiation. In contrast, a negligible amount of degradation of effluents was observed by irradiation in the absence of a photocatalyst.

The graph of $\ln \frac{C_0}{C}$ versus time for the photocatalytic reactions by TiO_2 , ZnO , and Fe_2O_3 is shown in Figure 4.18, which supports the degradation of SIER-1 followed approximately pseudo-first-order kinetics. Neppolian *et al.* (2001) reported that the disappearance of a dye RY 17 in the solution followed approximately pseudo-first-order kinetics. Another research on the photocatalytic degradation pathway of MB in water also observed similar results (Houas *et al.*, 2001). The linear regression coefficients on the fitted lines were (R^2 =) 0.9983, 0.9877, and 0.9993 for ZnO , TiO_2 , and Fe_2O_3 , respectively. The rate constants of the photodegradation reactions by ZnO , TiO_2 , and Fe_2O_3 were calculated to be 4.74×10^{-3} , 3.88×10^{-3} , and $3.63 \times 10^{-3} \text{ min}^{-1}$, respectively. Abo-Farha, (2010) described that the photocatalytic degradation rate depends on dye structure, dye concentration, catalyst concentration, and pH of the medium.

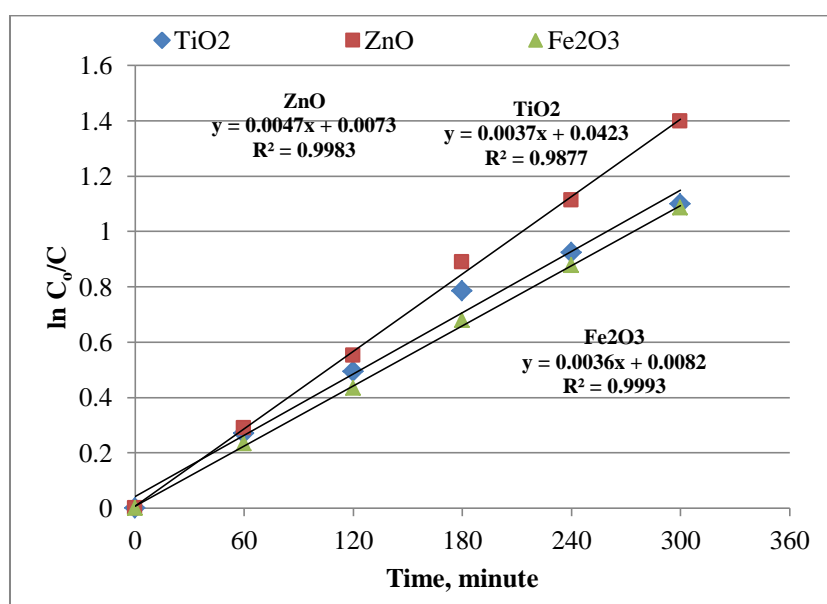


Figure 4.18 Kinetics of photodegradation of SIER-1

4.4.6 Effect of pH

Photocatalytic degradation experiments on SIER-1 by catalyst ZnO were performed at different pH values of 4 to 10. The results are shown in Figure 4.19. The results revealed that the photodegradation efficiency decreases with the increase in pH from 4 to 6. At low pH value (pH = 4) the photodegradation efficiency reached to 71%. When the pH value of effluent was increased from 4 to 6, the photodegradation efficiency decreased to 61% at pH 6. This is because the effluent might be negatively charged in an acidic medium, whereas ZnO is positively charged below pH 8, which is reported as pH of point of zero charges (pzc) for ZnO (Daneshvar *et al.*, 2007). So the increasing pH value tends to change the charge on ZnO from positive to negative by adsorbing HO^- ions, which favors the formation of $\text{HO}\cdot$ (Wang *et al.*, 2007) and consequently, the photocatalytic activity decreased due to the increase of the electrostatic repulsion between ZnO and anionic effluent gradually. Besides, electron/hole (e^-/h^+) pairs recombination rate might be increased by an increase in pH and thus, photocatalytic activity decreased (El-Bahy *et al.*, 2009). But further, at pH 10 of the effluents, the photodegradation efficiency achieved was 75.6%, which was the highest in pH ranges.

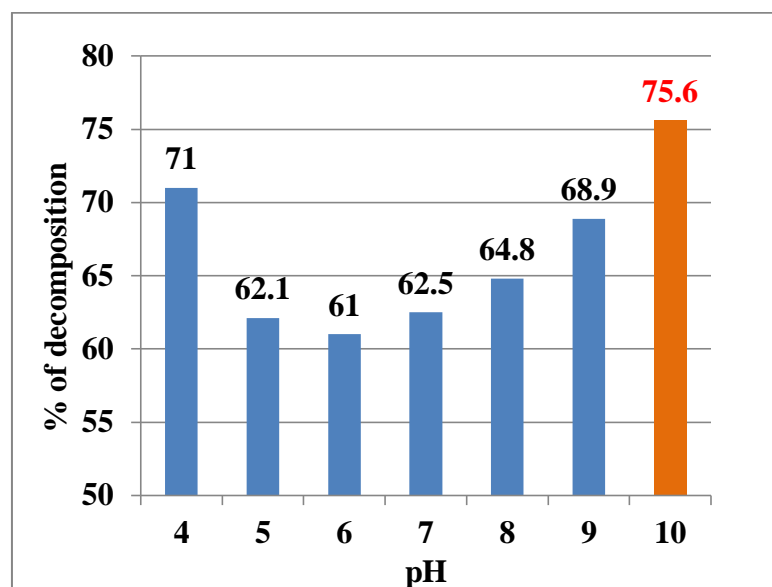


Figure 4.19 Effect of pH on % of decomposition of 60% SIER-1

(Catalyst = ZnO, Catalyst conc. = 200 ppm, Reaction time = 3 hrs, H_2O_2 = 300 ppm)

The reason may be a larger amount of OH^- available to react with the h^+ on the ZnO surface resulting in a larger production of $\text{HO}\cdot$ which is the main species for degradation. pH is a vital parameter in photocatalytic degradation as it determines the surface charge properties of the catalysts and dye molecules, aggregates size, adsorption on the catalyst surface, and the concentration of hydroxyl radicals (Sakthivel *et al.*, 2003; Aguedach *et al.*, 2005).

Understanding pH effects on photocatalytic decomposition is difficult since three probable reaction mechanisms can at a time contribute to the degradation process : (1) hydroxyl radical attack, (2) direct oxidation by the positive hole, and (3) direct reduction by the electron in the conducting band. Each one's contribution is determined by the substrate's properties and pH. (Tang *et al.* 1997). The solution pH influences the sorption–desorption processes and the separation of photogenerated electron/hole (e/h^+) pairs in the surface of semiconductor particles by altering the electrical double layer of the solid electrolyte interface. (Reza *et al.*, 2017). So, the optimal pH value for the photodegradation of SIER-1 was selected as $\text{pH} = 10$. Similar results were reported by Alkaykh and Ali-Shattle (2020), illustrated that photocatalytic degradation of MB in aqueous solution by MnTiO_3 nanoparticles under sunlight irradiation was favored in an alkaline medium.

4.4.7 Effect of catalyst concentration

The effect of different amounts of photocatalysts ZnO and TiO_2 viz., 100, 200, 300, and 400 ppm on the photocatalytic decomposition of SIER-1 for 3 hrs at pH 10 was investigated. The results showed that the degradation efficiency increased to reach a maximum value of about 76.1% with a catalyst dose of 300 ppm in the case of ZnO (Figure 4.20). The reason is that number of active sites for photocatalytic reaction increases due to an increase in catalyst concentration, which leads to higher production of $\text{OH}\cdot$ radicals up to the catalyst dose of 300 ppm. Further increase in the concentration of ZnO to 400 ppm resulted in a decrease in degradation percentage. The photocatalyst degradation efficiency was found highest at 100 ppm and decreased when the catalyst concentration was increased from 100 ppm to 400 ppm in the case of TiO_2 .

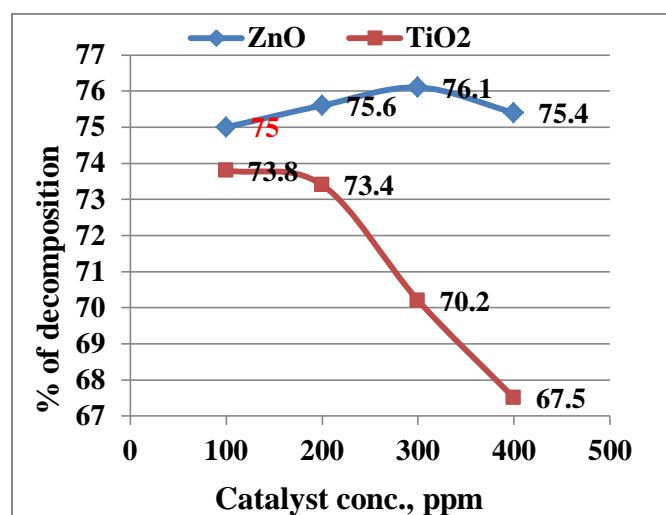


Figure 4.20 Effect of catalyst concentration on % of decomposition of SIER-1

(Effluent conc. = 60%, pH=10, Reaction time = 3 hrs, H₂O₂ = 300 ppm)

This was probably because further increases in catalyst dose increased turbidity and reduced the amount of light penetration in the effluent solution (Nomikos *et al.*, 2014; Martínez *et al.*, 2011). Another reason behind this phenomenon is the catalyst-powder agglomeration and the subsequent decrease in the active surface sites (Tayeb and Hussein, 2015). The results are in good agreement with those reported in the literature (Mills *et al.*, 1993; Chen and Mao, 2007). In all experiments, ZnO showed better degradation efficiency than TiO₂. Although a catalyst dose of 300 ppm shows the highest degradation (76.1%) in the case of ZnO, the dose of 100 ppm shows a degradation efficiency of 75% which is not much lower than the highest value. Hence for commercial purposes, 100 ppm concentration of ZnO catalyst should be the optimum choice.

4.4.8 Effect of oxidizing agent (H₂O₂) dose

The effect of oxidizing agent dose on the photodegradation of SIER-1 using the catalyst ZnO at pH 10 for 3 hrs was studied. Different photocatalytic degradation experiments were carried out by varying H₂O₂ doses viz., 200, 300, 400, 500, 600, and 700 ppm. The results are represented in Figure 4.21, which indicates that the percentage of photocatalytic decomposition increases with increasing concentration of H₂O₂. A higher concentration of H₂O₂ liberated more hydroxyl free radicals, which caused the dye decomposition. Oxidizing agents greatly enhance the photodegradation

rates (Guettai and Amar, 2005; Madhu *et al.*, 2007). The degradation increased from 68.4% at 200 ppm of H₂O₂ to 81.6% at 500 ppm of H₂O₂.

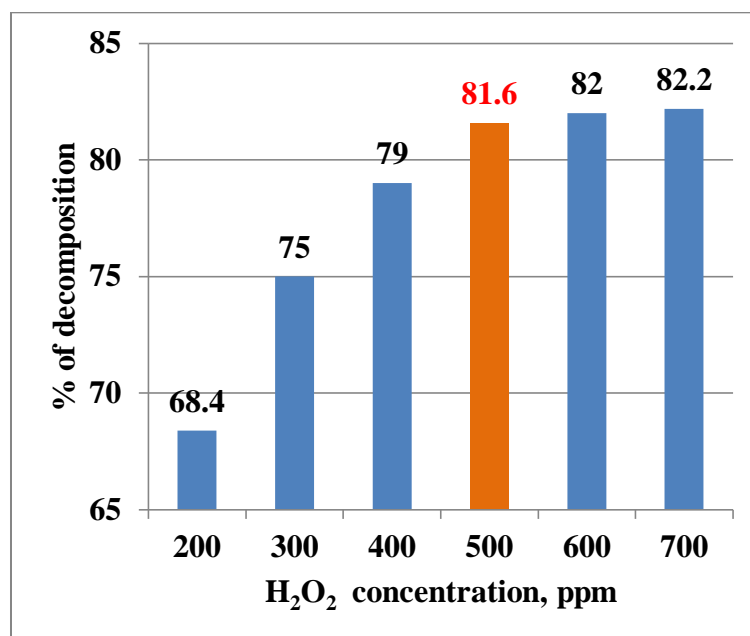


Figure 4.21 Effect of H₂O₂ dose on % of decomposition of SIER-1

(Effluent conc. = 60%, Catalyst = ZnO, Catalyst conc. = 100 ppm, pH= 10, Reaction time = 3 hrs)

Further increase in H₂O₂ dose (from 500 ppm to 700 ppm) had no significant effect on the degradation percentage. At a higher concentration of H₂O₂ reaction, the solution becomes acidic resulting in reduced decomposition rates. However, an increase in the H₂O₂ concentration beyond certain limits (critical concentration) does not increase the reaction rates as it tends to act as a hydroxyl radical scavenger instead of a free radical generator (Baxendale and Wilson, 1957; Guettai and Amar, 2005). Although in the H₂O₂ dose of 700 ppm, the highest degradation (82.2%) was observed, the dose of 500 ppm showed a degradation efficiency of 81.6%, which was not lower than the highest value. Hence for the commercial purpose, 500 ppm was considered as the optimum value of H₂O₂ loading for the photocatalytic degradation of SIER-1.

4.4.9 Mineralization of SIER-1

The extent of mineralization of SIER-1 by photocatalytic treatment was studied by measuring the COD and TOC values of the effluent before and after the treatment. The results are shown in Table 4.7. The results showed that excellent mineralization

of the effluent was observed as the TOC reduced was about 97.7%. It also showed that the TOC value decreased from 833 to 17 mg/L after 3 hrs of photocatalytic treatment. The results of two individual studies showed that about 89% and 80-82% of TOC reduction were achieved by Bulc and Ojstršek, (2008) and Ghaly *et al.*, (2014), respectively. The results obtained in these photocatalytic reduction studies were lower than that of the present study. The results showed that the COD of the effluent decreased from 2550 to 1440 mg/L by the treatment under the same conditions indicating 43.53% COD reduction. The results showed that the COD of the effluent decreased from 2550 to 1440 mg/L by the treatment under the same conditions indicating 43.53% COD reduction. It is observed that the COD reduction (43.53%) was lower than the concentration reduction (81.6%) of SIER-1 under optimized conditions, which may be due to the chromophore destruction resulting in the formation of smaller uncolored degraded products. Kulkarni and Thakur, (2014) conducted a study on photocatalytic degradation of textile industrial effluent by ZnO and they reported 37.5% COD reduction by 400 ppm catalyst for 5 hrs. The study finding was supported by another research result where a 29.2 % reduction in COD was achieved using a 500 ppm ZnO for 4 hrs of UV irradiation (Mondal and Bhagchandani, 2016).

Table 4.7 Reduction in TOC and COD of SIER-1 by photocatalytic treatment at optimized conditions

Parameters	Before treatment (mg/L)	After treatment (mg/L)	% of reduction
TOC	833	17	97.9
COD	2550	1440	43.53

(Effluent conc. = 60%, Catalyst = ZnO, Catalyst conc. = 100 ppm, pH= 10, Reaction time = 3 hr, H₂O₂ = 500 ppm)

4.4.10 Optimized parameters for the photodegradation of SIER-1

The study results showed that the textile effluent SIER-1 could be efficiently photocatalytically degraded using ZnO catalyst under UV irradiation. Photodegradation was maximum in an alkaline medium, and the degradation efficiency was influenced by the process parameters like catalyst concentration, dye concentration, irradiation time, oxidizing agent dose, and pH. The optimum catalyst dose for the degradation of 60%

Chapter Four : Results and Discussion

SIER-1 was 100 ppm of ZnO. TOC analysis of the effluent showed about 97.9% reductions in TOC under optimized conditions whereas, the COD reduction in the same conditions was 43.53%. The addition of oxidants like H₂O₂ enhanced the degradation significantly. The optimized values for the photocatalytic degradation of 60% SIER-1 are shown in Table 4.8. The maximum 81.6 % decomposition was achieved at the optimized parameters.

Table 4.8 Optimized parameters for the photocatalytic degradation of 60% SIER-1

Parameters	Optimized values
Catalyst	ZnO
Catalyst concentration	100 ppm
Irradiation time	3.0 hrs
pH	10
Oxidizing agent (H ₂ O ₂) concentration	500 ppm
Maximum decomposition achieved = 81.6 %	

4.5 Photocatalytic decomposition of Silk Industry Effluent, Rajshahi-2 (SIER-2)

This textile effluent SIER-2 (Silk Industry Effluent, Rajshahi-2) was collected from a silk industry at BSCIC, Rajshahi was light red color and almost neutral (pH=6.8). Like SIER-1, SIER-2 was also highly concentrated and so necessary dilution was made for conducting the photocatalytic decomposition study. Further, all calculations were done based on the diluted effluent. The decomposition performance of ZnO, TiO₂, and Fe₂O₃ photocatalysts was investigated by treatment on SIER-2 under UV light. The effect of variable parameters like initial effluent concentration, irradiation time, catalyst type and doses, pH, and oxidizing agent doses on the photocatalytic degradation efficiency were analyzed. The percentage of degradation was estimated in terms of reducing the COD and TOC. The concentration of the effluent was determined using the absorbance recorded on a UV-spectrophotometer at a wavelength of 414 nm (λ_{\max}).

4.5.1 Effect of initial effluent concentration

The effect of initial concentrations of SIER-2 (20%, 40%, 60%, 80%, and 100%) on their photocatalytic decomposition by TiO₂ at pH 6.8 (effluent's normal pH) was investigated. The results are represented in Figure 4.22, and it indicates that the percentage of photocatalytic decomposition decreased as the concentration of the effluents was increased. It showed that the percentage of decomposition decreased from 100 to 42.9% in 3 hrs, when the concentration of the effluents increased from 20 to 100%. The possible explanation for this behavior is that as the initial concentration of the effluent was increased, the path length of the photons entering the solution decreased, thereby decreasing the number of photon absorption by the catalyst surface at a higher concentration (Davis *et al.*, 1994). When the concentration of the dyeing effluent is raised, the dye molecules act as a filter for the incident UV radiation. Thus, the desired light intensity fails to reach the catalyst surface, and the percentage of degradation decreases (Ameta *et al.*, 2013). The same effect was observed by Neppolian *et al.* (2002a) during the photocatalytic degradation of three commercial textile dyes: Reactive Yellow, Reactive Red, and Reactive Blue. They found that

when initial dye concentration was increased from 0.0001 M to 0.0005 M, degradation fell from 98% to 32%, which supported the present findings. However, although 20% and 40% SIER-2 solutions showed better degradation percentages than others, for the optimization of other parameters, 60% SIER-2 was selected.

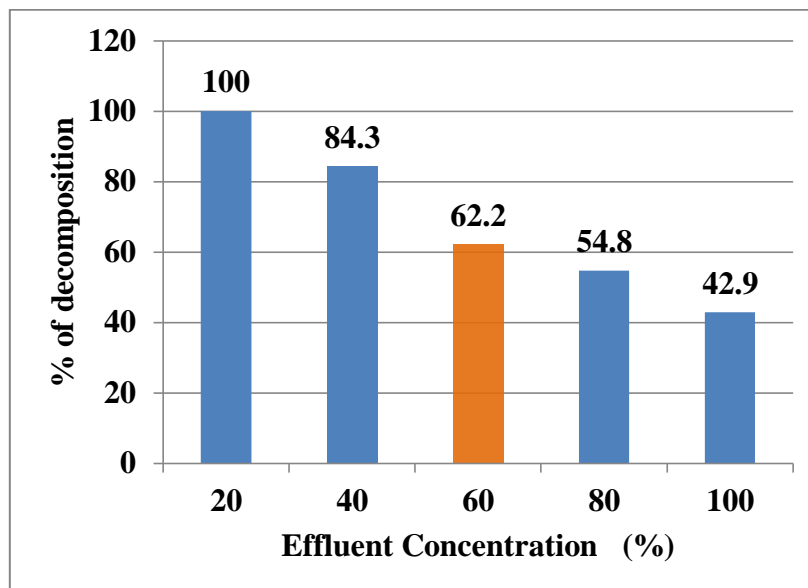


Figure 4.22 Effect of initial effluent concentrations on % of decomposition of SIER-2
(Catalyst = TiO₂, Catalyst conc. = 400 ppm, pH = 6.8, Reaction time = 3 hrs, H₂O₂ = 300 ppm)

4.5.2 Effect of catalyst

The decomposition efficiency of different photocatalysts, i.e., TiO₂, ZnO, Fe₂O₃, and their mixtures under UV light for the SIER-2 was examined. The results are represented in Figure 4.23. It is shown that the degradation efficiency of mixed catalysts was higher than that of single catalysts for SIER-2 in most cases, which might be because they acted as catalyst promoters. The maximum 71.5 % degradation of the effluent was achieved by Fe₂O₃. The next better photodegradation efficiency was shown by the mixed catalysts TiO₂+ZnO (1:1), and TiO₂+Fe₂O₃ (1:1) where degradation was 71.33% and 71.2%, respectively. When TiO₂, ZnO, and Fe₂O₃ were used for 3 hrs under the same conditions 62.22, 69.17, and 71.5% of degradation occurred, respectively. Their photocatalytic decomposition efficiency after 3 hrs of irradiation was of the following order: Fe₂O₃ > (TiO₂+ZnO) > (TiO₂+Fe₂O₃) > (TiO₂+ZnO+Fe₂O₃) > ZnO > (ZnO+Fe₂O₃) > TiO₂. There was no significant difference among the degradation percentages (71.5, 71.33, and 71.2%) achieved by

Fe_2O_3 , TiO_2+ZnO (1:1), and $\text{TiO}_2+\text{Fe}_2\text{O}_3$ (1:1) respectively. Maji *et al.* (2012) conducted research on the synthesis and photocatalytic activity of $\alpha\text{-Fe}_2\text{O}_3$ nanoparticles and observed that the prepared $\alpha\text{-Fe}_2\text{O}_3$ nanoparticles showed better photoactivity than that of the Commercial TiO_2 (Degussa-P25). Research on photocatalytic degradation of MB by nanostructured Fe/FeS powder under visible light illustrated that three and a half hrs of irradiation was able to degrade about 50% of dye (Esmaili *et al.*, 2018). The present study showed a comparatively better result, i.e., 71.54 % degradation of the dye solution was achieved by the catalyst Fe_2O_3 within 3 hrs. The study also found that the extent of degradation by photocatalysts varies among different effluents, and it is related to the nature of both effluents and catalysts. Figure 4.23 illustrated that Fe_2O_3 is the most suitable catalyst for the photocatalytic degradation of this specific effluent. Hence, Fe_2O_3 was selected as the photocatalyst for the optimization of other parameters.

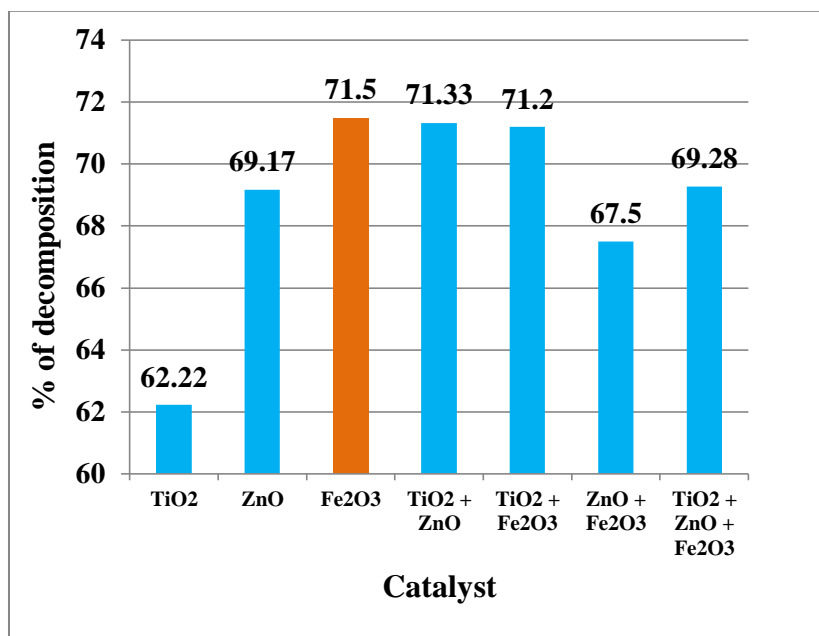


Figure 4.23 Effect of catalyst on % of decomposition of SIER-2

(Effluent conc. = 60%, Catalyst conc. = 400 ppm, pH = 6.8, Reaction time = 3 hrs, H_2O_2 = 300 ppm)

4.5.3 Comparison among decomposition processes

In a total photocatalytic decomposition process, each of catalyst, UV radiation, and an oxidizing agent has its contribution. Some experiments were carried out to find the contribution and efficiency of each decomposition processes viz., catalytic, photolytic, and photocatalytic. Each process was conducted with or without H_2O_2 as

the oxidizing agent. The results are presented in Figure 4.24, and it illustrated that the degradation efficiencies of these processes after 3 hrs of irradiation were of the following trends: photocatalytic (with H₂O₂) > photolytic (with H₂O₂) > photocatalytic (without H₂O₂) > photolytic (without H₂O₂) > with only H₂O₂ > catalytic (with H₂O₂) > catalytic (without H₂O₂). Photocatalysts, UV irradiation, and oxidizing agent are the major key factors of a total decomposition process of an effluent. The oxidizing agent played a vital role in these decomposition processes as most processes without H₂O₂ showed poor performance. The reason is that H₂O₂ increases the rate of hydroxyl radical formation, which is the main factor of dye decomposition (Guettai and Amar, 2005; Madhu *et al.*, 2007). Again the single key factors such as the photocatalyst, UV irradiation, and H₂O₂ achieved 1%, 16.8%, and 11% of decomposition, respectively, which proves that UV light had the highest contribution in the total decomposition process. The factors all together created a synergistic effect in the degradation process and thus the photocatalytic process with an oxidizing agent (H₂O₂) created the best decomposition result of 83.7%. Besides, the photolytic process with H₂O₂ also gave the second-best decomposition result of 74.4%.

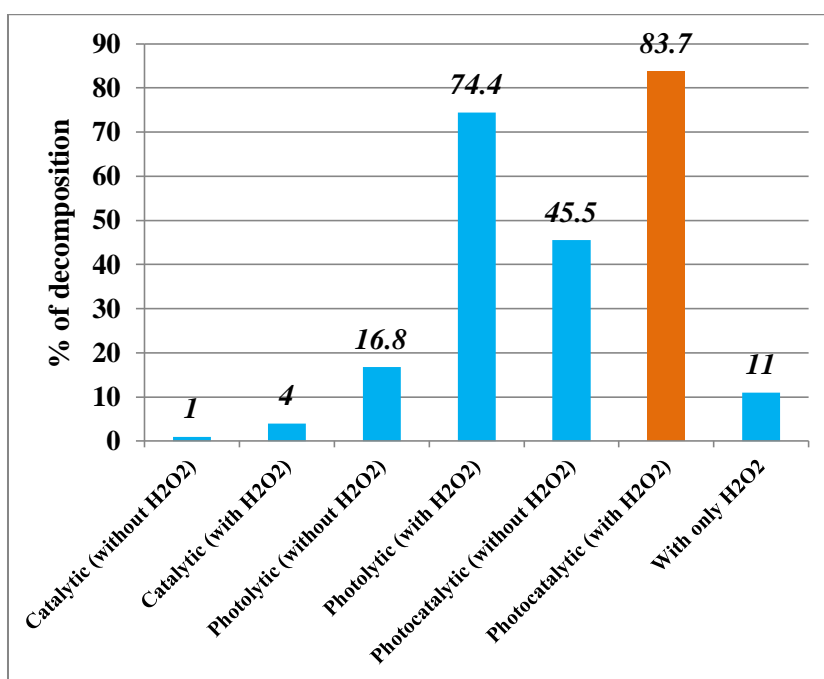


Figure 4.24 Comparison among different decomposition processes on SIER-2

(Catalyst = Fe₂O₃, Catalyst conc. = 400 ppm, pH = 6.8, Reaction time = 3 hrs, H₂O₂ = 300 ppm)

4.5.4 Effect of irradiation time

The effect of irradiation time on the photocatalytic decomposition efficiency of different catalysts like TiO₂, ZnO, Fe₂O₃, and their combinations for SIER-2 was investigated for different periods up to 7 hrs under UV light. The results indicated that in the case of Fe₂O₃ the degradation increased from 33.6% to 94.3% for the period from 1 to 7 hrs. (Figure 4.25). The figure shows that the degradation increased sharply with time and reached a maximum of five hours and then slowly increased with time. It means that the photocatalysts have potential in the degradation process. The results showed that the degradation reached the maximum of 92.8 % for ZnO and 84.42% for TiO₂ after 7 hrs.

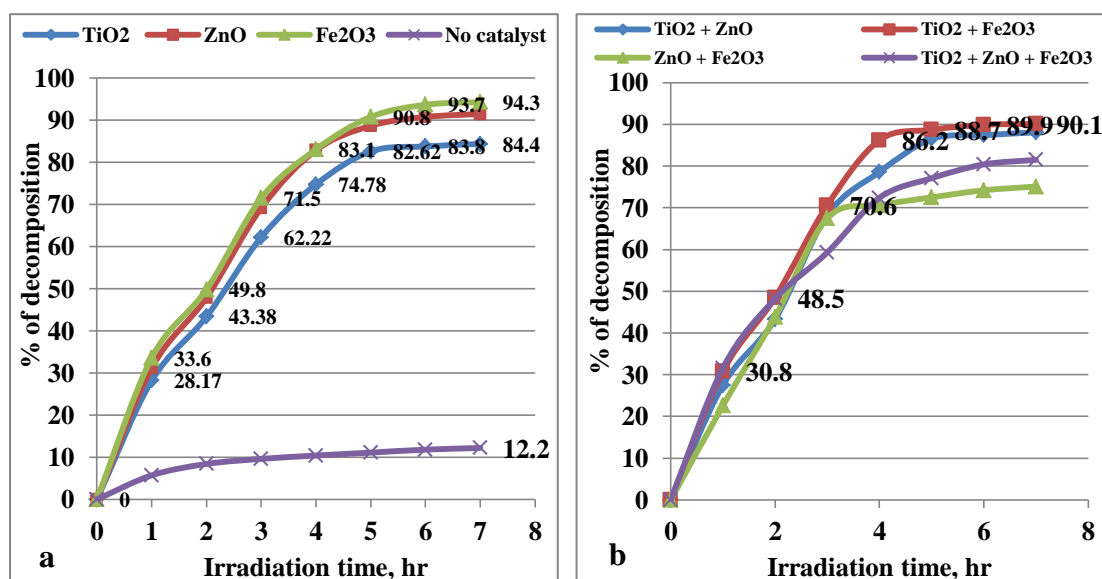


Figure 4.25 Effect of irradiation time on % of decomposition of SIER-2 by a) single catalysts and b) mixed catalyst.

(Effluent conc. = 60%, Catalyst conc. = 400 ppm, pH = 6.8, H₂O₂ = 300 ppm)

Afterward, the degradation rate gradually decreased, reaching 94.3 and 84.4% for Fe₂O₃ and TiO₂, respectively, after 7 hrs. This occurred because many electrons were excited from the valence to conduction bands at the start of the process generating plenty of hydroxyl free radicals which are mainly responsible for degradation. Thereafter, due to the consumption of the catalyst, this process slowed down resulting in a decrease in the degradation rate (Alshabanat and AL-Anazy, 2018). Salama *et al.* (2018) described that in the first hour of irradiation exposure the number of active

sites on the catalyst surface remained high. As a result greater degradation rate was observed. The degradation rate was then gradually reduced because of catalyst consumption. Similar results were observed by other studies (Ghasemi *et al.* 2016; Che Ramli *et al.*, 2014). No better result was observed by the mixed catalyst for 7 hrs of irradiation time (Figure 4.25b). Erdemoğlu *et al.* (2008) also observed the same effect in the photocatalytic degradation of Congo Red by hydrothermally synthesized nanocrystalline TiO₂. It is noticeable that for a 3 hrs reaction 71.5% decomposition of SIER-2 was found with Fe₂O₃ and more decomposition was possible by further reaction up to 7 hrs. But for any industrial operation time is a factor and continuing any process over a prolonged period is not desirable because it is cost-effective. Therefore, it is reasonable to improve degradation efficiency by optimizing other parameters. Hence, the next experiments were carried out for 3 hrs of irradiation time to optimize other parameters.

4.5.5 Photodegradation kinetics of SIER-2

Chemical kinetics is related with understanding the rates of chemical reactions. Kinetic studies are of fundamental importance in any investigation of the reaction mechanism. Experiments on 60% SIER-2 solution were conducted by UV irradiation in the presence of 400 ppm of different photocatalysts viz., TiO₂, ZnO, and Fe₂O₃ and also without a catalyst.

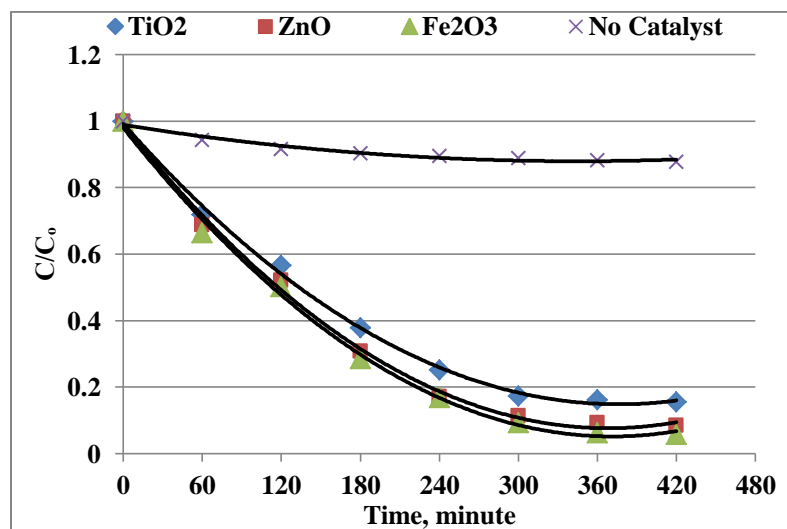


Figure 4.26 Photocatalytic degradation of SIER-2

(Effluent conc. = 60%, Catalyst conc. = 400 ppm, pH = 6.8, H₂O₂ = 300 ppm)

The change in concentration of the solution (C/C_0) is plotted as a function of irradiation time (C_0 = the initial concentration of the bulk solution, C = concentration at time t). The study observed that both photocatalyst and a light source were necessary for the degradation reaction to occur. Figure 4.26 shows that negligible degradation was observed without any catalyst in the presence of only UV light. However, when the dye solution was irradiated with photocatalysts, 80-90% degradation of the effluent was achieved within 7 hrs of irradiation.

The graph of $\ln \frac{C_0}{C}$ versus time for photocatalytic reaction by TiO_2 , ZnO , and Fe_2O_3 is shown in Figure 4.27 (almost straight line) which indicates that the degradation of SIER-2 followed nearly pseudo-first-order kinetics. Mukhlish *et al.* (2013) conducted a study on the photocatalytic degradation kinetics of MB and Congo Red and observed that the first-order and Freundlich model fit the kinetic data well. Houas *et al.* (2001) studied the photocatalytic degradation pathway of MB in water and observed similar results. Another research reported that the disappearance of a dye Reactive Yellow 17 in the solution followed approximately pseudo-first-order kinetics (Neppolian *et al.*, 2001). The linear regression coefficient of determination ($R^2 =$) on the fitted lines was 0.9863, 0.9879, and 0.9938 for Fe_2O_3 , ZnO , and TiO_2 , respectively, indicating that the best-fitted line obtained for TiO_2 .

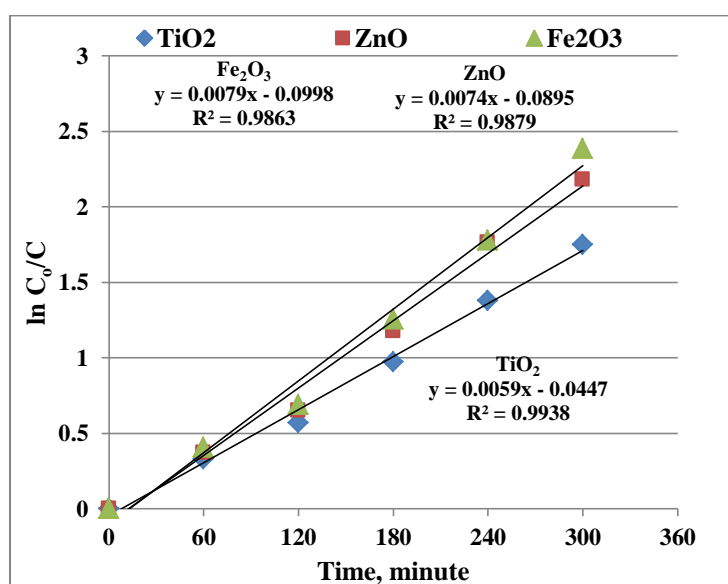


Figure 4.27 Kinetics of photodegradation of SIER-2

The rate constants of the photodegradation reactions by Fe₂O₃, ZnO, and TiO₂ were calculated to be 7.4×10^{-3} , 6.98×10^{-3} , and $5.73 \times 10^{-3} \text{ min}^{-1}$, respectively. The photocatalytic degradation rate depends on dye structure, dye, and catalyst concentration, and pH of the medium (Abo-Farha, 2010).

4.5.6 Effect of pH

Wastewater containing dyes are discharged at different pH. So, it is important to study the role of pH on their decomposition. The pH of the effluent may vary according to the type of dyes used and the organic and inorganic compounds added to it (Harikumar *et al.*, 2013). In the present study, the effect of pH of the effluent, SIER-2 on the percentage photodegradation was examined in the range of 3–11 for constant effluent concentration (60%) and 400 ppm of catalyst (Fe₂O₃) loading. Figure 4.28 shows the decomposition efficiency of SIER-2 as a function of pH. The results revealed that the photodegradation efficiency increased with the increase in pH from 3 to 7 and then decreased with increasing the pH.

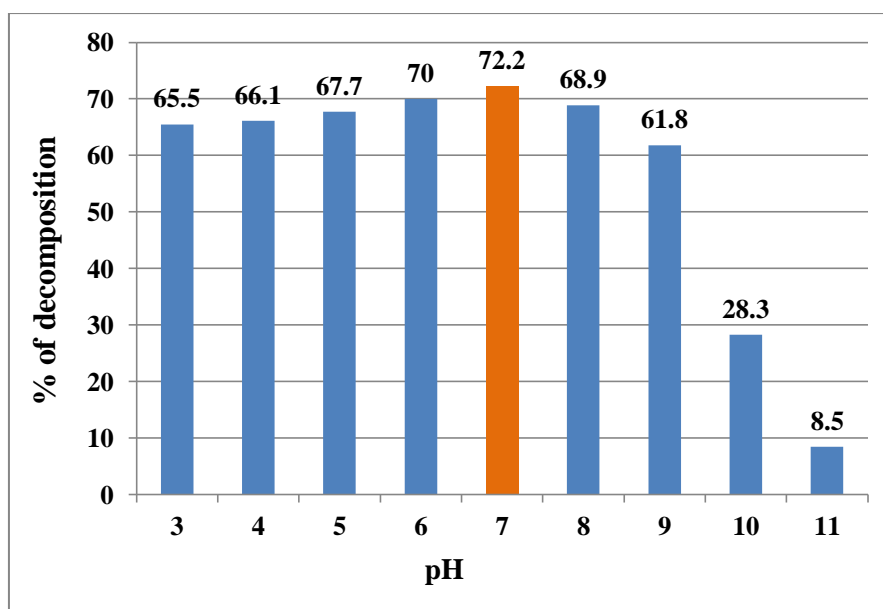


Figure 4.28 Effect of pH on % of decomposition of 60% SIER-2

(Catalyst = Fe₂O₃, Catalyst conc. = 400 ppm, Reaction time = 3 hrs, H₂O₂ = 300 ppm)

The effect of pH on photodegradation efficiency is very difficult to interpret. This is because three possible reaction mechanisms can contribute to dye degradation, (1) hydroxyl radical attack, (2) direct oxidation by the positive hole, and (3) direct

reduction by the electron in the conducting band. The contribution of each one depends on the substrate nature and pH (Tang *et al.*, 1997). At low pH value (pH = 3) the decomposition achieved was 65.5%. When the pH value of effluent increased from 3 to 7, the decomposition increased to 72.2% at pH 7. The reason for the increase in decomposition up to pH 7 might be due to strong adsorption of the dye onto the catalyst surface as a result of the electrostatic attraction between the positively charged catalyst and the ionized dye.

A decrease in the decomposition was observed, with a minimum at pH 11, reflected the difficulty of anionic dye in approaching the negatively charged catalyst surface when increasing the solution pH. Similar results were observed by Harikumar *et al.* (2013) in the case of photocatalytic degradation of Alizarin Red S by TiO₂. The effects of pH on the photocatalytic degradation of dibutyl phthalate (DBP) were investigated using α -Fe₂O₃ nanoparticles, and the results were in good agreement with the present study. They also observed higher degradation under the neutral conditions (Liu *et al.*, 2018). The reason for this might also be that at a higher pH value, the hydroxyl radicals are so rapidly scavenged that they do not have the opportunity to react with dyes (Neppolian *et al.* 2003; Tang *et al.* 1997). Based on the results shown in Figure 4.28, the optimal pH was selected as 7.

4.5.7 Effect of catalyst concentration

The effect of different amounts of photocatalyst Fe₂O₃, i.e., 200 to 700 ppm on the photocatalytic decomposition of SIER-2 for 3 hrs at pH 10 was investigated. The results showed that the degradation efficiency increased to reach a maximum value of about 72.2% with a catalyst dose of 400 ppm (Figure 4.29). The reason is that number of active sites for photocatalytic reaction increases due to an increase in catalyst concentration, which leads to higher production of OH• radicals up to the catalyst dose of 400 ppm. Further, an increase in concentration up to 700 ppm resulted in a decrease in degradation efficiency. This was probably because catalyst loading beyond 700 ppm contributed to additional opacity in liquid and light scattering by Fe₂O₃ particles, which caused a decrease in the photocatalytic active volume of the reactor (Nomikos *et al.*, 2014; Martínez *et al.*, 2011). Another reason behind this

phenomenon is an aggregation of catalyst particles is enhanced at high concentrations and subsequently active surface sites decrease (Tayeb and Hussein, 2015). Similar observations were reported by many researchers (Liu *et al.*, 2018; Chen and Mao, 2007). Based on the results shown in Figure 4.29, the optimal catalyst dose was selected as 400 ppm.

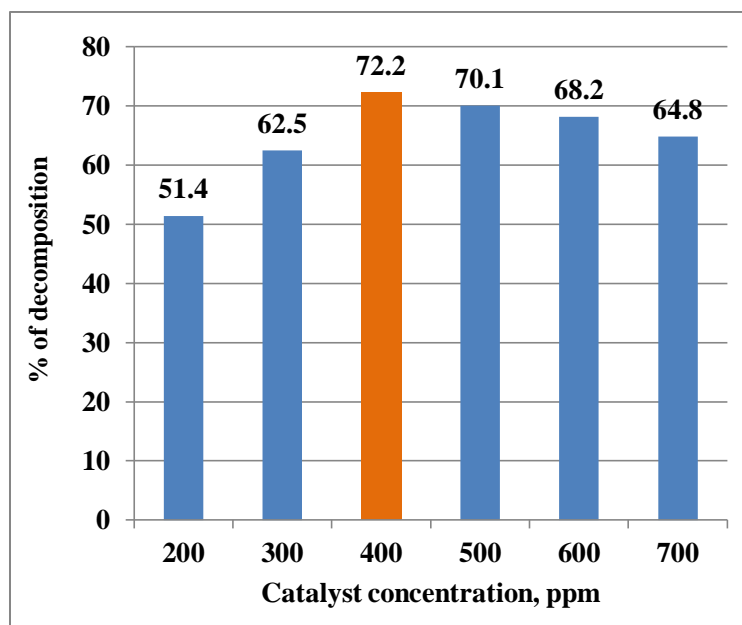


Figure 4.29 Effect of catalyst concentration on % of decomposition of SIER-2
(Effluent conc. = 60%, Catalyst = Fe₂O₃, pH=7, Reaction time = 3 hrs, H₂O₂ = 300 ppm)

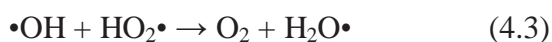
4.5.8 Effect of oxidizing agent (H₂O₂) dose

The effect of H₂O₂ doses viz., 200, 300, 400, 500, and 600 ppm on the photodegradation of SIER-2 by the catalyst Fe₂O₃ at pH 7 for 3 hrs was studied. The results are represented in Figure 4.30, which indicates that the percentage of decomposition increased with increasing concentration of H₂O₂. The addition of H₂O₂ as an oxidizing agent can increase the rate of hydroxyl radical formation, which is the key factor of dye decomposition (Guettai and Amar, 2005; Madhu *et al.*, 2007). According to Madhu *et al.* (2007), H₂O₂ has major effects as an oxidizing agent on photocatalytic degradation rates. H₂O₂ can be photolyzed to produce a hydroxyl radical group under light irradiation according to the following reaction:



Chapter Four : Results and Discussion

The degradation increased from 57% at 200 ppm to 97.1% at 500 ppm of H₂O₂. Further, an increase in H₂O₂ dose had no significant effect on the degradation percentage. This was because, when the H₂O₂ addition exceeded the critical value, the generation of •OH was inhibited. After all, excessive H₂O₂ had a capture effect on •OH, resulting in a decrease in degradation efficiency, which can be described by the following reactions (Liu *et al.*, 2018):



An increase in the H₂O₂ concentration beyond certain limits (critical concentration) did not increase the reaction rates as it tends to act as a hydroxyl radical scavenger instead of a free radical generator (Baxendale and Wilson, 1957; Guettai and Amar, 2005). Hence according to the results shown in Figure 4.30, the optimum value of H₂O₂ loading for the photocatalytic degradation of SIER-2 can be considered 500 ppm.

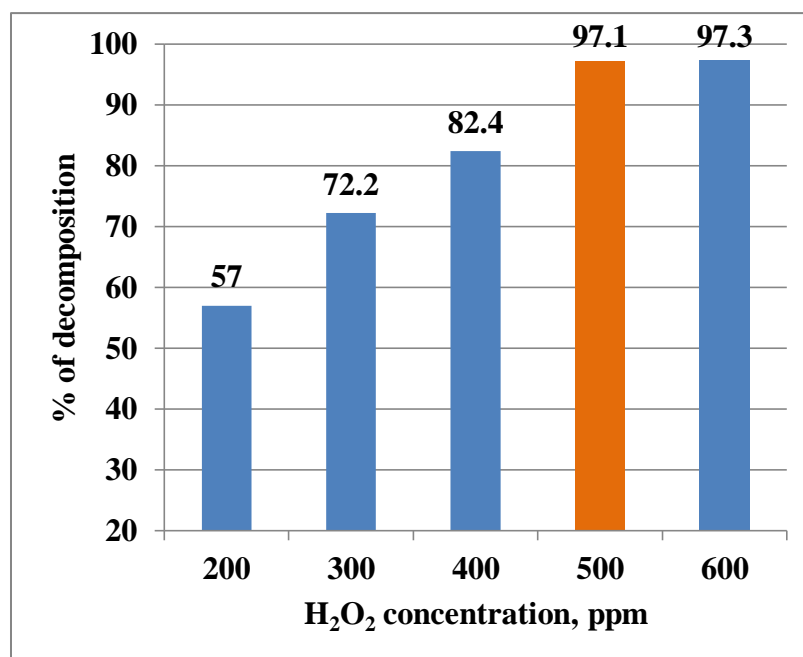


Figure 4.30 Effect of H₂O₂ dose on % of decomposition of SIER-2

(Effluent conc. = 60%, Catalyst = Fe₂O₃, Catalyst conc. = 400 ppm, pH=7, Reaction time = 3 hrs)

4.5.9 Mineralization of SIER-2

Mineralization study was done along with decomposition studies to evaluate the reduction in COD and TOC during photocatalysis of SIER-2. This was done by measuring the COD and TOC values of the effluent before and after the treatment at optimized conditions. The results are shown in Table 4.9. Good mineralization of the effluent was observed as the TOC values decreased from 874 to 329 mg/L after 3 hrs of photocatalytic treatment. It indicated that about 62.35% reductions whereas the decomposition was 97.1% at the same conditions. Kusvuran *et al.* (2004) also observed that greater decomposition of RR120 was accompanied by lesser TOC reduction indicating that stable intermediates had been formed. It has been observed that such stable intermediates include strongly recalcitrant chemicals, such as acetic acid (Kacar *et al.*, 2003). Bulc and Ojstršek, (2008) and Ghaly *et al.*, (2014) reported 89% and 80-82% of TOC reduction in their studies respectively, which support the present study results. The COD of the effluent decreased from 2670 to 1580 mg/L by the treatment under the same conditions indicating a 40.82% COD reduction. Research on the photocatalytic degradation of textile industrial effluent by 400 ppm ZnO catalyst reported 37.5% COD reduction for 5 hrs (Kulkarni and Thakur, 2014). The result of the present study is also supported by another research result where a 29.2 % reduction in COD was achieved by 500 ppm ZnO for 4 hrs of UV irradiation (Mondal and Bhagchandani, 2016).

Table 4.9 Reduction in TOC and COD of SIER-2 by photocatalytic treatment at optimized conditions

Parameters	Before treatment (mg/L)	After treatment (mg/L)	% of reduction
COD	2670	1580	40.82
TOC	874	329	62.35

(Effluent conc. = 60%, Catalyst = Fe₂O₃, Catalyst conc. = 400 ppm, pH=7, Reaction time = 3 hr, H₂O₂ = 500 ppm)

4.5.10 Optimized parameters for the photodegradation of SIER-2

The results of the present study showed that the textile effluent SIER-2 can be photocatalytically decomposed using Fe₂O₃ catalyst efficiently under UV irradiation. Photodegradation was maximum in neutral condition, and the degradation efficiency was influenced by the process parameters like catalyst concentration, dye concentration, irradiation time, oxidizing agent dose, and pH. The optimum catalyst dose for the degradation of 60% SIER-2 was 400 ppm of Fe₂O₃. TOC analysis of the effluent showed a 62.35% reduction in TOC under optimized conditions, whereas the COD reduction in the same conditions was 40.82%. The addition of oxidants like H₂O₂ increased the degradation significantly. The optimized values for the photocatalytic degradation of 60% SIER-2 are shown in Table 4.10. Maximum 97.1 % decomposition was achieved at the optimized parameters.

Table 4.10 Optimized parameters for the photocatalytic degradation of 60% SIER-2

Parameters	Optimized values
Catalyst	Fe ₂ O ₃
Catalyst concentration	400 ppm
Irradiation time	3.0 hrs
pH	7
Oxidizing agent (H ₂ O ₂) concentration	500 ppm
Maximum decomposition achieved = 97.1 %	

4.6 Photocatalytic decomposition of Yarn Dyeing Industry Effluent, Sirajganj (YDIES)

This textile effluent YDIES collected from a yarn dyeing industry at Pipulbaria, Sirajganj district, Bangladesh was of pink color and slightly alkaline. Unlike SIER-1 and SIER-2 the YDIES was not so highly concentrated. It was diluted 2 times and further all experiments and calculations were done based on the diluted effluent. The photocatalytic decomposition of YDIES by ZnO, TiO₂, and Fe₂O₃ as photocatalysts was investigated under UV light. The effect of variable parameters like initial effluent concentration, irradiation time, catalyst type and doses, pH, and oxidizing agent doses on the photocatalytic degradation efficiency were analyzed. The percentage of degradation was estimated in terms of reducing the COD and TOC. The concentration of the effluent was determined using the absorbance recorded on a UV-spectrophotometer at a wavelength of 414 nm (λ_{\max}).

4.6.1 Effect of initial effluent concentration

The effects of initial concentrations of YDIES (10%, 20%, 30%, 40%, 50%, 60%, and 70%) on their photocatalytic decomposition by TiO₂ at pH 7.8 (effluent's normal pH) were investigated. The results are represented in Figure 4.31, and it indicated that when the concentration of the effluents was increased the percentage of photocatalytic decomposition decreased. It showed that the percentage of decomposition decreased from 100 to 16.37% in 2 hrs when the concentration of the effluents increased from 10 to 70 %. The possible explanation for this behavior is that as the initial concentration of the effluent was increased, the path length of the photons entering the solution decreased, thereby decreasing the number of photon absorption by the catalyst surface at a higher concentration (Davis *et al.*, 1994). When the concentration of the dyeing effluent is raised, the dye molecules act as a filter for the incident UV radiation. . Thus, the desired light intensity fails to reach the catalyst surface, and the percentage of degradation decreases (Ameta *et al.*, 2013). The same effect was observed by Neppolian *et al.* (2002a) during the photocatalytic degradation of three commercial textile dyes: Reactive Yellow, Reactive Red, and Reactive Blue. They found that when initial dye concentration was increased from 0.0001 M to 0.0005 M,

degradation fell from 98% to 32%, which supported the present findings. However, although YDIES solutions of lower concentration showed better degradation percentage than those of higher concentration, for the optimization of other parameters, 50% YDIES was selected.

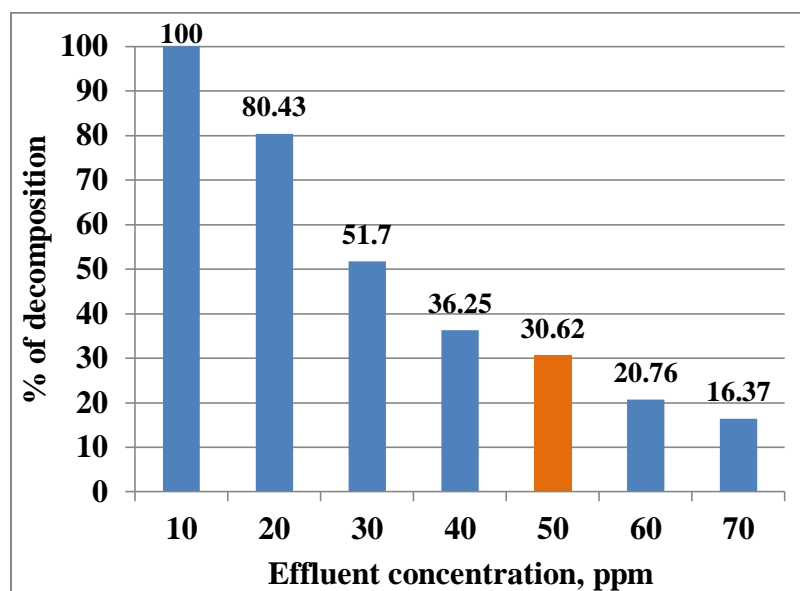


Figure 4.31 Effect of effluent concentrations on % of decomposition of YDIES

(Catalyst = TiO₂, Catalyst conc. = 100 ppm, pH = 7.8, Reaction time = 2 hrs, H₂O₂ = 300 ppm)

4.6.2 Effect of catalyst

The decomposition efficiency of different photocatalysts, i.e., TiO₂, ZnO, Fe₂O₃, and their mixtures under UV light for the YDIES was examined. The results are represented in Figure 4.32. It is shown that the degradation efficiency of mixed catalysts was higher than that of single catalysts for YDIES in most cases, which might be because they acted as catalyst promoters. The maximum 43.8 % degradation of the effluent was achieved by TiO₂. The next better photodegradation efficiency was observed by the mixed catalysts ZnO+Fe₂O₃ (1:1) and TiO₂+Fe₂O₃ (1:1) where degradation was 42.72% and 41.72%, respectively. When TiO₂, ZnO, and Fe₂O₃ were lonely used for 3 hrs under the same conditions 43.8, 38.98, and 35.42% of degradation were achieved, respectively. Their decomposition efficiency was as follows: TiO₂ > (ZnO+Fe₂O₃) > (TiO₂+Fe₂O₃) > (TiO₂+ZnO) > ZnO > (TiO₂+ZnO+Fe₂O₃) > Fe₂O₃. However, TiO₂ showed the best photocatalytic activity over all other catalysts and their mixtures. Khan *et al.* (2016) conducted a study on the

photocatalytic degradation of textile wastewater from Gul Ahmad textile industry in Karachi, Pakistan, using TiO_2 and ZnO . They observed better degradation (95.29%) by TiO_2 than by using ZnO (64.41%) at pH 9 within 150 minutes of irradiations. The extent of degradation by photocatalysts is dependent on the nature of both effluents and catalysts. There was no significant difference among the degradation percentages achieved by mixed catalysts. Figure 4.32 illustrated that TiO_2 is the most suitable catalyst for the photocatalytic degradation of this specific effluent. Hence, TiO_2 was selected as the photocatalyst for the optimization of other parameters.

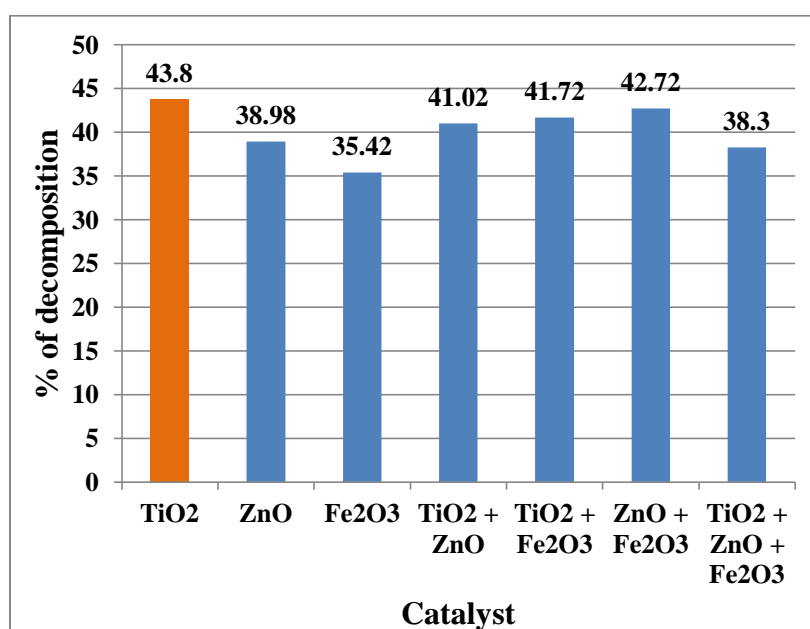


Figure 4.32 Effect of catalyst on % of decomposition of YDIES

(Effluent conc. = 50%, Catalyst conc. = 100 ppm, pH = 7.8, Reaction time = 3 hrs, H_2O_2 = 300 ppm)

4.6.3 Effect of irradiation time

The effect of irradiation time on the photocatalytic decomposition efficiency of different catalysts like TiO_2 , ZnO , Fe_2O_3 , and their combinations on YDIES was investigated for different periods up to 8 hrs under UV light. The results obtained are represented in Figure 4.33 which illustrates the influence of the irradiation time on the photodegradation percentage. The results indicated that in the case of TiO_2 the degradation increased from 20.65 to 78.3% for the period from 1 to 8 hrs (Figure 4.33a). The figure shows that the degradation increased sharply with time up to 6 hrs and then slowly increased with time. It means that the photocatalysts have potential in

the degradation process. The study observed that the degradation reached the maximum of 78.3% for TiO₂ and 63.5% for ZnO after 8 hrs. The greater degradation rate at the start of the process was caused by the presence of high amounts of active sites on the catalyst surface. The degradation rate was then gradually reduced because of catalyst consumption (Salama *et al.*, 2018). The slow kinetics of degradation after a certain time limit is mainly attributed to the difficulty in the reaction of short-chain aliphatics with •OH radicals, and the short lifetime of photocatalyst because of active sites deactivation by strong by-products deposition (Kumar and Pandey, 2017).

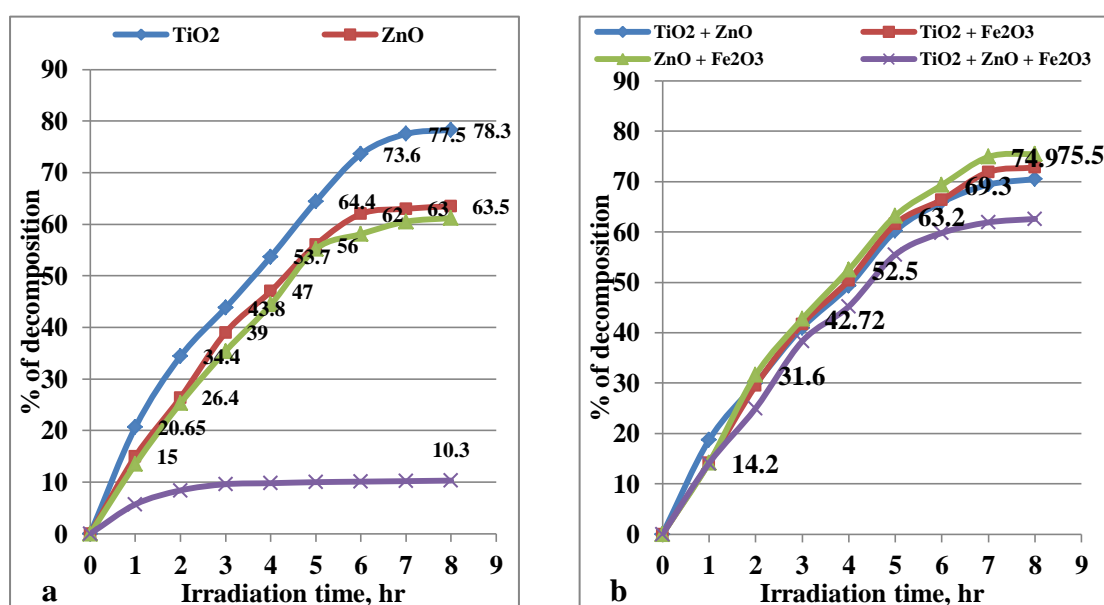


Figure 4.33 Effect of irradiation time on % of decomposition of YDIES by a) single catalysts and b) mixed catalyst.

(Effluent conc. = 50%, Catalyst conc. = 100 ppm, pH = 7.8, H₂O₂ = 300 ppm)

In research, TiO₂ was used for the photocatalytic decomposition of model textile wastewaters containing azo dyes where C.I Reactive Black 5 was degraded from 75% at 30 minutes to 93% at 120 minutes with 1 g/L of TiO₂ (Saggiaro *et al.*, 2011). Experiments with the mixed catalyst for 7 hrs of irradiation time observed no better result (Figure 4.33b). It is noticeable that for a 3 hrs reaction 43.8% decomposition was achieved by TiO₂ and further reaction up to 8 hrs produced more decomposition. But for any industrial operation time is a factor and continuing any process over a longer period is cost-effective and less desirable. Therefore, it is wise to improve

degradation efficiency by changing other parameters. Hence, the next experiments were carried out for 3 hrs of irradiation to optimize other parameters.

4.6.4 Photodegradation kinetics of YDIES

Chemical kinetics is concerned with understanding the rates of chemical reactions. Kinetic studies are of fundamental importance in any investigation of the reaction mechanism. By understanding how a reaction takes place, many processes can be improved. The results of photocatalysis of the textile effluent YDIES by different catalysts viz., TiO₂, ZnO, and Fe₂O₃, and also without a catalyst are shown in Figure 4.34. The change in concentration of the effluent (C/C_0) is plotted as a function of irradiation time (C_0 = the initial concentration of the bulk solution, C = concentration at time t). The study observed that both photocatalyst and a light source were necessary for the degradation reaction to occur. It was evident that about 60-80% of the effluent concentration was removed after 8 hrs irradiation. In contrast, a negligible decrease in the concentration of dye was observed by irradiation in the absence of a photocatalyst.

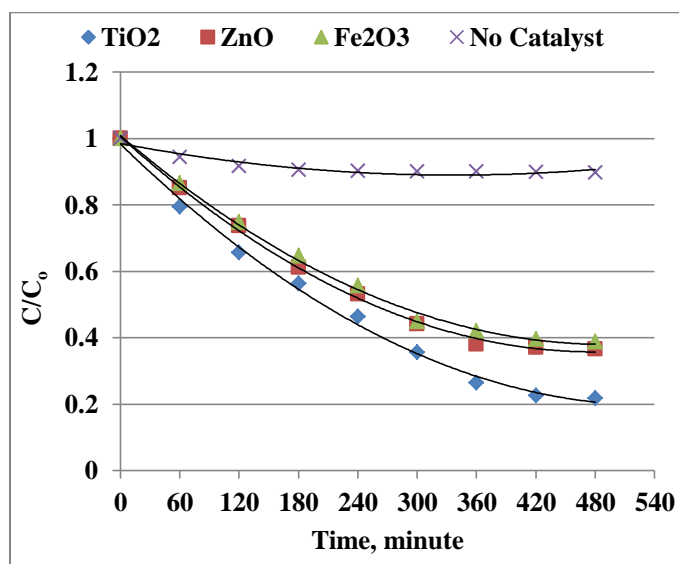


Figure 4.34 Photocatalytic degradation of YDIES

(Effluent conc. = 50%, Catalyst conc. = 100 ppm, pH = 7.8, H₂O₂ = 300 ppm)

The graph of $\ln \frac{C_0}{C}$ versus time for the photocatalytic reactions by TiO₂, ZnO, and Fe₂O₃ is shown in Figure 4.35 (almost straight line) which supports the observation

that the degradation of YDIES followed approximately pseudo-first-order kinetics. Neppolian *et al.* (2001) reported that the disappearance of a dye Reactive Yellow 17 in the solution followed approximately pseudo-first-order kinetics.

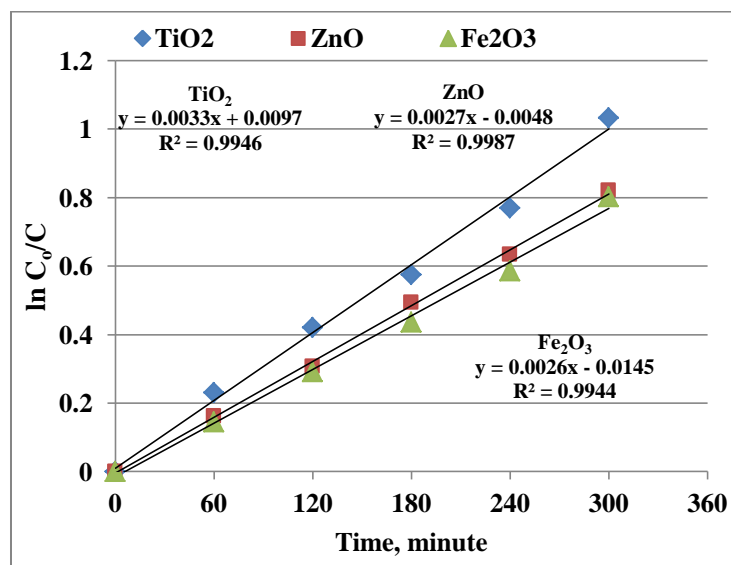


Figure 4.35 Kinetics of photodegradation of YDIES

Another research on the photocatalytic degradation pathway of MB in water also observed similar results (Houas *et al.*, 2001). Mukhlis *et al.* (2013) conducted a study on the photocatalytic degradation kinetics of MB and Congo Red and observed that the first order and Freundlich model fit the kinetic data well. The linear regression coefficients of determination ($R^2 =$) on the fitted lines were 0.9946, 0.9987, and 0.9944 for TiO₂, ZnO, and Fe₂O₃, respectively indicating that the best-fitted line was obtained for ZnO. The rate constants of the photodegradation reactions by TiO₂, ZnO, and Fe₂O₃ were calculated to be 3.37×10^{-3} , 2.68×10^{-3} , and $2.54 \times 10^{-3} \text{ min}^{-1}$, respectively. Abo-Farha, (2010) described that the photocatalytic degradation rate depends on dye structure, dye concentration, catalyst concentration, and pH of the medium.

4.6.5 Effect of pH

pH is an important parameter because its variation can influence the adsorption of dye molecules onto the catalyst surfaces (Wang *et al.*, 2008a). Different photocatalytic degradation experiments on YDIES were performed with TiO₂ as the photocatalyst at different pH values of 3 to 10. The results are represented in Figure 4.36. The

interpretation of pH effects on the photodegradation efficiency is not easy because three possible reaction mechanisms can contribute to the process at a time. These are (1) hydroxyl radical attack, (2) direct oxidation by the positive hole, and (3) direct reduction by the electron in the conducting band. The contribution of each one depends on the substrate nature and pH (Tang *et al.* 1997).

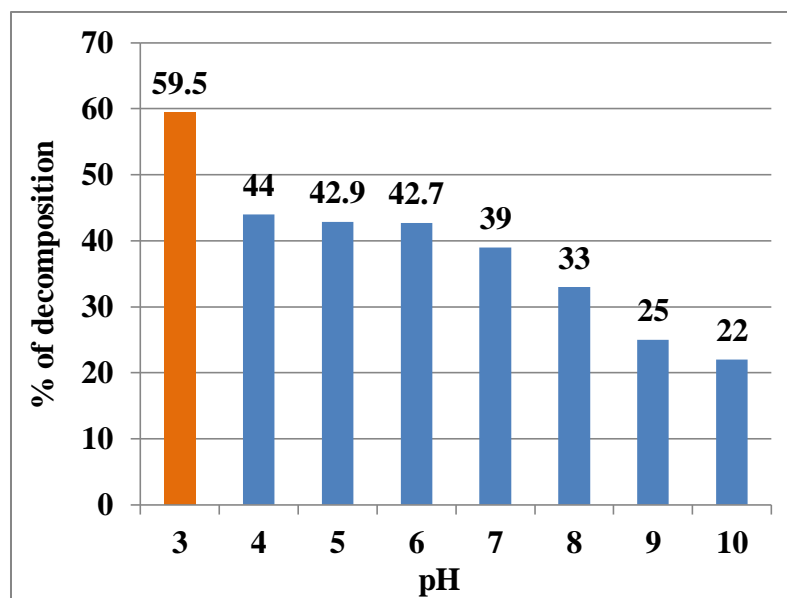


Figure 4.36 Effect of pH on % of decomposition of 50% YDIES

(Catalyst = TiO₂, Catalyst conc. = 100 ppm, Reaction time = 3 hrs, H₂O₂ = 300 ppm)

The results revealed that the photodegradation efficiency decreased with the increase in pH. Photodegradation was highest in acidic media with degradation of 59.5% at pH 3. Up to a pH value of 7, the degradation efficiency decreased to 39%. Above pH 7, the degradation continued to decrease to about 22% at pH 10. This behavior can be explained by TiO₂ surface charge density. The point of zero charge (pzc) of TiO₂ is at pH 6.8. In acid media (pH ≤ 6.8) the TiO₂ surface is positively charged, whereas in alkaline conditions (pH ≥ 6.8) it is negatively charged (Dostanić *et al.*, 2011). In acidic conditions, the positive charges on the TiO₂ surface promote a strong electrostatic attraction between the catalyst and the anionic groups of the dye contained in the effluent. As a result, catalytic activity is accelerated. On the other hand, in basic conditions negative charges of the catalyst promote the repulsion of the dye by the titanium surface, diminishing the catalytic activity of this semiconductor

(Saggiaro *et al.*, 2011). The increasing pH value tends to change the charge on TiO₂ from positive to negative by adsorbing HO⁻ ions, which favors the formation of HO• (Wang *et al.*, 2007) and consequently, the photocatalytic activity decreased due to the increase of the electrostatic repulsion between TiO₂ and anionic effluent gradually. Based on the results shown in Figure 4.36, the optimal pH for the photocatalytic decomposition of YDIES was selected as 3. Similar results were reported by Kansal *et al.* (2009), who found that the photocatalytic degradation of Reactive Black 5 and Reactive Orange 4 dyes was favored in an acidic medium with TiO₂.

4.6.6 Effect of catalyst concentration

The dose of catalyst is an important factor influencing the photodegradation process significantly because it can affect the degradation rate. Hence, it is important to determine the concentration of the catalyst required to degrade the maximum amount of effluent. The effect of different amounts of photocatalyst TiO₂, i.e., 100 to 400 ppm on the photocatalytic decomposition of YDIES for 3 hrs at pH 3 was investigated. The results are shown in Figure 4.37 indicating that there was almost no effect of catalyst loading on the percentage of decomposition of YDIES. When the catalyst concentration was increased from 100 ppm to 400 ppm, the percentage of degradation obtained was 40.2%, 40%, 41%, and 40.8% respectively. Wei and Wan (1991) have reported that the amount of catalyst has both positive and negative effects on the rate of photodecomposition. Increased catalyst loading increases the number of photons adsorbed and, as a result, the rate of degradation also increases. (Muruganandham and Swaminathan 2006). On the other hand, increasing the catalyst loading enhances the turbidity of the solution, which lowers the photon flux penetration in the reactor and thus lowers the photocatalytic degradation rate. (Kamble *et al.*, 2003; Gogate and Pandit 2004). Furthermore, at high solid concentrations, agglomeration creates a reduction of surface area (Kaneco *et al.*, 2004). Excessive light scattering by suspended particles has a steadily decreasing effect on the reaction rate. Neppolian *et al.* (2002a) conducted a study on the effect of TiO₂ loading on percentage degradation of the dyes Reactive Red 2, Reactive Blue 4, and Reactive Yellow 17. In the case of Reactive Red 2 and Reactive Blue 4, the percentage degradation increased only slightly while in the case of Reactive Yellow 17, percentage degradation was found to

be constant with an increase in TiO₂ loading suggesting that an upper level for catalyst effectiveness existed. This is in agreement with the present study results. Therefore, a TiO₂ dose of 100 ppm can be the optimum value for the degradation of YDIES.

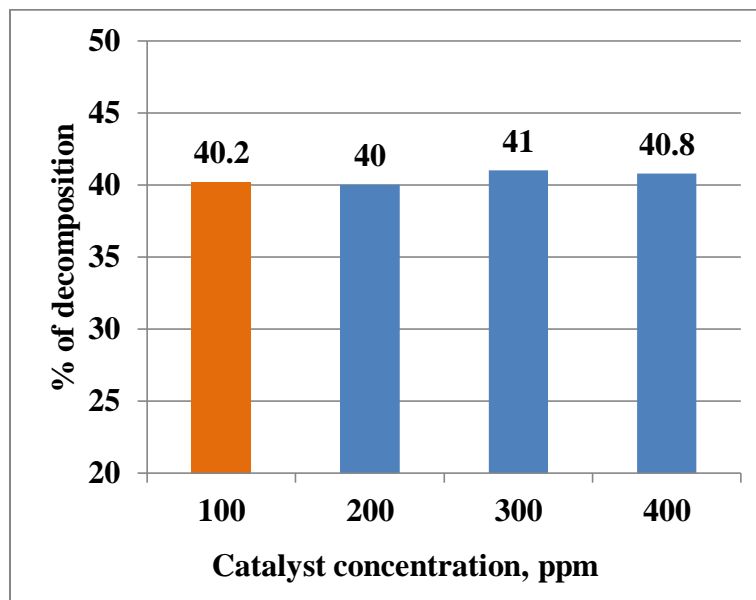


Figure 4.37 Effect of catalyst concentration on % of decomposition of YDIES

(Effluent conc. = 50%, Catalyst = TiO₂, pH=3, Reaction time = 3 hrs, H₂O₂ = 300 ppm)

4.6.7 Effect of oxidizing agent (H₂O₂) dose

According to Madhu *et al.* (2007), H₂O₂ has a major effect on the degradation rates as an oxidant. Photocatalytic decomposition experiments were carried out for varying H₂O₂ doses viz., 300, 400, 500, 600, and 700 ppm on YDIES at pH 3 for 3 hrs. The results are plotted in Figure 4.38 from which it can be observed that the percentage of photocatalytic decomposition increases with increasing concentration of H₂O₂. A higher concentration of H₂O₂ liberated more of the hydroxyl free radicals which caused the dye decomposition. The degradation increased from 41% at 300 ppm of H₂O₂ to 95.8% at 600 ppm of H₂O₂. No significant effect was observed on further increase in H₂O₂ dose on the degradation. In low concentrations, H₂O₂ enhances the degradation of compounds due to a more efficient generation of hydroxyl radical and inhibition of electron–hole pair recombination (Aguedach *et al.*, 2005; Prado *et al.*, 2008; Saggiaro *et al.*, 2011) When the concentration of H₂O₂ rises, the electron

acceptor interacts with hydroxyl radicals, scavenging the photoproducted holes (Daneshvar *et al.*, 2003; Malato *et al.*, 1998). Furthermore, H₂O₂ can alter the surface of TiO₂, lowering its photocatalytic ability (Zhu *et al.*, 2000). From the observed results, 600 ppm can be considered as the optimum value of H₂O₂ loading for the degradation of YDIES.

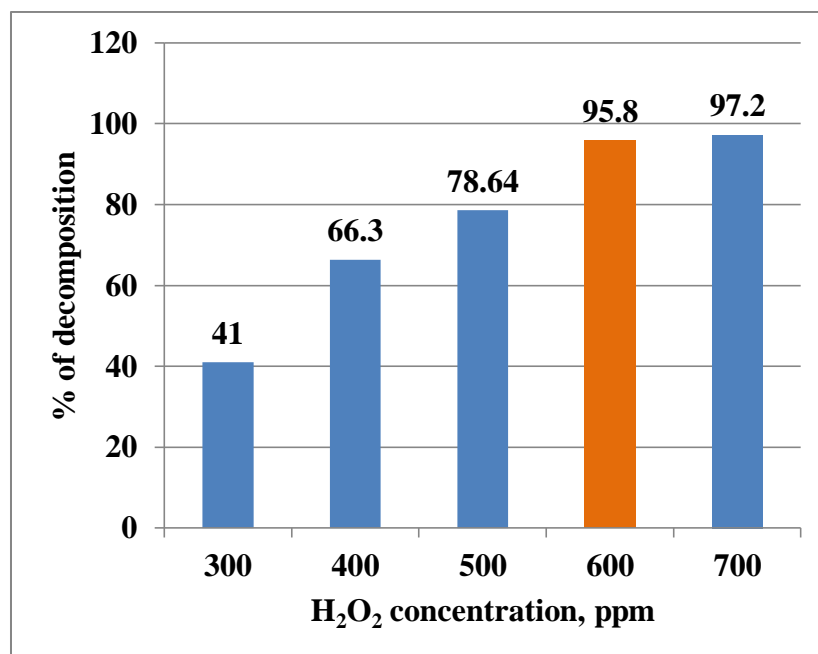


Figure 4.38 Effect of H₂O₂ concentrations

(Effluent conc. = 50%, Catalyst = TiO₂, Catalyst conc. = 100 ppm, pH= 3, Reaction time = 3 hrs)

4.6.8 Mineralization of YDIES

As the reduction in chemical oxygen demand (COD) and total organic carbon (TOC) reflects the extent of degradation or mineralization of an organic species, the percentage reduction in COD and TOC was studied for YDIES by photocatalytic degradation under optimized conditions i.e., by TiO₂ of 100 ppm at pH 3 for 3 hrs of UV irradiation. To enhance the photocatalytic degradation rate, 600 ppm of H₂O₂ was used as an oxidizing agent. The results are shown in Table 4.11. Excellent mineralization of the effluent was observed as the TOC value decreased from 710 to 184 mg/L after 3 hrs of photocatalytic treatment. It indicated that about 74.08% reductions whereas the decomposition was 95.8% at the same conditions. Similar results have been reported by Bulc and Ojstršek (2008) and Ghaly *et al.* (2014) who

reported 89% and 80-82% of TOC reduction in their studies respectively. The COD of the effluent decreased from 2180 to 945 mg/L by the treatment under the same conditions indicating a 56.65% COD reduction. It is noticeable the COD reduction is lesser than percentage decomposition (95.8%) under optimized conditions which may be due to chromophore destruction resulting in the formation of smaller uncolored products. These products were counted in COD measurement but not in spectrophotometric measurement to evaluate the decomposition percentage. Kulkarni and Thakur (2014) conducted a study on photocatalytic degradation of textile industrial effluent by ZnO and they reported 37.5% COD reduction by 400 ppm catalyst for 5 hrs. The result of the present study is also supported by another research result where a 29.2 % reduction in COD was achieved by 500 ppm ZnO for 4 hrs of UV irradiation (Mondal and Bhagchandani, 2016).

Table 4.11 Reduction in TOC and COD of YDIES by photocatalytic treatment at optimized conditions

Parameters	Before treatment (mg/L)	After treatment (mg/L)	% of reduction
TOC	710	184	74.08
COD	2180	945	56.65

(Effluent conc. = 50%, Catalyst = TiO₂, Catalyst conc. = 100 ppm, pH= 3, Reaction time = 3 hr, H₂O₂ = 600 ppm)

4.6.9 Optimized parameters for photocatalytic degradation of YDIES

The results of the present study showed that the textile effluent YDIES can be efficiently photocatalytically degraded using TiO₂ catalyst under UV irradiation. Photodegradation was maximum in an acidic medium and the degradation efficiency was influenced by the process parameters like catalyst concentration, dye concentration, irradiation time, oxidizing agent dose, and pH. The optimum catalyst dose for the degradation of 50% YDIES was 100 ppm of TiO₂. TOC analysis of the effluent showed a 74.08% reduction in TOC under optimized conditions whereas the COD reduction in the same conditions was 56.65%. The addition of oxidants like H₂O₂ enhanced the degradation significantly.

The optimized values for the photocatalytic degradation of 50% YDIES are shown in Table 4.12. Maximum 95.8 % decomposition was achieved at the optimized parameters.

Table 4.12 Optimized parameters for the photocatalytic degradation of 50% YDIES

Parameters	Optimized values
Catalyst	TiO ₂
Catalyst concentration	100 ppm
Irradiation time	3.0 hrs
pH	3
Oxidizing agent (H ₂ O ₂) concentration	600 ppm
Maximum decomposition achieved = 95.8 %	

4.7 Comparative studies

The comparative results of the photocatalytic activity of TiO₂, ZnO, Fe₂O₃, on the degradation of MB and three textile dyeing effluents namely SIER-1, SIER-2, and YDIES at optimized conditions are shown in Table 4.13.

Table 4.13 Comparison of optimized parameters for photocatalytic degradation of MB, SIER-1, SIER-2, YDIES

Optimized Parameters	MB	SIER-1	SIER-2	YDIES
Initial effluent conc.	40 ppm	60%	60%	50%
Catalyst	ZnO	ZnO	Fe ₂ O ₃	TiO ₂
Catalyst doses., ppm	200	100	400	100
Irradiation time, hrs	3	3	3	3
pH	4	10	7	3
H ₂ O ₂ doses., ppm	600	500	500	600
Maximum decomposition, %	82.75	81.60	97.10	95.80

At the optimized conditions, these effluents showed about 83 to 98% degradation. It indicates that different photocatalysts were suitable for the treatment of different

Chapter Four : Results and Discussion

effluents. The only ZnO was the most suitable catalyst for the photocatalytic degradation of both MB and SIER-1. Catalyst doses of 100 ppm to 400 ppm showed the best degradation results for different effluents. MB and YDIES were more efficiently degraded in acidic conditions whereas SIER-1 in alkaline conditions. Again neutral condition was best for the treatment of SIER-2. Oxidizing agent doses of 500 – 600 were sufficient to achieve remarkable degradation results.

The comparative results among the photocatalytic degradation of MB (present study) and that of other dyes of different research work are represented in Table 4.14. Daneshvar *et al.* (2004) investigated the photocatalytic degradation of a commonly used textile dye Acid red 14 by ZnO. They achieved about 70% degradation of 20 ppm dye solution with 160 ppm catalyst in 3.5 hrs. The photocatalytic degradation of two azo-dyes, Reactive Black 5 (RB5) and reactive yellow (RY145) was investigated by UV-irradiated TiO₂ coated on non-woven paper. Among them, 40 ppm of RB5 and RY145 showed about 64 and 62% degradation respectively (Aguedach *et al.*, 2005). Another report showed that the photocatalytic degradation of 50 ppm Reactive Violet 1 using TiO₂-P25 (Degussa) catalyst in slurry form achieved about 85% degradation in 20 minutes of solar irradiations (Giwa *et al.*, 2012).

Table 4.14 Comparison of photocatalytic degradation of MB and other dyes

Photocatalysts	Dyes	Light source	Time (min)	Degradation (%)	References
ZnO	Acid red 14	UV	210	70	Daneshvar <i>et al.</i> , 2004
TiO ₂	Reactive black 5	UV	300	64	Aguedach <i>et al.</i> , 2005
TiO ₂	Reactive yellow 145	UV	300	62	Aguedach <i>et al.</i> , 2005
ZnO	Reactive red 2	Solar light	480	85	Neppolian <i>et al.</i> , 2002b
MnTiO ₃	Methylene blue	Solar light	240	70	Alkaykh <i>et al.</i> , 2020
MnTiO ₃ /TiO ₂	Methylene blue	Solar light	240	75	Alkaykh <i>et al.</i> , 2020
ZnO	Methylene blue	UV	180	82.75	Present study

Chapter Four : Results and Discussion

The photocatalytic degradation of some commercial textile dyes was investigated using TiO₂ photocatalyst in an aqueous solution under solar irradiation. Among them, Reactive red 2 (conc. = 0.64g/L) showed about 85% degradation (Neppolian *et al.*, 2002b). Alkaykh *et al.* (2020) studied the photocatalytic activities of pure MnTiO₃ and mixed MnTiO₃/TiO₂ on MB (1×10^{-5} M) under sunlight irradiation and achieved 70% and 75% degradation respectively after 4 hrs. The present study showed a better or almost similar degradation, i.e., 82.75 % of MB (40 ppm) in 3 hrs using ZnO catalyst.

The comparative results among the photocatalytic degradation of SIER-1, SIER-2, and YDIES and those of other real or simulated textile effluents of different studies are represented in Table 4.15. Ganesan and Thanasekaran, (2011) investigated the degradation of a real textile dyeing wastewater collected from an industry at Tirupur, Tamilnadu, India and achieved about 89% degradation by Steel scrap/ H₂O₂ under solar radiation. Another report showed that the photocatalytic degradation of wastewater collected from an industry at Kalol, Gujarat, India using TiO₂ and ZnO catalyst achieved about 90% COD reduction under UV light (Mondal, and Bhagchandani, 2016). The photocatalytic degradation of textile wastewater from Gul Ahmad textile industry in Karachi, Pakistan, using TiO₂, ZnO, and H₂O₂ as photocatalyst was investigated under UV irradiation. The maximum decolorization achieved was 95.29% by using TiO₂ and 64.41% by using ZnO at pH 9, within 150 minutes of irradiations (Khan *et al.*, 2016). Table 4.15 showed that the present study achieved good degradation percentages in all textile dyeing effluents compare to the results reported in the literature.

Table 4.15 Comparison of photocatalytic degradation of SIER-1, SIER-2, YDIES and other effluents/mixture of dyes

Effluents/ mixture of dyes	Parameters	Degradation, (%)	References
Methylene blue + bromophenol blue	Catalyst: CuO-clinoptilolite composite, pH: 5.9, catalyst dose: 0.2 g L ⁻¹ , irradiation time: 3 hrs	61 and 32	Nezamzadeh-Ejhieh and Zabihi-Mobarakeh, 2014
Acid orange 7 + reactive red 2	Catalyst: TiO ₂ , pH: 6.8, catalyst dose: 0.5 g/L	45-60	Juang <i>et al.</i> , 2010
Methylene blue + methyl orange	Catalyst: BiVO ₄ /CeO ₂ nano- composites, visible-light	90-98	Wetchakun <i>et al.</i> , 2012
Binary mixture of reactive dyes	Photocatalyst: TiO ₂ , irradiation time: 15 h	90-95	Chatterjee <i>et al.</i> , 2008
Textile dyeing effluent, Tamilnadu, India	Catalyst: Steel scrap/ H ₂ O ₂ , H ₂ O ₂ doses: 15 ppm, pH: 3	89	Ganesan and Thanasekaran, 2011
Bharat Vijay Mills effluent, Gujarat, India	Catalyst: TiO ₂ and ZnO , irradiation time: 6 hrs, catalyst conc.: 3-4g/L	90 % COD reduction	Mondal, and Bhagchandani, 2016
Textile wastewater, Gul Ahmad textile industry, Karachi, Pakistan	Catalyst: TiO ₂ and ZnO , pH: 9, irradiation time: 150 minutes	95.29% by TiO ₂ 64.41% by ZnO	Khan <i>et al.</i> , 2016
SIER-1	Catalyst: ZnO, catalyst conc.: 100 ppm, irradiation time: 3 hrs, pH: 10, H ₂ O ₂ doses: 500 ppm	81.60	This study
SIER-2	Catalyst: Fe ₂ O ₃ , catalyst conc.: 400 ppm, irradiation time: 3 hrs, pH: 7, H ₂ O ₂ doses: 500 ppm	97.10	This study
YDIES	Catalyst: TiO ₂ , catalyst conc.: 100 ppm, irradiation time: 3 hrs, pH: 3, H ₂ O ₂ doses: 600 ppm	95.80	This study

It is noteworthy that photocatalytic decomposition is not a self-sufficient treatment process for textile effluents on an industrial scale but it can be an auxiliary step in the conventional effluent treatment process. It is a unique destructive technology for non-biodegradable components of the effluent. It can be incorporated after chemical treatment of the effluent. A schematic diagram of the total effluent treatment process including the photocatalytic decomposition unit is represented in the following Figure 4.39.

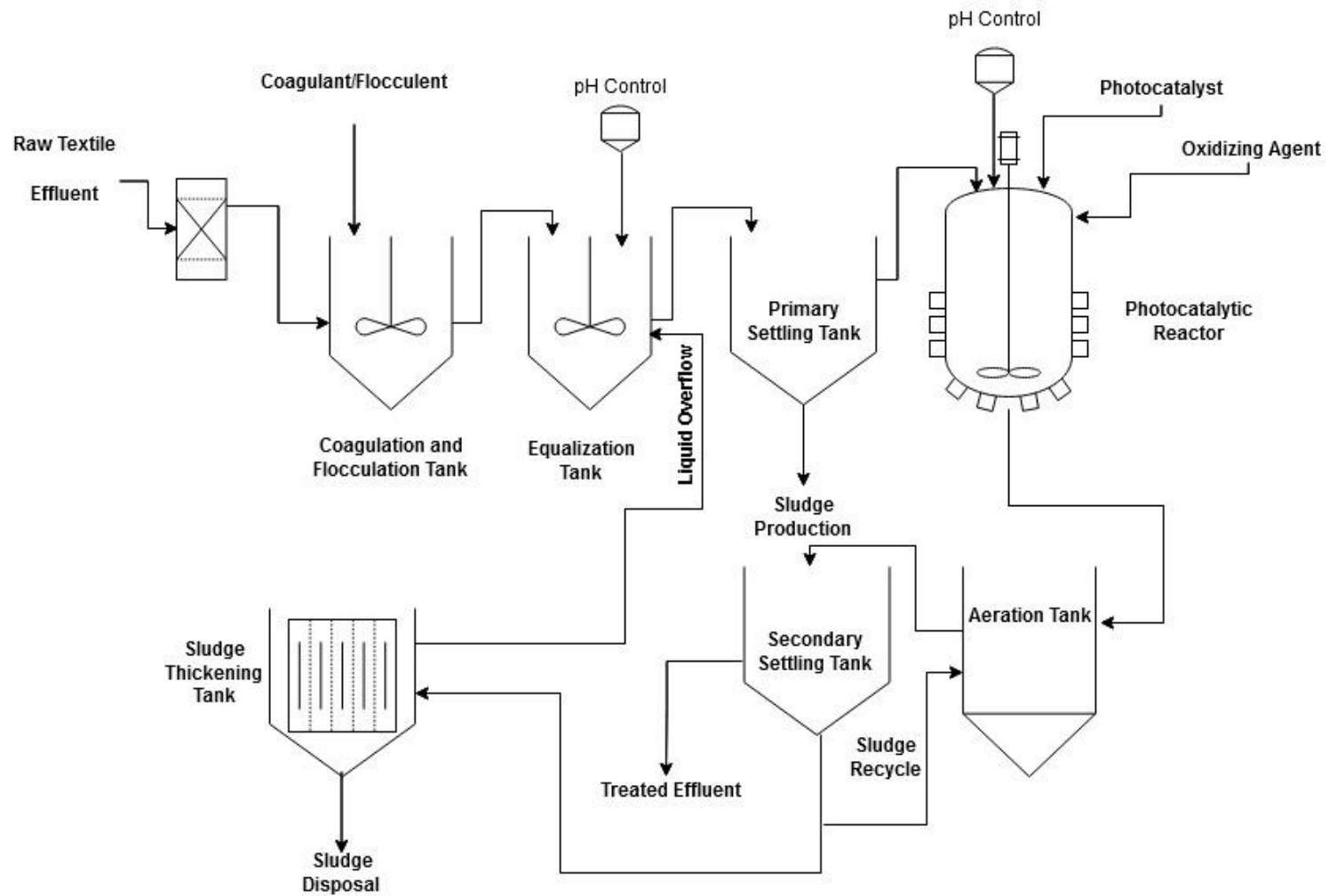


Figure 4.39 Flow diagram of a novel approach for combination of photocatalytic decomposition of textile dyeing effluent treatment plant



CHAPTER FIVE
CONCLUSION

CONCLUSION

The textile dyeing and printing industries produce a huge volume of wastewater containing various toxic chemicals that cause harm to the environment. The complexity of the organic load and the toxicity of these textile effluents have far-reaching environmental consequences. The study aimed to reduce the pollutants due to discharge the untreated or partially treated textile dyeing effluents. The study optimized the process parameters of the photocatalytic treatment for each effluent and observed the reaction kinetics.

A total of three (3) textile effluent samples were collected, two of them from the BSCIC (Bangladesh Small and Cottage Industries Corporation) industrial area, Rajshahi, and the other from a yarn dyeing industry, Pipulbaria, Sirajganj. The photocatalytic activity of TiO_2 , ZnO , and Fe_2O_3 was studied for the degradation of these effluents as well as the methylene blue solution. The decomposition efficiency of the photocatalysts was measured in terms of a decrease in effluent concentration.

The analysis results showed that the color of the effluents was dark with a noxious smell. Among those, YDIES was slightly alkaline ($\text{pH}=7.8$), whereas SIER-1 ($\text{pH}=6.7$) and SIER-2 ($\text{pH}=6.8$) were almost neutral. The DO values of the effluents indicated that there was a depletion of necessary oxygen in the water. The value of EC, TSS, TDS, BOD, and COD of the effluents exceeded the DoE, BD standard limits by several times indicated that these effluents were highly polluted. The concentrations of five anions (Cl^- , HCO_3^- , NO_3^- , SO_4^{2-} , and PO_4^{3-}) of the effluents were measured. Among the effluents SIER-1 showed higher Cl^- and SO_4^{2-} pollution than others, whereas SIER-2 showed comparatively higher NO_3^- and HCO_3^- pollution. All the effluents were almost free from PO_4^{2-} pollution. SO_4^{2-} concentration of SIER-1 was about 10 times higher than the DoE, BD standard limit. The study analyzed eight (8) trace elements named Cr, Mn, Fe, Ni, Cu, Zn, Pb, and Cd of three textile effluent samples. Among those, Cr in one industrial effluent (SIER-1) and Pb in two industrial effluents (SIER-1 and SIER-2) exceeded the limits of DoE, BD. The results of other trace elements indicated that all the effluents had concentrations within the

Chapter Five : Conclusion

permissible limit of the DoE, BD standard, 2003. The effluents contained similar TOC compared to others reported values in different papers.

The photocatalytic treatment results of the effluent samples obtained in the present study have shown the great efficiency of AOP's in significant degradation and mineralization of real textile industrial effluents as well as dyes like MB which are resistant to other conventional treatment processes. The photocatalytic degradation reactions were carried out by using different photocatalysts such as TiO_2 , ZnO , and Fe_2O_3 . Optimization of different process parameters such as effluent concentration, catalyst concentration, pH, irradiation time, oxidizing agent dose has been carried out on the basis of percentage (%) of decomposition of the effluents. Although TiO_2 is the most well-known photocatalyst, the results of this study indicate that ZnO and Fe_2O_3 can be very effective and suitable alternatives to TiO_2 . The maximum degradation efficiency of dye/effluent was achieved with the combination of UV, H_2O_2 , and photocatalyst. The results showed that the percentage of photocatalytic decomposition decreased with increasing dye/effluent concentrations.

Comparisons among the efficiencies of different decomposition processes, viz., catalytic, photolytic, and photocatalytic were observed for SIER-1 and SIER-2. These followed the trends: photocatalytic (with H_2O_2) > photolytic (with H_2O_2) > photocatalytic (without H_2O_2) > catalytic (with H_2O_2) > catalytic (without H_2O_2) > with only H_2O_2 > photolytic (without H_2O_2) in the case of SIER-1. Besides, the trends shown for the SIER-2 follows: photocatalytic (with H_2O_2) > photolytic (with H_2O_2) > photocatalytic (without H_2O_2) > photolytic (without H_2O_2) > with only H_2O_2 > catalytic (with H_2O_2) > catalytic (without H_2O_2).

Among the three photocatalysts (TiO_2 , ZnO , and Fe_2O_3) and their combinations, ZnO showed the best photodegradation efficiency for MB and SIER-1, whereas Fe_2O_3 and TiO_2 were the best for SIER-2 and YDIES, respectively. The decomposition percentage sharply increased with the increase in reaction time within the first few hours and then slowly increased to reach an equilibrium. All the three catalysts and their mixtures showed similar behavior. After 3 hours of irradiation about 63, 59, 71.5, and 44% of decomposition were observed for MB, SIER-1, SIER-2, and YDIES, respectively for their best-suited catalyst at the original pH of the effluents.

Chapter Five : Conclusion

Further reactions that allow over three (3) hours might produce higher decomposition percentages. But the long operation period of an industrial process needs a larger treatment tank and thus enhances the operational and maintenance cost. Hence, the study considered the degradation experiments would be carried out for three (3) hrs to make the process more feasible from an economic point of view.

The study found that the photocatalytic degradation of MB and all the three effluents by different catalysts obeyed approximately pseudo-first-order kinetics. The rate constants of the photodegradation reactions of MB by Fe₂O₃, ZnO, and TiO₂ were 4.88×10^{-3} , 5.89×10^{-3} , and $4.51 \times 10^{-3} \text{ min}^{-1}$, respectively. In the case of SIER-1, the rate constants of photodegradation by ZnO, TiO₂, and Fe₂O₃ were 4.74×10^{-3} , 3.88×10^{-3} , and $3.63 \times 10^{-3} \text{ min}^{-1}$, respectively. The rate constants of the photodegradation of SIER-2 by Fe₂O₃, ZnO, and TiO₂ were 7.4×10^{-3} , 6.98×10^{-3} , and $5.73 \times 10^{-3} \text{ min}^{-1}$, respectively. The rate constants of the photodegradation of YDIES by TiO₂, ZnO, and Fe₂O₃ were 3.37×10^{-3} , 2.68×10^{-3} , and $2.54 \times 10^{-3} \text{ min}^{-1}$, respectively.

The results revealed that the photodegradation efficiency initially decreased with the increase in pH up to pH 7 for MB and pH 6 for SIER-1, and then increased with pH. In the case of SIER-2 the reverse trend was observed and fortunately, the maximum decomposition was observed at pH 7. Besides, the efficiency continuously decreased with increasing pH in the case of YDIES.

The maximum photodegradation of MB, SIER-1, SIER-2, and YDIES were recorded at pH 4, 10, 7, and 3, respectively. It indicated that the acidic conditions were favorable for the degradation of MB and YDIES, whereas SIER-1 and SIER-2 were better degraded in alkaline and neutral conditions, respectively. The percentage of degradation increased in the beginning and then decreased with increasing catalyst doses for MB and SIER-2. However, the effects of catalyst concentration on the degradation of the effluents in most cases were not so significant. Higher catalyst doses increased turbidity and inhibited light penetration through the effluent solution and reduced the degradation. The study considered 200 and 100 ppm ZnO, 400 ppm Fe₂O₃, and 100 ppm TiO₂ as the optimum doses of catalysts for MB, SIER-1, SIER-2, and YDIES, respectively.

Chapter Five : Conclusion

Besides, H_2O_2 is an oxidizing agent to the photocatalytic treatment process up to a critical limit was found to enhance the degradation greatly. Increase in the H_2O_2 concentration beyond the limit does not increase the reaction rates as it tends to act as a hydroxyl radical scavenger instead of a free radical generator. The study considered 600, 500, 500, and 600 ppm of H_2O_2 as the optimum dose of oxidizing agent for MB, SIER-1, SIER-2, and YDIES, respectively.

The optimized parameters for the photodegradation of MB, SIER-1, SIER-2, and YDIES were (dye conc.- 40 ppm, catalyst-ZnO, catalyst conc. - 200 ppm, irradiation time- 3 hrs, pH- 4.0, and H_2O_2 dose-600 ppm), (effluent conc.- 60%, catalyst-ZnO, catalyst conc. - 100 ppm, irradiation time- 3 hrs, pH- 10.0, and H_2O_2 dose-500 ppm), (effluent conc.- 60%, catalyst- Fe_2O_3 , catalyst conc. - 400 ppm, irradiation time- 3 hrs, pH- 7.0, and H_2O_2 dose-500 ppm), and (effluent conc.- 50%, catalyst- TiO_2 , catalyst conc. - 100 ppm, irradiation time- 3 hrs, pH- 3.0, and H_2O_2 dose-600 ppm), respectively.

The TOC reductions achieved were about 45, 98, 62, and 74% for MB, SIER-1, SIER-2, and YDIES, respectively at the optimized conditions of the parameters indicating a moderate to excellent mineralization of the effluents were observed. At the same conditions, COD reduction was about 44, 41, and 57% for SIER-1, SIER-2, and YDIES, respectively. Maximum 82.75, 81.6, 97, and 95.8% of decomposition of MB, SIER-1, SIER-2, and YDIES, respectively were achieved by the photocatalytic degradation at their optimized parameters.

Addition of H_2O_2 to the above system made the degradation much faster. The catalyst ZnO proved its efficiency in the case of MB and SIER-1 over TiO_2 . Another catalyst Fe_2O_3 also proved its performance over TiO_2 in the case of SIER-2. Hence, although TiO_2 is the most well-known photocatalyst, ZnO and Fe_2O_3 can be very effective and suitable alternatives to TiO_2 . Optimum parameters vary from one effluent to another, there are no universal trends. Selection of optimum degradation parameters such as catalyst, effluent concentration, catalyst concentration, pH, irradiation time, oxidizing agent dose, etc. is very important for photocatalytic treatment. Each of these parameters has to be optimized before the photocatalytic treatment of a particular effluent. Photocatalytic degradation is not sufficient alone for the treatment of textile

Chapter Five : Conclusion

effluents on an industrial scale but it must be an auxiliary process with the conventional treatment techniques because it is a unique destructive technology for non-biodegradable organic components of the effluent. The study has proposed a typical flow diagram of the textile effluent treatment process incorporating photocatalytic decomposition unit operation. It is an eco-friendly and low-cost way to minimize the pollution load of wastewater generated from textile industries. Other advantages include high color removal, lower sludge production, and simpler to operate. Hence the study suggested that photocatalytic degradation technology should be incorporated with all ETPs in the textile and other industries as well.

The three photocatalysts TiO_2 , ZnO and Fe_2O_3 have proved their efficiency for the degradation of a model dye as well as three textile effluents. Hence optimization of the operational parameters for the degradation of more real effluents needs extensive research so that the efficiency of the technique can be increased further and extended to industrial scale. Future research is needed for the development of more efficient catalysts for harnessing solar light which is much more cost effective. An efficient photocatalytic reactor is to be designed for both the small and large-scale textile industries in combination with the physicochemical and biological treatment plants to get the maximum reduction in pollutants from the industrial wastewaters.



REFERENCES

REFERENCES

- Aber, S. and Esfahlan, F.H., 2011. Removal of CI Basic Yellow 2 from aqueous solution by adsorption onto granular activated carbon using an on-line spectrophotometric analysis system: Kinetic and equilibrium study. *Global Nest Journal*, 13(3), pp.246-254. <https://doi.org/10.30955/gnj.000621>
- Abo-Farha, S.A., 2010. Photocatalytic degradation of monoazo and diazo dyes in wastewater on nanometer-sized TiO₂. *Journal of American science*, 6(11), pp.130-42.
- Addy, K., Green, L. and Herron, E., 2004. pH and Alkalinity. *Kingston: University of Rhode Island*.
- Aguedach, A., Brosillon, S. and Morvan, J., 2005. Photocatalytic degradation of azo-dyes reactive black 5 and reactive yellow 145 in water over a newly deposited titanium dioxide. *Applied Catalysis B: Environmental*, 57(1), pp.55-62. <https://doi.org/10.1016/j.apcatb.2004.10.009>
- Ahmed, M.K., Baki, M.A., Islam, M.S., Kundu, G.K., Habibullah-Al-Mamun, M., Sarkar, S.K. and Hossain, M.M., 2015. Human health risk assessment of heavy metals in tropical fish and shellfish collected from the river Buriganga, Bangladesh. *Environmental science and pollution research*, 22(20), pp.15880-15890. <https://doi.org/10.1007/s11356-015-4813-z>
- Ahmed, S., Akter, T., Ahsan, M.A., Yasmin, S., Jamal, A.H.M., Molla, S.I., and Shajahan, M., 2019. Textile dyeing and tannery industries effluent physico-chemicals conditions before discharge to river around Dhaka, Bangladesh. *International Journal of Scientific & Engineering Research*, 10(7), pp. 1029-1045.
- Akpor, O.B., Ohiobor, G.O. and Olaolu, D.T., 2014. Heavy metal pollutants in wastewater effluents: sources, effects and remediation. *Advances in Bioscience and Bioengineering*, 2(4), pp.37-43. <https://eprints.lmu.edu.ng/id/eprint/1012>
- Aksu, Z., 2005. Application of biosorption for the removal of organic pollutants: a review. *Process biochemistry*, 40(3-4), pp.997-1026. <https://doi.org/10.1016/j.procbio.2004.04.008>

References

- Akyol, A., Yatmaz, H.C. and Bayramoglu, M., 2004. Photocatalytic decolorization of Remazol Red RR in aqueous ZnO suspensions. *Applied Catalysis B: Environmental*, 54(1), pp.19-24. <https://doi.org/10.1016/j.apcatb.2004.05.021>
- Alalm, M.G., Tawfik, A. and Ookawara, S., 2015. Comparison of solar TiO₂ photocatalysis and solar photo-Fenton for treatment of pesticides industry wastewater: operational conditions, kinetics, and costs. *Journal of Water Process Engineering*, 8, pp.55-63. <https://doi.org/10.1016/j.jwpe.2015.09.007>
- Aleboye, A., Aleboye, H. and Moussa, Y., 2003. Decolorisation of Acid Blue 74 by ultraviolet/H₂O₂. *Environmental Chemistry Letters*, 1(3), pp.161-164. <https://doi.org/10.1007/s10311-003-0039-2>
- Alkaykh, S., Mbarek, A. and Ali-Shattle, E.E., 2020. Photocatalytic degradation of methylene blue dye in aqueous solution by MnTiO₃ nanoparticles under sunlight irradiation. *Heliyon*, 6(4), p.e03663. <https://doi.org/10.1016/j.heliyon.2020.e03663>
- Al-Kdasi, A., Idris, A., Saed, K. and Guan, C.T., 2004. Treatment of textile wastewater by advanced oxidation processes—a review. *Global nest: the Int. J.*, 6(3), pp.222-230.
- Alkhateeb, A.N., Hussein, F.H. and Asker, K.A., 2005. Photocatalytic decolorization of industrial wastewater under natural weathering conditions. *Asian journal of chemistry*, 17(2), pp.1155-1159.
- Almazán-Sánchez, P.T., Linares-Hernández, I., Solache-Ríos, M.J. and Martínez-Miranda, V., 2016. Textile wastewater treatment using iron-modified clay and copper-modified carbon in batch and column systems. *Water, Air, and Soil Pollution*, 227(4), pp.100. <https://doi.org/10.1007/s11270-016-2801-7>
- Almquist, C.B., Sahle-Demessie, E., Enriquez, J. and Biswas, P., 2003. The photocatalytic oxidation of low concentration MTBE on titanium dioxide from groundwater in a falling film reactor. *Environmental progress*, 22(1), pp.14-23. <https://doi.org/10.1002/ep.670220113>
- Alshabanat, M.N. and AL-Anazy, M.M., 2018. An experimental study of photocatalytic degradation of congo red using polymer nanocomposite films. *Journal of Chemistry*, 2018. <https://doi.org/10.1155/2018/9651850>

References

- Ameta, A., Ameta, R. and Ahuja, M., 2013. Photocatalytic degradation of methylene blue over ferric tungstate. *Scientific Reviews and Chemical Communications*, 3(3), pp.172-180.
- Amini, M., Arami, M., Mahmoodi, N.M. and Akbari, A., 2011. Dye removal from colored textile wastewater using acrylic grafted nanomembrane. *Desalination*, 267(1), pp.107-113. <https://doi.org/10.1016/j.desal.2010.09.014>
- Anjaneyulu, Y., Chary, N.S. and Raj, D.S.S., 2005. Decolourization of industrial effluents—available methods and emerging technologies—a review. *Reviews in Environmental Science and Bio/Technology*, 4(4), pp.245-273. <https://doi.org/10.1007/s11157-005-1246-z>
- Annadurai, G., Juang, R.S., Yen, P.S. and Lee, D.J., 2003. Use of thermally treated waste biological sludge as dye absorbent. *Advances in Environmental Research*, 7(3), pp.739-744. [https://doi.org/10.1016/S1093-0191\(02\)00044-8](https://doi.org/10.1016/S1093-0191(02)00044-8)
- Aranda, P.R., Moyano, S., Martinez, L.D. and De Vito, I.E., 2010. Determination of trace chromium (VI) in drinking water using X-ray fluorescence spectrometry after solid-phase extraction. *Analytical and bioanalytical chemistry*, 398(2), pp.1043-1048. <https://doi.org/10.1007/s00216-010-3950-y>
- Arslan, I., Balcioglu, I.A., Tuhkanen, T. and Bahnemann, D., 2000. H₂O₂/UV-C and Fe²⁺/H₂O₂/UV-C versus TiO₂/UV-A treatment for reactive dye wastewater. *Journal of Environmental Engineering*, 126(10), pp.903-911. [https://doi.org/10.1061/\(ASCE\)0733-9372\(2000\)126:10\(903\)](https://doi.org/10.1061/(ASCE)0733-9372(2000)126:10(903))
- Atchariyawut, S., Phattaranawik, J., Leiknes, T. and Jiraratananon, R., 2009. Application of ozonation membrane contacting system for dye wastewater treatment. *Separation and purification technology*, 66(1), pp.153-158. <https://doi.org/10.1016/j.seppur.2008.11.011>
- Attia, A.J., Kadhim, S.H. and Hussein, F.H., 2008. Photocatalytic degradation of textile dyeing wastewater using titanium dioxide and zinc oxide. *Journal of Chemistry*, 5(2), pp.219-223. <https://doi.org/10.1155/2008/876498>

References

- Augugliaro, V., Litter, M., Palmisano, L. and Soria, J., 2006. The combination of heterogeneous photocatalysis with chemical and physical operations: A tool for improving the photoprocess performance. *Journal of Photochemistry and Photobiology C: Photochemistry Reviews*, 7(4), pp.127-144. <https://doi.org/10.1016/j.jphotochemrev.2006.12.001>
- Ayers, R.S. and Westcot, D.W., 1985. *Water quality for agriculture* (Vol. 29). Rome: Food and Agriculture Organization of the United Nations.
- Azbar, N., Kestioglu, K. and Yonar, T., 2004. Comparison of various advanced oxidation processes and chemical treatment methods for COD and color removal from a polyester and acetate fiber dyeing effluent. *Chemosphere*, 55(1), pp.35-43. <https://doi.org/10.1016/j.chemosphere.2003.10.046>
- Azbar, N., Kestioglu, K. and Yonar, T., 2005. Application of Advanced Oxidation Processes (AOPs) to wastewater treatment. Case studies: decolourization of textile effluents, detoxification of olive mill effluent, treatment of domestic wastewater. *Water Pollution: New Research*, New York, Nova Science Publishers, Ed. AR Burk, pp.99-118.
- Baban, A., Yediler, A. and Ciliz, N.K., 2010. Integrated water management and CP implementation for wool and textile blend processes. *CLEAN–Soil, Air, Water*, 38(1), pp.84-90. <https://doi.org/10.1002/clen.200900102>
- Bal, W., Kozłowski, H. and Kasprzak, K.S., 2000. Molecular models in nickel carcinogenesis. *Journal of Inorganic Biochemistry*, 79(1-4), pp.213-218. [https://doi.org/10.1016/S0162-0134\(99\)00169-5](https://doi.org/10.1016/S0162-0134(99)00169-5)
- Baldwin, D.R. and Marshall, W.J., 1999. Heavy metal poisoning and its laboratory investigation. *Annals of clinical biochemistry*, 36(3), pp.267-300. <https://doi.org/10.1177/000456329903600301>
- Bansal, P. and Sud, D., 2011. Photodegradation of commercial dye, Procion Blue HERD from real textile wastewater using nanocatalysts. *Desalination*, 267(2-3), pp.244-249. <https://doi.org/10.1016/j.desal.2010.09.034>
- Bash, J., Berman, C.H. and Bolton, S., 2001. Effects of turbidity and suspended solids on salmonids. University of Washington Water Center. <http://hdl.handle.net/1773/16382>

References

- Baxendale, J.H. and Wilson, J.A., 1957. The photolysis of hydrogen peroxide at high light intensities. *Transactions of the Faraday Society*, 53, pp.344-356.
- Baysal, A., Ozbek, N. and Akman, S., 2013. Determination of trace metals in waste water and their removal processes. *Intech Open Science, Wastewater treatment technologies and recent analytical developments*. Retrieved September, 20(2014), pp.145-171. DOI: 10.5772/52025
- Belal, A.R., Cooper, S.M. and Khan, N.A., 2015. Corporate environmental responsibility and accountability: what chance in vulnerable Bangladesh?. *Critical Perspectives on Accounting*, 33, pp.44-58. <https://doi.org/10.1016/j.cpa.2015.01.005>
- Bizani, E., Fytianos, K., Poullos, I. and Tsiridis, V., 2006. Photocatalytic decolorization and degradation of dye solutions and wastewaters in the presence of titanium dioxide. *Journal of Hazardous Materials*, 136(1), pp.85-94. <https://doi.org/10.1016/j.jhazmat.2005.11.017>
- Blomqvist, A., 1996. *Food and fashion. Water management and collective action among irrigation farmers and textile industrialists in South India*. Linköping University.
- Bremner, I. and Beattie, J.H., 1990. Metallothionein and the trace minerals. *Annual review of nutrition*, 10(1), pp.63-83. <https://doi.org/10.1146/annurev.nu.10.070190.000431>
- Bringolf, R.B., Kwak, T.J., Cope, W.G. and Larimore, M.S., 2005. Salinity tolerance of flathead catfish: implications for dispersal of introduced populations. *Transactions of the American Fisheries Society*, 134(4), pp.927-936. <https://doi.org/10.1577/T04-195.1>
- Bulc, T.G. and Ojstršek, A., 2008. The use of constructed wetland for dye-rich textile wastewater treatment. *Journal of hazardous materials*, 155(1-2), pp.76-82. <https://doi.org/10.1016/j.jhazmat.2007.11.068>
- Bulut, Y. and Aydın, H., 2006. A kinetics and thermodynamics study of methylene blue adsorption on wheat shells. *Desalination*, 194(1-3), pp.259-267. <https://doi.org/10.1016/j.desal.2005.10.032>
- Casey, J.R., 2006. Why bicarbonate?. *Biochemistry and cell biology*, 84(6), pp.930-939. <https://doi.org/10.1139/o06-184>

References

- Casey, T.J., 1997. *Unit treatment processes in water and wastewater engineering*, Chichester: Wiley, pp.166-170.
- Catanho, M., Malpass, G.R.P. and Motheo, A.D.J., 2006. Evaluation of electrochemical and photoelectrochemical methods for the degradation of three textile dyes. *Quimica Nova*, 29(5), pp.983-989. <https://doi.org/10.1590/S0100-40422006000500018>
- Chatterjee, D., Patnam, V.R., Sikdar, A., Joshi, P., Misra, R. and Rao, N.N., 2008. Kinetics of the decoloration of reactive dyes over visible light-irradiated TiO₂ semiconductor photocatalyst. *Journal of Hazardous Materials*, 156(1-3), pp.435-441. <https://doi.org/10.1016/j.jhazmat.2007.12.038>
- Chaudhari, K., Bhatt, V., Bhargava, A. and Seshadri, S., 2011. Combinational system for the treatment of textile waste water: a future perspective. *Asian Journal of Water, Environment and Pollution*, 8(2), pp.127-136.
- Che Ramli, Z.A., Asim, N., Isahak, W.N., Emdadi, Z., Ahmad-Ludin, N., Yarmo, M.A. and Sopian, K., 2014. Photocatalytic degradation of methylene blue under UV light irradiation on prepared carbonaceous. *The Scientific World Journal*, 2014. <https://doi.org/10.1155/2014/415136>
- Chen, X. and Mao, S.S., 2007. Titanium dioxide nanomaterials: synthesis, properties, modifications, and applications. *Chemical reviews*, 107(7), pp.2891-2959. <https://doi.org/10.1021/cr0500535>
- Chequer, F.D., De Oliveira, G.R., Ferraz, E.A., Cardoso, J.C., Zanoni, M.B. and de Oliveira, D.P., 2013. Textile dyes: dyeing process and environmental impact. *Eco-friendly textile dyeing and finishing*, 6(6), pp.151-176.
- Correia, V.M., Stephenson, T. and Judd, S.J., 1994. Characterisation of textile wastewaters-a review. *Environmental technology*, 15(10), pp.917-929. <https://doi.org/10.1080/09593339409385500>
- Cox, B.A., 2003. A review of currently available in-stream water-quality models and their applicability for simulating dissolved oxygen in lowland rivers. *Science of the total environment*, 314, pp.335-377. [https://doi.org/10.1016/S0048-9697\(03\)00063-9](https://doi.org/10.1016/S0048-9697(03)00063-9)

References

- Crittenden, J.C., Liu, J., Hand, D.W. and Perram, D.L., 1997. Photocatalytic oxidation of chlorinated hydrocarbons in water. *Water Research*, 31(3), pp.429-438. [https://doi.org/10.1016/S0043-1354\(96\)00267-9](https://doi.org/10.1016/S0043-1354(96)00267-9)
- da Silva, C.G. and Faria, J.L., 2003. Photochemical and photocatalytic degradation of an azo dye in aqueous solution by UV irradiation. *Journal of Photochemistry and Photobiology A: Chemistry*, 155(1-3), pp.133-143. [https://doi.org/10.1016/S1010-6030\(02\)00374-X](https://doi.org/10.1016/S1010-6030(02)00374-X)
- Daneshvar, N., Aber, S., Dorraji, M.S., Khataee, A.R. and Rasoulifard, M.H., 2007. Photocatalytic degradation of the insecticide diazinon in the presence of prepared nanocrystalline ZnO powders under irradiation of UV-C light. *Separation and purification Technology*, 58(1), pp.91-98. <https://doi.org/10.1016/j.seppur.2007.07.016>
- Daneshvar, N., Salari, D. and Khataee, A.R., 2003. Photocatalytic degradation of azo dye acid red 14 in water: investigation of the effect of operational parameters. *Journal of Photochemistry and Photobiology A: Chemistry*, 157(1), pp.111-116. [https://doi.org/10.1016/S1010-6030\(03\)00015-7](https://doi.org/10.1016/S1010-6030(03)00015-7)
- Daneshvar, N., Salari, D. and Khataee, A.R., 2004. Photocatalytic degradation of azo dye acid red 14 in water on ZnO as an alternative catalyst to TiO₂. *Journal of photochemistry and photobiology A: chemistry*, 162(2-3), pp.317-322. [https://doi.org/10.1016/S1010-6030\(03\)00378-2](https://doi.org/10.1016/S1010-6030(03)00378-2)
- Das, S., Kamat, P.V., Padmaja, S., Au, V. and Madison, S.A., 1999. Free radical induced oxidation of the azo dye Acid Yellow 9. *Journal of the Chemical Society, Perkin Transactions 2*, (6), pp.1219-1224. <https://doi.org/10.1039/A809720H>
- Davis, R.J., Gainer, J.L., O'Neal, G. and Wu, I.W., 1994. Photocatalytic decolorization of wastewater dyes. *Water environment research*, 66(1), pp.50-53. <https://doi.org/10.2175/WER.66.1.8>
- Demirbas, E., Kobya, M., Öncel, S. and Şencan, S., 2002. Removal of Ni (II) from aqueous solution by adsorption onto hazelnut shell activated carbon: equilibrium studies. *Bioresource technology*, 84(3), pp.291-293. [https://doi.org/10.1016/S0960-8524\(02\)00052-4](https://doi.org/10.1016/S0960-8524(02)00052-4)

References

- Dostanić, J.M., Lončarević, D.R., Banković, P.T., Cvetković, O.G., Jovanović, D.M. and Mijin, D.Ž., 2011. Influence of process parameters on the photodegradation of synthesized azo pyridone dye in TiO₂ water suspension under simulated sunlight. *Journal of Environmental Science and Health, Part A*, 46(1), pp.70-79. <https://doi.org/10.1080/10934529.2011.526905>
- Duran, N. and Esposito, E., 2000. Potential applications of oxidative enzymes and phenoloxidase-like compounds in wastewater and soil treatment: a review. *Applied catalysis B: environmental*, 28(2), pp.83-99. [https://doi.org/10.1016/S0926-3373\(00\)00168-5](https://doi.org/10.1016/S0926-3373(00)00168-5)
- Edition, F., 2011. Guidelines for drinking-water quality. *WHO chronicle*, 38(4), pp.104-8.
- El-Bahy, Z.M., Ismail, A.A. and Mohamed, R.M., 2009. Enhancement of titania by doping rare earth for photodegradation of organic dye (Direct Blue). *Journal of Hazardous Materials*, 166(1), pp.138-143. <https://doi.org/10.1016/j.jhazmat.2008.11.022>
- Erdemoğlu, S., Aksu, S.K., Sayilkan, F., Izgi, B., Asiltürk, M., Sayilkan, H., Frimmel, F. and Güçer, Ş., 2008. Photocatalytic degradation of Congo Red by hydrothermally synthesized nanocrystalline TiO₂ and identification of degradation products by LC–MS. *Journal of Hazardous Materials*, 155(3), pp.469-476. <https://doi.org/10.1016/j.jhazmat.2007.11.087>
- Erswell, A., Brouckaert, C.J. and Buckley, C.A., 1988. The reuse of reactive dye liquors using charged ultrafiltration membrane technology. *Desalination*, 70(1-3), pp.157-167. [https://doi.org/10.1016/0011-9164\(88\)85051-3](https://doi.org/10.1016/0011-9164(88)85051-3)
- Esmaili, H., Kotobi, A., Sheibani, S. and Rashchi, F., 2018. Photocatalytic degradation of methylene blue by nanostructured Fe/FeS powder under visible light. *International Journal of Minerals, Metallurgy, and Materials*, 25(2), pp.244-252. <https://doi.org/10.1007/s12613-018-1567-x>
- Eswaramoorthi, S., Dhanapal, K. and Chauhan, D., 2008. Advanced in textile waste water treatment: The case for UV-ozonation and membrane bioreactor for common effluent treatment plants in Tirupur, Tamil Nadu, India. *Environment with People's Involvement and Co-ordination in India. Coimbatore, India.*

References

- Fang, S., Jiang, Y., Wang, A., Yang, Z. and Li, F., 2004. Photocatalytic performance of natural zeolite modified by TiO₂. *China. Non-Metallic Mines*, 27(1), pp.14-21.
- Fennessy, M.S. and Cronk, J.K., 1997. The effectiveness and restoration potential of riparian ecotones for the management of nonpoint source pollution, particularly nitrate. *Critical reviews in environmental science and technology*, 27(4), pp.285-317. <https://doi.org/10.1080/10643389709388502>
- FIBRE2FASHION, 2006. <https://www.fibre2fashion.com/industry-article/740/textile-effluent-treatment> (last visit: 25-06-2020)
- FIBRE2FASHION, 2012. <https://www.fibre2fashion.com/industry-article/6262/various-pollutants-released-into-environment-by-textile-industry> (last visit: 25-06-2020)
- Frank, S.N. and Bard, A.J., 1977. Heterogeneous photocatalytic oxidation of cyanide ion in aqueous solutions at titanium dioxide powder. *Journal of the American Chemical Society*, 99(1), pp.303-304. <https://doi.org/10.1021/ja00443a081>
- Fujishima, A. and Honda, K., 1972. Electrochemical photolysis of water at a semiconductor electrode. *nature*, 238(5358), pp.37-38. <https://doi.org/10.1038/238037a0>
- Fujishima, A., Rao, T.N. and Tryk, D.A., 2000. Titanium dioxide photocatalysis. *Journal of photochemistry and photobiology C: Photochemistry reviews*, 1(1), pp.1-21. [https://doi.org/10.1016/S1389-5567\(00\)00002-2](https://doi.org/10.1016/S1389-5567(00)00002-2)
- Galindo, C., Jacques, P. and Kalt, A., 2000. Photodegradation of the aminoazobenzene acid orange 52 by three advanced oxidation processes: UV/H₂O₂, UV/ TiO₂ and VIS/ TiO₂: comparative mechanistic and kinetic investigations. *Journal of Photochemistry and Photobiology A: Chemistry*, 130(1), pp.35-47. [https://doi.org/10.1016/S1010-6030\(99\)00199-9](https://doi.org/10.1016/S1010-6030(99)00199-9)
- Galindo, C., Jacques, P. and Kalt, A., 2001. Photochemical and photocatalytic degradation of an indigoid dye: a case study of acid blue 74 (AB74). *Journal of Photochemistry and Photobiology A: Chemistry*, 141(1), pp.47-56. [https://doi.org/10.1016/S1010-6030\(01\)00435-X](https://doi.org/10.1016/S1010-6030(01)00435-X)

References

- Ganesan, R. and Thanasekaran, K., 2011. Decolourisation of textile dyeing Wastewater by modified solar Photo-Fenton Oxidation. *International Journal of Environmental Sciences*, 1(6), pp.1168.
- Geetha, A., Palanisamy, P.N., Sivakumar, P., Kumar, P.G. and Sujatha, M., 2008. Assessment of underground water contamination and effect of textile effluents on Noyyal River basin in and around Tiruppur Town, Tamilnadu. *E-journal of Chemistry*, 5(4), pp.696-705. <https://doi.org/10.1155/2008/394052>
- Georgiou, D., Melidis, P., Aivasidis, A. and Gimouhopoulos, K., 2002. Degradation of azo-reactive dyes by ultraviolet radiation in the presence of hydrogen peroxide. *Dyes and pigments*, 52(2), pp.69-78. [https://doi.org/10.1016/S0143-7208\(01\)00078-X](https://doi.org/10.1016/S0143-7208(01)00078-X)
- Ghaly, A.E., Ananthashankar, R., Alhattab, M.V.V.R. and Ramakrishnan, V.V., 2014. Production, characterization and treatment of textile effluents: a critical review. *J Chem Eng Process Technol*, 5(1), pp.1-19. <http://dx.doi.org/10.4172/2157-7048.1000182>
- Gharbani, P., Tabatabaie, S.M. and Mehrizad, A., 2008. Removal of Congo red from textile wastewater by ozonation. *International Journal of Environmental science and Technology*, 5(4), pp.495-500. <https://doi.org/10.1007/BF03326046>
- Ghasemi, B., Anvaripour, B., Jorfi, S. and Jaafarzadeh, N., 2016. Enhanced photocatalytic degradation and mineralization of furfural using UVC/TiO₂/GAC composite in aqueous solution. *International Journal of Photoenergy*, 2016. <https://doi.org/10.1155/2016/2782607>
- Giller, P.S., Giller, P. and Malmqvist, B., 1998. *The biology of streams and rivers*. Oxford University Press.
- Giwa, A., Nkeonye, P.O., Bello, K.A., Kolawole, E.G. and Campos, A.O., 2012. Solar photocatalytic degradation of reactive yellow 81 and reactive violet 1 in aqueous solution containing semiconductor oxides. *International Journal of Applied*, 2(4), pp.90-105.

References

- Gnanaprakasam, A., Sivakumar, V.M. and Thirumarimurugan, M., 2015. Influencing parameters in the photocatalytic degradation of organic effluent via nanometal oxide catalyst: a review. *Indian Journal of Materials Science*, 2015. <http://dx.doi.org/10.1155/2015/601827>
- Gogate, P.R. and Pandit, A.B., 2004. A review of imperative technologies for wastewater treatment I: oxidation technologies at ambient conditions. *Advances in Environmental Research*, 8(3-4), pp.501-551. [https://doi.org/10.1016/S1093-0191\(03\)00032-7](https://doi.org/10.1016/S1093-0191(03)00032-7)
- Goldhaber, S.B., 2003. Trace element risk assessment: essentiality vs. toxicity. *Regulatory toxicology and pharmacology*, 38(2), pp.232-242. [https://doi.org/10.1016/S0273-2300\(02\)00020-X](https://doi.org/10.1016/S0273-2300(02)00020-X)
- Grau, P., 1991. Textile industry wastewaters treatment. *Water Science and Technology*, 24(1), pp.97-103. <https://doi.org/10.2166/wst.1991.0015>
- Gray, M.A., Harrins, A. and Centeno, J.A., 2005. The role of cadmium, zinc, and selenium in prostate disease. *Metal contaminants in New Zealand: sources, treatments, and effects on ecology and human health*, 20, pp.393-414.
- Greenberg, A.E., Clesceri, L.S. and Eaton, A.D., 1992. Standard methods for the examination of water and wastewater. Published by American public health association, 18th edition, Washington, DC. In *Library congress ISBN 0-87553-207-1*.
- Grzechulska, J. and Morawski, A.W., 2002. Photocatalytic decomposition of azo-dye acid black 1 in water over modified titanium dioxide. *Applied Catalysis B: Environmental*, 36(1), pp.45-51. [https://doi.org/10.1016/S0926-3373\(01\)00275-2](https://doi.org/10.1016/S0926-3373(01)00275-2)
- Guettai, N. and Amar, H.A., 2005. Photocatalytic oxidation of methyl orange in presence of titanium dioxide in aqueous suspension. Part I: Parametric study. *Desalination*, 185(1-3), pp.427-437. <https://doi.org/10.1016/j.desal.2005.04.048>

References

- Guillard, C., Lachheb, H., Houas, A., Ksibi, M., Elaloui, E. and Herrmann, J.M., 2003. Influence of chemical structure of dyes, of pH and of inorganic salts on their photocatalytic degradation by TiO₂ comparison of the efficiency of powder and supported TiO₂. *Journal of Photochemistry and Photobiology A: Chemistry*, 158(1), pp.27-36. [https://doi.org/10.1016/S1010-6030\(03\)00016-9](https://doi.org/10.1016/S1010-6030(03)00016-9)
- Gümüş, D. and Akbal, F., 2011. Photocatalytic degradation of textile dye and wastewater. *Water, Air, and Soil Pollution*, 216(1-4), pp.117-124. <https://doi.org/10.1007/s11270-010-0520-z>
- Gupta, U.C. and Gupta, S.C., 1998. Trace element toxicity relationships to crop production and livestock and human health: implications for management. *Communications in Soil Science and Plant Analysis*, 29(11-14), pp.1491-1522. <https://doi.org/10.1080/00103629809370045>
- Gupta, V.K., Ali, I., Saleh, T.A., Nayak, A. and Agarwal, S., 2012. Chemical treatment technologies for waste-water recycling—an overview. *Rsc Advances*, 2(16), pp.6380-6388. <https://doi.org/10.1039/C2RA20340E>
- Habibi, M.H., Hassanzadeh, A. and Mahdavi, S., 2005. The effect of operational parameters on the photocatalytic degradation of three textile azo dyes in aqueous TiO₂ suspensions. *Journal of Photochemistry and Photobiology A: Chemistry*, 172(1), pp.89-96. <https://doi.org/10.1016/j.jphotochem.2004.11.009>
- Harikumar, P.S., Joseph, L. and Dhanya, A., 2013. Photocatalytic degradation of textile dyes by hydrogel supported titanium dioxide nanoparticles. *Journal of Environmental Engineering and Ecological Science*, 2(2). <http://dx.doi.org/10.7243/2050-1323-2-2>
- Harper, D.D., Farag, A.M. and Skaar, D., 2014. Acute toxicity of sodium bicarbonate, a major component of coal bed natural gas produced waters, to 13 aquatic species as defined in the laboratory. *Environmental toxicology and chemistry*, 33(3), pp.525-531. <https://doi.org/10.1002/etc.2452>
- Harris, Z.L. and Gitlin, J.D., 1996. Genetic and molecular basis for copper toxicity. *The American journal of clinical nutrition*, 63(5), pp.836S-841S. <https://doi.org/10.1093/ajcn/63.5.836>

References

- Hasan, M.K., Shahriar, A. and Jim, K.U., 2019. Water pollution in Bangladesh and its impact on public health. *Heliyon*, 5(8), p.e02145. <https://doi.org/10.1016/j.heliyon.2019.e02145>
- Hasani, A., Seyf, S., Javid, A.H. and Borgheei, M., 2008. Comparison of adsorption process by GAC with novel formulation of coagulation–flocculation for color removal of textile wastewater. *International Journal of Environmental Research*, 2(3), pp.239-248.
- Hassaan, M.A. and El Nemr, A., 2017. Advanced oxidation processes for textile wastewater treatment. *International Journal of Photochemistry and Photobiology*, 2(3), pp.85-93. doi: 10.11648/j.ijpp.20170203.13
- Heizer, W.D., Sandler, R.S., Seal, E., Murray, S.C., Busby, M.G., Schliebe, B.G. and Pusek, S.N., 1997. Intestinal effects of sulfate in drinking water on normal human subjects. *Digestive diseases and sciences*, 42(5), pp.1055-1061. <https://doi.org/10.1023/A:1018801522760>
- Hooper, P.L., Visconti, L., Garry, P.J. and Johnson, G.E., 1980. Zinc lowers high-density lipoprotein-cholesterol levels. *Jama*, 244(17), pp.1960-1961. doi:10.1001/jama.1980.03310170058030
- Hossain, L., Sarker, S.K. and Khan, M.S., 2018. Evaluation of present and future wastewater impacts of textile dyeing industries in Bangladesh. *Environmental Development*, 26, pp.23-33. <https://doi.org/10.1016/j.envdev.2018.03.005>
- Hossain, M.D., 2019. Waste Water Production in Fabric Processing in Bangladesh. *European Online Journal of Natural and Social Sciences*, 8(3), pp-558.
- Houas, A., Lachheb, H., Ksibi, M., Elaloui, E., Guillard, C. and Herrmann, J.M., 2001. Photocatalytic degradation pathway of methylene blue in water. *Applied Catalysis B: Environmental*, 31(2), pp.145-157. [https://doi.org/10.1016/S0926-3373\(00\)00276-9](https://doi.org/10.1016/S0926-3373(00)00276-9)
- Hsueh, C.L., Huang, Y.H., Wang, C.C. and Chen, C.Y., 2005. Degradation of azo dyes using low iron concentration of Fenton and Fenton-like system. *Chemosphere*, 58(10), pp.1409-1414. <https://doi.org/10.1016/j.chemosphere.2004.09.091>

References

- Hussain, M. and Rao, T.P., 2013. Effect of Industrial Effluents on Surface Water Quality-A Case Study of Patancheru, Andhra Pradesh, India. *Current World Environment*, 8(3), pp. 445-454. <http://dx.doi.org/10.12944/CWE.8.3.14>
- Hussein, F.H. and Abass, T.A., 2010. Photocatalytic treatment of textile industrial wastewater. *International Journal of Chemical Sciences*, 8(3), pp.1353-1364.
- Imed, M., Fatima, H. and Abdelhamid, K., 2008. Protective effects of selenium (Se) and zinc (Zn) on cadmium (Cd) toxicity in the liver and kidney of the rat: histology and Cd accumulation. *Food and chemical toxicology*, 46(11), pp.3522-3527. <https://doi.org/10.1016/j.fct.2008.08.037>
- Ince, N.H. and Tezcanlı, G., 1999. Treatability of textile dye-bath effluents by advanced oxidation: preparation for reuse. *Water Science and Technology*, 40(1), pp.183-190 [https://doi.org/10.1016/S0273-1223\(99\)00379-0](https://doi.org/10.1016/S0273-1223(99)00379-0)
- Islam, M.M., Mahmud, K., Faruk, O. and Billah, M.S., 2011. Textile dyeing industries in Bangladesh for sustainable development. *International Journal of Environmental Science and Development*, 2(6), p.428.
- Islam, M.R. and Mostafa, M.G., 2020. Characterization of textile dyeing effluent and its treatment using polyaluminum chloride. *Applied Water Science*, 10(5), pp.1-10. <https://doi.org/10.1007/s13201-020-01204-4>
- Islam, R., Al Foisal, J., Rahman, M., Lisa, L.A. and Paul, D.K., 2016. Pollution assessment and heavy metal determination by AAS in waste water collected from Kushtia industrial zone in Bangladesh. *African Journal of Environmental Science and Technology*, 10(1), pp.9-17. [10.5897/AJEST2014.1994](https://doi.org/10.5897/AJEST2014.1994)
- Jain, R. and Shrivastava, M., 2008. Photocatalytic removal of hazardous dye cyanosine from industrial waste using titanium dioxide. *Journal of Hazardous materials*, 152(1), pp.216-220. <https://doi.org/10.1016/j.jhazmat.2007.06.119>
- Jain, S.K. and Singh, V.P., 2003. *Water resources systems planning and management*. Elsevier.
- Joshi, K.M. and Shrivastava, V.S., 2015. Detection and identification of metals, nonmetals and organic compounds from industrial wastewater by analytical methods. *Journal of Advanced Chemical Sciences*, pp.56-58.

References

- Juang, R.S., Lin, S.H. and Hsueh, P.Y., 2010. Removal of binary azo dyes from water by UV-irradiated degradation in TiO₂ suspensions. *Journal of Hazardous materials*, 182(1-3), pp.820-826. <https://doi.org/10.1016/j.jhazmat.2010.06.113>
- Kacar, Y., Alpay, E. and Ceylan, V.K., 2003. Pretreatment of Afyon alcaloide factory's wastewater by wet air oxidation (WAO). *Water Research*, 37(5), pp.1170-1176. [https://doi.org/10.1016/S0043-1354\(02\)00448-7](https://doi.org/10.1016/S0043-1354(02)00448-7)
- Kamble, S.P., Sawant, S.B. and Pangarkar, V.G., 2003. Batch and continuous photocatalytic degradation of benzenesulfonic acid using concentrated solar radiation. *Industrial and engineering chemistry research*, 42(26), pp.6705-6713. <https://doi.org/10.1021/ie030493r>
- Kanan, A.H., Marine, S.S., Raihan, F., Redowan, M. and Miah, M., 2014. Textile effluents changes physiochemical parameters of water and soil: Threat for agriculture. *African Journal of Agronomy*, 2(10), pp.219-223.
- Kaneco, S., Rahman, M.A., Suzuki, T., Katsumata, H. and Ohta, K., 2004. Optimization of solar photocatalytic degradation conditions of bisphenol A in water using titanium dioxide. *Journal of photochemistry and photobiology A: Chemistry*, 163(3), pp.419-424. <https://doi.org/10.1016/j.jphotochem.2004.01.012>
- Kang, S.F., Yen, H.Y. and Yang, M.H., 2003. Treatment of textile effluents by H₂O₂/UV oxidation combined with RO separation for reuse. *Journal of Environmental Science and Health, Part A*, 38(7), pp.1327-1339. <https://doi.org/10.1081/ESE-120021129>
- Kannan, N. and Sundaram, M.M., 2001. Kinetics and mechanism of removal of methylene blue by adsorption on various carbons—a comparative study. *Dyes and pigments*, 51(1), pp.25-40. [https://doi.org/10.1016/S0143-7208\(01\)00056-0](https://doi.org/10.1016/S0143-7208(01)00056-0)
- Kansal, S.K., Kaur, N. and Singh, S., 2009. Photocatalytic degradation of two commercial reactive dyes in aqueous phase using nanophotocatalysts. *Nanoscale research letters*, 4(7), p.709. <https://doi.org/10.1007/s11671-009-9300-3>

References

- Kansal, S.K., Singh, M. and Sud, D., 2007. Studies on photodegradation of two commercial dyes in aqueous phase using different photocatalysts. *Journal of hazardous materials*, 141(3), pp.581-590. <https://doi.org/10.1016/j.jhazmat.2006.07.035>
- Kasanen, J., Salstela, J., Suvanto, M. and Pakkanen, T.T., 2011. Photocatalytic degradation of methylene blue in water solution by multilayer TiO₂ coating on HDPE. *Applied Surface Science*, 258(5), pp.1738-1743. <https://doi.org/10.1016/j.apsusc.2011.10.028>
- Kestioğlu, K., Yonar, T. and Azbar, N., 2005. Feasibility of physico-chemical treatment and advanced oxidation processes (AOPs) as a means of pretreatment of olive mill effluent (OME). *Process Biochemistry*, 40(7), pp.2409-2416. <https://doi.org/10.1016/j.procbio.2004.09.015>
- Khan, S. and Malik, A., 2014. Environmental and health effects of textile industry wastewater. In *Environmental deterioration and human health* (pp. 55-71). Springer, Dordrecht. https://doi.org/10.1007/978-94-007-7890-0_4
- Khan, W.Z., Najeeb, I. and Ishtiaque, S., 2016. Photocatalytic degradation of a real textile wastewater using titanium dioxide, zinc oxide and hydrogen peroxide. *Int J Eng Sci*, 5(7), pp.61-70.
- Khataee, A.R., Pons, M.N. and Zahraa, O., 2010. Photocatalytic decolorisation and mineralisation of orange dyes on immobilised titanium dioxide nanoparticles. *Water Science and Technology*, 62(5), pp.1112-1120. <https://doi.org/10.2166/wst.2010.438>
- Kondakis, X.G., Makris, N., Leotsinidis, M., Prinou, M. and Papapetropoulos, T., 1989. Possible health effects of high manganese concentration in drinking water. *Archives of Environmental Health: An International Journal*, 44(3), pp.175-178. <https://doi.org/10.1080/00039896.1989.9935883>
- Kondarides, D.I., 2010. Photocatalysis. *Catalysis. Encyclopedia of life support systems (EOLSS), developed under the auspices of the UNESCO. EOLSS Publishers, Paris.*
- Konstantinou, I.K. and Albanis, T.A., 2004. TiO₂-assisted photocatalytic degradation of azo dyes in aqueous solution: kinetic and mechanistic investigations: a

References

- review. *Applied Catalysis B: Environmental*, 49(1), pp.1-14.
<https://doi.org/10.1016/j.apcatb.2003.11.010>
- Kulkarni, M. and Thakur, P., 2014. Photocatalytic degradation of real textile industrial effluent under UV light catalyzed by metal oxide nanoparticles. *Nepal Journal of Science and Technology*, 15(2), pp.105-110.
<https://doi.org/10.3126/njst.v15i2.12124>
- Kumar, A. and Pandey, G., 2017. A review on the factors affecting the photocatalytic degradation of hazardous materials. *Mater. Sci. Eng. Int. J*, 1(3), pp.1-10.
10.15406/mseij.2017.01.00018
- Kunz, A., Peralta-Zamora, P., de Moraes, S.G. and Duran, N., 2002. New tendencies on textile effluent treatment. *Quimica Nova*, 25(1), pp.78-82.
<http://dx.doi.org/10.1590/S0100-40422002000100014>
- Kusvuran, E., Gulnaz, O., Irmak, S., Atanur, O.M., Yavuz, H.I. and Erbatur, O., 2004. Comparison of several advanced oxidation processes for the decolorization of Reactive Red 120 azo dye in aqueous solution. *Journal of Hazardous Materials*, 109(1-3), pp.85-93. <https://doi.org/10.1016/j.jhazmat.2004.03.009>
- Lachheb, H., Puzenat, E., Houas, A., Ksibi, M., Elaloui, E., Guillard, C. and Herrmann, J.M., 2002. Photocatalytic degradation of various types of dyes (Alizarin S, Crocein Orange G, Methyl Red, Congo Red, Methylene Blue) in water by UV-irradiated titania. *Applied Catalysis B: Environmental*, 39(1), pp.75-90. [https://doi.org/10.1016/S0926-3373\(02\)00078-4](https://doi.org/10.1016/S0926-3373(02)00078-4)
- Langland, M. and Cronin, T., 2003. A summary report of sediment processes in Chesapeake Bay and watershed: US Geological Survey water-resources investigations report 2003–4123. <https://doi.org/10.3133/wri034123>
- Lathasree, S., Rao, A.N., SivaSankar, B., Sadasivam, V. and Rengaraj, K., 2004. Heterogeneous photocatalytic mineralisation of phenols in aqueous solutions. *Journal of Molecular Catalysis A: Chemical*, 223(1-2), pp.101-105.
<https://doi.org/10.1016/j.molcata.2003.08.032>
- Ledakowicz, S., Solecka, M. and Zylla, R., 2001. Biodegradation, decolourisation and detoxification of textile wastewater enhanced by advanced oxidation processes. *Journal of biotechnology*, 89(2-3), pp.175-184.
[https://doi.org/10.1016/S0168-1656\(01\)00296-6](https://doi.org/10.1016/S0168-1656(01)00296-6)

References

- Legrini, O., Oliveros, E. and Braun, A.M., 1993. Photochemical processes for water treatment. *Chemical reviews*, 93(2), pp.671-698. <https://doi.org/10.1021/cr00018a003>
- Li, F., Sun, S., Jiang, Y., Xia, M., Sun, M. and Xue, B., 2008. Photodegradation of an azo dye using immobilized nanoparticles of TiO₂ supported by natural porous mineral. *Journal of Hazardous Materials*, 152(3), pp.1037-1044. <https://doi.org/10.1016/j.jhazmat.2007.07.114>
- Li, X.Z. and Zhang, M., 1996. Decolorization and biodegradability of dyeing wastewater treated by a TiO₂-sensitized photo-oxidation process. *Water Science and Technology*, 34(9), pp.49-55. [https://doi.org/10.1016/S0273-1223\(96\)00786-X](https://doi.org/10.1016/S0273-1223(96)00786-X)
- Ling, C.M., Mohamed, A.R. and Bhatia, S., 2004. Performance of photocatalytic reactors using immobilized TiO₂ film for the degradation of phenol and methylene blue dye present in water stream. *Chemosphere*, 57(7), pp.547-554. <https://doi.org/10.1016/j.chemosphere.2004.07.011>
- Liu, Y., Sun, N., Hu, J., Li, S. and Qin, G., 2018. Photocatalytic degradation properties of α -Fe₂O₃ nanoparticles for dibutyl phthalate in aqueous solution system. *Royal Society open science*, 5(4), pp.172196. <https://doi.org/10.1098/rsos.172196>
- Lokhande, R.S., Singare, P.U. and Pimple, D.S., 2011. Toxicity study of heavy metals pollutants in waste water effluent samples collected from Taloja industrial estate of Mumbai, India. *Resources and Environment*, 1(1), pp.13-19. [10.5923/j.re.20110101.02](https://doi.org/10.5923/j.re.20110101.02)
- Maas, R. and Chaudhari, S., 2005. Adsorption and biological decolourization of azo dye Reactive Red 2 in semicontinuous anaerobic reactors. *Process biochemistry*, 40(2), pp.699-705. <https://doi.org/10.1016/j.procbio.2004.01.038>
- Madhu, G.M., Raj, A., Lourdu, M.A., Pai, K. and Rao, S., 2007. Photodegradation of methylene blue dye using UV/BaTiO₃, UV/H₂O₂ and UV/H₂O₂/BaTiO₃ oxidation processes. *Indian Journal of Chemical Technology*, 14(2), pp.139-144. <http://hdl.handle.net/123456789/1074>

References

- Madhu, G.M., Raj, M.L.A. and Pai, K.V.K., 2009. Titanium oxide (TiO₂) assisted photocatalytic degradation of methylene blue. *Journal of environmental biology*, 30(2), pp.259-264.
- Mahlambi, M.M., Ngila, C.J. and Mamba, B.B., 2015. Recent developments in environmental photocatalytic degradation of organic pollutants: the case of titanium dioxide nanoparticles—a review. *Journal of Nanomaterials*, 2015. <https://doi.org/10.1155/2015/790173>
- Mahmoodi, N.M. and Arami, M., 2006. Bulk phase degradation of Acid Red 14 by nanophotocatalysis using immobilized titanium (IV) oxide nanoparticles. *Journal of Photochemistry and Photobiology A: Chemistry*, 182(1), pp.60-66. <https://doi.org/10.1016/j.jphotochem.2006.01.014>
- Mahmoodi, N.M. and Arami, M., 2008. Modeling and sensitivity analysis of dyes adsorption onto natural adsorbent from colored textile wastewater. *Journal of Applied Polymer Science*, 109(6), pp.4043-4048. <https://doi.org/10.1002/app.28547>
- Mahmoodi, N.M. and Arami, M., 2009. Degradation and toxicity reduction of textile wastewater using immobilized titania nanophotocatalysis. *Journal of Photochemistry and Photobiology B: Biology*, 94(1), pp.20-24. <https://doi.org/10.1016/j.jphotobiol.2008.09.004>
- Mahmoodi, N.M. and Arami, M., 2010. Immobilized titania nanophotocatalysis: Degradation, modeling and toxicity reduction of agricultural pollutants. *Journal of alloys and compounds*, 506(1), pp.155-159. <https://doi.org/10.1016/j.jallcom.2010.06.164>
- Maji, S.K., Mukherjee, N., Mondal, A. and Adhikary, B., 2012. Synthesis, characterization and photocatalytic activity of α -Fe₂O₃ nanoparticles. *Polyhedron*, 33(1), pp.145-149. <https://doi.org/10.1016/j.poly.2011.11.017>
- Malato, S., Blanco, J., Richter, C., Braun, B. and Maldonado, M.I., 1998. Enhancement of the rate of solar photocatalytic mineralization of organic pollutants by inorganic oxidizing species. *Applied Catalysis B: Environmental*, 17(4), pp.347-356. [https://doi.org/10.1016/S0926-3373\(98\)00019-8](https://doi.org/10.1016/S0926-3373(98)00019-8)
- Manahan, S.E., 2002. *Toxicological chemistry and biochemistry*. CRC Press.

References

- Mandal, A., Ojha, K., De Asim, K. and Bhattacharjee, S., 2004. Removal of catechol from aqueous solution by advanced photo-oxidation process. *Chemical engineering journal*, 102(2), pp.203-208. <https://doi.org/10.1016/j.cej.2004.05.007>
- Manekar, P., Patkar, G., Aswale, P., Mahure, M. and Nandy, T., 2014. Detoxifying of high strength textile effluent through chemical and bio-oxidation processes. *Bioresource technology*, 157, pp.44-51. <https://doi.org/10.1016/j.biortech.2014.01.046>
- Martínez, C.M.C.L., Fernández, M.I., Santaballa, J.A. and Faria, J., 2011. Kinetics and mechanism of aqueous degradation of carbamazepine by heterogeneous photocatalysis using nanocrystalline TiO₂, ZnO and multi-walled carbon nanotubes–anatase composites. *Applied Catalysis B: Environmental*, 102(3-4), pp.563-571. <https://doi.org/10.1016/j.apcatb.2010.12.039>
- Mester, T. and Tien, M., 2000. Oxidation mechanism of ligninolytic enzymes involved in the degradation of environmental pollutants. *International biodeterioration and biodegradation*, 46(1), pp.51-59. [https://doi.org/10.1016/S0964-8305\(00\)00071-8](https://doi.org/10.1016/S0964-8305(00)00071-8)
- Mills, A., Davies, R.H. and Worsley, D., 1993. Water purification by semiconductor photocatalysis. *Chemical Society Reviews*, 22(6), pp.417-425.
- Minussi, R.C., De Moraes, S.G., Pastore, G.M. and Duran, N., 2001. Biodecolorization screening of synthetic dyes by four white-rot fungi in a solid medium: possible role of siderophores. *Letters in applied microbiology*, 33(1), pp.21-25. <https://doi.org/10.1046/j.1472-765X.2001.00943.x>
- Mohabansi, N.P., Patil, V.B. and Yenkie, N., 2011. A comparative study on photo degradation of methylene blue dye effluent by advanced oxidation process by using TiO₂/ZnO photo catalyst. *Rasayan Journal of Chemistry*, 4(4), pp.814-819.
- Mohamed, R.M., Mkhallid, I.A., Baeissa, E.S. and Al-Rayyani, M.A., 2012. Photocatalytic degradation of methylene blue by Fe/ZnO/SiO₂ nanoparticles under visiblelight. *Journal of Nanotechnology*, 2012. <https://doi.org/10.1155/2012/329082>

References

- Momtaz, H., Alam, F., Ahsan, M.A., Akbor, M.A. and Rashid, M.M., 2012. Surface water quality around DEPZ industrial area, Savar, Dhaka. *Bangladesh Journal of Scientific and Industrial Research*, 47(3), pp.279-286. <https://doi.org/10.3329/bjsir.v47i3.13061>
- Mondal, S. and Bhagchandani, C., 2016. Novel effluent treatment technique in textile industry. *International Journal of Advance Research and Innovative Ideas in Education*, 2(3), pp. 573-588.
- Mostafa, M.G., Uddin, S.H. and Haque, A.B.M.H., 2017. Assessment of hydro-geochemistry and groundwater quality of Rajshahi City in Bangladesh. *Applied Water Science*, 7(8), pp.4663-4671. <https://doi.org/10.1007/s13201-017-0629-y>
- Mozia, S., Morawski, A.W., Toyoda, M. and Inagaki, M., 2008. Effectiveness of photodecomposition of an azo dye on a novel anatase-phase TiO₂ and two commercial photocatalysts in a photocatalytic membrane reactor (PMR). *Separation and purification technology*, 63(2), pp.386-391. <https://doi.org/10.1016/j.seppur.2008.05.029>
- Mukhlis, M.B., Najnin, F., Rahman, M.M. and Uddin, M.J., 2013. Photocatalytic degradation of different dyes using TiO₂ with high surface area: a kinetic study. *Journal of Scientific Research*, 5(2), pp.301-314. <https://doi.org/10.3329/jsr.v5i2.11641>
- Muruganandham, M. and Swaminathan, M., 2006. Photocatalytic decolourisation and degradation of Reactive Orange 4 by TiO₂-UV process. *Dyes and pigments*, 68(2-3), pp.133-142. <https://doi.org/10.1016/j.dyepig.2005.01.004>
- Muruganandham, M., Sobana, N. and Swaminathan, M., 2006. Solar assisted photocatalytic and photochemical degradation of Reactive Black 5. *Journal of hazardous materials*, 137(3), pp.1371-1376. <https://doi.org/10.1016/j.jhazmat.2006.03.030>
- Neppolian, B., Choi, H.C., Sakthivel, S., Arabindoo, B. and Murugesan, V., 2002a. Solar/UV-induced photocatalytic degradation of three commercial textile dyes. *Journal of hazardous materials*, 89(2-3), pp.303-317. [https://doi.org/10.1016/S0304-3894\(01\)00329-6](https://doi.org/10.1016/S0304-3894(01)00329-6)

References

- Neppolian, B., Choi, H.C., Sakthivel, S., Arabindoo, B. and Murugesan, V., 2002b. Solar light induced and TiO₂ assisted degradation of textile dye reactive blue 4. *Chemosphere*, 46(8), pp.1173-1181. [https://doi.org/10.1016/S0045-6535\(01\)00284-3](https://doi.org/10.1016/S0045-6535(01)00284-3)
- Neppolian, B., Kanel, S.R., Choi, H.C., Shankar, M.V., Arabindoo, B. and Murugesan, V., 2003. Photocatalytic degradation of reactive yellow 17 dye in aqueous solution in the presence of TiO₂ with cement binder. *International journal of Photoenergy*, 5. <https://doi.org/10.1155/S1110662X03000126>
- Neppolian, B., Sakthivel, S., Arabindoo, B., Palanichamy, M. and Murugesan, V., 2001. Kinetics of photocatalytic degradation of reactive yellow 17 dye in aqueous solution using UV irradiation. *Journal of Environmental Science and Health, Part A*, 36(2), pp.203-213. <https://doi.org/10.1081/ESE-100102618>
- Nezamzadeh-Ejehieh, A. and Zabihi-Mobarakeh, H., 2014. Heterogeneous photodecolorization of mixture of methylene blue and bromophenol blue using CuO-nano-clinoptilolite. *Journal of Industrial and Engineering Chemistry*, 20(4), pp.1421-1431. <https://doi.org/10.1016/j.jiec.2013.07.027>
- Nielsen, G.D., S oderberg, U., J rgensen, P.J., Templeton, D.M., Rasmussen, S.N., Andersen, K.E. and Grandjean, P., 1999. Absorption and retention of nickel from drinking water in relation to food intake and nickel sensitivity. *Toxicology and applied pharmacology*, 154(1), pp.67-75. <https://doi.org/10.1006/taap.1998.8577>
- Nomikos, G.N., Panagiotopoulou, P., Kondarides, D.I. and Verykios, X.E., 2014. Kinetic and mechanistic study of the photocatalytic reforming of methanol over Pt/ TiO₂ catalyst. *Applied Catalysis B: Environmental*, 146, pp.249-257. <https://doi.org/10.1016/j.apcatb.2013.03.018>
- Ntuli, F., Omoregbe, D.I., Kuipa, P.K., Muzenda, E. and Belaid, M., 2009. Characterization of effluent from textile wet finishing operations. World Congress on Engineering and Computer Science. San Francisco, USA
- O'Neill, C., Hawkes, F.R., Hawkes, D.L., Louren o, N.D., Pinheiro, H.M. and Del e, W., 1999. Colour in textile effluents—sources, measurement, discharge consents and simulation: a review. *Journal of Chemical Technology and Biotechnology: International Research in Process, Environmental and Clean Technology*, 74(11), pp.1009-1018. [https://doi.org/10.1002/\(SICI\)1097-4660\(199911\)74:11<1009::AID-JCTB153>3.0.CO;2-N](https://doi.org/10.1002/(SICI)1097-4660(199911)74:11<1009::AID-JCTB153>3.0.CO;2-N)

References

- Okamoto, K.I., Yamamoto, Y., Tanaka, H., Tanaka, M. and Itaya, A., 1985. Heterogeneous photocatalytic decomposition of phenol over TiO₂ powder. *Bulletin of the Chemical Society of Japan*, 58(7), pp.2015-2022. <https://doi.org/10.1246/bcsj.58.2015>
- Olukanni, O.D., Osuntoki, A.A. and Gbenle, G.O., 2006. Textile effluent biodegradation potentials of textile effluent-adapted and non-adapted bacteria. *African Journal of Biotechnology*, 5(20), pp.1980-1984.
- Olukanni, O.D., Osuntoki, A.A. and Gbenle, G.O., 2009. Decolourization of azo dyes by a strain of *Micrococcus* isolated from a refuse dump soil. *Biotechnology*, 8(4), pp.442-448. 10.3923/biotech.2009.442.448
- Pal, M.K. and Mazumdar, K.K., 1974. Photoreduction of dyes catalysed by organic and bio-molecules. *Histochemistry*, 40(3), pp.267-274. <https://doi.org/10.1007/BF00501962>
- Panswad, T., Polprasert, C. and Yamamoto, K. eds., 2016. *Water Pollution Control in Asia: Proceeding of Second IAWPRC Asian Conference on Water Pollution Control Held in Bangkok, Thailand, 9-11 November, 1988*. Elsevier.
- Patel, R.K., 2016. Nitrates-its generation and impact on environment from mines: a review. In *National conference on sustainable mining practice* (pp. 2-3).
- Patel, V. and Parikh, P., 2013. Assessment of seasonal variation in water quality of River Mini, at Sindhrot, Vadodara. *International journal of environmental sciences*, 3(5), pp.1424-1436.
- Pekakis, P.A., Xekoukoulotakis, N.P. and Mantzavinos, D., 2006. Treatment of textile dyehouse wastewater by TiO₂ photocatalysis. *Water research*, 40(6), pp.1276-1286. <https://doi.org/10.1016/j.watres.2006.01.019>
- Peralta-Zamora, P., Kunz, A., de Moraes, S.G., Pelegrini, R., de Campos Moleiro, P., Reyes, J. and Duran, N., 1999. Degradation of reactive dyes I. A comparative study of ozonation, enzymatic and photochemical processes. *Chemosphere*, 38(4), pp.835-852. [https://doi.org/10.1016/S0045-6535\(98\)00227-6](https://doi.org/10.1016/S0045-6535(98)00227-6)
- Pignatello, J.J., Oliveros, E. and MacKay, A., 2006. Advanced oxidation processes for organic contaminant destruction based on the Fenton reaction and related chemistry. *Critical reviews in environmental science and technology*, 36(1), pp.1-84. <https://doi.org/10.1080/10643380500326564>

References

- Poulios, I. and Tsachpinis, I., 1999. Photodegradation of the textile dye Reactive Black 5 in the presence of semiconducting oxides. *Journal of Chemical Technology and Biotechnology: International Research in Process, Environmental and Clean Technology*, 74(4), pp.349-357. [https://doi.org/10.1002/\(SICI\)1097-4660\(199904\)74:4<349::AID-JCTB5>3.0.CO;2-7](https://doi.org/10.1002/(SICI)1097-4660(199904)74:4<349::AID-JCTB5>3.0.CO;2-7)
- Prado, A.G., Bolzon, L.B., Pedroso, C.P., Moura, A.O. and Costa, L.L., 2008. Nb₂O₅ as efficient and recyclable photocatalyst for indigo carmine degradation. *Applied catalysis B: environmental*, 82(3-4), pp.219-224. <https://doi.org/10.1016/j.apcatb.2008.01.024>
- Prieto, O., Feroso, J., Nuñez, Y., Del Valle, J.L. and Irusta, R., 2005. Decolouration of textile dyes in wastewaters by photocatalysis with TiO₂. *Solar Energy*, 79(4), pp.376-383. <https://doi.org/10.1016/j.solener.2005.02.023>
- Qamar, M., Saquib, M. and Muneer, M., 2005a. Photocatalytic degradation of two selected dye derivatives, chromotrope 2B and amido black 10B, in aqueous suspensions of titanium dioxide. *Dyes and Pigments*, 65(1), pp.1-9. <https://doi.org/10.1016/j.dyepig.2004.06.006>
- Qamar, M., Saquib, M. and Muneer, M., 2005b. Semiconductor-mediated photocatalytic degradation of an azo dye, chrysoidine Y in aqueous suspensions. *Desalination*, 171(2), pp.185-193. <https://doi.org/10.1016/j.desal.2004.04.005>
- Rai, H.S., Bhattacharyya, M.S., Singh, J., Bansal, T.K., Vats, P. and Banerjee, U.C., 2005. Removal of dyes from the effluent of textile and dyestuff manufacturing industry: a review of emerging techniques with reference to biological treatment. *Critical reviews in environmental science and technology*, 35(3), pp.219-238. <https://doi.org/10.1080/10643380590917932>
- Rajesh, K.M., 2011. Studies on photocatalysis by nano titania modified with nonmetals. PhD Dissertation (unpubl). Faculty of Science, Cochin University of Science and Technology, Kerala, India
- Ram, C., Pareek, R.K. and Singh, V., 2012. Photocatalytic degradation of textile dye by using titanium dioxide nanocatalyst. *International Journal of Theoretical and Applied Sciences*, 4(2), pp.82-88.

References

- Restiani, P., 2016. Water Governance Mapping Report: Textile Industry Water Use in Bangladesh. *Stockholm International Water Institute (SIWI) and Sweden Textile Water Initiative (STWI): Stockholm, Sweden.*
- Reza, K.M., Kurny, A.S.W. and Gulshan, F., 2017. Parameters affecting the photocatalytic degradation of dyes using TiO₂: a review. *Applied Water Science*, 7(4), pp.1569-1578. <https://doi.org/10.1007/s13201-015-0367-y>
- Robinson, T., McMullan, G., Marchant, R. and Nigam, P., 2001. Remediation of dyes in textile effluent: a critical review on current treatment technologies with a proposed alternative. *Bioresource technology*, 77(3), pp.247-255. [https://doi.org/10.1016/S0960-8524\(00\)00080-8](https://doi.org/10.1016/S0960-8524(00)00080-8)
- Rouse, R.D., 1979. Water quality management in pond fish culture. *Research and development series*, 22. Auburn University, Alabama, USA.
- Rupa, A.V., Vaithyanathan, R. and Sivakumar, T., 2011. Noble metal modified titania catalysts in the degradation of Reactive Black 5: a kinetic approach. *Water Science and Technology*, 64(5), pp.1040-1045. <https://doi.org/10.2166/wst.2011.524>
- Saggiaro, E.M., Oliveira, A.S., Pavesi, T., Maia, C.G., Ferreira, L.F.V. and Moreira, J.C., 2011. Use of titanium dioxide photocatalysis on the remediation of model textile wastewaters containing azo dyes. *Molecules*, 16(12), pp.10370-10386. <https://doi.org/10.3390/molecules161210370>
- Sahel, K., Perol, N., Chermette, H., Bordes, C., Derriche, Z. and Guillard, C., 2007. Photocatalytic decolorization of Remazol Black 5 (RB5) and Procion Red MX-5B—Isotherm of adsorption, kinetic of decolorization and mineralization. *Applied Catalysis B: Environmental*, 77(1-2), pp.100-109. <https://doi.org/10.1016/j.apcatb.2007.06.016>
- Sakthivel, S., Neppolian, B., Shankar, M.V., Arabindoo, B., Palanichamy, M. and Murugesan, V., 2003. Solar photocatalytic degradation of azo dye: comparison of photocatalytic efficiency of ZnO and TiO₂. *Solar energy materials and solar cells*, 77(1), pp.65-82. [https://doi.org/10.1016/S0927-0248\(02\)00255-6](https://doi.org/10.1016/S0927-0248(02)00255-6)
- Salama, A., Mohamed, A., Aboamara, N.M., Osman, T.A. and Khattab, A., 2018. Photocatalytic degradation of organic dyes using composite nanofibers under UV irradiation. *Applied Nanoscience*, 8(1-2), pp.155-161. <https://doi.org/10.1007/s13204-018-0660-9>

References

- Salem, H.M., Eweida, E.A. and Farag, A., 2000. Heavy metals in drinking water and their environmental impact on human health. *ICEHM2000, Cairo University, Egypt*, pp.542-556. <https://eprints.lmu.edu.ng/id/eprint/1012>
- Salleh, M.A.M., Mahmoud, D.K., Karim, W.A.W.A. and Idris, A., 2011. Cationic and anionic dye adsorption by agricultural solid wastes: a comprehensive review. *Desalination*, 280(1-3), pp.1-13. <https://doi.org/10.1016/j.desal.2011.07.019>
- Saltabas, Ö., Teker, M. and Konuk, Z., 2012. Biosorption of cationic dyes from aqueous solution by water hyacinth roots. *Global Nest Journal*, 14, pp.24-31.
- Sandstead, H.H., 1978. Zinc interference with copper metabolism. *Jama*, 240(20), pp.2188-2189.
- Sauer, T., Neto, G.C., Jose, H.J. and Moreira, R.F.P.M., 2002. Kinetics of photocatalytic degradation of reactive dyes in a TiO₂ slurry reactor. *Journal of Photochemistry and Photobiology A: Chemistry*, 149(1-3), pp.147-154. [https://doi.org/10.1016/S1010-6030\(02\)00015-1](https://doi.org/10.1016/S1010-6030(02)00015-1)
- Schivello, M. (Ed.). 1997. Heterogeneous photocatalysis In: *Photoscience and Photo engineering. John Wiley and Sons, Chichester*, 3: pp.208
- Secula, M.S., Suditu, G.D., Poullos, I., Cojocar, C. and Cretescu, I., 2008. Response surface optimization of the photocatalytic decolorization of a simulated dyestuff effluent. *Chemical Engineering Journal*, 141(1-3), pp.18-26. <https://doi.org/10.1016/j.cej.2007.10.003>
- Shrivastava, R., Upreti, R.K., Seth, P.K. and Chaturvedi, U.C., 2002. Effects of chromium on the immune system. *FEMS Immunology and Medical Microbiology*, 34(1), pp.1-7. <https://doi.org/10.1111/j.1574-695X.2002.tb00596.x>
- Singh, D., Singh, V. and Agnihotri, A.K., 2013. Study of textile effluent in and around Ludhiana district in Punjab, India. *International Journal of Environmental Sciences*, 3(4), pp.1271-1278.
- Singh, R. and Kulkarni, A.D., 2012. Application of immobilized photocatalyst for the degradation of Textile waste water. *Int. J. Engineering Research and Applications*, 2, pp.460-472.

References

- Slokar, Y.M. and Le Marechal, A.M., 1998. Methods of decoloration of textile wastewaters. *Dyes and pigments*, 37(4), pp.335-356. [https://doi.org/10.1016/S0143-7208\(97\)00075-2](https://doi.org/10.1016/S0143-7208(97)00075-2)
- Sobana, N. and Swaminathan, M., 2007. The effect of operational parameters on the photocatalytic degradation of acid red 18 by ZnO. *Separation and purification technology*, 56(1), pp.101-107. <https://doi.org/10.1016/j.seppur.2007.01.032>
- Sohrabi, M.R. and Ghavami, M., 2008. Photocatalytic degradation of Direct Red 23 dye using UV/ TiO₂: Effect of operational parameters. *Journal of hazardous materials*, 153(3), pp.1235-1239. <https://doi.org/10.1016/j.jhazmat.2007.09.114>
- Solmaz, S.A., Üstün, G.E., Birgül, A. and Yonar, T., 2009. Advanced oxidation of textile dyeing effluents: comparison of Fe⁺²/H₂O₂, Fe⁺³/H₂O₂, O₃ and chemical coagulation processes. *Fresenius Environmental Bulletin*, 18(8), pp.1424-1433.
- Soloman, P.A., Basha, C.A., Velan, M., Ramamurthi, V., Koteeswaran, K. and Balasubramanian, N., 2009. Electrochemical degradation of Remazol Black B dye effluent. *CLEAN–Soil, Air, Water*, 37(11), pp.889-900. <https://doi.org/10.1002/clen.200900055>
- Soltani, T. and Entezari, M.H., 2013. Photolysis and photocatalysis of methylene blue by ferrite bismuth nanoparticles under sunlight irradiation. *Journal of Molecular Catalysis A: Chemical*, 377, pp.197-203. <https://doi.org/10.1016/j.molcata.2013.05.004>
- Sonwane, G. and Mahajan, V., 2016. Effective degradation and mineralization of real textile effluent by sonolysis, photocatalysis, and sonophotocatalysis using ZnO nano catalyst. *Nanochemistry Research*, 1(2), pp.258-263. <https://doaj.org/article/7774456cefe64b13812e80743d88e0ba>
- Sousa, J., Freitas, O.M. and Figueiredo, S.A., 2012. Basic dyestuffs removal from textile effluents using feathers: Equilibrium, kinetic and column studies. *Global Nest Journal*, 14, pp.100-107.

References

- Soutsas, K., Karayannis, V., Poullos, I., Riga, A., Ntampeglitis, K., Spiliotis, X. and Papapolymerou, G., 2010. Decolorization and degradation of reactive azo dyes via heterogeneous photocatalytic processes. *Desalination*, 250(1), pp.345-350. <https://doi.org/10.1016/j.desal.2009.09.054>
- Stock, N.L., Peller, J., Vinodgopal, K. and Kamat, P.V., 2000. Combinative sonolysis and photocatalysis for textile dye degradation. *Environmental science and technology*, 34(9), pp.1747-1750. <https://doi.org/10.1021/es991231c>
- Sultana, M.S., Islam, M.S., Saha, R. and Al-Mansur, M.A., 2009. Impact of the effluents of textile dyeing industries on the surface water quality inside DND embankment, Narayanganj. *Bangladesh Journal of Scientific and Industrial Research*, 44(1), pp.65-80. <https://doi.org/10.3329/bjsir.v44i1.2715>
- Suteu, D., Zaharia, C., Bilba, D., Muresan, R., Popescu, A. and Muresan, A., 2009. Decolorization waste waters from the textile industry-physical methods, chemical methods. *Industria Textila*, 60(5), pp.254-263.
- Syafalni, S., Abustan, I., Dahlan, I., Wah, C.K. and Umar, G., 2012. Treatment of dye wastewater using granular activated carbon and zeolite filter. *Modern Applied Science*, 6(2), p.37.
- Syoufian, A., Satriya, O.H. and Nakashima, K., 2007. Photocatalytic activity of titania hollow spheres: Photodecomposition of methylene blue as a target molecule. *Catalysis Communications*, 8(5), pp.755-759. <https://doi.org/10.1016/j.catcom.2006.08.047>
- Tang, C. and Chen, V., 2004. The photocatalytic degradation of reactive black 5 using TiO₂/UV in an annular photoreactor. *Water Research*, 38(11), pp.2775-2781. <https://doi.org/10.1016/j.watres.2004.03.020>
- Tang, W.Z. and An, H., 1995. UV/ TiO₂ photocatalytic oxidation of commercial dyes in aqueous solutions. *Chemosphere*, 31(9), pp.4157-4170. [https://doi.org/10.1016/0045-6535\(95\)80015-D](https://doi.org/10.1016/0045-6535(95)80015-D)
- Tang, W.Z. and Huang, C.P., 1995. Photocatalyzed oxidation pathways of 2, 4-dichlorophenol by CdS in basic and acidic aqueous solutions. *Water Research*, 29(2), pp.745-756. [https://doi.org/10.1016/0043-1354\(94\)00151-V](https://doi.org/10.1016/0043-1354(94)00151-V)

References

- Tang, W.Z., Zhang, Z., An, H., Quintana, M.O. and Torres, D.F., 1997. TiO₂/UV photodegradation of azo dyes in aqueous solutions. *Environmental technology*, 18(1), pp.1-12. 10.1080/09593330.1997.9618466
- Tariq, M.A., Faisal, M., Saquib, M. and Muneer, M., 2008. Heterogeneous photocatalytic degradation of an anthraquinone and a triphenylmethane dye derivative in aqueous suspensions of semiconductor. *Dyes and Pigments*, 76(2), pp.358-365. <https://doi.org/10.1016/j.dyepig.2006.08.045>
- Tatawat, R.K., Chandel, C.P.S., 2008. A hydrochemical profile for assessing the groundwater quality of Jaipur City. *Environmental Monitoring and Assessment*, 143, pp.337–343. <https://doi.org/10.1007/s10661-007-9936-3>
- Tayade, R.J., Natarajan, T.S. and Bajaj, H.C., 2009. Photocatalytic degradation of methylene blue dye using ultraviolet light emitting diodes. *Industrial and Engineering Chemistry Research*, 48(23), pp.10262-10267. <https://doi.org/10.1021/ie9012437>
- Tayeb, A.M. and Hussein, D.S., 2015. Synthesis of TiO₂ nanoparticles and their photocatalytic activity for methylene blue. *American Journal of Nanomaterials*, 3(2), pp.57-63. DOI:10.12691/ajn-3-2-2
- Teh, C.M. and Mohamed, A.R., 2011. Roles of titanium dioxide and ion-doped titanium dioxide on photocatalytic degradation of organic pollutants (phenolic compounds and dyes) in aqueous solutions: A review. *Journal of Alloys and Compounds*, 509(5), pp.1648-1660. <https://doi.org/10.1016/j.jallcom.2010.10.181>
- Thiruvengkatachari, R., Vigneswaran, S. and Moon, I.S., 2008. A review on UV/TiO₂ photocatalytic oxidation process (Journal Review). *Korean Journal of Chemical Engineering*, 25(1), pp.64-72. <https://doi.org/10.1007/s11814-008-0011-8>
- Tomei, M.C., Pascual, J.S. and Angelucci, D.M., 2016. Analysing performance of real textile wastewater bio-decolourization under different reaction environments. *Journal of Cleaner Production*, 129, pp.468-477. <https://doi.org/10.1016/j.jclepro.2016.04.028>

References

- Toor, A.P., Verma, A., Jotshi, C.K., Bajpai, P.K. and Singh, V., 2006. Photocatalytic degradation of Direct Yellow 12 dye using UV/ TiO₂ in a shallow pond slurry reactor. *Dyes and pigments*, 68(1), pp.53-60. <https://doi.org/10.1016/j.dyepig.2004.12.009>
- Tünay, O., Germirli, F., Meriç, S., Orhon, D. and Gonenc, E., 1996. Assessment of industrial waste loads in Istanbul watershed areas. *Water Science and Technology*, 34(3-4), pp.79-86. [https://doi.org/10.1016/0273-1223\(96\)00559-8](https://doi.org/10.1016/0273-1223(96)00559-8)
- Türkdoğan, M.K., Kilicel, F., Kara, K., Tuncer, I. and Uygan, I., 2003. Heavy metals in soil, vegetables and fruits in the endemic upper gastrointestinal cancer region of Turkey. *Environmental toxicology and pharmacology*, 13(3), pp.175-179. [https://doi.org/10.1016/S1382-6689\(02\)00156-4](https://doi.org/10.1016/S1382-6689(02)00156-4)
- Uygur, A. and Kök, E., 1999. Decolorisation treatments of azo dye waste waters including dichlorotriazinyl reactive groups by using advanced oxidation method. *Coloration Technology*, 115(11), pp.350-354. <https://doi.org/10.1111/j.1478-4408.1999.tb00325.x>
- Vandevivere, P.C., Bianchi, R. and Verstraete, W., 1998. Treatment and reuse of wastewater from the textile wet-processing industry: Review of emerging technologies. *Journal of Chemical Technology and Biotechnology*, 72(4), pp.289-302. [https://doi.org/10.1002/\(SICI\)1097-4660\(199808\)72:4<289::AID-JCTB905>3.0.CO;2-%23](https://doi.org/10.1002/(SICI)1097-4660(199808)72:4<289::AID-JCTB905>3.0.CO;2-%23)
- Vautier, M., Guillard, C. and Herrmann, J.M., 2001. Photocatalytic degradation of dyes in water: case study of indigo and of indigo carmine. *Journal of Catalysis*, 201(1), pp.46-59. <https://doi.org/10.1006/jcat.2001.3232>
- Venceslau, M.C., Tom, S. and Simon, J.J., 1994. Characterization of textile wastewaters-a review. *Environmental technology*, 15(9), pp.17-29. <https://doi.org/10.1080/09593339409385500>
- Vinodgopal, K. and Kamat, P.V., 1995. Enhanced rates of photocatalytic degradation of an azo dye using SnO₂/ TiO₂ coupled semiconductor thin films. *Environmental science and technology*, 29(3), pp.841-845. <https://doi.org/10.1021/es00003a037>

References

- Walker, G.M. and Weatherley, L.R., 1997. Adsorption of acid dyes on to granular activated carbon in fixed beds. *Water Research*, 31(8), pp.2093-2101. [https://doi.org/10.1016/S0043-1354\(97\)00039-0](https://doi.org/10.1016/S0043-1354(97)00039-0)
- Wang, C.C., Lee, C.K., Lyu, M.D. and Juang, L.C., 2008a. Photocatalytic degradation of CI Basic Violet 10 using TiO₂ catalysts supported by Y zeolite: An investigation of the effects of operational parameters. *Dyes and Pigments*, 76(3), pp.817-824. <https://doi.org/10.1016/j.dyepig.2007.02.004>
- Wang, H., Xie, C., Zhang, W., Cai, S., Yang, Z. and Gui, Y., 2007. Comparison of dye degradation efficiency using ZnO powders with various size scales. *Journal of Hazardous materials*, 141(3), pp.645-652. <https://doi.org/10.1016/j.jhazmat.2006.07.021>
- Wang, K.S., Chen, H.Y., Huang, L.C., Su, Y.C. and Chang, S.H., 2008b. Degradation of Reactive Black 5 using combined electrochemical degradation-solar-light/immobilized TiO₂ film process and toxicity evaluation. *Chemosphere*, 72(2), pp.299-305. <https://doi.org/10.1016/j.chemosphere.2008.02.012>
- Wei, T.Y. and Wan, C.C., 1991. Heterogeneous photocatalytic oxidation of phenol with titanium dioxide powders. *Industrial and engineering chemistry research*, 30(6), pp.1293-1300. <https://doi.org/10.1021/ie00054a033>
- Wetchakun, N., Chaiwichain, S., Inceesungvorn, B., Pingmuang, K., Phanichphant, S., Minett, A.I. and Chen, J., 2012. BiVO₄/CeO₂ nanocomposites with high visible-light-induced photocatalytic activity. *ACS applied materials and interfaces*, 4(7), pp.3718-3723. <https://doi.org/10.1021/am300812n>
- Wijannarong, S., Aroonsrimorakot, S., Thavipoke, P. and Sangjan, S., 2013. Removal of reactive dyes from textile dyeing industrial effluent by ozonation process. *APCBEE procedia*, 5, pp.279-282. <https://doi.org/10.1016/j.apcbee.2013.05.048>
- Willmott, N., Guthrie, J. and Nelson, G., 1998. The biotechnology approach to colour removal from textile effluent. *Journal of the Society of Dyers and Colourists*, 114(2), pp.38-41. <https://doi.org/10.1111/j.1478-4408.1998.tb01943.x>
- Winton, E.F., Tardiff, R.G. and McCabe, L.J., 1971. Nitrate in drinking water. *Journal-American Water Works Association*, 63(2), pp.95-98.

References

- Wojnarovits, L. and Takacs, E., 2008. Irradiation treatment of azo dye containing wastewater: an overview. *Radiation physics and chemistry*, 77(3), pp.225-244. <https://doi.org/10.1016/j.radphyschem.2007.05.003>
- Wu, Y., Hu, Y., Xie, Z., Feng, S., Li, B. and Mi, X., 2011. Characterization of biosorption process of acid orange 7 on waste brewery's yeast. *Applied biochemistry and biotechnology*, 163(7), pp.882-894. <https://doi.org/10.1007/s12010-010-9092-z>
- Wuana, R.A. and Okieimen, F.E., 2011. Heavy metals in contaminated soils: a review of sources, chemistry, risks and best available strategies for remediation. *Isrn Ecology*, 2011. doi:10.5402/2011/402647
- Xu, X.R., Li, H.B., Wang, W.H. and Gu, J.D., 2005. Decolorization of dyes and textile wastewater by potassium permanganate. *Chemosphere*, 59(6), pp.893-898. <https://doi.org/10.1016/j.chemosphere.2004.11.013>
- Yang, Y., Guo, Y., Hu, C., Wang, Y. and Wang, E., 2004. Preparation of surface modifications of mesoporous titania with monosubstituted Keggin units and their catalytic performance for organochlorine pesticide and dyes under UV irradiation. *Applied Catalysis A: General*, 273(1-2), pp.201-210. <https://doi.org/10.1016/j.apcata.2004.06.032>
- Yang, Y., Wyatt, I.I., Travis, D. and Bahorsky, M., 1998. Decolorization of Dyes Using UV/H₂O₂ Photochemical Oxidation. *Textile Chemist and Colorist*, 30(4), pp. 27-35.
- Yeber, M.C., Rodríguez, J., Freer, J., Durán, N. and Mansilla, H.D., 2000. Photocatalytic degradation of cellulose bleaching effluent by supported TiO₂ and ZnO. *Chemosphere*, 41(8), pp.1193-1197. [https://doi.org/10.1016/S0045-6535\(99\)00551-2](https://doi.org/10.1016/S0045-6535(99)00551-2)
- Yonar, T., Yonar, G.K., Kestioglu, K. and Azbar, N., 2005. Decolorisation of textile effluent using homogeneous photochemical oxidation processes. *Coloration technology*, 121(5), pp.258-264. <https://doi.org/10.1111/j.1478-4408.2005.tb00283.x>
- Yusuff, R.O. and Sonibare, J.A., 2004. Characterization of textile industries' effluents in Kaduna, Nigeria and pollution implications. *Global Nest: the int. J.*, 6(3), pp.212-221. <https://doi.org/10.30955/gnj.000284>

References

- Zaharia, C., Suteu, D., Muresan, A., Muresan, R. and Popescu, A., 2009. Textile wastewater treatment by homogenous oxidation with hydrogen peroxide. *Environmental Engineering and Management Journal*, 8(6), pp.1359-1369.
- Zainal, Z., Hui, L.K., Hussein, M.Z., Taufiq-Yap, Y.H., Abdullah, A.H. and Ramli, I., 2005. Removal of dyes using immobilized titanium dioxide illuminated by fluorescent lamps. *Journal of hazardous materials*, 125(1-3), pp.113-120. <https://doi.org/10.1016/j.jhazmat.2005.05.013>
- Zayani, G., Bousselmi, L., Mhenni, F. and Ghrabi, A., 2009. Solar photocatalytic degradation of commercial textile azo dyes: Performance of pilot plant scale thin film fixed-bed reactor. *Desalination*, 246(1-3), pp.344-352. <https://doi.org/10.1016/j.desal.2008.03.059>
- Zhang, L., Wan, L., Chang, N., Liu, J., Duan, C., Zhou, Q., Li, X. and Wang, X., 2011. Removal of phosphate from water by activated carbon fiber loaded with lanthanum oxide. *Journal of hazardous materials*, 190(1-3), pp.848-855. <https://doi.org/10.1016/j.jhazmat.2011.04.021>
- Zhu, C., Wang, L., Kong, L., Yang, X., Wang, L., Zheng, S., Chen, F., MaiZhi, F. and Zong, H., 2000. Photocatalytic degradation of AZO dyes by supported TiO₂+ UV in aqueous solution. *Chemosphere*, 41(3), pp.303-309. [https://doi.org/10.1016/S0045-6535\(99\)00487-7](https://doi.org/10.1016/S0045-6535(99)00487-7)



Appendix-1 Standard curves for heavy metals

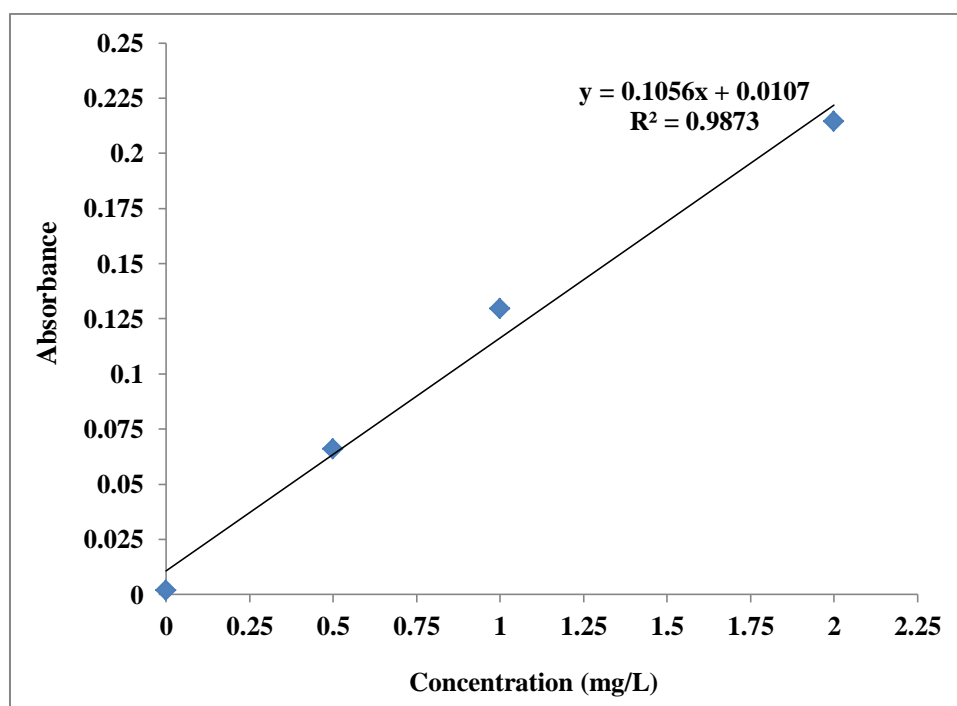


Figure 1.1 Standard curve of Chromium (Cr)

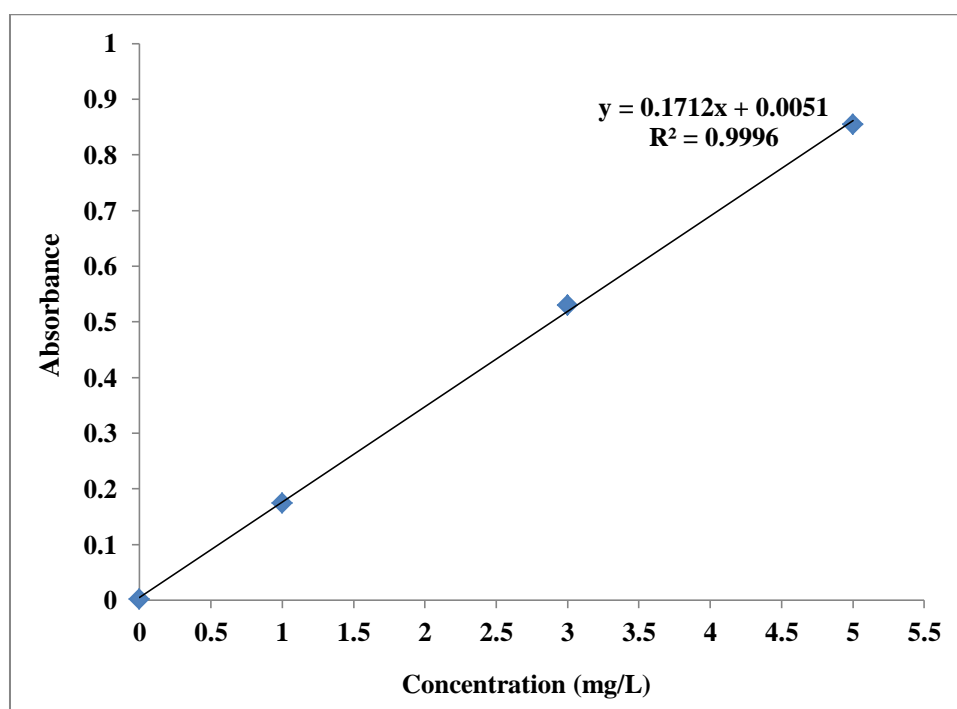


Figure 1.2 Standard curve of Manganese (Mn)

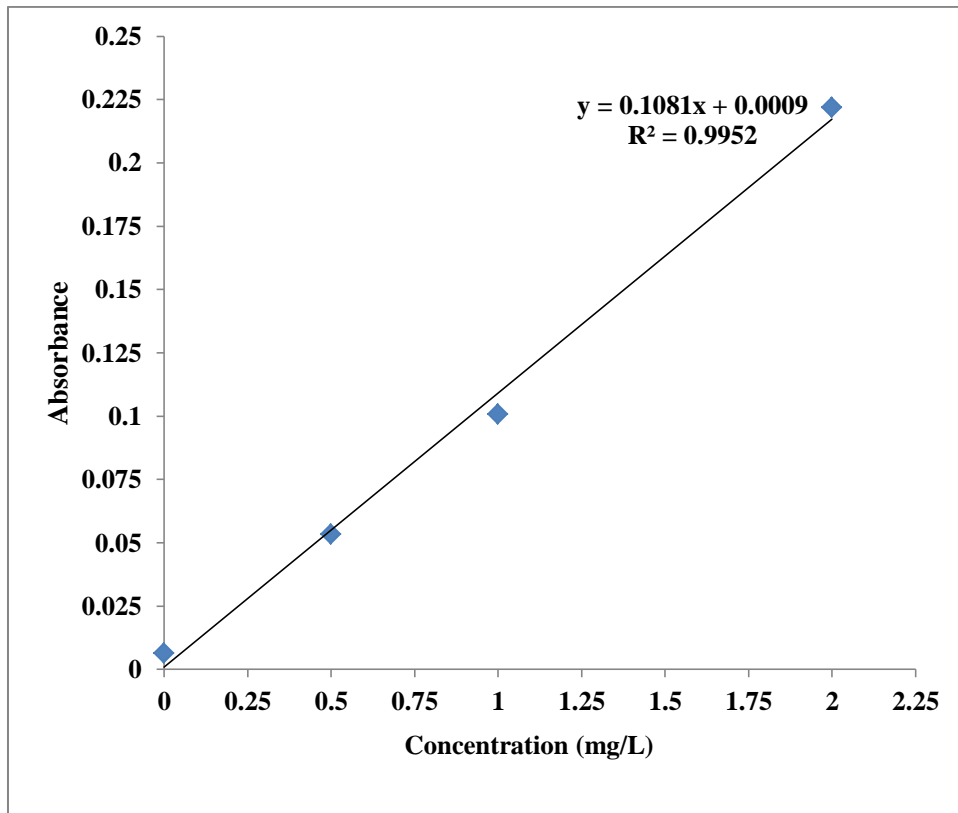


Figure 1.3 Standard curve of Iron (Fe)

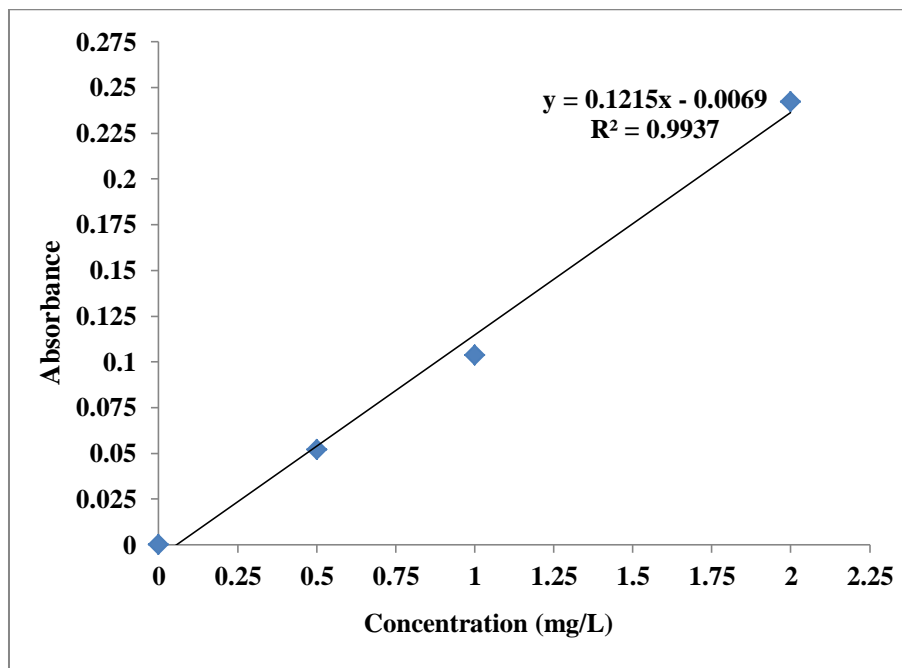


Figure 1.4 Standard curve of Nickel (Ni)

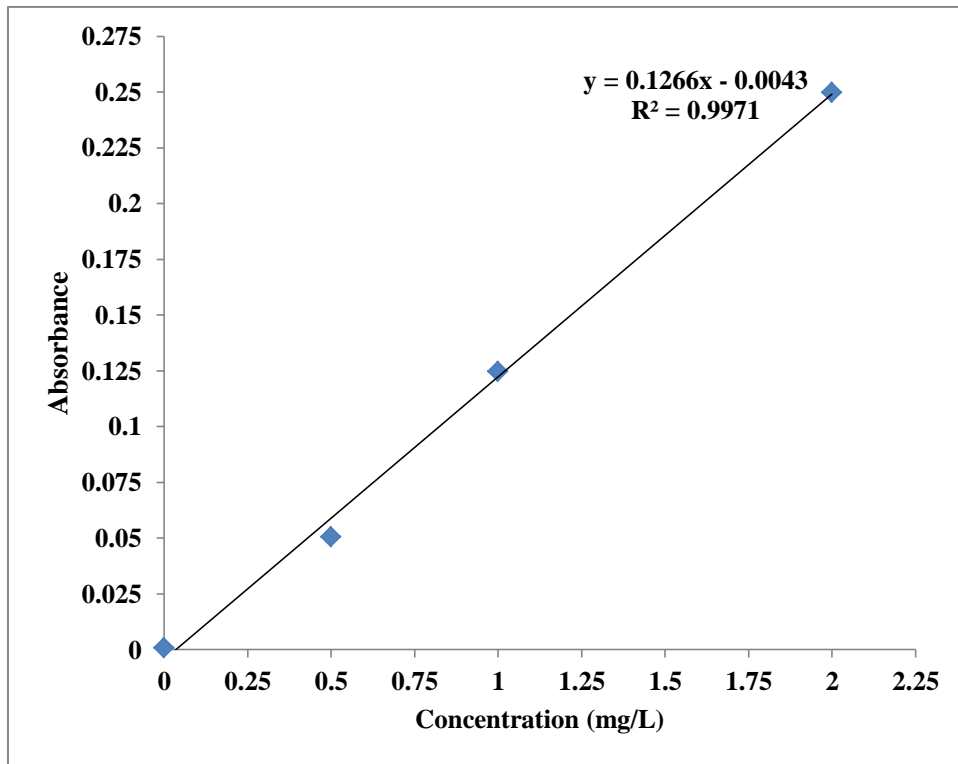


Figure 1.5 Standard curve of Copper (Cu)

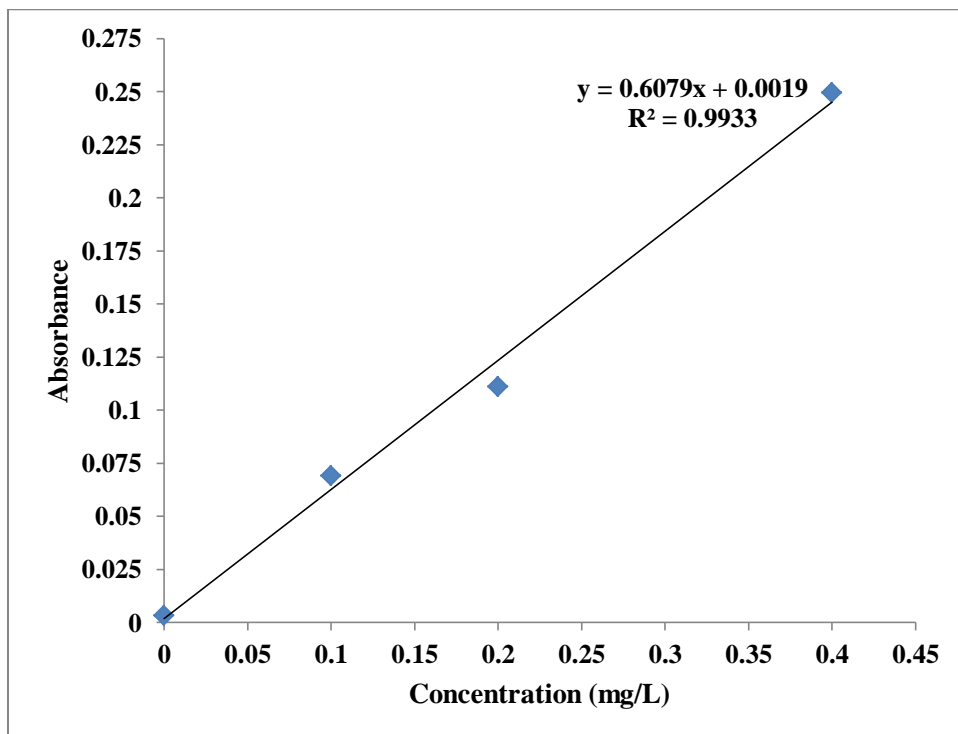


Figure 1.6 Standard curve of Zinc (Zn)

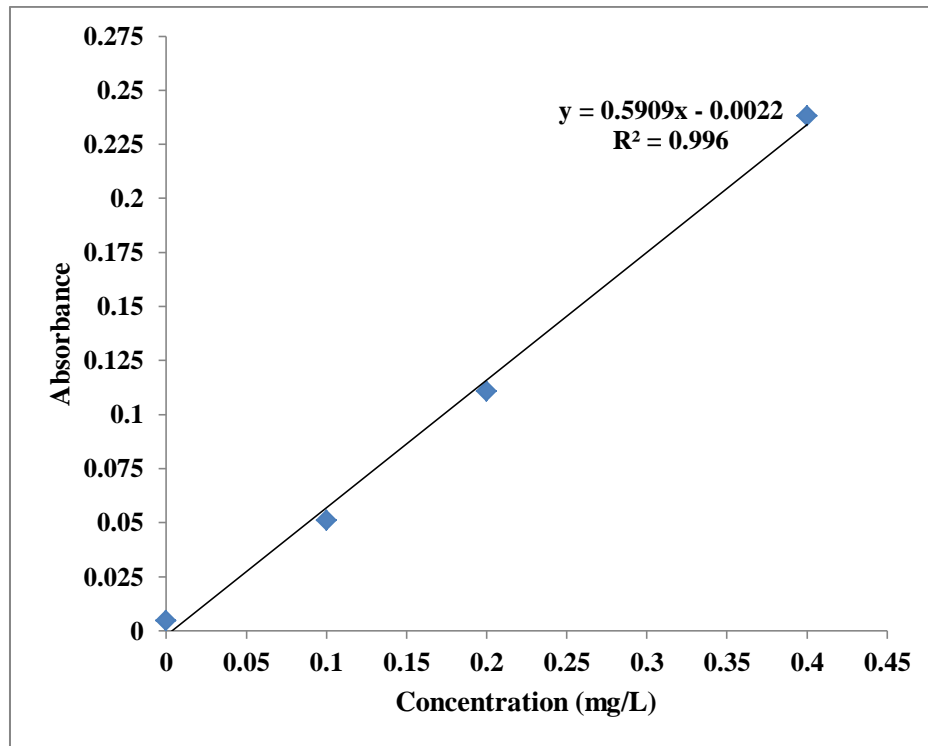


Figure 1.7 Standard curve of Cadmium (Cd)

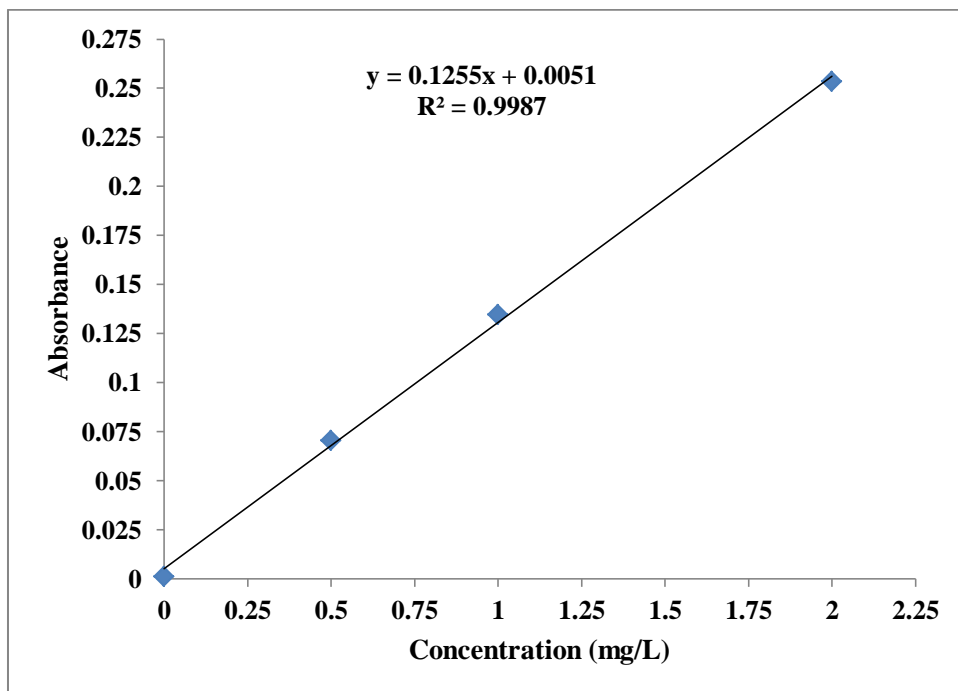


Figure 1.8 Standard curve of Lead (Pb)

Appendix-2 Standard curves for anions

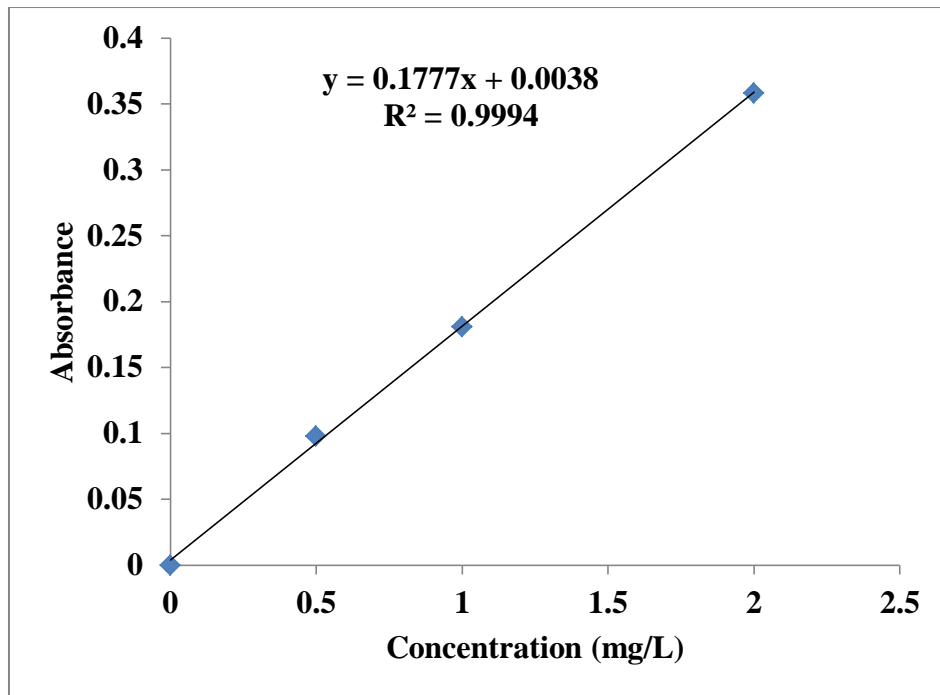


Figure 2.1 Standard curve of Nitrate ion (NO₃⁻)

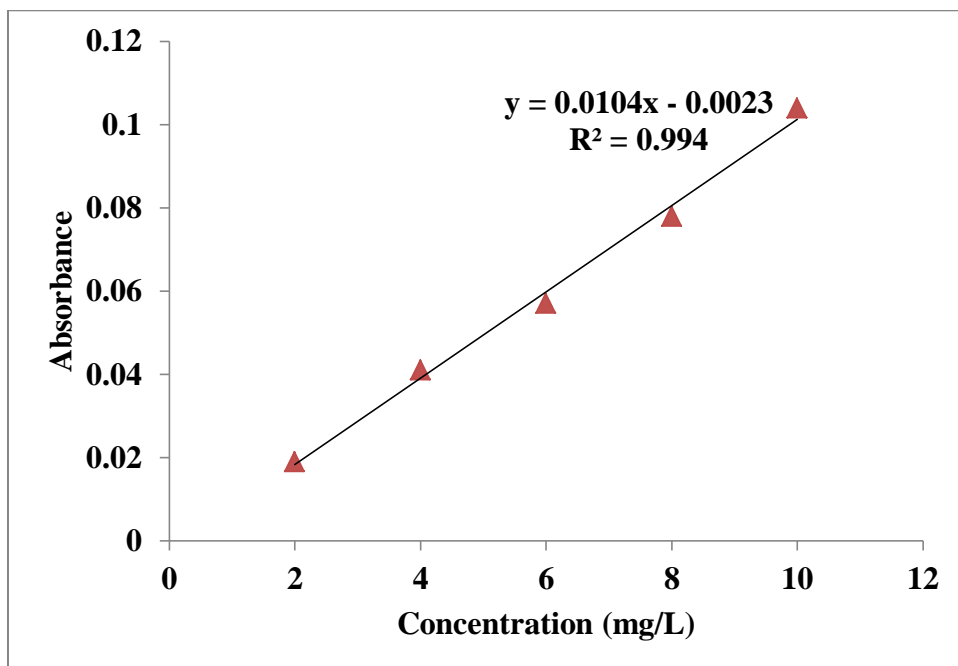


Figure 2.2 Standard curve of Sulfate ion (SO₄²⁻)

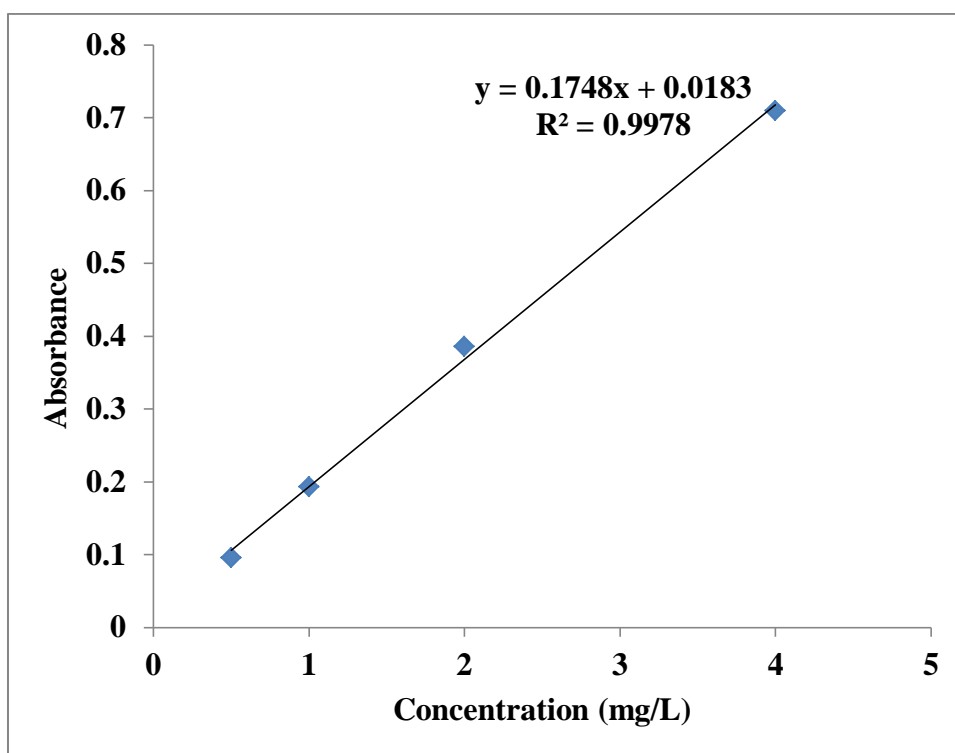


Figure 2.3 Standard curve of Phosphate ion (PO_4^{3-})

Appendix-3 Standard curves for effluent samples

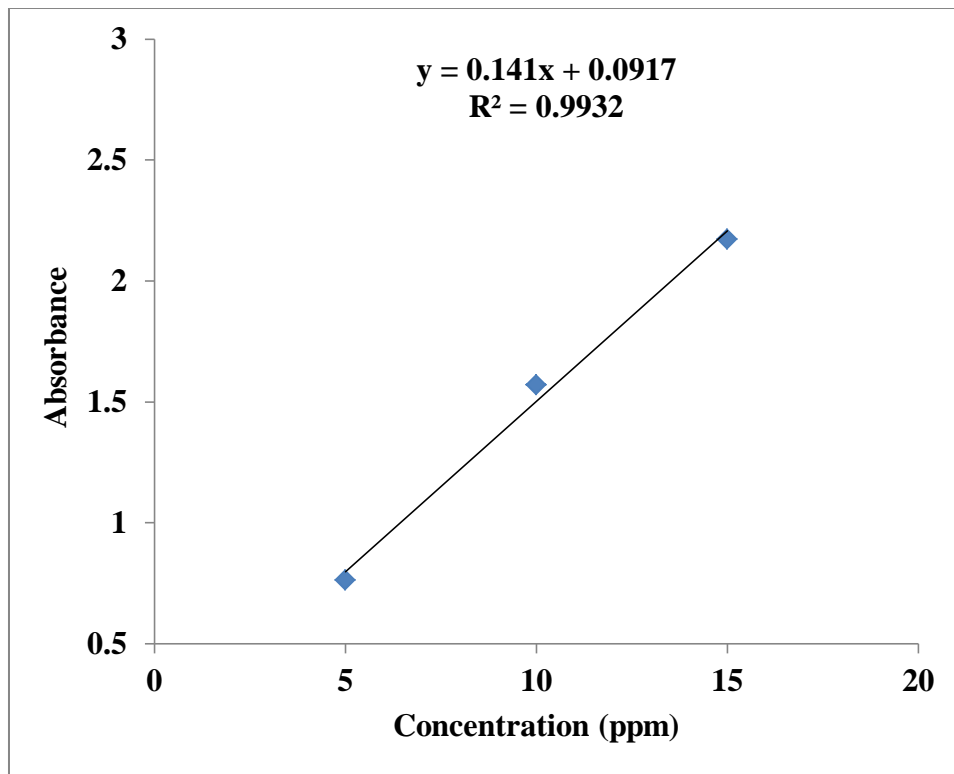


Figure 3.1 Standard curve of MB

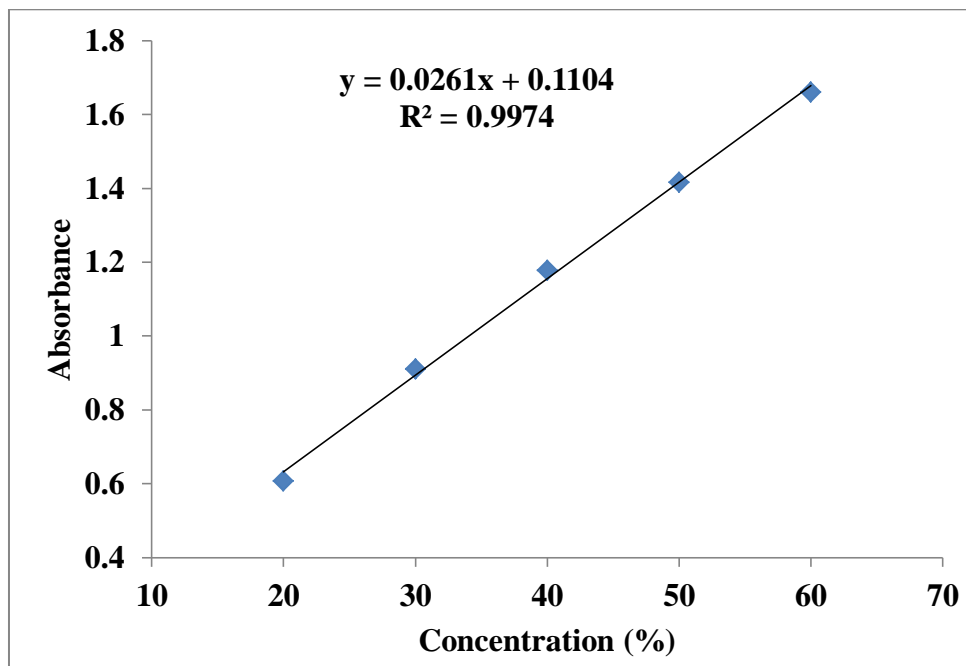


Figure 3.2 Standard curve of SIER-1

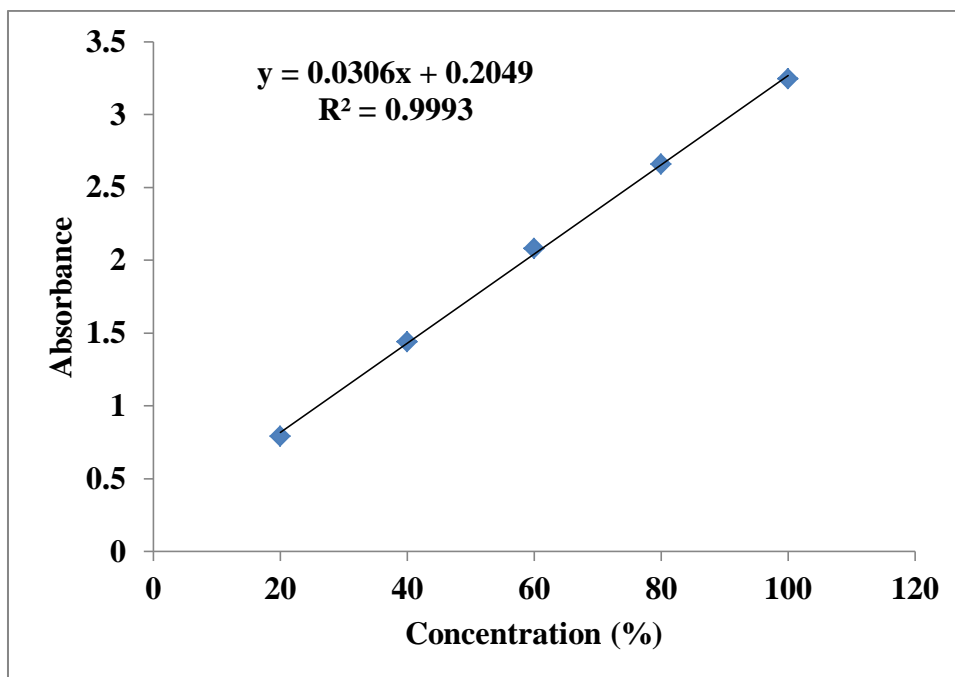


Figure 3.3 Standard curve of SIER-2

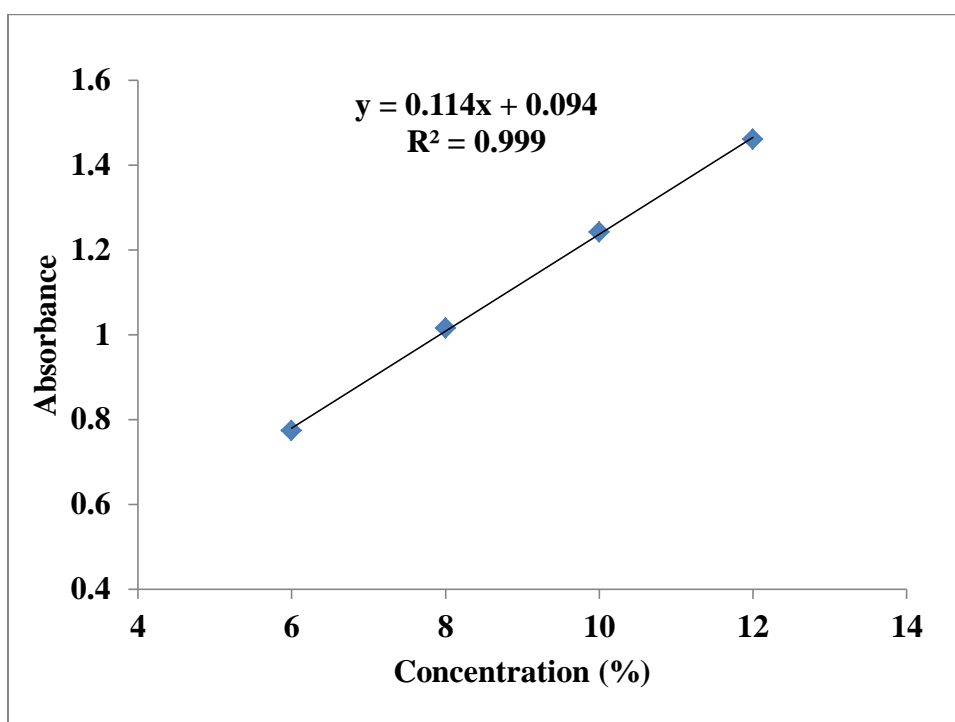


Figure 3.4 Standard curve of YDIES

Appendix-4 Standards

Table 4.1 Waste quality standards for discharge point of industrial units

Parameters	Units	DoE, BD standards
Ammoniacal Nitrogen	mg/L	50
Arsenic (As)	mg/L	0.05
Biological Oxygen Demand (BOD ₅)	mg/L	50
Bicarbonate (HCO ₃ ⁻)	mg/L	300
Cadmium (Cd)	mg/L	0.05
Chemical Oxygen Demand (COD)	mg/L	200
Chloride (Cl)	mg/L	150-600
Chromium (Cr)	mg/L	0.5
Copper (Cu)	mg/L	0.5
Cyanide	mg/L	0.1
Dissolved Oxygen (DO)	mg/L	4.5-8
Electrical Conductivity (EC)	µS/cm	1200
Fluoride	mg/L	7.0
Iron (Fe)	mg/L	2.0
Lead (Pb)	mg/L	0.1
Manganese (Mn)	mg/L	5.0
Mercury (Hg)	mg/L	5.0
Nickel (Ni)	mg/L	1.0
Nitrate (NO ₃ ⁻)	mg/L	10
Oil and Grease	mg/L	10
pH	-	6.5-8
Phosphate	mg/L	25
Phenol compounds	mg/L	1.0
Sulfate (SO ₄ ²⁻)	mg/L	400
Temperature	°C	40
Total Dissolved Solids (TDS)	mg/L	2100
Total Hardness	mg/L	
Total Suspended solids (TSS)	mg/L	150
Zinc	mg/L	5.0